The Identification of the novel gene SENEX and its role in Endothelial Cell Senescence and Survival

Paul Coleman

A thesis submitted in fulfillment of the requirements for the degree of

Doctor of Philosophy

Faculty of Medicine

University of Sydney

2013

Table of Contents

DECLARATION

The work described in this thesis was performed personally by the author in the Vascular Biology Laboratory at the Institute of Medical and Veterinary Science, Adelaide, Australia and at the Vascular Biology Laboratory in the Centenary Institute, Sydney, Australia. The work was conducted between March 2005 and August 2010. This work is original and has not been previously submitted for the purpose of obtaining any other degree at any other institution.

Paul Coleman

BSc (Laboratory Medicine) Honours (Class I)

University of South Australia

August 2010

Acknowledgements

Firstly and most importantly to my supervisor, Jenny Gamble, I thank you and apologies to you at the same time. Firstly I apologies for all the grief I have given you and for the fact I have made everything harder than it needs to be. With experiments and especially with the writing of the thesis, I always made the situation that little bit more difficult than it should be. For these reasons I would like to thank you for your patience, understanding and never ending encouragement. I have been through break ups and break downs during my PhD and you never waivered in your support and faith in the fact I would finish, even if I had nearly given up. Without you I would definitely not have finished the thesis and would probably not be doing my PhD any longer. I truly believe with any other supervisor I would not be writing these words or completing my thesis. I will never forget the massive role you have played in sending me on my path into the research world. Mathew I have to thank you for all your advice over the years and I maybe have to thank you for calming Jenny down at the end of the day and advising her it was a good idea to keep me as a student.

I need to thank two labs and I will start with the VB lab in Adelaide where it all began. I spent a wonderful 3 years in Adelaide with a wonderful group of people in the greatest lab in the world. I don't think there could have been a better combination of people assembled at the one time. Firstly to Chris, I cannot praise you enough to justify how important you were in my PhD. You have taught me so much about science and about life. Your incredible passion for science, which I hope to develop one day, made learning so much more enjoyable. You are a fantastic scientist and teacher and I would be happy in the future to have half of your knowledge and skills in the lab. You have never stopped encouraging me even when I left Adelaide and knowing that I could ring you any time has been a comfort which I have needed many times. I also would have

frustrated you a lot over the years and I will always appreciate your patience and understanding. To Xiao and Claudine, thankyou both so much for all your help in Adelaide. You were both wonderful teachers and have been wonderful friends. Xiao I always appreciated your brutal honesty and your advice. I miss drinking and eating with you and Wayne on the weekends and weeknights so much. Claudine you are a scientist to which a PhD student can look up to. You have been an inspiration with all your success at a young age and you always remained warm and helpful. I have always appreciated your advice and the fact you always involved me in sports and exercise. I assume you were trying to repair the damage which I did to my body when I drank with Xiao.

To Milena, Peter and Kiwi, thankyou you all so much for all your help while I learned the art of science and thankyou for been such great people. There were many times when coming to work was the last thing I wanted to do, but the fact I had such good friends waiting for me made the task so much easier. You were each such an important part of why the lab was such a great place to learn and practice science. Peter I miss the runs and talks, Milena I miss all the laughs and Kiwi I miss your happiness and big smile.

To the mothers of the lab, Jenny, Anna and Michelle. Thankyou for everything, obviously I would have never done an experiment without your efforts, which may not have been a bad thing. I have missed you all in Sydney, you always had good advice for all my problems and you were all caring and wonderful people.

My time at the IMVS was fantastic and that is a reflection on all the fabulous people in the Immunology Department. I made so many good friends and I received so much support and help from many members of the department. I especially would like to thank Paul and Jason. You are both great friends who made my time at the IMVS fun and enjoyable. You were always there

when I needed a drink or twenty, but your are also excellent scientists and had sound advice when I needed it. I will always appreciate the role you played in my PhD.

To my current VB lab in Sydney, the transition from Adelaide could never have gone so smooth without helpful and supportive lab members. I have always received help and excellent advice as I have tried to finish my PhD. A special mention goes to Ying, you have been essential to my progress in Sydney. With your help and support and patience you have made sure I have completed the experiments that were required. I thankyou so much and I will never forget what you have done for me. I also have received help from other members of the Centenary Institute and I thank you all.

To my old friends and new friends, thankyou all for your encouragement and support over my long journey. I will not name everyone, but so many people have helped me or just come to the pub with me and most have respected the fact I don't like to talk about my thesis. Just having good people around me has made the process just that little bit easier.

To Jennifer and Dom, what can I say? There would be no thesis without the two of you. You have played a role in my PhD which extends beyond science and has been just as important as all my experiments put together. You celebrated my ups and most importantly have been the two people that have pulled me out of my repeated and huge downs. Words cannot express fully my gratitude and appreciation for your patience and support you have given me. Our friendship has been forged through very tough times for me and I will always cherish it and appreciate it.

Lastly to my family, I have made strange decisions over the years, including moving to a different state. I know my decisions have worried you and upset you. But through all the time and pain you never questioned me and supported me unconditionally. Through all my worries and stresses I have always had the backing of a wonderful and caring family and knowing this has

always helped me take the next step. I hope you are proud of my PhD and I dedicate my thesis to you. I have finally finished

Publications

Paul R. Coleman, Christopher N. Hahn, Matthew Grimshaw, Ying Lu, Xiaochun Li, Peter J. Brautigan, Konstanze Beck, Roland Stocker, Mathew A. Vadas, and Jennifer R. Gamble. Stress-induced premature senescence mediated by a novel gene, SENEX, results in an anti-inflammatory phenotype in endothelial cells. Blood. Jul 27

List of Figures

List of Abbreviations

ADMA	Asymmetrical Dimethyl l-arginine
Ang	Angiopoietin
Ang II	Angiotensin II
aRNA	Amplified RNA
ATM	Ataxia Talengiectasia Mutated gene
bp	Base Pairs
cDNA	Complementary DNA
CDK	Cyclin-dependent kinase
CDKI	Cyclin-dependent kinase inhibitor
COX2	Cyclooxygenase
CTX	Cyclophosphamide
CVD	Cardiovascular disease
DNA	Deoxyribonucleic acid
DDR	DNA Damage Response
DSBs	Double Stranded Breaks
EC	Endothelial Cell
ECM	Extracellular Matrix
ELISA	Enzyme-linked immunosorbent assay
EGF	Epidermal Growth Factor
FACS	Fluorescence Activated Cell Sorting
FCS	Foetal Calf Serum
FGF	Fibroblast Growth Factor
GFP	Green Fluorescent Protein
H_2O_2	Hydrogen Peroxide
HEK293	Human Embryonic Kidney 293 Cells
HDF	Human Diploid fibroblasts
HIF-1	Hypoxia Inducible Factor 1
HMT	Histone Methyltransferase
HSC	Hepatic Stellate Cells
HUVEC	Human Umbilical Vein Endothelial Cells
ICAM1	Intercellular adhesion molecule-1
IGFBP7	Insulin Growth Factor Binding Protein 7
IL	Interleukin
kb	Kilobases
LB	Luria Bertani
M	Molar (mol/L)
MCP-1	Monocyte Chemotactic protein-1
MCS	Multiple Cloning Site
MEF	Murine embryonic Fibroblasts
ml/mm/mM	Millilitre/millimetre/millimolar
MMP	Matrix Metalloproteinase
MOI	Multiplicity of Infection
mRNA	Messenger ribonucleic acid
nt	Nucleotides
O_2^-	Superoxide Anions
p14	$p14^{ARF}$
p16	$p16^{INK4a}$
pAEAT	pAdEasy1-AdTrackCMV
PAI-1	Plasminogen Activator Inhibitor 1

PBS	Phosphate buffered saline
PCR	Polymerase Chain Reaction
PDGF	Platelet Derived Growth Factor
PHB1	Prohibitin-1
PMA	Phorbol Myristate Acetate
PPIA	Peptidylprolyl isomerase A
PHB1	Prohibitin-1
PRR	Proline Rich Region
PTB	Phosphotyrosine Binding domain
Q-RT-PCR	Real Time Quantitative Reverse Transcription PCR
Rb	Retinoblastoma protein
RE1	Repressor Element-1
REST	Repressor Element 1 Silencing Transcription Factor
RNA	Ribonucleic acid
RNAi	RNA interfernece
ROS	Reactive Oxygen Species
RS	Replicative senescence
RT	Room temperature
SA β-gal	Senescence Associated β-galactosidase
SAGE	Serial analysis of gene expression
SAFH	Senescence Associated Heterochromatin Foci
SASP	Senescence Associated Secretory Phenotype
SEM	Standard error of the mean
SIPS	Stress Induced Premature Senescence
siRNA	Short Interfering RNA
SMC	Smooth muscle cells
$TCID_{50}$	Tissue Culture Infectious Dose 50
TERT	Telomerase Reverse Transcriptase
TGF-β	Transforming Growth Factor β
TNFα	Tumour Necrosis Factor α TNFα
UTR	Untranslated Region
µg/µl/µM	Microgram/microlitre/micromolar
VCAM1	Vascular Cell Adhesion Molecule-1
VEGF	Vascular Endothelial Growth Factor
VEGI	Vascular Endothelial Growth Inhibitor
VPF	Vascular Permeability Factor
v/v	Volume per volume
2D or 3D	Two dimensional or Three dimensional

Abstract

Cellular senescence is a mechanism to inhibit the growth of mammalians cells after oncogenic activation, or in response to damage or stress. Senescence significantly changes the phenotype of the cell and permanently stops cell replication. Senescence was originally thought of as a cell culture artifact, but recent research has demonstrated a significant role in human pathologies, such as tumour development and cardiovascular disease. We describe here the identification of a novel gene, *SENEX* that regulates stress induced premature senescence pathways in endothelial cells (EC) involving $p16^{INK4a}$ and Rb activation. Endogenous levels of *SENEX* remain unchanged during replicative senescence but are regulated by H_2O_2 mediated stress. Indicating a role for SENEX in stress induced senescence and not in replicative induced senescence. In contrast to that previously described for senescence in other cell types, the *SENEX* induced senescent EC are profoundly anti-inflammatory. The cells are resistant to TNFα induced apoptosis, adhesion of neutrophils and mononuclear cells and the surface (but not cytoplasmic) expression of E-selectin and VCAM1 is decreased after SENEX induced senescence. Furthermore they are resistant to thrombin induced vascular leak. Senescent ECs such as those lining atherosclerotic lesions may therefore function to limit the inflammatory response. *SENEX* is also essential for EC survival since depletion either ectopically by siRNA or by high dose H_2O_2 treatment causes apoptosis. Preliminary results indicate that SENEX plays a role in the induction of apoptosis through the extrinsic pathway. Together, these findings expand our understanding of the role of senescence in the vasculature and identify *SENEX* as a fulcrum for driving the resultant phenotype of the endothelium.

CHAPTER 1

INTRODUCTION

1.1 Cellular Senescence

In 1961 Hayflick and Moorhead challenged the idea that cells are immortal by demonstrating that many cells enter a phase of irreversible growth arrest following serial cultivation *in vitro [1]*. This cellular phenomenon was referred to as 'cellular senescence' and for many years was considered to be an artefact of tissue culture [1]. This view has now been reversed. *S*enescent cells have been observed *in vivo* under both normal physiological conditions, for example in the skin of elderly people [2] and in pathological conditions such as cancer suggesting a physiological role for senescence [3-6]. Together with apoptosis, senescence is now considered a key mechanism for the control of cell proliferation and inappropriate activation [7]. Recent research also indicates that senescent cells are not an insignificant population of cells and since they are metabolically active, although halted from proliferation, it is proposed that they play a role in regulation of their microenvironment [8].

1.1.1 Forms of Senescence

Senescence can be divided into two types: 1) Replicative (telomere-dependent) senescence (RS), where telomere shortening during replication results in growth arrest and senescence and 2) Stress-induced premature senescence (SIPS) which is seen under situations of cellular stress and may be induced by DNA damage, oxidative stress, activated oncogenes and certain chemotherapeutic drugs [9]. The major characteristic of both RS and SIPS is that the cells permanently exit the cell cycle but remain metabolically active. This activity has profound effects on the phenotype of the senescent cell itself and on surrounding cells and the environment in

which they reside. With the possible exception of embryonic stem cells, most division-component cells, including some tumour cells, can undergo senescence when appropriately stimulated [10].

1.2 Features of Senescence

Senescent cells are characterised by a markedly enlarged cell size. They have a flattened vacuolated morphology and are inhibited in their proliferative capacity and are not responsive to physiologic mitogenic stimuli. The growth arrest of senescent cells occurs mostly in the G1/S interface. Senescent cells often display polyploidy, and have accumulated senescence-associated β-galactosidase activity (SA β-gal), a widely used marker of senescence [2]. SA β-gal enables the detection of increased lysosomal β-galactosidase evident in senescent cells at a pH 6.0. It is visualised by means of a cytochemical reaction which stains cells blue. Although its function is unknown, SA β gal is generally accepted as a marker of senescence *in vitro* and *in vivo* (Figure 1.1) [11]. Until recently SA-β-gal has been the most reliable marker of the senescence state, although there is some evidence that suggests that it is not specific for senescence [12]. Cotter et al found that given the fact that pH 6 β-gal staining simply detects the lysosomal expansion associated with cellular passages and is not required for senescence development *in vitro*, they suggest the need for more specific and biologically relevant markers of senescence *in vivo [13]*.

A further marker of senescent cells is the detection of Senescence Associated Heterochromatin Foci (SAHF). Senescent cells undergo modifications in their chromatin structure due to the accumulation of heterochromatin proteins on E2F promoters [14] which can contribute to the gene expression profile characteristic of senescence. The organisation of DNA into heterochromatin contributes to nuclear organisation, chromosome structure and gene silencing. SAHF are observed in interphase nuclei and contain the heterochromatin associated proteins histone 3 methylated at lysine 9 (K9M-H3) and heterochromatin protein 1γ (HP1), exclude

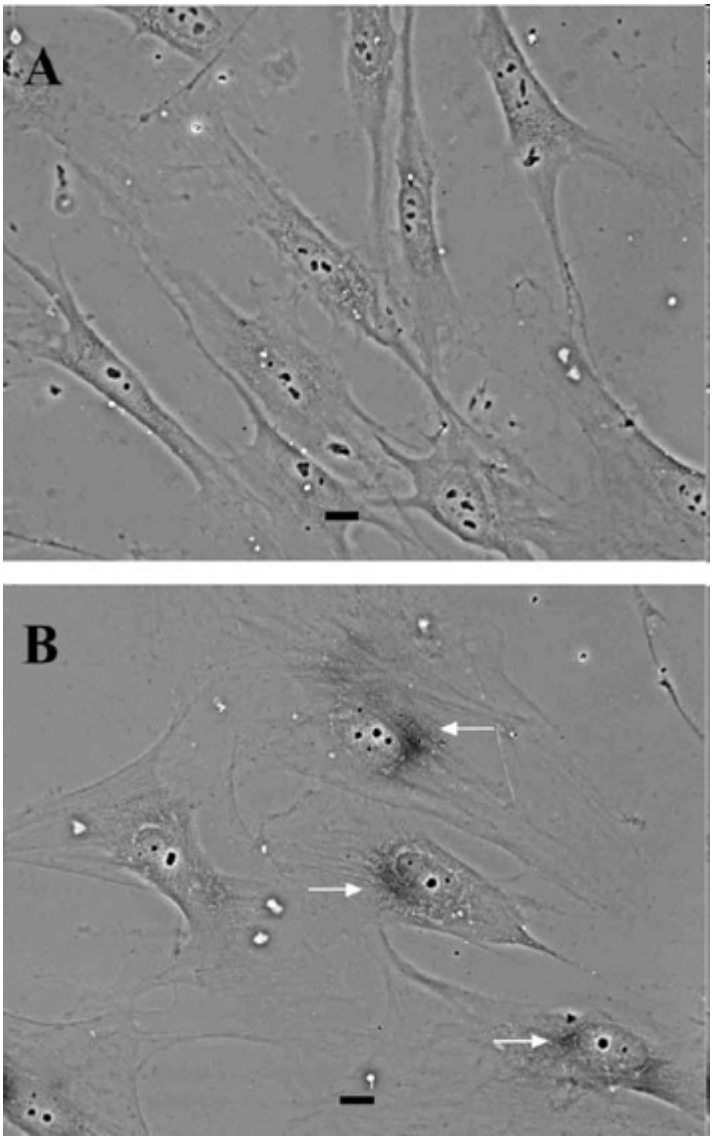

Figure 1.1. Morphology of senescent human fibroblasts. Normal human dermal diploid fibroblasts exhibit a typically thin, elongated appearance with dense cytoplasm when subconfluent in culture (**A**). Senescent fibroblasts become much larger with diffuse, thin cytoplasm with prominent stress fibers becoming visible under phase contrast (**B**). *Arrows*, Areas of dark perinuclear staining due to SA -gal activity. (Muller, 2009)

histone modifications found in euchromatin and are not sites of active transcription. Their appearance is accompanied by an increase in HP1 incorporation into senescent chromatin and an enhanced resistance of senescent DNA to nuclease digestion. SAHF formation requires an intact Retinoblastoma (Rb) pathway and they contribute to cellular senescence by controlling the stability of the arrest. Rb acts directly on E2F target promoters to nucleate regions of heterochromatin leading to the silencing of E2F target genes. The decision for a cell to enter senescence is determined by a histone methyltransferase (HMT) that acts with Rb and HP1 proteins to alter chromatin structure and silence E2F target genes. The failure to silence
E2F target genes reduce the chances that a damaged cell will become senescent and/or makes the senescence state more difficult to sustain [14].

Unfortunately no marker or hallmark of senescence identified thus far is entirely specific to the senescent state. Further, not all senescent cells express all possible senescence markers. Nonetheless, senescent cells display several phenotypes, which, in aggregate, define the senescent state [15].

1.2.1 Apoptosis and Senescence

Senescent cells also display a feature of altered responsiveness to apoptotic stimuli, a feature which can be cell type and stimuli specific. For example, senescent WI-38 fibroblasts are non responsive to serum removal and display increased levels of the antiapoptotic Bcl2 protein and the proapoptotic caspase, caspase 3 is downregulated [16]. Ceramide can induce apoptosis in both young and senescent fibroblasts and endothelial cells (ECs), but senescent fibroblasts are more resistant to apoptosis induction compared to young fibroblasts and ECs [17].

Within the process of senescence development a small subset of normal human fibroblasts undergo apoptosis. The activation of caspases in H_2O_2 induced and spontaneously senescent fibroblast indicates that the apoptosis pathway is activated during senescence of fibroblasts. Thus

both the death receptor and the mitochondrial pathway are involved during senescent fibroblast development [18].

In the case of EC there is an increase in apoptosis when the cells become senescent [17]. When EC undergo a cell cycle arrest and become senescent there is a subpopulation of senescent cells that become apoptotic as measured by caspase 3. Also when premature senescence is induced by oxidative stress, a certain population of treated cells do not respond and continue to proliferate. The proportion of unresponsive cells depends on the experimental conditions. If the subpopulation is significant then over time the senescent cells will be diluted by the proliferating population [19].

The diverse finding indicates that not all cell types respond in the same way when they become senescent. The ability of the senescent cell to become apoptotic seems to depend on the cell type, signaling pathways involved and the expression levels of the apoptotic machinery. The relationship between senescence and apoptosis is still at an early stage and needs further work to clarify what is really happening when the cell becomes senescent.

1.3 Types of Senescence

1.3.1 Replicative Senescence

The process of DNA synthesis is made up of two essential steps: i) DNA polymerases synthesising a new complementary polynucleotide strand in the 5' to 3' direction and ii) DNA polymerases initiating DNA synthesis through an RNA primer which is subsequently removed. This results in the loss of sequences at the 5' end of linear molecules with each round of cell division, the 'end-replication problem'. Telomeres are sequences - $(TTAGGG)_n$ - that cap the ends of linear chromosomes and maintain the stability of the genome by preventing DNA ends

from degradation and recombination [20, 21]. Under normal conditions, DNA base pairs are lost from the telomeric ends of each chromosome with every round of cell division [22]. For each population doubling, telomeres lose approximately 100 base pairs. The ribonucleoprotein telomerase (which is upregulated in cancer cells), is able to compensate for the loss of terminal sequences encountered during replication through the addition of newly synthesised telomeric repeats to the 3' end of chromosomal DNA. However in primary human somatic cells the levels of telomerase are low to non-detectable and therefore in these cells there is a shortening of their chromosomes at each round of cell division. Thus, telomeres eventually reach a critical minimum length and cell division is inhibited through a DNA damage response (DDR), to prevent the chromosomes from becoming dysfunctional [23]. These cells are said to have undergone replicative senescence.

The formation of RS has been found to follow a linear sequence of events which involve the transcriptional activator and tumour suppressor protein, p53, the cyclin dependent kinase inhibitor, p21 and the cell cycle regulator, retinoblastoma protein. The recognition of DNA damage resulting from telomere shortening leads to the activation of p53 and halts the cell in the G1 phase of the cell cycle preventing abnormal DNA being replicated in S phase. This response limits the ability of damaged cells to pass on their altered DNA or to develop neoplastic potential [24].

1.3.2 Stress-Induced Premature Senescence (SIPS).

Although RS has been studied extensively, SIPS has only been described relatively recently[25]. In SIPS, senescence is induced in cells prematurely (before chromosomal dysfunction can trigger senescence) by various cellular stresses. These include suboptimal culture conditions, activated oncogenes, oxidative damage and several chemotherapeutic drugs [6, 26-29] (Figure 1.2). Some of these same extrinsic stimuli can also induce excessive proliferation of cells which ultimately

results in RS [29]. The "decision" to undergo proliferation or SIPS is unknown at present but appears to depend on the cell type and the strength and duration of the stimulant [30].

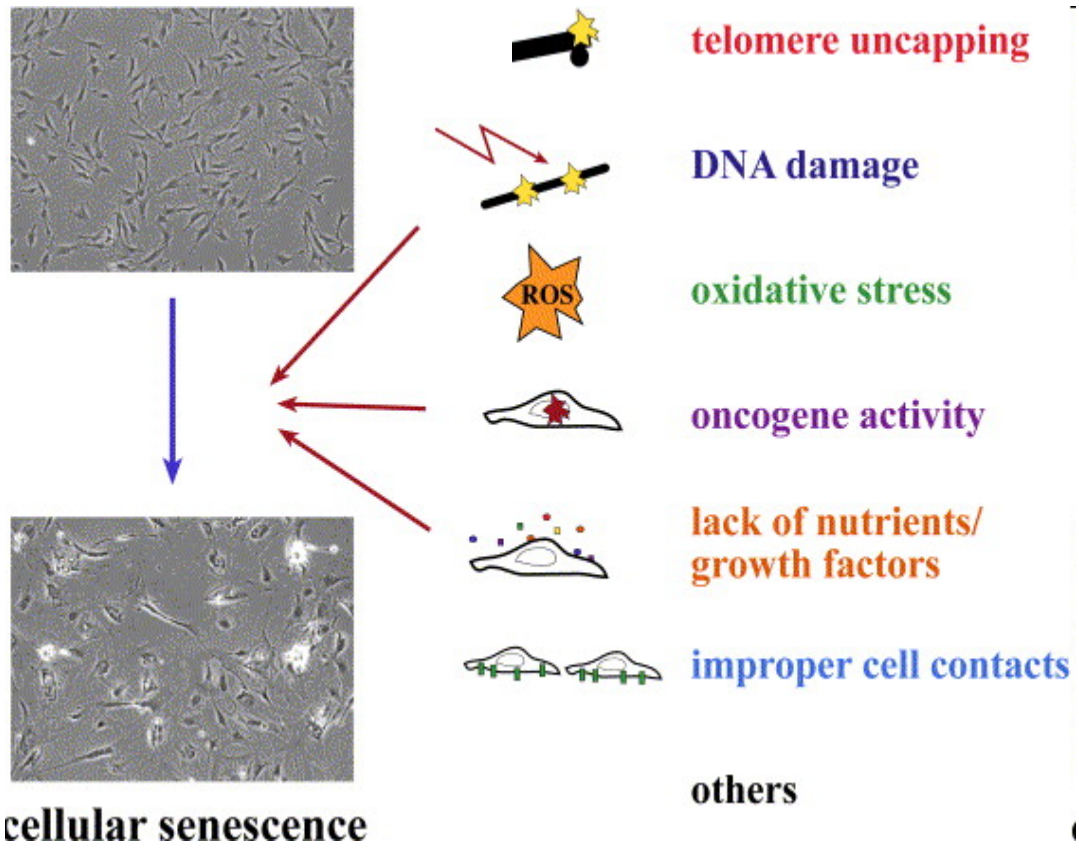

Figure 1.2. The signals activating SIPS. Multiple types of stress can induce cells to undergo stress induced senescence. The combined levels of stress determine how rapidly the entry into senescence will occur (Ben-Porath, 2005).

1.4 Senescence signaling pathways

The p53 and $p16^{INK4a}$ (p16) tumour suppressor networks are essential for initiation of senescence [31]. Although it was originally believed that RS induced a p53 response whereas SIPS was p16 dependent, it is now clear that a senescent signal can activate multiple inhibitory pathways that may vary depending on the stimulus inducing the response and the signaling components present in the cell.

1.4.1 The CDKN2A locus

The CDKN2A locus, located on chromosome 9p21 in humans and chromosome 4 in mice, is highly conserved and encodes two critical tumour suppressor proteins and important induces of cellular senescence: $p16^{INK4a}$ and $p14^{ARF}$ (humans) or $p19^{ARF}$ (mice). The $p16^{Ink4a}$ gene is encoded by the α transcript containing exons 1α, 2 and 3 whilst $p14^{Arf}$ is encoded by the β transcript comprised of exons 1 β, 2 and 3. Although they share exons 2 and 3 they are unique as they are read in different open-reading frames [32].

The p16 protein is normally expressed at low or undetectable constitutive levels in normal cells. Expression of p16 however, is significantly up-regulated during cellular senescence and functions as a negative regulator of cell proliferation. The p16 protein is a cyclin dependent kinase inhibitor (CDKI) which, through its binding to cyclin dependent kinase 4 (CDK4) and CDK6 is able to induce a conformational change that disrupts binding with D-type cyclins, antagonising cyclin binding and activation of the CDK [33]. Failure to activate CDK4/6 ultimately results in failure to phosphorylate the Rb protein. Rb in its active hypo-phosphorylated form inhibits the expression of genes regulated by the E2F transcriptions factor halting cells in the G1 phase of the cell cycle [34] (Figure 1.3). The E2F family of cell cycle transcription factors facilitates the transcription of genes necessary for G1/S phase transition. pRb binds the transcription factor

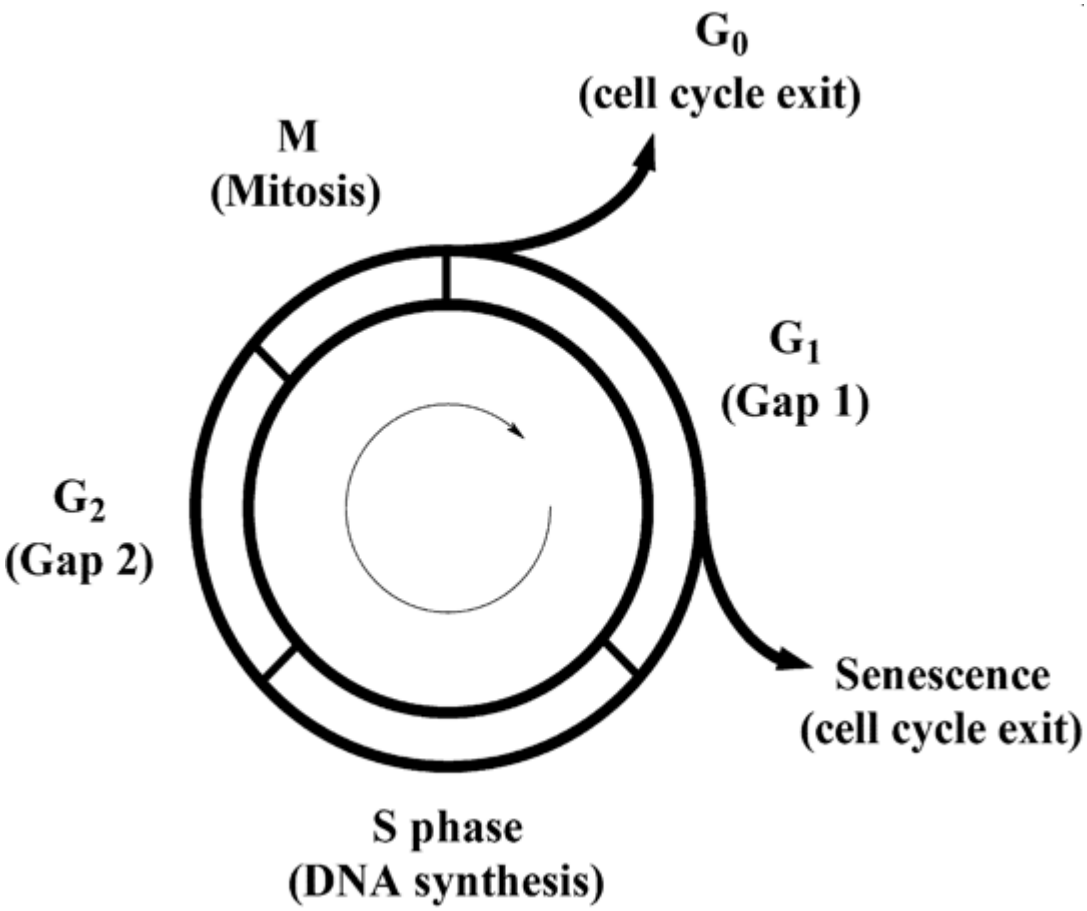

Figure 1.3 The cell cycle. The cell cycle represents an ordered progression of events that result in cell replication with the production of two offspring cells. On entering the cycle, cells progress through phases G1 (Gap1), S (synthesis), G2 (Gap2), and M (mitosis) with check-points at the G1/S and G2/M interfaces to ensure that genomic integrity is maintained. DNA replication occurs during the synthesis (S) stage. Mitosis encompasses chromosomal separation and cytokinesis. After mitosis, cells reenter G0 and leave the cell cycle. Failure to pass the G1/S check-point results in exit from the cycle and the onset of cellular senescence or, in some cases, apoptosis. (Muller, 2009)

E2F, inhibiting it from facilitating gene transcription, and consequently repressing G1/S transition. Inactivation of the Rb protein is therefore essential for the progression of cells from the G1 phase to the S phase, where DNA synthesis takes place. Failure to phosphorylate the Rb protein results in a halt in the cell cycle and cells are induced to stop dividing [34].

1.4.2 The p53 pathway

The p53/p21 ^{Cip1} pathway (Figure 1.4), also known as the DNA damage pathway, is activated in response to critical telomere length [35, 36], DNA damage and in response to cellular stressors, such as oncogene activation [31, 37] and oxidative stress [38].

DNA damage is sensed by a host of factors which leads to the recruitment of phosphatidyl-inositol-3-OH kinase-like kinase (PIKK) ATM (ataxia telangicstasia mutated). This immediately phosphorylates the histone variant H2AX, into its modified form, γH2AX [10]. For this reason, γH2AX has become widely used as a marker for immediate detection of DNA double stranded breaks [39]. γH2AX recruits downstream mediators such as Checkpoint kinase 1 and 2 (Chk1 and Chk2) to the site of damage. At this point, the signal is transduced to effector proteins including tumour suppressor and transcription factor p53 [10]. ATM phosphorylates and thus activates p53, leading to its stabalisation [37]. ATM increases p53 activation by two other means - it phosphorylates the transducing kinase Chk2 which phosphorylates p53 [40] and phosphorylates/deactivates ubiquitin ligase human double minute (HDM2), a negative regulator of p53 [35]. Evidence suggests that Chk2 phosphorylation does not lead to direct activation of p53, but rather, sensitizes it to acetylation by p300 which is ultimately responsible for its activation [41].

The importance of these DNA damage signaling components in replicative senescence has been demonstrated through loss of function experiments. Inactivation of ATM alone allowed senescent cells to re-enter the cell cycle [42], while inactivation of Chk2 was shown to increase the lifespan

of cells [43]. If ATM and Chk2 are absent, the related PIKK ATR (AMT-andRad3-related) and transducing kinase Chk1 can perform the same roles but are mainly involved in the responses to dysfunction in DNA replication machinery, as opposed to DNA damage [35, 37].

p53 acts as a transcription factor [44] to induce a number of anti-proliferative cell states including G1 arrest, apoptosis and senescence [35, 37]. How cell fate is decided is not completely understood but is partly determined by cell type, type of stressor and intensity of signal [35]. These cell fates are aimed at preventing the proliferation of damaged cells which may allow accumulation of the mutations necessary for neoplastic transformation. The importance of this role is evidenced by the presence of a mutated or dysfunctional p53 protein in 50% of all human tumours [45, 46].

p53 induces senescence by increasing transcription of the cdk inhibitor $p21^{Cip1}$ which silences the G1/S –promoting cyclinE/Cdk2 [47]and cyclinE/Cdk4 [48]. This prevents the phosphorylation of Rb and subsequent activation of E2F genes, resulting in G1 arrest [37]

DNA damage-induced senescence strongly depends on p53 and expression of p21 [10]. However, in many cells, DNA damage can also induce p16 at a later stage which provides a second layer of reinforcement for the senescence program [49, 50] (Figure 1.4).

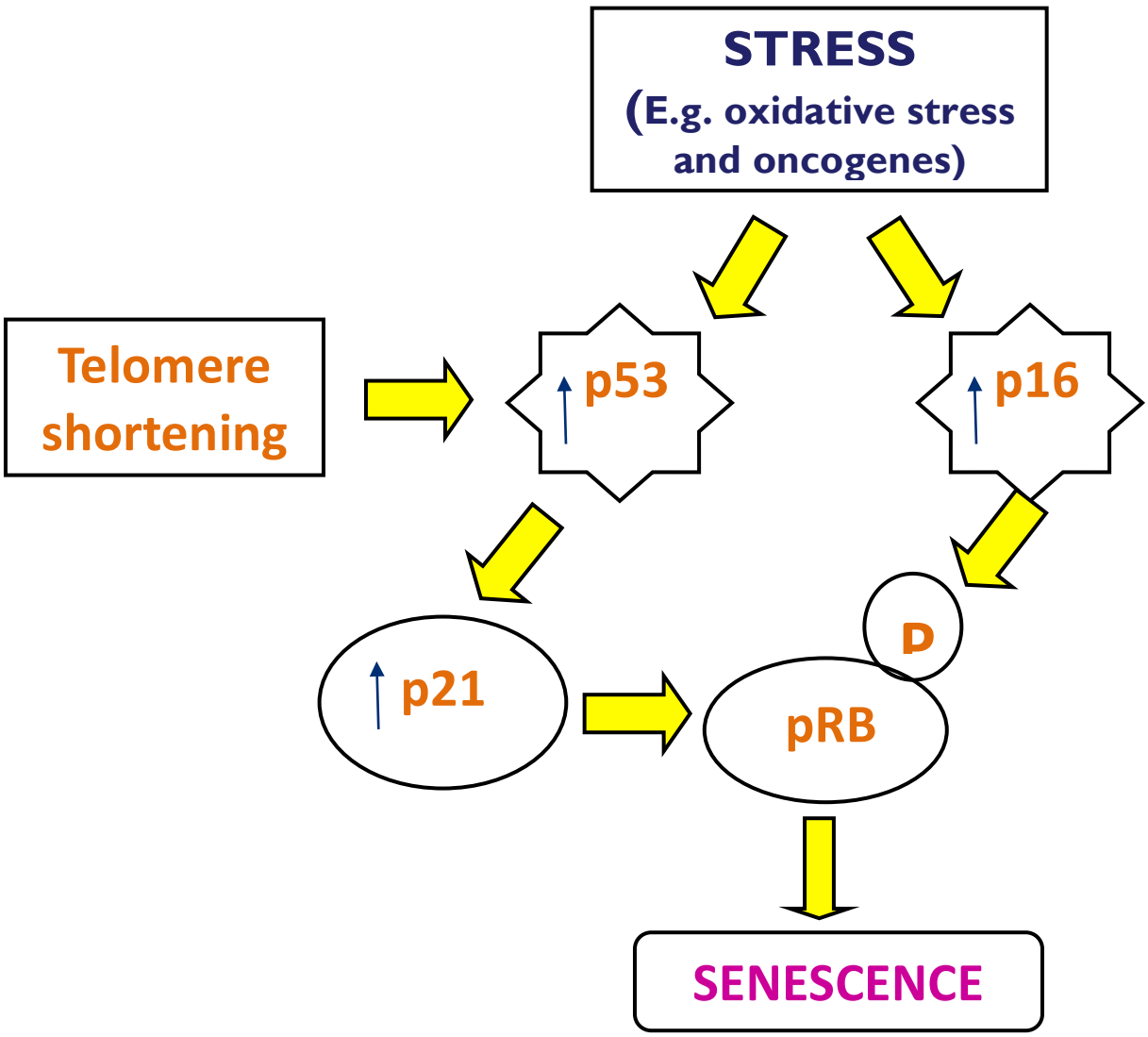

Figure 1.4 Senescence Pathways. The induction of senescence occurs through two pathways. Replicatve senescence induced by telomere shortening, typically induces senescence through the p53/p21 pathway. SIPS iduced senescence can also be induced through the p53/p21 pathway, but can also involve the p16/pRb pathway.

1.5 Mediators of Senescence

1.5.1 Oncogene induced senescence

In response to the activation of mitogenic oncogenes, checkpoint mediated failsafe mechanisms such as apoptosis or cellular senescence may be recruited to terminate a pre-malignant condition before a fully transformed stage can develop[51]. When expressed in primary cells, activated oncogenes can also block cellular proliferation by inducing senescence or apoptosis. [24]. For example, BRAF is a protein kinase which is an immediate downstream effector of Ras. Activating BRAF mutations are present in up to 82% of melanocytic nevi, which are benign skin lesions that rarely progress to melanoma. The nevi are growth arrested and display hallmarks of senescence including β-gal staining and p16 expression. The oncogenic BRAF initiates a senescence response through the MAP kinase pathway, preventing the progression of nevi to malignancy. [52]. The importance of activated BRAF and the induction of senescence are demonstrated by the fact that BRAF mutations are found in high frequency in human cancers and are particularly prevalent in melanoma where they occur at a frequency of 50%-70% [53]. Theimportance of oncogene induced senescence is further demonstrated by the fact that inactivation of the senescence inducer p53 in mice overexpressing the oncogene Ras leads to the development of invasive T cell lymphomas. Mice overexpressing Ras but having wild type p53, develop a delayed non-lymphoid neoplasia. These studies show the importance of senescence mediated through p53 to prevent the development of a malignant tumour [3].

1.5.1.1 Mechanisms of oncogene induced senescence

Oncogene induced senescence is thought to result from DNA damage caused in 2 ways. The first suggests that the DNA damage is caused by an oncogene driven accumulation of reactive oxygen species (ROS) [28]. The other model suggests the DDR is triggered by excessive replication caused by a sustained oncogenic signal which eventually leads to RS [26].

1.5.1.2 Ras

Normal cells in culture will undergo senescence in response to the overexpression of the Ras oncogene or its downstream effectors such as RAF activated MAP kinase [29]. The activation of the MEK-ERK pathway by oncogenic Ras leads to the activation of another MAPK, P38 and the activated p38 then induces the accumulation of growth inhibitors and premature senescence. The activation of p38 is sufficient to induce the increases in protein levels of p16 and p53 and induce the senescence pathways. The increase in protein levels is a result of p38 stabilising p16 and p53 mRNA [54]. Sun et al has also found that PRAK, a kinase downstream of Ras and p38 is essential for oncogenic Ras induced senescence of both murine embryonic fibroblasts (MEFs) and human diploid fibroblast (HDFs) in vitro. PRAK contributed to the senescence induction by directly phosphorylating and activating p53 in both cell lines [55].

Tumour senescence induced by Ras signaling can occur in the absence of p16 or Rb and is not interrupted by the inactivation of Rb, p107 or p130. In contrast the inactivation of p21 disrupts Ras induced tumour senescence [56]. Furthermore in murine cells the functional inactivation of p53 or its direct upstream regulator p19, is sufficient to bypass Ras induced senescence [29]. In human fibroblast the knockdown of p16 is able to prevent Ras induced senescence [57]. Brookes et al also found that human fibroblast cells which are p16 deficient do not form senescent after treatment with oncogenic Ras [58]. These results indicate that Ras driven senescence involves both the p53/p21 pathway and the p16/Rb pathway, and both pathways are essential for Ras induced senescence in certain cell lines.

Ras-induced senescence also appears to be dose-dependent: low levels of Raf-1 expression induced proliferation in NIH3t3 dells whereas high levels of raf-1 caused cells to senesce [59]. To confirm this further Sarkisian et al went on to demonstrate that the decision of mammary epithelial cells to proliferate, senesce or undergo malignant transformation was dependent on the intensity of Ras signaling [60]. Low levels of Ras activation - similar to those found in non-

transformed mouse tissues expressing endogenous oncogenic KRas2 - stimulate cellular proliferation and mammary epithelial hyperplasias. In contrast, high levels of Ras activation - similar to those found in tumours bearing endogenous KRas2 mutations - induce cellular senescence. Chronic low-level Ras induction results in tumour formation, but only after the spontaneous upregulation of activated Ras and evasion of senescence checkpoints. Thus, high-level, but not low-level, Ras activation activates tumour suppressor pathways and triggers an irreversible senescent growth arrest in vivo.

The activation of endogenous Ras can also induce dramatically different phenotypes in different cell types. In MEFs the loss of the NF1 tumour suppressor results in sustained Ras activation, a hypersensitivity to growth factors and immortalisation. In normal diploid fibroblasts loss of NF1 results in a transient activation of Ras and Ras effectors, followed by dramatic suppression of these signals to lower the baseline levels. These cells are not immortalised, they become senescent [30].

1.5.1.3 c-Myc

Overexpression of c-myc causes proliferation and growth but also sensitises the cells to apoptosis and senescence [61]. C-myc is able to induce senescence through two mechanisms. Reduced levels of c-myc protein results in an induction of a telomere independent form of senescence. This is caused by a decrease in the activation of BMI-1 which normally represses p16, resulting in upregulation of p16 and the induction of senescence [62]. C-Myc can also directly act on E boxes within the p16 gene leading to the upregulation of p16 expression and senescence development [61].

1.5.1.4 Akt

In mammalian cells, activation of Akt has been reported to induce proliferation and survival, thereby promoting tumourigenesis. In primary culture human endothelial cells the constitutive activation of Akt promotes a senescence-like growth arrest via a p53/p21 pathway. The inhibition of the forkhead transcription factor FOXO3a by Akt is essential for the growth arrest to occur. FOXO3a is able to induce the senescence response by regulating the ROS levels [63].

1.5.2 Oxidative stress

There is strong evidence that acute or chronic exposure to sublethal doses of oxidative stress can induce both RS and SIPS in a variety of cell types.

1.5.2.1 SIPS

From an experimental point of view, oxidative stress is the most common inducer of SIPS. Reactive oxygen species (ROS), such as superoxide anions (O_2^-) and hydrogen peroxide (H_2O_2) are toxic by-products of aerobic metabolism capable of damaging DNA. A sustained increase in ROS can activate a premature senescence program, through the up-regulation of p53 and p16 [27] [64] [65].

In vitro H_2O_2 is a well known trigger of senescence and has been shown to act in a variety of cells including fibroblasts [66] and ECs [67]. However the pathways responsible can be different and may depend on the cell types. For example, treatment of human diploid fibroblasts with sublethal doses of H_2O_2 caused cells to senesce prematurely as observed by the arrest in G1 stage of the cell cycle through the sustained up-regulation of p21 [27]. Iwasa et al also found that in WI-38 cells treated with low dose H_2O_2 a senescent phenotype is formed and this is induced by p38 [68]. Zhan et al [69] found that oxidative stress induced senescence in ECs occurs through the activation of a DDR which leads to an ATM/Akt/p53/p21 dependent signaling pathway.

V12Ras expression induces an increased intracellular level of ROS. ROS can induce DNA damage resulting from oxidative modifications to DNA and then subsequent up regulation of p53 and p21 and this may eventually lead to senescence [28]. The overexpression of p53 or p21 has also been associated with an increase in ROS and the induction of SIPS [70].

1.5.2.2 Replicative senescence

Oxidative stress does not always induce SIPS. In normal EC mild chronic oxidative stress induced by interference with the glutathione-dependent anti-oxidant defenses accelerates telomere erosion and the onset of RS. In human EC the glutathione redox cycle has been shown to play a predominant role in the maintenance of redox homeostasis. By changing this system the cells are placed under physiologically relevant oxidative stress [71]. The increased telomere erosion and induction of replicative senescence is caused by the inability of the cells to repair telomere damage induced through oxidative stress, compared to elsewhere on the chromosome [72].

1.6 Physiological Role of Senescence

1.6.1 Senescence in Cancer

The observation of senescent cells in tumours has been found in both mouse models and in humans [5, 6]. Apoptosis and senescence are cellular fail safe programs that protect against excessive mitogenic signals from activated oncogenes. For a tumour to become malignant, apoptosis and senescence responses need to be circumvented [73]. This theory is supported by the discovery of senescent cells in the pre malignant stages of tumorigenesis, but the absence of senescent cells in malignant tumours. The original identification of senescent tumour cells was obtained from lung adenomas, pancreatic intraductal neoplasias, PIN lesions and melanocytic nevi. By contrast senescence was absent in their corresponding malignant stages, which are lung adenocarcinomas, pancreatic ductal adenocarcinomas, prostate adenocarcinomas and melanomas

[4-6, 74]. Senescence was originally considered a cultured cell artifact. However the observation of senescent cells in premalignant tumours and the absence of senescence in malignant tumours exposed the possibility that senescence maybe a barrier to transformation. There have been a large number of reports confirming this possibility [51] (Figure 1.5).

1.6.1.1 Senescence acts as a tumour suppressor

It is believed senescence can serve as a tumour suppressor in two ways. First, since tumour growth depends on cell proliferation, senescence associated proliferation arrest would block tumour growth. Secondly the proliferation arrest should suppress the acquisition of additional oncogenic events during DNA replication and mitosis [75].

The data to date supports the concept that senescence in human preneoplastic lesions is a result of oncogene induced DNA replication stress and together with apoptosis provides a barrier to malignant progression [26]. Human naevi are benign tumours of melanocytes that contain oncogenic mutations in BRAF, a protein kinase and downstream effector of Ras. The naevi typically remain in a growth arrested state and rarely progress into a malignant melanoma. Research has shown that the premalignant naevi *in vivo* and *in vitro* contain classical hallmarks of senescent cells including an increase in p16 expression and positive SA-β-gal activity [6]. A role for senescence in the prevention of melanoma development has been confirmed by Ha et al [76] who found a genetic deficiency in Arf , which is a positive regulator of p53, facilitates a rapid development of melanoma in a genetically engineered mouse model. They found that the senescence control in melanocytes is strongly regulated by Arf and not p53 and Arf helps restrict melanoma progression by executing the oncogene-induced senescence program in benign nevi

Similar results have also been found with p53 studies in prostate cancer. The Pten and p53 tumour suppressors are among the most commonly inactivated or mutated genes in human cancer [77, 78]. In the prostrate, the inactivation of p53 fails to produce a tumour phenotype, while the

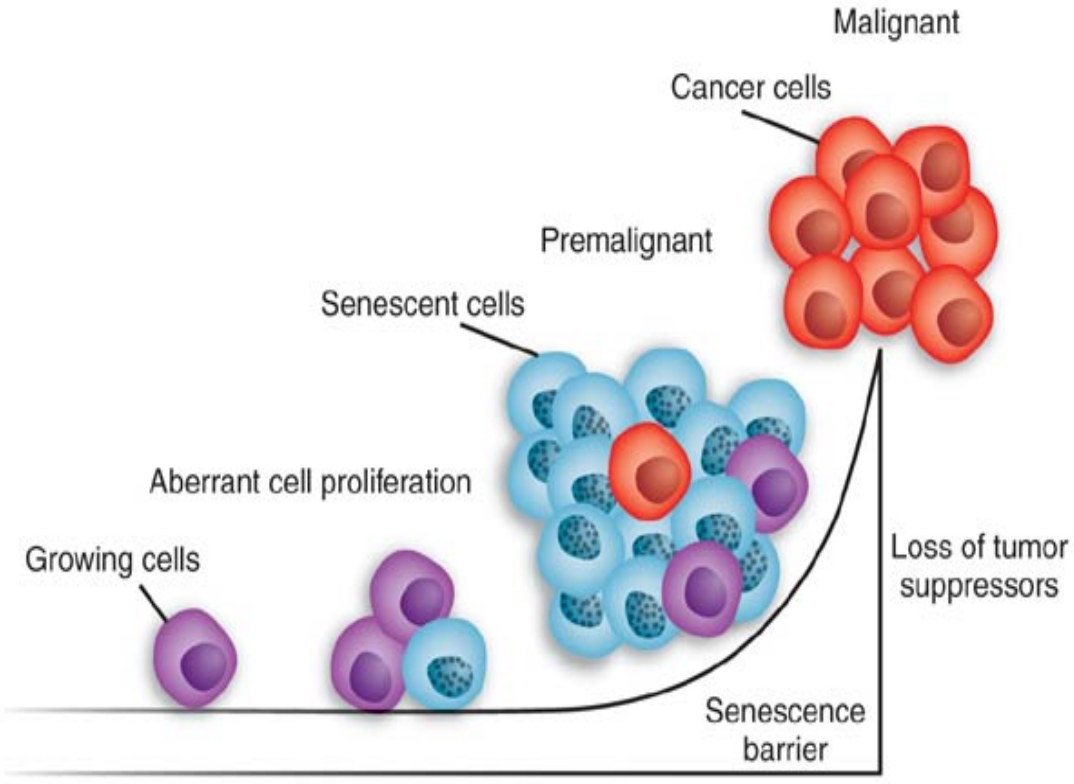

Figure 1.5 Senescence prevents tumour growth. Abnormal activation of oncogenic Ras, BRAF, or loss of the PTEN tumor suppressor can promote aberrant cell proliferation (purple cells), which eventually provokes the activation of a cellular senescence program. Senescent cells frequently exhibit SA- -galactosidase activity and heterchromatic foci (blue cells with prominent nuclei). If the program remains intact, the neoplastic growth may remain benign for many years. However, mutations that disable cellular senescence (such disruption of p53, p16INK4a, orange cells) cooperate with the initiating lesions to promote tumor progression and, in some instances, contribute to drug resistance. (Narita 2005).

complete Pten inactivation in the prostrate causes a non lethal invasive prostrate cancer. The combined inactivation of Pten and p53 results in an invasive prostrate cancer. During the Pten inactivation, growth is arrested through a p53-dependent cellular senescence pathway both in vitro and in vivo, which can be fully rescued by the loss of transformation protein 53(Trp53), which encodes for the tumour protein p53. Therefore cellular senescence induced by p53 is able to prevent tumorigenesis in animals with a Pten mutation [4]. Similar results have also been found in the development of non lymphoid neoplasia into invasive T cell lymphomas. Proliferation of primary lymphocytes is stopped by senescent induced growth arrest in response to oncogenic Ras. This is able to halt lymphomagenesis at the initial step [3].

Senescence caused by shortened telomeres also can prevent tumour growth. Short telomeres impair tumour formation by inducing apoptosis, but if the apoptosis is blocked the shortened telomeres are still able to suppress tumour development through the induction of senescence [79]. Cosme-Blanco et al found the same response in vivo where telomere dysfunction prevented spontaneous tumourigenesis by inducing p53 and p21. These changes were accompanied by the senescence marker SA β-gal [80]. These results indicate that telomere shortening can prevent the development of a malignant tumour by the induction of a p53 dependent senescence response.

Together these results support the idea that the induction of senescence during tumour development is able to halt the tumour in a pre malignant stage and prevent the formation of a malignant tumour.

1.6.1.2 Senescence contributes to tumour regression.

p53 is an important tumour suppressor which acts to restrict proliferation in response to DNA damage or deregulation of mitogenic oncogenes, by leading to the induction of various cell cycle

checkpoints, apoptosis or cellular senescence [81, 82]. Consequently, p53 mutations increase cell proliferation and survival, and in some settings promote genomic instability and resistance to certain chemotherapies [7]. Using RNAi it is possible to conditionally regulate endogenous p53 expression in a mosaic model of liver carcinoma. Brief reactivation of endogenous p53 in p53 deficient tumours can produce complete tumour regressions. The primary response to p53 was not apoptosis, but instead involved the induction of cellular senescence, which was associated with differentiation and the upregulation of inflammatory cytokines. The upregulation of inflammatory cytokines produced an innate immune response that targeted the tumour cells and contributed to tumour clearance [83]. Similar results by Ventura et al [84] found that restoring endogenous p53 expression leads to regression of lymphomas and sarcomas in mice without affecting normal tissues. The mechanism responsible for tumour regression is dependent on the tumour type, with the main consequence of p53 restoration being apoptosis in lymphomas and suppression of cell growth with features of cellular senescence in sarcomas.

1.6.1.3 Senescence and Anti Cancer Drugs

Cyclophosphamide (CTX) has been successfully used to treat many human malignancies [85]. The anti-tumour activity of CTX depends on its ability to induce both apoptosis and senescence. Tumours lacking both programs rapidly progress to a lethal stage [86]. CTX induced senescence was accompanied by increases in the expression of p53, p16, PML and SA-β-gal activity. Knockdown of either the p53 or p16 pathway prevented senescence formation and allowed tumours to progress to a terminal stage. Senescence was therefore able to contribute to the treatment outcome, especially when apoptosis was not possible. In fact drug induced senescence was most prominent in the presence of an apoptotic block. This suggests that senescence can be a back up to apoptosis [86]. Topoisomerase inhibitors are commonly used anticancer drugs, and

like most cytotoxics are used to induce DNA damage in tumour cells, activating p53 and leading to cell cycle arrest or apoptosis [87]. Te Poele et al showed that DNA damage induced by clinically relevant concentrations of topoisomerase inhibitors is able to induce irreversible growth arrest involving p53, p21, and $p16^{I}$. These cells had the morphological and biochemical characteristics of cellular senescence. The onset of the senescence program was coincident with increased levels of p53 and p21, whereas p16 levels remained unchanged during treatment. When cells were recultured in drug-free medium, the p53 and p21 levels decreased to normal. However, p16 levels increased soon after drug withdrawal, and cells remained senescent. These data suggest that p53 and p21 play a central role in the onset of senescence, whereas p16 may be involved in maintaining senescence [88].

1.6.2 Senescence and Liver fibrosis

The senescence of activated hepatic stellate cells (HSCs) limits the accumulation of fibrotic tissue following chronic liver damage and facilitates the resolution of fibrosis following the withdrawal of the damaging agent. This is possible because the senescent activated stellate cells exhibit gene expression profiles consistent with cell cycle exit, reduced secretion of extracellular matrix components, enhanced secretion of extracellular matrix degradation enzymes and enhanced immune surveillance. The natural killer cells which are recruited into the area by the cytokines produced by the senescent cells themselves, preferentially kill the senescent activated stellate cells in vitro and in vivo. The increased expression of metalloproteinases (MMPs) also leads to the degradation of the extracellular matrix which is contributing to the development of the fibrotic scar [8].

1.7 Senescence associated secretory phenotype

Cellular senescence is accompanied by an increase in the secreted levels of factors involved in intercellular signaling. This phenotype has been termed the senescence associated secretory phenotype, or SASP [89]. The cells which have been shown to senesce and secrete the biologically active molecules are liver stellate cells [8], endothelial cells [90, 91], and epithelial cells [92]. The senescence associated changes in gene expression are specific and conserved within individual cell types [93]. The SASP includes several families of soluble and insoluble factors. The factors affect surrounding cells by activating cell surface receptors and initiate signal transduction pathways that can lead to multiple pathologies. The SASP factors can be divided into a number of major categories including soluble signaling factors (interleukins, chemokines and growth factors, secreted proteases), and secreted insoluble components. [94].

1.7.1 Soluble factors

The factors released from senescent cells are capable of regulating the phenotype of surrounding cells. In addition some factors can act in an autocrine manner to initiate the senescent phenotype. Two of these described to have such a role are interleukin (IL)-6 and insulin growth factor binding protein 7 (IGFBP7).

IL-6 is a pro inflammatory cytokine and is associated with DNA damage and oncogenic stress induced senescence of mouse and human keratinocytes, melanocytes, monocytes, fibroblasts and epithelial cells [89]. In response to oncogenic stress, both IL6 and IL8 genes are activated by the transcription factor C/EBPβ upon its recruitment to either promoter. C/EBP deletion results in a bypass of oncogene induced senescence which correlated with a loss of expression of both interleukins. Because IL-6 depletion was followed by a decrease in the levels of both C/EBP and IL-8 it suggests that the C/EBP and IL-6 are involved in a positive feedback network regulating oncogene induced senescence [95].

Similarly in primary melanocytes, the BRAF oncogene BRAFV600E results in the synthesis and secretion of IGFBP7, which then acts in an autocrine and paracrine fashion to inhibit BRAF signaling and induce senescence. [52].

Most senescent cells overexpress IL-8 and GROα and GROβ [93]. Fibroblasts undergoing oncogene arrest upregulate the cytokine receptor CXCR2 (IL-8RB) and its ligands and by manipulating their levels it is possible to promote or delay senescence. This suggests the existence of a positive feedback loop involving chemokine signaling via CXCR2 and acts to reinforce senescence [96]. Two of the ligands for CXCR2 are IL-8 and GROα. IL-8 has multiple paracrine and autocrine effects. As a paracrine agent, it controls endothelial cell migration and is a chemoattractant for neutrophils. As an autocrine agent IL-8 promotes the growth of different cancer cell types [97]. GROα is also an autocrine factor which stimulates melanoma cells to proliferate [98]. Cells in which CXCR2 signaling has been compromised are less able to engage senescence in response to oncogenic signaling from Ras or MEK. Expressing CXCR2 increases DNA damage and its depletion diminishes the activation of a DDR. Secreted CXCR2 binding chemokines mainly reinforce senescence in cells that have already upregulated CXCR2 as opposed to spreading senescence to proliferative neighbouring cells [96].

1.7.2 Secreted Proteases

SASP proteases have three major effects which include the shedding of membrane associated proteins resulting in soluble versions of membrane bound receptors, cleavage of signaling molecules and degradation of the extracellular matrix [94].

Senescent cells secrete increased levels of (MMPs). They are upregulated in mouse fibroblasts undergoing replicative or stress induced senescence. Senescent cells have been indentified in fibrotic livers of CCL4 treated mice and they arise from activated stellate cells, a cell type that initially proliferates in response to hepatocyte cell death and is responsible for the extracellular

matrix (ECM) production through the action of MMPs. The altered ECM is a hallmark of the fibrotic scar [8]. The secretion of MMPs also enhances the invasion of epithelial cells. Human fibroblasts which have undergone SIPS as a result of exposure to the DNA-damaging agent bleomycin increase the growth of transplanted cancer cells in immunodeficient mice. It is believed this response is the result of increased MMP expression by the senescent fibroblasts, which leads to an increase in the permeability of adjacent capillaries. This results in increased levels of mitogens, cytokines and other plasma products and causes increased proliferation of cancer cells [99].

1.7.3 SASPs effect on cell behavior

The factors secreted by senescent cells can promote tumour development *in vivo* and malignant phenotypes such as proliferation and invasiveness in cell culture models. These effects have been observed in a number of tissues including breast, skin, prostate and pancreas [93].

1.7.3.1 Cell Proliferation

One of the most pro-tumorigenic effects of SASP is to promote cell proliferation. It has been found that senescent fibroblasts can stimulate the growth of premalignant and malignant mammary epithelial cells [100]. MMP secretion was found to be responsible for tumorigenicity of breast epithelial cell xenografts in mice when secreted by senescent fibroblast. It is believed that the MMPs allow mitogenic and chemotactic signals greater access to the breast cancer cells [99]. Fibroblasts from the human prostate gland that undergo senescence in culture have been shown to create a local tissue environment that favours prostate epithelial cell hyperproliferation, as a result of amphiregulin secretion [101].

1.7.3.2 Cell Motility

Senescent cells secrete factors which can create a gradient to promote cell migration and invasion. In breast cancer the high levels of IL-6 and -8 secreted by senescent fibroblasts are responsible for enhancing the invasiveness of cancer cell lines [102]. In cell culture models it has been found that EC are induced to migrate by vascular endothelial growth factor (VEGF) which can be secreted by senescent fibroblasts [103].

1.7.3.3 Inflammation

Gene expression profiles have demonstrated that senescence is associated with gene expression patterns similar to those observed in an inflammatory response. There is an increased expression of inflammatory associated genes including the chemokines monocyte chemotactic protein-1 (MCP-1) and Groα, cytokines IL-15 and IL-1β and intercellular adhesion molecule-1 (ICAM1). The expression of these molecules was observed in replicative senescent fibroblasts [104] and replicative senescent human hepatic stellate cells [105]. The induction of the inflammatory network is also linked to premature senescence induced by oncogenes. The increased expression of the inflammatory regulators has been observed in primary human fibroblasts induced to undergo senescence by oncogenic Ras [106] and in senescent melanocytes expressing BRAF [95].

Senescent tumour cells can be cleared by an innate immune response triggered by the inflammatory cytokines secreted by the senescent cells [83]. This was possible because the senescent cells caused a progressive infiltration of host leukocytes (neutrophils, macrophages and natural killer cells) into the tumour tissues. It was accompanied by increased production of inflammatory cytokines known to attract these leukocytes, and adhesion molecules including ICAM1 and vascular cell adhesion molecule-1 (VCAM1). On the other hand the inflammatory mediators produced by senescent cells are also known to enhance tumour angiogenesis and

tumour cell proliferation, invasion and metastasis. IL-6 stimulates the proliferation of tumour cells, protects tumour cells from apoptosis and promotes tumour metastasis and angiogenesis by inducing the expression of adhesion molecules and angiogenic factors.[107].

The work so far has shown that senescence can be both beneficial to tumour development by preventing tumours from becoming malignant, but can also enhance tumour progression with the secretion of pro-tumorigenic factors.

The theory that a biological process such as cellular senescence can be both beneficial as a tumour suppressor and deleterious when pro-tumorigenic is consistent with a major evolutionary theory of aging termed antagonistic pleiotrophy. The theory states that natural selection has favoured genes conferring short-term benefits to the organism at the cost of deterioration in later life. This is occurring with senescence initially stopping the development of malignant tumours by stopping uncontrolled proliferation. But in the long term as more senescence develops, the microenvironment created by the senescence begins to become pro-tumorigenic and is therefore a negative influence on the organism. [10].

1.7.4 SASP and the Senescence Pathways

Although senescence induction and the development of SASP occur together, the pathways that regulate them do not completely overlap. For example, $p16^{INK4a}$ expression is sufficient to induce a senescence growth arrest, but does not induce or modify the SASP [93]. Likewise, p53 is required for the growth arrest [10], but not the SASP; in fact, cells lacking functional p53 secrete markedly higher levels of most SASP factors. The SASP is not an acute (rapid, transient) inflammatory response. It does not develop immediately after cells experience a senescence-inducing stimulus but, once established, it persists for long intervals [89]. One regulator of the

SASP is the DNA damage response (DDR), the signalling cascade that senses and ultimately repairs DNA damage. ATM, CHK2, and NBS1 which are involved in the DDR pathway are essential for establishing and maintaining the expression of several SASP proteins, particularly inflammatory cytokines such as IL-6 and IL-8[108]. However, canonical DDR signalling is not sufficient for the SASP: a transient DDR, caused by low-level ionizing radiation, does not induce an SASP[108]. Additionally, the SASP, like some other features of the senescent phenotype (e.g., cell enlargement, SA-βgal activity), takes several days to develop after the damaging event, whereas the canonical DDR is activated immediately after damage. Thus, at least one additional, slower event which cooperates with the DDR, but is independent of rapid-response DDR factors must be required for the SASP [109].

1.8 Senescence and Aging

Human aging is marked by the onset of a wide spectrum of pathologies. Many of these, for example, osteoporosis, Alzheimer's disease, and heart disease, are degenerative, whereas others, like cancer, result from unregulated and excessive cell proliferation. Both situation represent uncontrolled age-associated decline in normal cells and tissue homeostasis. While controlled senescence may have a positive role in cancer, there is evidence that uncontrolled senescence promotes the degenerative and cancerous pathologies of aging [75].

Senescence may impact on aging through two mechanisms. The first is that accumulation of senescent cells in tissues may reach a point that compromises the tissues functionality, and, secondly, senescence may limit the regenerative potential of adult stem cells [110].

1.8.1 Evidence of senescence in aging

Cells with the characteristics of senescence, such as β-gal staining and p16 expression, accumulate with age in multiple tissues from both humans and rodents. These cells are also

present at sites of age related pathologies, including atherosclerotic lesions, skin ulcers and arthritic joints [111]. The senescence observed is often the result of decreased telomeres and indeed, there is an inverse correlation between telomere length and age in a variety of tissues and between telomere length and diseases associated with aging [112]. Indeed, factors that can decrease longevity, such as physiological stress or obesity, decrease telomerase activity and telomere length. There is also an age associated accumulation of DNA damage which is attributed to an age related increase in ROS production and a decline in DNA repair capacity. The increase in DNA damage results in an increase in cellular senescence and leads to compromised tissue homeostasis [113]. The accumulation of senescent cells in animal organs may also contribute to the aging process by depleting the renewal capacity of tissues an/or by altering tissue structure and function through the secretion of MMPs, epithelial growth factors and inflammatory cytokines which could interfere with the tissue microenvironment [24]. Some studies have also shown

1.9 Senescence and the Vascular System

My thesis will concentrate on the impact of senescence in the vascular system. For this reason I have included a specific section on the role which senescence plays in the vascular system.

One process that has been increasingly linked to both aging and vascular pathologies is EC senescence. In EC the changes result in a phenotype that is pro-inflammatory, pro atherosclerotic and pro-thrombotic. EC senescence can also be induced by a number of factors implicated in vascular pathologies, including sustained cell replication and oxidative stress [114]. The importance of senescence in EC has been demonstrated recently by the identification of senescent cells in a range of vascular pathologies. Using β-galactosidase staining evidence of senescent EC

has been found in rabbit carotid arteries after repeated balloon endothelial denudation, an injury model which promotes endothelial and smooth muscle proliferation [115] (Figure 1.6). Research

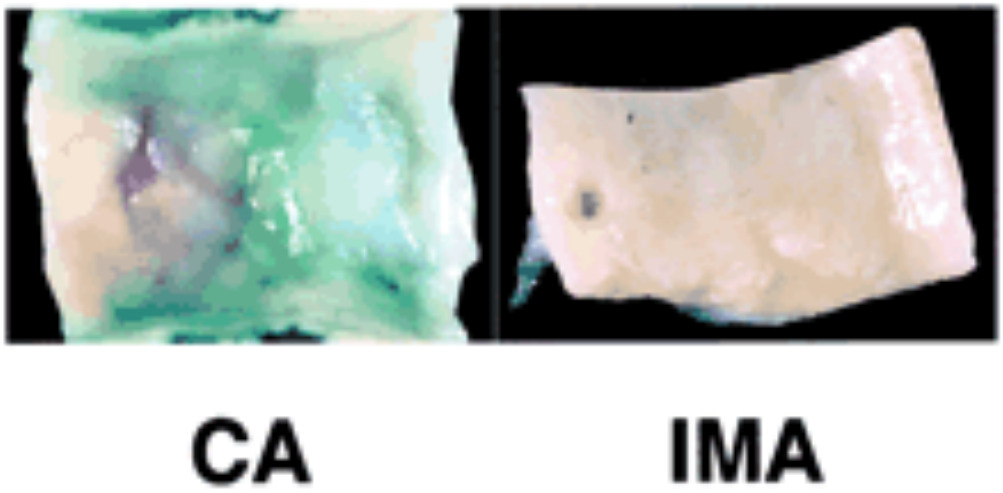

Figure 1.6. SA ß-gal–positive vascular cells in human atheroma. Photographs of the luminal surface of human coronary artery (CA) (left) and internal mammary artery (IMA) (right) stained with ß-gal staining. Senescent-associated ß-gal activity was observed in human coronary arteries but not in internal mammary arteries. Adapted from Minamino et al 2002.

has also shown the presence of EC senescence overlying atherosclerotic plaques of human aorta and coronary arteries [116] and on the aorta of diabetic rats [90].

Studies on cultured EC have shown that the induction of senescence can be initiated by a number of factors which are also involved in vascular function.

1.9.1 Telomere dependent senescence in vascular disease

There is evidence indicating that telomere shortening occurs in human vessels, and this may be related to age associated vascular diseases. Telomere shortening is also more enhanced in coronary artery EC from patients with coronary heart disease compared with cells from healthy subjects. The enhanced telomere shortening leads to increased development of senescence at these sites [112]. The rate of telomere loss was also greater in the intimal cells of iliac arteries, a region of the arterial tree subjected to higher haemodynamic stress, than in the internal mammary arteries. It is likely that the increased rate of cell turnover in the region of disturbed flow accelerates telomere loss.[117] Telomere length can also be reduced by treatment with cardiovascular risk factors. The rate of endothelial senescence is increased after repeated addition of asymmetrical dimethyl l-arginine (ADMA), a novel cardiovascular risk factor. The telomere length in ADMA treated cells is significantly shortened compared with control cells, as a result of the significant reduction in telomerase activity in ADMA treated cells leading to the development of RS [118]. Similar results have been found with homocysteine, which is also a risk factor for atherosclerosis and can induce telomere shortening and accelerates EC senescence [119].

1.9.2 Telomere independent induction of senescence in vascular disease

The duration of exposure to risk factors for cardiovascular disease (CVD), particularly to hypertension, was associated with an early onset of senescence. The senescent EC showed markers of both senescent pathways. The RS pathway was shown by a shortened telomere length

and lower levels of TRF-1 a telomeric repeat binding factor known to protect telomere integrity. There was also increased expression of ATM, the DNA damage signal inducer and of p53 and p21, known inducers of replicative senescence. But the telomeres were not significantly shortened which suggests that EC from patients with a heavy burden of risk factors for CVD enter senescence before telomeres shortened to their threshold length. Since risk factors for CVD are associated with an increase in oxidative stress, oxidative stress induced senescence was studied. Senescence was strongly associated with an increase in lipid peroxidation levels. Lipid peroxidation and the onset of cellular senescence were positively correlated with levels of caveolin-1. Cellular levels of cholesterol increased with aging and this is associated with an upregulation of caveolin-1, which is linked to senescence induction. Cox 2, an inflammatory marker known to increase in the presence of oxidative stress increased in expression after senescence. The increase in these markers confirmed that stress induced senescence is occurring in EC from patients with CVD [120]

1.9.2.1 Angiotensin II contributes to atherosclerosis

Arterial components of the angiotensin II (AngII) signaling cascade increase with aging and contribute to the pathogenesis of atherosclerosis [121]. Ang II has also been reported to induce premature senescence of human VSMCs via the p53/p21 pathway. Ang II also induces the production of pro-inflammatory cytokines. The increase in pro-inflammatory molecules associated with the induction of premature senescence contributes to the development of atherosclerosis [122]. Ang II is also able to activate the Ras signaling pathway. Consistent with the influence of Ang II on senescence, activated Ras has been found to induce vascular cell senescence and is also associated with inflammation. The activation of Ras leads to an increase in the expression of proinflammatory cytokines in EC. The introduction of Ras into balloon injured arteries enhances vascular inflammation and cellular senescence compared with responses seen in

control injured arteries. Thus the Ang II/Ras signaling pathway appears to promote atherogenesis in humans by inducing vascular cell senescence via the p53/p21 pathway [123].

1.9.2.2 Mitochondrial dysfunction

There is a key role for mitochondrial dysfunction in the aging process in many species and the increased ROS production has the ability to lead to EC senescence. Mitochondria by themselves generate ROS during normal respiration. The importance of mitochondrial derived ROS in the induction of EC senescence has been highlighted in a study examining prohibitin-1 (PHB1). PHB1 is a constituent of the inner mitochondrial membrane and important for the maintenance of mitochondrial functional integrity. The knockdown of PHB1 in EC increases mitochondrial ROS generation leading to cellular senescence [124]. Mitochondrial dysfunction also correlates with the extent of atherosclerosis, with vascular complications often seen in young subjects with mitochondrial disease in the absence of risk factors for cardiovascular disease. These results suggest that mitochondrial dysfunction may promote atherogenesis by inducing vascular cell senescence [125].

1.9.2.3 PAI1

Type 1 plasminogen activator inhibitor (PAI 1) is the primary inhibitor of plasminogen activator and is increased in a number of clinical conditions defined as prothrombotic. During EC senescence there is a correlated increase in the mRNA expression of PAI1. The EC expression of PAI1 is characteristic of an activated endothelium and has been detected in atherosclerotic human arteries and in the ECs surrounding invasive tumor cells. The expression of PAI1 is also increased in response to IL-1 a known marker of EC senescence [126].

1.9.2.4 Akt

Akt is activated through phosphorylation. Detection of phosphorylated Akt is seen in human atheroma, but not in normal arteries In addition, Akt activity is increased in endothelial cells undergoing replicative senescence and the inhibition of Akt leads to prolonged cellular lifespan. The knockdown of p53 prevented Akt induced senescence suggesting a role of p53 in the Akt induced senescence pathway. Akt also increases the transcriptional activity of p53, resulting in upregulation of p21 and the induction of senescence [63].

1.9.3 Senescence and cardiovascular disease

Age associated changes of the blood vessels include a decrease in compliance and an increase of inflammation. Aging also decreases the antithrombogenic properties of the endothelium. These changes of vascular structure and function have been suggested to have a role in the increased risk of atherosclerotic cardiovascular disease in the elderly [127].

A number of studies have shown that many of the changes seen in senescent vascular cells are consistent with those seen in human atherosclerosis.

1.9.3.1 Contribution of senescent endothelial cells to plaque development.

Not only are senescent EC present at the site of atherosclerotic plaques, they also have an effect on plaque development. Both nitric oxide production and endothelial nitric oxide synthase activity are reduced in senescent EC. NO regulates vascular tone, dilatation and homeostasis and the loss of NO leads to the progression of atherosclerosis [128]. The production of ROS is increased which leads to a further decrease in the bioavailability of NO [129]. There is also an upregulation of plasminogen activator inhibitor-1, which decreases fibinolytic activity [126]. These changes as a result of endothelial cell senescence formation will contribute to the

impairment of endothelium–dependent vasodilation and an increased occurrence of thrombogenesis in human atherosclerosis [130].

The interaction between monocytes and the vascular endothelial cells is also enhanced after EC senescence. This interaction also promotes atherogenesis [131]. The increased interaction is caused by the upregulation of proinflammatory cytokines in the senescent cells along with the decreased production of NO. The main cytokine found to be upregulated is ICAM-1 [130].

These features are all characteristic of the pro-inflammatory/pro-thrombotic phenotype of endothelial cells found in atherosclerotic human arteries.

These results indicate that senescence is not only found on the surface of atherosclerotic plaques but the senescent cells contribute to the development of atherosclerosis [130, 132].

1.9.3.2 Prevention of atherosclerosis through prevention of senescence.

Premature endothelial cell senescence becomes progressively worse in the aorta, especially in the areas surrounding branching points of the intercostal arteries in young ZDF rats, and is associated with signs of vasculopathy. These signs include impaired vasorelaxation and NO production and defective angiogenic competence. The premature senescence used in these studies was developed using cellular oxidative stress. Ebselen a peroxynitrite scavenger and antioxidant was able to prevent the development of senescent endothelial cells in the ZDF rats. The development of vasculopathy as judged by acetylcholine induced vasorelaxation, NO production, angiogenic competence and the number of circulating microparticles was almost completely prevented when ebselen was administered from 8 to 22 weeks. [133]. Hayashi et al found by maintaining a high expression of NO the development of atherosclerosis was reduced and there was a partial regression of advanced atherosclerosis. These changes are attributed to the decrease in development of endothelial cell senescence when the levels of NO are maintained [134].

1.9.4 Diabetes

Senescent endothelial have also been found to play a role in diabetes. Constitutive activation of Akt in human vascular endothelial cells not only leads to vascular dysfunction, but also to cellular senescence. Akt dependent vascular senescence can also be induced by features of type 2 diabetes, including insulin resistance and hyperinsulinemia [63]. Endothelial senescence occurs in the arteries of type 2 diabetic rats and the expression of the cell cycle proteins p53 and p16 are also induced in the endothelium of these rats. The animals also show evidence of vascular dysfunction such as impaired endothelium dependent relaxation and reduced angiogenesis [133]. Endothelial cells treated with glycated collagen I, an advanced glycation end product (AGEs) which are considered among the leading causes of diabetic complications, develop premature senescence within 3-5 days, as judged by an increase SA-B-gal staining, decreased proliferation and an increase in cell size. This treatment mimics a diabetic situation. During this process there is a dysfunction in the lysosomes. Aging affects many cellular components, but the mitochondria and lysosomes show some of the most significant changes. After ECs are exposed to GC there is a collapse of the lysosomal pH gradient and lysosomal permeabilisation. The change in lysosomal pH is relevant to premature senescence, as the reduced proteolytic activity may contribute to age associated pathologies [135].

With these results taken together type 2 diabetes can be regarded as a premature aging syndrome in which dysregulation of insulin/Akt signaling promotes cellular senescence and leads to various complications.

1.10 Summary

Senescence has made the transition from cell-culture artifact to potential regulator of cancer and ageing and the importance of senescence has been realised. But cellular senescence still remains enigmatic and continues to pose a host of questions. Precisely how do the p53 and p16–pRB pathways establish and, equally importantly, maintain the senescent growth arrest? Both of these tumour-suppressor pathways also cause transient or reversible cell-cycle arrests, so how are their activities modified by senescence-inducing signals? How do cells 'decide' whether to undergo a transient growth arrest, senescence or apoptosis in response to damage or stress signals? The signals that induce p16, both in culture and in vivo, are especially obscure at present.

There is also little is known about the mechanisms that are responsible for the apparently deleterious senescent secretory phenotype. How and why does this phenotype develop? How does the senescence response balance tumour suppression, tissue regeneration and ageing phenotypes? It would be undesirable to reverse the senescence growth arrest — this would allow damaged, stressed or oncogene-expressing cells to proliferate and therefore increase the risk of cancer. But will it be possible to eliminate the deleterious (pro-ageing) aspects of cellular senescence (for example, the senescent secretory phenotype) without reversing the tumour-suppressive growth arrest?

The impact of senescence on vascular function, and in particular the effects on EC function are only just being elucidated. Studies of senescence in EC and the expression in atherosclerotic plaques, at this stage, would imply a detrimental effect. This may make anti-senescence therapy a novel strategy for the treatment of atherosclerosis. However it is not appreciated at this stage the effect of senescence on the initiation of early lesions and the transition of early fatty streaks to advanced full-blown atherosclerotic plaques. In order to move into more detailed analysis and

understanding of senescence in vascular disease, it is critical that more markers are available for senescence in EC.

1.11 Project Aims

My project has been made up in two parts. When I initially began my PhD the aim of the laboratory was to identify novel genes involved in the regulation of angiogenesis and was the basis for the first aim and the results in chapter 3.

Aim 1: Establish the function of the gene repressor element 1 silencing factor (*REST*) in angiogenesis and determine if expression manipulation of *REST* would affect angiogenesis.

The work for this aim was not successful and as my data will show a decision was made to change my projects. I began work on a new gene *SENEX*. The introduction in Chapter 1 is based on the following aims.

Aim 2: To determine and confirm that overexpression of SENEX in endothelial cells is inducing a senescent phenotype.

Aim 3: To identify the signaling pathway through which SENEX is able to induce the senescent phenotype.

Aim 4: To determine whether, SENEX is expressed in atherosclerotic lesions and to determine the effect SENEX induced senescence has on the cellular function.

CHAPTER 2

Materials and Methods

2.1 Materials

2.1.1 Chemical Reagents

Agarose (DNA Grade)	Progen Industries Ltd, QLD, Australia
Ampicillin/Kanamycin/Gentamicin	Roche, Mannheim, Germany
MTS	Promega, WI, USA
TRIZOL	Invitrogen Life Technologies, CA, USA

2.1.2 Cells and Plasmids

Human Umbilical Vein Endothelial Cells (HUVEC)	Isolated from Human umbilical cords, obtained with ethics approval from the Royal Prince Alfred Hospital (Sydney)
pEG	Invitrogen Life Technology, CA, USA
pcDNA3	Invitrogen Life Technology, CA, USA
pAEAT-G	Constructed by Samuel Yu, Vascular Biology Laboratory, Hanson Institute, Adelaide, SA, Australia

2.1.3 Tissue Culture and Adenovirus Production Reagents

Endothelial cell growth Supplement (ECGS)	Becton Dickinson, MA, USA
Fibronectin, Vitronectin, Laminin	Boehringer, Mannheim, Germany
Foetal Calf Serum	Hyclone, In Vitro, Vic, Australia
Heparin	Sigma, MI, USA
Gelatin	Sigma, MI, USA
LIPOFECTAMINE™ 2000	Invitrogen Life Technology, CA, USA
Matrigel®	Becton Dickinson, MA, USA
Tissue Culture Reagents	CSL Ltd, Vic, Australia

2.1.4 Kits

Qiaquick® Gel Extraction Kit	QIAGEN, Vic, Australia
Qiafilter® MIDI and MAXIprep Kit	QIAGEN, Vic, Australia
Qiafiter® PCR Purification Kit	QIAGEN, Vic, Australia

2.1.5 Enzymes

Pfu Ultra	Stratagene, CA, USA
AmpliTaq Gold®	Applied Biosystems, CA, USA
Calf Intestinal Alkaline Phosphotase	Boehringer Mannheim, Mannheim, Germany
T4 DNA Ligase	Boehringer Mannheim, Mannheim, Germany
Bgl *II*, BstX *I*, EcoR *I*, Pac *I*, Stu *I*, Xho *I*	New England Biolabs (NEB), Ontario, Canada OR Promega, WI, USA

LR Clonase Enzyme Mix	Invitrogen Life Technology, CA, USA
Superscript™III	Invitrogen Life Technology, CA, USA

2.1.6 Other

QuantiTech SYBR Green PCR Master Mix	QIAGEN, Vic, Australia

2.2 Cloning Procedures

2.2.1 PCR Amplification

Filtered tips were used to prepare all PCR amplification reactions and thermal cycling was performed on a Perkin Elmer 2400 thermal cycler.

PCR conditions were as follows:

Initial Denaturation	95°C, 1 min	
Denaturation	95°C, 30 sec	
Annealing	63°C, 30 sec	3 cycles
Extension	72°C, 4 min	

Denaturation	95°C, 30 sec
Annealing	68°C, 30 sec

Extension	72°C, 4 min	32 cycles
Final Extension	72°C, 10 min	

In order to ensure high sequence integrity, the high fidelity proof-reading enzyme, *Pfu* Ultra (Applied Biosystems, CA, USA), was used to obtain PCR products. Following their amplification, all PCR reaction were purified via the QIAquick® PCR Purification Kit (see QIAquick® Spin Handbook, 2000, QIAGEN) and the product was viewed via agarose gel electrophoresis.

The PCR temperature (T_p) of all designed primers was between 50 - 72°C, with the PCR reaction performed at 2-5°C below this value [136]. T_p refers to the maximum temperature value at which priming occurs within a given oligonucleotide pair and it is also the temperature at which maximum specificity is achieved [136]. T_p values were used over T_m which relate more specifically to hybridisation reactions. In order to calculate T_p the following formula was used: $T_p = 22 + 1.46$ (2GC+ AT), where GC + AT refers to the number of G and C residues and A and T residues, respectively [136].

2.2.2 Prparation of samples for Sequencing

Sequencing of all clones was performed using the BigDye ™ 3.0 system (Applied Biosystems, CA, USA). The sequencing primers used were T7 and SP6, which flanked the MCS containing the gene of interest. Internal primers, which were designed for specificity for each of the individual cloned cDNAs, enabled sequence determination beyond the range of the T7 and SP6 primers.

The cycling conditions for sequencing reactions were as follows:

Denaturation	96°C, 1 min	
Denaturation	96°C, 10 sec	} 30 cycles
Annealing	50°C, 5 sec	
Extension	60°C, 4 min	

Subsequent to the sequencing reaction, the products were purified using isopropanol. In brief, 80µl of 75% isopropanol (made fresh) was added to the sequencing reaction which was vortexed and incubated at room temperature for 15 min in order to precipitate the sequencing products. After the incubation period, samples were centrifuged (13,000 x g, 20min, RT) and the supernatant was carefully aspirated. The pellet was then washed in 250µl of 75% isopropanol and vortexed briefly. Samples were subsequently centrifuged for a further 5 min and the supernatant was again aspirated. After air-drying, samples were sent for sequencing.

2.2.3 Restriction Endonuclease Digestion

Restriction enzyme digestions were performed under conditions suiting each individual enzyme, according to the manufacturer's instructions. Both New England Biolabs and Promega enzymes were used. Digested DNA fragments were subsequently separated via agarose gel electrophoresis (1-3% agarose) in order to determine the efficiency of digestion.

2.2.4 Extraction of DNA Fragments from Gels

DNA fragments were gel extracted following directions from the QIAquick® Gel Extraction Kit (see QIAquick® Spin Handbook, 2001, QIAGEN).

2.2.5 Ligation of DNA fragments into Plasmid Vectors

After appropriate restriction enzyme digestion, the 5' ends of plasmid vectors with compatible termini were CIAP (Calf Intestine Alkaline Phosphatase) dephosphorylated. The vector and insert

were then ligated together using T4 DNA ligase (NEB, Canada) at a mole ratio of 1:1 and 1:3, with approximately 40-50ng of vector.

2.2.6 Transformation of Plasmid DNA into competent *E.coli* DH5α Cells

Competent *E.coli* DH5α were produced via the calcium and magnesium chloride protocol at stored at -80°C. 1µl of the ligation reaction was added to 50µl of competent *E.coli* and mixed. This mixture was then incubated on ice for 30min and then subsequently placed in a 42°C water bath for 2 min, in ice water for 1 min, then 1ml of SOC medium (2% Tryptone, 0.5% Yeast Extract, 10mM NaCl,10mM $MgSO_4$,10mM $MgCl_2$) was added and this mix was incubated at 37°C for 20-40 min. Transformed cells were then plated onto Luria Bertani (LB) agar which contained the necessary amount of the appropriate antibiotic (Ampicillin at 100µg/ml, Kanamycin at 50µg/ml or Gentamicin at 7µg/ml) and incubated at 37°C overnight.

2.2.7 Small Scale Plasmid DNA Purification

Desired colonies, picked using sterile toothpicks, were inoculated in 2ml of LB Broth containing the appropriate antibiotic and were incubated in a 37°C shaker overnight. An alkaline lysis method was used to purify the plasmid DNA from the 2ml cultures [137]. In brief, 1.5ml of each culture was centrifuged (13,000 x g, 20 sec, RT) and the supernatant was then discarded. The cell pellet was resuspending by vortexing in 100µl of TES (25mM Tris-HCl,pH 8.0, 10mM EDTA, 15% sucrose). To this, 200µl of 0.2M NaOH, 1% SDS solution was added and then mixed by inversion and left for 5 min. Sodium acetate (3M,pH 5.2, 125µl) was then added, mixed by inversion and then left at RT for a further 5 min. The sample was centrifuged for 5 min and the supernatant transferred to a clean tube which contained 30µg/ml RNase (final concentration). This was then incubated at 37°C for 30 min. 700µl of phenol/chloroform/isoamyl alcohol (25:24:1 v:v:v) was then added, vortexed and centrifuged for 5 min and the upper phase was

transferred to a clean tube with care to avoid the interface. Plasmid DNA was then precipitated with 2 volumes of 100% ethanol (80µl), vortexed and centrifuged for 10 min. In order to remove residual salt, one volume of 70% ethanol (400µl) was added. The mixture was then vortexed well and then centrifuged for a further 5 min. The purified plasmid DNA pellet was air dried and resuspended on 20µl TE buffer (10 mM Tris-Cl,pH 7.5, 1 mM EDTA). All centrifugations were performed at room temperature using a microcentrifuge at 13,000 x g.

2.2.8 Large Scale Plasmid DNA Purification

In order to prepare large-scale plasmid DNA, the Qiafilter® MIDI or MAXI preparation procedures (see QIAGEN Plasmid Purification manual 2001) were performed and either the Qiagen 100 or 500 columns were used. Either 100ml or 500ml bacterial cultures were used depending on the amount of plasmid DNA required and this volume was passed over MIDI or MAXIprep columns, respectively. The quantity and purity of DNA was determined via UV spectrophotometry. Purified DNA was also rum on an agarose gel in order to determine the level of RNA contamination and the proportion of plasmid that was nicked, dimerised or supercoiled. Following quantification and gel electrophoresis, samples were digested with appropriate restriction enzymes to confirm the validity of the cloned DNA.

2.3 Generation of Adenoviral Constructs

Adenoviral vectors were generated in accordance with the manufacturer's instructions (http://www.qbiogene.com/products/adenovirus/adeasy.shtml), as described below. A gene of interest is cloned into a shuttle vector (pEG) and is then inserted into a much larger adenoviral vector (pAdEasy-AdTrackG) via homologous recombination in *E.coli.* pAEATG is a vector in which the GFP gene and gene of interest are driven by two strong CMV promoters/enhancers (see section 4.1.2). The vector also contains a kanamycin resistance gene and right and left arms

which are homologous to the adenoviral vector, pAEATG to enable insertion of the pEG cassette via homologous recombination. Firstly, the cDNA versions of the genes of interest were cloned into the pEG shuttle vector, which was followed by linerisation by *Pac I.* Next, *E.coli* which already contained the pAEATG plasmid, were transformed with the recombinant pEG constructs via Gateway recombination using the LR Clonase enzyme mix in accordance with manufacturer's instruction (http://www.invitrogen.com/content.cfm?pageid=10600#lr). The transformation mixture was then resuspended in 1ml of SOC medium and incubated at 37°C for 1h, in order to allow the cells to recover. The mixture was then plated on LB kanamycin (50μg/ml) plates and incubated overnight at 37°C. The colonies were then picked and cultured in 2ml LB broth (Kan 50μg/ml) for a minimum of 24 h. Plasmid DNA was then purified and visualised on a 1% agarose gel, in order to confirm the size of the pAEAT recombinants. *E.coli* DH5α cells were transformed with the pAEATG recombinant plasmids, plated on LB agar (Kan 50μg/ml) plates and incubated overnight at 37°C. The colonies were picked once again and 500ml cultures were prepared and grown overnight at 37°C. The recombinant pAEATG plasmid DNA was purified via the Qiafilter® MIDIprep protocol, using Qiagen 100 columns. Purified plasmid DNA was then quantified and checked for successful recombination via *Pac I* and *Bs tXI* restriction enzyme digestion and visualisation on agarose gels.

2.4 Real Time Quantitative Reverse Transcription PCR (Q-RT-PCR)

RNA was isolated from HUVEC via an RNeasy Mini-Kit (QIAGEN, Australia) according to the manufacturer's instructions. Isolated RNA was then run on a 1% agarose TAE gel to check the integrity of the RNA, which was subsequently quantified by spectrophotometry at A_{260}. In order to remove residual DNA from isolated RNA, DNase treatment (DNA-free kit, Ambion**)** was performed according to manufacturer's instructions.

Reverse transcription was used to generate the first strand cDNA for the Q-RT-PCR. Superscript III (Invirogen) was used.

Q-RT-PCR was carried out on RotorGene 2000 (Corbett Research, Sydney, Australia) using the QuantiTech SYBR Green PCR Master Mix protocol (QIAGEN). The primers used were designed using the Primer3 program (http://frodo.wi.mit.edu/cgi-bin/primer3/primer3_www.cgi) and made specific for the genes of interest.

Q-RT-PCR conditions were as follows:

Denaturation	95°C, 15 min	
Denaturation	95°C, 10 sec	
Annealing	60°C, 20 sec	} 40 cycles
Extension	72°C, 30 sec	
Melt	72°C to 95°C	

All melting curves were checked to ensure an appropriate single PCR product was obtained.

2.5 TISSUE CULTURING TECHNIQUES

2.5.1 Human Umbilical Vein Endothelial Cells

Human umbilical vein endothelial cells (HUVEC), were isolated by collagenase treatment [138]. The cells were cultured in gelatin (Sigma Aldrich) coated 25cm^2 flasks in HUVEC medium (M199 with Earles Salts, 20mM HEPES, 20% foetal calf serum, sodium bicarbonate (Invitrogen), 2mM glutamine, 1% nonessential amino acids (Invitrogen), 1mM sodium pyruvate (invitrogen), , penicillin and gentamicin(Invitrogen). Cells were grown at 37°C, 5% CO_2. HUVEC formed a

confluent monolayer within two to four days and were then harvested by trypsin-EDTA (Invitrogen) treatment and transferred into a gelatin coated 75cm^2 flask. Endothelial growth supplement (50μg/ml, BD, USA)) and 50μg/ml heparin (Sigma, Missouri, USA) were added. Cells were passaged (1:2 split) every three to four days and were used only up to passage four.

2.5.2 Human Embryonic Kidney 293 Cells

Human Embryonic Kidney 293 cells (HEK293 cells) were grown at 37°C, 5% CO_2, in complete DMEM containing 1% 1M HEPES, 10% FCS and antibiotics (1% Penicillin/Streptomycin).

2.5.3 Cell Counting

Cells, which were plated in either a T75 or T25 flask, were harvested three days after plating (unless otherwise indicated) using trypsin and resuspended in the appropriate amount of medium. An equal volume of cell suspension and trypan blue were added to a haemocytometer and the viable cells were counted manually.

2.6 Generation of Adenovirus

2.6.1 Transfection of HEK293 Cells

Human Embryonic Kidney 293 cells were plated, using antibiotic free DMEM, in a fibronectin-coated T25 tissue culture flask at a density of 2x10^6 cells, so as to be approximately 90-95% confluent after 48 h. On the day of the transfection, 4μg (in 20μl) of *PacI* digested pAEATG recombinant DNA was mixed with 500μl of OPTI-MEM ® I Reduced Serum Medium (Invitrogen Life Technologies, CA, USA). 20μl of Lipofectamine™ 2000 (LF2000, Invitrogen Life Technologies, CA, USA) reagent was also mixed with 500μl of OPTI-MEM ®. The two solutions were incubated separately for 5 min at room temperature before they were combined, mixed and incubated at room temperature for a further 15-30 min. Subsequent to this, the entire

volume (1ml) of the LF2000/DNA mixture was added to the T25 flask of HEK293 cells. The transfected cells were incubated at 37°C, 5% CO_2 for 48 h. After this 48 h period, the medium was changed to complete DMEM (with Penicillin/Streptomycin) and returned to the incubator until ready for viral harvesting.

2.6.2 Harvesting Adenovirus

Viral particles were harvested five to seven days after transfection when, upon observation, cells were floating and at least 50% of the cells were fluorescing green (due to the GFP gene located on the pAEATG plasmid) as visualised under the fluorescence microscope. Briefly, the cells were scraped from the bottom of the T25 flask and the cell suspension was transferred to a 10ml tube. After centrifugation (2000 x g, 5 min, RT), the medium was removed and the pellet was resuspended in 1ml of ice cold 1x Phosphate Buffered Saline (PBS) and then vortexed. Freeze-thawing was then performed four times, using liquid nitrogen and a 37°C water bath, in order to ensure complete lysis of the cells. The suspension was then transferred into an eppendorf tube and centrifuged at 8,000 rpm for 10 min, with the centrifuge rotor pre-cooled to 4°C. Next, the 'transfection supernatant' was stored at -20°C in 250µl aliquots until required.

2.6.3 Large Scale production of Adenoviral Particles

The titre and quantity of viral particles was increased by performing a series of three infections. For the first infection (infection #1), a 1/20 volume (250µl) of 'transfection supernatant' was mixed with 5ml of Complete DMEM (with Penicillin/Streptomycin) and then added to a T75 flask of 70-90% confluent 293 cells. The T75 was then incubated at 37°C, 5% CO_2 for a minimum of 2 h and agitated periodically through the day. The volume of medium was kept to a minimum to enable closer contact between cells and viral particle which therefore increases the efficiency of infection. 5ml of complete DMEM (with Penicillin/Streptomycin) was then added

to the infected cells to give a total volume of 10ml. The fluorescence of the cells was checked every day and virus was harvested when a minimum of 50% of cells were floating and fluorescing green. Viral particles were harvested as described above, except that the cell pellet was resuspended in 0.5ml cold 1xPBS.

A 1 in 50 volume (100µl) of infection #1 supernatant was used to infect each of two T75 flasks as described above. The remaining supernatant from infection #1 was stored at -20°C in 100µl aliquots for future use. In the same way, viral particles were harvested when at least 50% of cells were fluorescing green, to produce viral supernatant from infection #2. For the third infection, 100µl of infection #2 supernatant was used to infect each of four T75 flasks as above. The supernatant was then collected and a small amount was used to perform an estimate viral titration in HEK293 cells. This estimate infection (see 2.2.5.4) was performed prior to the final large scale infection of HEK293 cells in T75 flasks at a dilution of 1/2500 for the sense and 1/2200 for the antisense.

2.6.4 Estimate Titre of Adenovirus

At dilutions ranging from 1/25 to 1/3200, the adenoviral supernatant was titrated in HEK293 cells plated in a 24 well plate at 2 x 10^5 cells per well. After 48 h, the GFP production and cytopathic effect (CPE) of the virus was observed and recorded. The dilution chosen for the large scale infection is that which corresponds to the one which resulted in at least 4/5 of cells being detached and 100% green fluorescent.

2.6.5 Purification of Adenovirus via a Double Caesium Chloride Gradient

Recombinant adenovirus was purified via a caesium chloride (CsCl) purification procedure, as described in the Qbiogene Version 1.4 AdEasy™ Vector System manual (http://www.qbiogene.com/products/adenovirus/adeasy.shtml). Alterations to this protocol

included ultracentrifugation being performed in a SW41 Beckman rotor at 32,000 rpm rather than a SW28 rotor at 23,000 rpm as well as the collection of both upper and lower viral bands via bottom puncture rather than side puncture of the tube.

2.6.6 Desalting and Concentration of Adenovirus by Dialysis

The removal of CsCl via dialysis is a crucial step to this procedure, as high concentration of salt may potentially interfere with subsequent infection of cells with virus. The dialysis was performed using a Slide-A-Lyzer ◦ Dialysis Cassettes (Pierce, IL, USA) and occurred according to the manufacturer's procedure.

2.6.7 Tissue Culture Infectious Dose 50 ($TCID_{50}$)

The $TCID_{50}$ method for viral titration of viral particles is based on the development of a cytopathic effect in HEK293 cells via end point dilutions to estimate the titre. The $TCID_{50}$ was performed in accordance with the Qbiogene Version 1.4 AdEasy™ Vector System manual (http://www.qbiogene.com/products/adenovirus/adeasy.shtml). In brief, various dilutions of virus were incubated with HEK293 cells in 96 well plates for ten days after which the presence or absence of a cytopathic effect (CPE) in each well was determined and the $TCID_{50}$ was calculated as per the equation provided in the manual. The calculated values correspond to the number of infectious particles and their ratio with respect to the cells infected with adenovirus, which will be referred to as the multiplicity of infection (MOI).

Also, the total number of viral particles (both infectious and non-infectious) which are present in the viral stock was calculated using an optical density (OD) of 260nm as described in the Qbiogene Version 1.4 AdEasy™ Vector System manual. Comparing the values obtained from this assay with the corresponding $TCID_{50}$ allows a rough estimate of the ratio of infectious to

non-infectious viral particles. The optimal ratio is anything less than 1:50; however, a ratio of approximately 1:100 is satisfactory.

2.6.8 Titration of Recombinant Adenovirus for Infection of HUVEC

Various dilutions of virus were incubated with HUVEC, first in 24 well plates and later in T25 flasks, for a period of 48 h. Cells were then harvested and analysed via FACS for mean GFP production (using a Coulter® Epics® XL2 Analyser). Results from FACS analysis relate to both efficiency of infection as well as the level of GFP expression which is assumed to reflect the specific level of gene expression which is occurring.

2.7 HUVEC Proliferation Assay

2.7.1 MTS

MTS(3-(4,5-dimethylthiazol-2-yl)-5-(3-carboxymethoxyphenyl)-2-(4-sulfophenyl)-2H-tetrazolium, inner salt) is a colourless compound which is converted to a coloured compound by metabolically active cells. This is used as a measure of cell number. The MTS assay (Promega, WI, USA) was performed in accordance with the manufacturer's protocol. Infected HUVEC were plated at 4 x 10^4 cells per well with eight replicates in each of two 96 well plates, coated with gelatin (one plate for 'Day 0' and one for 'Day 3' measurement). Cells were plated in a final volume of 150μl; 20% FCS + ECGS/Heparin. After 2 h incubation at 37°C, 5% CO_2 , to allow for cell attachment, 30μl of MTS was added to each well of the 'Day 0' plate and it was then incubated for a further 2 h at the above conditions. Subsequent to this second incubation period, the 'Day 0' plate was read at 490nm on the ELISA plate reader. From previous work performed by members of the Vascular Biology Laboratory, the above conditions were established. There is a linear relationship between the absorbance reading at 490nm and the number of viable cells in

culture. The 'Day 3' plate was incubated for three days prior to the addition of MTS and the MTS readings were made as above.

2.8 HUVEC Migration Assay

2.8.1 Wounding Assay

The migration assay was performed using a 6 well plate, coated with gelatin. Cells were plated at a density of 8 x 10^5 cells per well in 20% FCS + ECGS/Heparin and grown for at least 24 h post infection and at least 3 h prior to wounding. Cells were wounded using a rubber policeman, washed 3 times and the medium changed. Photographs of cells were taken at various time points over a 24h period so as to observe the rate of migration of cells over the wound until closure of the wound occurred.

2.9 MATRIGEL® TUBE FORMATION ASSAY

The Matrigel® (Becton Dickinson, MA, USA) was thawed on ice overnight. Once thawed, using pre-cooled pipette tips, 100µl of Matrigel® was added per well to a pre-cooled 96 well plate. Care was taken to avoid air bubbles. The plate was then incubated at 37°C for approximately 30min to allow the Matrigel® to gel. Whilst this incubation period was occurring, HUVEC were harvested and counted. 4 x 10^4 cells are plated onto the Matrigel.Photographs are taken 30mins after plating and further photographs are taken every 6 hours for 24 hours. The tubes are compared between treated and untreated cells.

2.10 ATTACHMENT ASSAY

Ninety six well plates were coated in 70µl of gelatin, fibronectin or laminin in quadruplicate and were incubated at 37°C for approximately 30 min and then removed. Infected cells were harvested and collected in serum free medium and counted cells were plated in 2% Bovine Serum

Albumin (BSA) at 4 x 10^4 cells per 96 well. A 1:6 mix of MTS and serum free medium was made and on each plate 120µl of this mix was added to one non-coated well as a blank. 100µl of cells were also plated in duplicate into non-coated wells as plating controls. Cells were incubated at 37°C for either 20 min or 60 min, then each well (excluding plating controls and blank) was washed twice with 1x PBS and then 120µl of the MTS mix was added to each well. 20µl of MTS was also added to the plating control wells at this point. Two hours after the addition of MTS, the plates were read on the ELISA plate reader.

2.11 Senescence staining

Senescence-associated β galactosidase staining was performed at pH 6.0, as previously described *(Dimri et al, 1995; Van der loo, 1998)* and using the Cell signaling Technology Senescence β-galactosidase staining kit. Cells believed to be exhibiting senescence characteristics, were washed once with 1 x PBS and fixed in 1x fixative solution (20% formaldehyde, 2% glutaraldehyde in 1 x PBS) for 15 mins at room temperature. Cells were washed twice with 1 x PBS and incubated at 37oC overnight in a solution containing 400mM citric acid/sodium phosphate 9pH 6.0), 1.5M NaCl, 20mM MgCl2, 500mM potassium ferricyanide, 500mM potassium ferrocyanide and 20mg/ml X-gal (5-bromo-4-chloro-3-indolyl-βD-galactopyranoside powder). Some improvements were made to the protocol which included not using a stock solution of X-Gal but rather making a 20mM solution in N-N-Dimethylformamide (DMF) with each use and the addition of 0.02% Nonidet® P40 Substitute (NP40) and 0.01% sodium deoxycholate to the staining solution. The pH of the staining solution was measured and adjusted with monobasic sodium phosphate NaH_2PO_4, to ensure that it was at a pH of 6.0 required to detect senescent cells. Stained cells were viewed under a microscope. The development of a blue colour is indiciative of SA-β gal positive cells.

2.12 siRNA transfection

HUVEC were transfected with validated Stealth siRNAs (50 nM (Invitrogen)) in parallel with corresponding non-specific Stealth siRNA negative control (50 nM Invitrogen). The cells were transfected using HiPerFect transfection reagent according to the manufacturer's protocol (Qiagen).

2.13 Protein Methodologies

2.13.1 Protein Lysates

Lysates were prepared from HUVEC for use in western blot analysis and caspase-3 assays. Media from each T25 was collected and centrifuged at 4^{o}C, 14000 rpm for 15 min to ensure that any apoptotic cells floating in the media are accounted for. Cells were washed twice with ice cold PBS and 100ul of Lysis buffer (refer to appendix 1) was added to each well. Cells were incubated on ice for 15 min and then removed with a cell scraper. Lysates were then transferred to a 1.5ml eppendorf tube and centrifuged at 4^{o}C,14000 rpm for 15 min. The supernatant was transferred to a new eppendorf tube and protein concentration calculated using the Bradford Assay.

2.13.2 Determining protein concentration: Bradford Assay

Protein standards were made using Bio-Rad Protein Assay Standard II (Bio-Rad, NSW, Australia) in lysis buffer. 5µl of each of these, as well as 5µl of each protein extract was added in duplicate to a 96-well plate. 25µl of Bio-Rad Protein Assay Reagent A/S (1:50) (Bio-Rad) and 200µl of Bio-Rad Protein Assay Reagent B was added to each well. The absorbance was read at 690nm on the Labsystems Multiskan® Multisoft (Labsystems, VIC, Australia) plate reader. To prepare extracts for Western Blotting (Section 2.2.13), each was diluted in appropriate amounts of lysis buffer to achieve equal concentrations. NuPAGE® 4x LDS Sample Buffer (Invitrogen), and 10x Sample Reducing Agent (Invitrogen) were added to diluted samples and heated at 70°C for 10 minutes.

2.13.3 Western blotting

Protein samples were run using the *SureLock*™ Mini-Cell Apparatus (Invitrogen). 25µl of protein samples were loaded onto a NuPAGE® 4-12% Bis-Tris Gel (Invitrogen) and run

according to manufacturer's instructions with either 1x MES running buffer (for small proteins) or 1x MOPs running buffer (refer to appendix 1) made by diluting 20x buffers in TDW. 4µl of 1x SeeBlue Pre-stained Standard (Invitrogen) was loaded as a protein ladder. Transfers were performed using XCell II™ Blot Module™ (Invitrogen) according to manufacturer's instruction. Proteins were transferred onto a polyvinylidene difluoride (PVDF) membrane. Membranes were blocked for one hour with 5% skim milk powder in PBS with 0.1% Tween-20 (PBS-T). After blocking, membranes were put in primary antibody diluted in PBS-T (refer to **appendix 3**) and left overnight on a rotator at 4°C.

Membranes were washed twice with PBS-T over a half an hour period. Appropriate secondary antibody (refer **appendix 3)** were added to membranes for 1 hour at RT with gentle rocking. Membranes were then washed 30 minutes. Protein was detected by the use of Enhanced ChemiLuminescence (ECL) Western Blotting Detection System (GE Healthcare, NSW, Australia) or ECL Plus (Thermo Scientific, Illinois, USA). Images were taken using the Kodak 4000MM Image Station (IS4000, Kodak, Australia). Band intensity was quantified using Image J (National Institute of Mental Health, MD, USA).

2.13.4 Caspase 3 ELISA

20µl of lysates from adjusted samples (so that protein concentration in each sample is equivalent) was added to wells of a white 96 well plate in quadruplicate, with three repeats per lysate. A 1x positive Caspase solution mix was prepared consisting of 1ml Caspase 3 Buffer (refer to appendix 7), 10µl 1M DTT and 5µl caspase-3 substrate The 'negative' mix was prepared as the positive mix, without the addition of the substrate. 100µl of 'positive' and 'negative' mix were added to corresponding wells (2 x 'positive' wells + 2 x 'negative wells). The plate was incubated at room temperature overnight and read on a fluorescence plate reader. Caspase-3 is a protein expressed during apoptosis which enzymatically cleaves DVED-AFC to release a

fluorescent product and thus the level of fluorescence correlated to the level of apoptosis in the cells.

2.14 Telomere length analysis

Genomic DNA was extracted from cells using a DNA extraction kit (Qiagen). 20 μg of DNA was digested with HinfI and RsaI (Boehringer Mannheim). The digested DNA was quantified by nanodrop (Thermo Scientific) and 1.0 μg was electrophoresed through a 0.8% agarose gel in 1x Tris-acetate-EDTA (TAE) buffer at 2 V/cm for 17 h. The gel was dried at 60°C for 2 h, denatured for 30-60 min in 0.5 M NaOH and 1.5 M NaCl and neutralized for 30-60 min in 1 M Tris-HCl, pH 8.0 and 1.5 M NaCl. The gel was then hybridized to a [γ-^{32}P]dATP 5' end-labeled telomeric oligonucleotide probe [γ-^{32}P-$(TTAGGG)_3$]. Hybridization and washing were carried out as described (77). The gel was autoradiographed on Kodak XAR-5 X-ray film for 12-24 h at room temperature.

2.15 Transwell permeability assay

Polycarbonate membrane (3μm) transwells (Corning Incorporated) were coated with 50 μg/ml fibronectin. Three x10^5 passage two HUVEC in complete medium were added to each well and incubated for 24 h after which another 1x10^5 cells were added to each well to produce a confluent monolayer. After 6 h, non-adhered cells were removed and the monolayer was infected with adenovirus (EV or SENEX) at an MOI sufficient to give 100% infection but without toxicity. After 48 h, the medium in both upper and lower wells was replaced with HUVEC medium containing 2% serum. To the upper well, 300 ng of FITC-dextran (Sigma-Aldrich) was added that contained 1.0U/ml thrombin (Sigma-Aldrich) where appropriate. 40 μl of medium was removed from the bottom well of each assay well after 50 minutes and fluorescence was quantified using a Wallac luminescence spectrometer (excitation 485 nm, emission 530 nm).

2.16 Neutrophil and mononuclear cell adhesion assay

Neutrophils and mononuclear cells were prepared from fresh blood from healthy volunteers. Blood was dextran sedimented, cells were separated by Histopaque (Sigma-Aldrich) gradient centrifugation. The buffy coat was collected and purified to obtain mononuclear cells and the neutrophils were purified from the cell pellet with hypotonic lysis of the remaining red cells. HUVECs were plated on fibronectin coated labtek slides (Invitro technologies) at $6x10^4$ for 24 h. Monolayers cultured on the slides were preincubated with TNFα (5 ng/ml) for 5 h before the assay, and then washed. Neutrophils and mononuclear cells (10^6) were added to the HUVECs. After 60 min the wells were washed and photographed and counts of adherent cells were made.

2.17 Dapi Staining

HUVECs were plated on fibronectin coated labtek slides (Invitro Technologies) at $6x10^4$ for 24 h. They were then fixed with 100% methanol and stained with Dapi (1 μg/ml) (Sigma-Aldrich) for 15 mins at 37°C, then washed and mounted.

2.18 Cell Cycle Analysis

Detached cells were washed with phosphate-buffered saline (PBS) and fixed in 70% ethanol at -20°C for 30 min and stained at 37°C for 30 min in 1 ml of PBS containing 20 μg/ml propidium iodide and 20 μg/ml RNase A. Cells were analyzed using a FACS Canto, FACS Diva for data acquisition (BD Biosciences) and FlowJo software (Tree Star) for data analysis.

2.19 Immunostaining

HUVECs were plated on fibronectin coated labtek slides (Invitro technologies) at $6x10^4$ for 24 h. Monolayers cultured on the slides were preincubated with TNFα (5 ng/ml) for 5 h for E-selectin or 24h for VCAM1 before the assay, and then washed. The cells were fixed in 4% paraformaldehyde/PBS for 10 min, and when needed permeabilized by treatment with 0.1% Triton X-100. Primary antibodies were used at 20μg/ml and binding detected by incubation with Alexa 594 fluorophore-coupled secondary antibody (Invitrogen).

2.20 Replicative Senescence

EC were maintained under subconfluent conditions at all times and were passaged every 3–4 days. During passaging, cells were lifted using 0.5% (w/v) trypsin and between $0.6x10^6$ and $1x10^6$ cells were replated onto fresh 75-cm^2 flasks.

2.21 Cell Cycle Array

HUVECs were infected with EV and SENEX containing adenovirus. After 24 and 72 hours RNA was harvested as previously described. RNA was pooled from 3 HUVEC lines and then analysed using the Cell Cycle Array (SuperArray) as per manufacturers instructions.

2.22 FACS Analysis

HUVECs were trypsinised and then washed with HUVEC wash. The cells were spun and re-suspended in 100 μl of FACS fix (see appendix). Twenty μg/ml of primary antibody was added and the cells were incubated at 4°C for 30min. The cells are then spun and washed with 0.5ml of FACS fix. Then spun at 4°C for 5min. The pellet is re-suspended in 100 μl FACS fix. Then add 1

µl of secondary antibody and incubate in the dark at 4°C for 30min. Then spin and wash the pellet with 0.5ml of FACS fix. Spin and resuspend the pellet in 200 µl of FACS fix. Then analysis using the FACS Canto, FACS Diva for data acquisition (BD Biosciences) and FlowJo software (Tree Star) for data analysis.

2.23 Virtual Northern Blot

VN blots were performed using the SMART PCR cDNA synthesis procedure (Clontech). In brief, full-length double-stranded cDNAs were generated from 1 µg of total RNA by the SMART procedure according to the manufacturer's protocol, ensuring optimization of the number of PCR cycles (typically 18–21) to remain within the linear range of amplification. Approximately 1 µg of cDNA from each time point was run on a 1% agarose gel. The cDNA was transferred by capillary transfer to nylon membranes (Hybond-N, Amersham Biosciences) and cross-linked (Stratalinker, Stratagene) to the membrane. For probe generation, cloned cDNA fragments were PCR amplified using T7 and T3 primers, and the products were labeled with [α-^{32}P]dATP using either a MegaPrime Kit (Amersham) or StripEZ Kit (Ambion). Hybridization was performed in ExpressHyb solution (Clontech) for 2 h, and blots were washed in 2x SSC and 0.1% SDS at 25°C (twice) and 0.1x SSC and 0.1% SDS at 60°C for 20 min. Blots were visualized and quantified using a Typhoon 9410 PhosporImager and Imagequant 3.3 software (Molecular Dynamics and Amersham Biosciences). All blots were exposed for the appropriate time to ensure that the signal was within the linear range of the machine for quantification.

2.25 Plasmid Transfection

pcDNA3-*SENEX* constructs were transfected into HUVECs using the Amaxa nucleofector kit according to the manufacturer's protocol (Amaxa Biosystems).

2.25 Statistics

Statistical analyses using a two-tailed Student's *t* test and 2 way ANOVA with Bonferroni posttest were performed using Prism software (version 4; GraphPad Software, Inc.). Data that satisfy confidence levels of $p < 0.05$, 0.01 or 0.001 are noted. Data are presented as means ± SEM.

CHAPTER 3

Functional Analysis of REST

My PhD has been made up in two parts. I initially began my PhD working on the gene that will be covered in the following chapter. I spent a year working on this gene trying to determine its function in angiogenesis. As you will find from my results detailed in chapter 3 the study of the gene was unsuccessful. For this reason I then started research on a new gene which is the major part of my thesis. I have still included this chapter as the methods used were also involved in the development of the research involved in Chapters 4 and 5.

Cancer is the second leading cause of death in the Western world. Despite advances in diagnosis and treatment, the overall survival of patients still remains poor. Tumour cells themselves have been the primary target for anticancer therapy. This has improved patient survival for several types of solid tumours, but treatment related toxicity and the emergence of drug resistant clones, together with consequent disease relapse, have been the major causes of morbidity and mortality. Since tumour growth is dependent on new blood vessel growth, through at least the process of angiogenesis, anti-angiogenic therapies have been proposed to have potential clinical importance. Indeed 80 anti-angiogenic drugs are currently in clinical trials, 12 of which target the key angiogenic factor vascular endothelial growth factor. A convincing regression of tumours has been reported for drugs against this target [139]. However, recent data has shown that targeting VEGF is selective for some tumours, and there are problems with longterm effects. It is apparent that further drug targets must be identified [140].

Thus the approach to understand the process of angiogenesis is still important in future attempts to prevent tumour growth.

In the tumour model of angiogenesis, tumour cells secrete angiogenic factors, which diffuse through the tissues to the host vasculature. At the same time, angiogenic inhibitors are also down-regulated. Tumour cells can also recruit macrophages and mast cells which secrete a number of angiogenic factors. The most important angiogenic promoters known in the literature include (VEGF), fibroblast growth factor (FGF), angiopoietins, Tie receptors, platelet derived growth factors, integrins and cadherins [141]. But the identification of more is essential.

It is vital to further the understanding of the angiogenesis process. One way to achieve this is to identify the genes specifically involved.

To do this an *in vitro* angiogenesis model developed in the Vascular Biology Laboratory of the Hanson Institute was used to obtain and characterise genes potentially involved in angiogenesis. Both *in vitro* and *in vivo* studies have shown that angiogenesis involves several discrete steps. These are the activation, migration, proliferation, differentiation and maturation. It can be assumed that genes important in tube-formation will be regulated in the critical stages of angiogenesis at the mRNA level. The genes that are regulated at the mRNA level may be important in the angiogenic phenotype. But mRNA regulation is only being used as an indicator of a potential involvement in angiogenesis and regulation will need to be verified in future experiments.

3.1. Isolation and Identification of a Gene Novel to Angiogenesis – REST

3.1.1 Screen for Angiogenic Genes.

Prior to commencing my PhD project, the Vascular Biology Laboratory embarked on a project to identify genes involved and crucial to angiogenesis. The approach taken was to utilize a well

characterized *in vitro* model of angiogenesis and to perform an array to screen for regulated genes. The model uses Human Umbilical Vein Endothelial Cell (HUVEC) placed in a 3D collagen gel, stimulated with the PKC activator, phorbol myristate acetate (PMA) and also with an antibody (clone RMAC11) directed against the integrin anti-$\alpha_2\beta_{1\ [142]}$. This antibody promotes tube formation by inhibiting cell attachment to the collagen matrix and promotes cell-cell interactions, including migration vacuole formation and fusion, lumen formation and vessel stabilization but not the proliferative response [143]. The cells reorganize over 24 hours in a process that recapitulates most of the events known to take place in *in vivo* angiogenesis [143]. The capillary tubes generated in this system are a combination of multicellular tubes similar to that seen for large vessels and unicellular similar to post capillary venules [143].

RNA was isolated at various time points (0, 0.5, 3, 6 and 24h) relating to distinct morphological events in the genesis of capillary tubes, being cell migration (0.5hours), vacuole coalescence and fusion (3 hours), lumen formation and apoptosis (6 hours) and capillary tube maturation and survival (24 hours). A suppression subtractive hybridisation approach was used to generate cDNA libraries enriched for genes whose transcripts were either upregulated or downregulated between adjacent time points.

Colonies from the forward (upregulated) subtracted libraries (0–0.5 h, 3,200 colonies; 0.5–3 h, 3,000 colonies; 3–6 h, 2,800 colonies; and 6–24 h, 1,000 colonies) were robotically picked, and glycerols stocks were generated. A total of 10,000 clones were picked. Each clone was then PCR amplified using primers to the T7 and T3 promoters in the vector that flank the cloning site. The PCR products were microarrayed onto glass slides in duplicate along with controls known to be regulated in this angiogenic model [e.g., prostaglandin endoperoxidase synthase 2 (PTGS2), matrix metalloproteinase 10 (MMP10), and connective tissue growth factor (CTGF)] together with genes predicted not to be regulated [thymosin-$ß_4$ (TMSB4X) and heat shock protein 150 kDa (HSPH1)]. A dilution series of a pool of the 10,000 clones was also incorporated, along with

cDNAs from other species as negative controls. We refer to these slides as "angiogenic" microarray chips.

The angiogenic microarray chip was established and contained cDNA fragments of genes potentially upregulated during capillary tube formation. For probing of this, to identify those regulated genes, RNA isolated from cells taken at 0, 0.5, 3, 6, and 24 h after plating onto a 3-D collagen matrix was linearly amplified and subsequently labeled with Cy3 or Cy5 dyes. Labeled aRNA from each time point was hybridized against that at *time 0*. Individual spot (performed in quadruplicate) intensities were normalised to the entire microarray and the fold change with respect to time zero was calculated. After scanning, background subtraction, local and global normalization, and ratio determination, Bayesian analysis was used to rank clones according to the likelihood of their corresponding genes being truly regulated. Expression profiles for each clone were generated by plotting fold induction versus time for each spot in each individual experiment. This work was performed by Anna Tyskin [144]. Approximately 550 clones were identified as significantly regulated and were isolated and the inserts were sequenced by the Australian Genome Research Facility (Figure 3.1)[144].

Figure 3.1: Isolation and Characterisation of Genes Involved in Angiogenesis. (A). The strategy for identification of genes regulated during capillary tube formation. From a well characterised *in vitro* 3D model of angiogenesis, RNA was prepared from cells isolated at specific time points over a 24h time period. Suppression subtractive hybridisation was used to generate four libraries of regulated cDNAs. A custom made microarray was generated containing 10,000 clones, known as the 'AngioChip'. This microarray was probed for changes in gene expression during *in vitro* capillary tube formation. Approximately 550 regulated genes were isolated, one of them was REST. **(B).** Generation of custom made AngioChip cDNA microarray. This figure demonstrates the number of clones isolated from each of the generated subtracted libraries which were enriched for on the microarray.

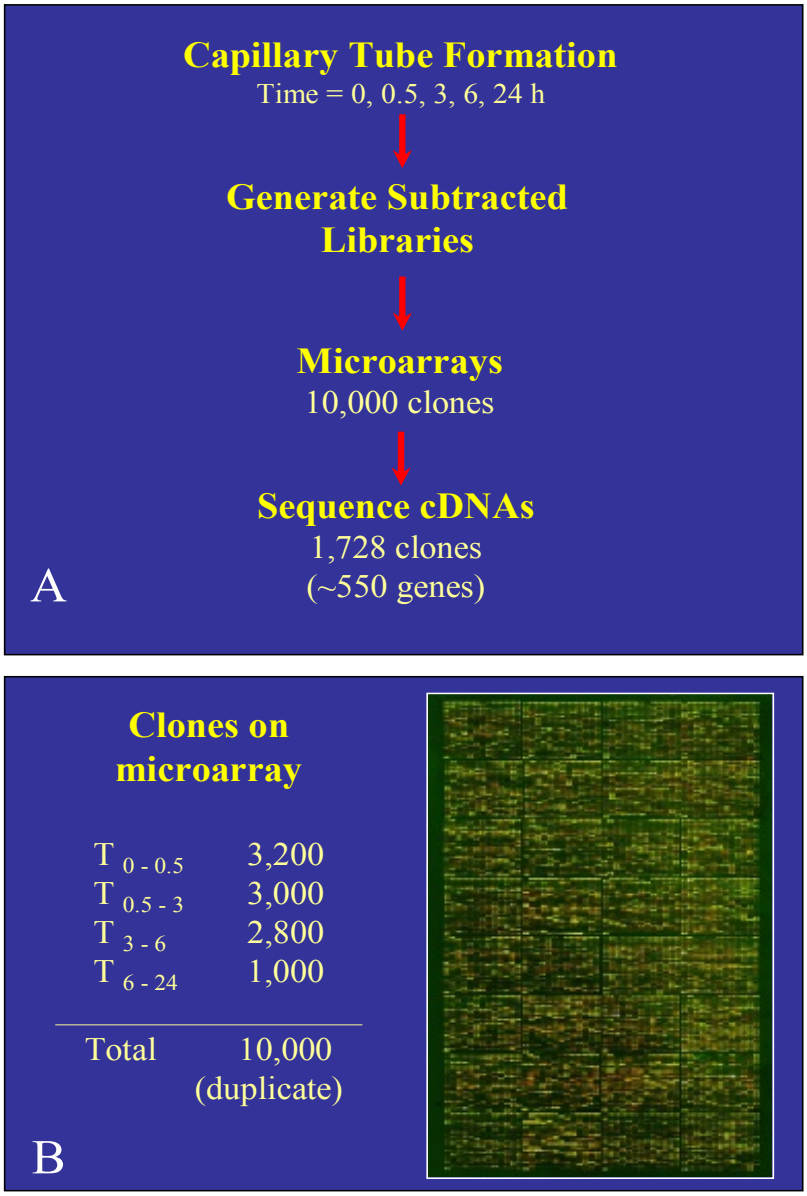

3.1.2 Isolation of REST

Selection of clones for further work was based on a number of criteria.

1. Number of times the clone was isolated – as an indication of confidence in the regulation of the gene.

2. The clone identification – as a possible gene with known or predicted involvement in angiogenesis or related differentiation processes.

3. Whether there was EC specificity or enrichment.

4. The pattern of regulation.

From the 550 sequenced clones, 10 clones were selected for further study based on the above criteria.

Of these 10, Repressor Element 1 Silencing Transcription Factor (REST) was chosen for further study in my PhD project because it was identified 10 times, and it's interesting mRNA expression profile, being upregulated from 30min to 6h and then downregulated at the 24h time period back to time 0 levels. The rapid induction in its expression level may reflect a major regulator of the process (Figure 3.2).

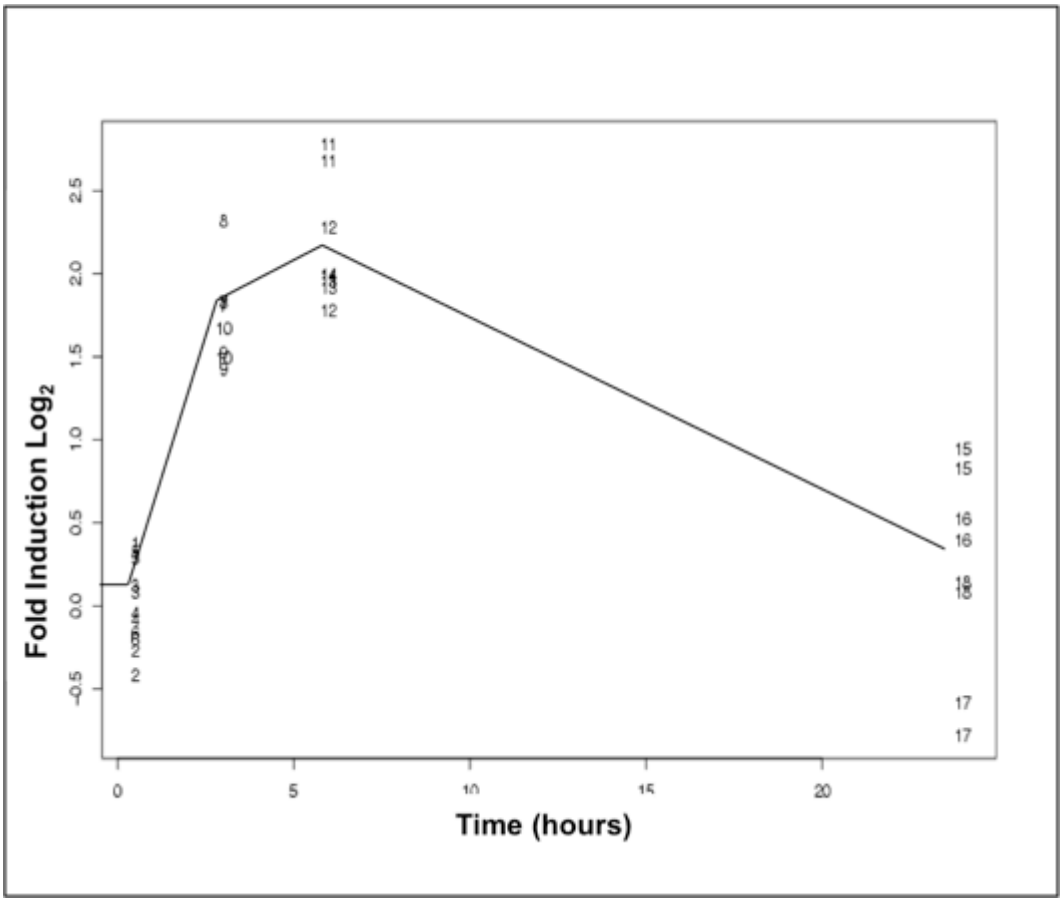

Figure 3.2 Expression profile of *REST* from angiogenic microarray. Individual spot intensities from the microarray were normalised to the whole microarray and plotted as the fold induction (log2) with respect to time zero versus time. Expression of *REST* was upregulated at 3 and 6 hours compared to time 0 and downregulated at 24 hours.

REST, or NRSF (neuron-restrictive silencing factor), is a transcriptional repressor regulating a number of genes. It binds to a 21–23 base pair repressor element 1 (RE1) of which there are ~ 1900 copies in the human genome. REST plays critical roles in preventing differentiation and maintaining the self-renewal capability of neuronal stem cells. In accordance with its function in silencing of both neuronal and nonneuronal genes, REST is essential for embryonic development and for a number of cellular responses in neurons and other cell types (Figure 3.3B). REST can function as either a tumor suppressor or an oncogene depending on the cellular context. Diminished REST expression is associated with colon cancer and transformation of human mammary epithelial cells (HMEC) [145]. High levels of forms truncated in the DNA binding domain due to alternative splicing, which are similar to a normally occurring alternative splice product, are implicated in small-cell lung cancer and neuroblastoma [146, 147]. Likewise, a frameshift mutant truncated just beyond the DNA binding domain (REST-FS) (Figure 3.3A) is found in colon cancer and can transform epithelial cells [145]. All of these truncated forms can presumably function to some extent as "dominant negatives." An oncogenic role for REST has been established in medulloblastoma, an aggressive childhood malignancy of neural progenitors, where high REST levels coupled with Myc overexpression drive cells toward proliferation and tumorigenesis rather than differentiation [148, 149]. There have been many genes showing common regulation and function between the neuronal and vascular systems (eg, ephrins, slits, metrins and VEGF) [150]. Therefore this possibility was considered for REST.

3.1.3 Confirmation of Regulation of REST

It is well accepted that microarray data, while indicative of the direction of regulation, is not quantitative. Therefore, the expression profile of *REST* was determined by real time Q-RT-PCR using cDNA synthesised from RNA obtained from HUVEC in a 3D setting as given above (3.1.1). Total cell RNA was harvested at various time points (0, 0.5, 1, 3, 6, 12 and 24h), purified

Figure 3.3. Structure and Function of REST(A.) Schematic representation of REST/NRSF. REST has N and C terminal repressor domains (RD1 and RD2) that serve as scaffolds for distinct gene repressor/silencing complexes. The DNA binding domain is followed by lysine- and proline-rich domains and two β-TrCP binding sites. Alternative splicing leads to truncated forms of REST that terminate in the region indicated by the arrow. These include a naturally occurring neuron-specific form and forms associated with small-cell lung cancer and neuroblastoma. The position of an oncogenic truncation found in colon cancer resulting from a frameshift (REST-FS) is also indicated by an arrow. **(B).** Proposed functions of REST. (Upper panel) In neuronal stem/progenitor cells, REST suppresses expression of neuron-specific genes maintaining cells in an undifferentiated state. Likewise, in normal epithelial cells, REST protein level is maintained, and it functions as a tumor suppressor. REST also suppresses expression of MAD2, a component of the mitotic checkpoint complex/spindle-assembly checkpoint, until degradation of REST by SCFβ-TrCP during the G2 phase of the cell cycle. (Lower panel) During neuronal differentiation, REST is degraded in a SCFβ-TrCP-dependent manner, allowing for expression of genes necessary for differentiation. When β-TrCP is overexpressed, as occurs in some epithelial cancers, REST levels are dysregulated, contributing to transformation. **Weissman et al 2008**

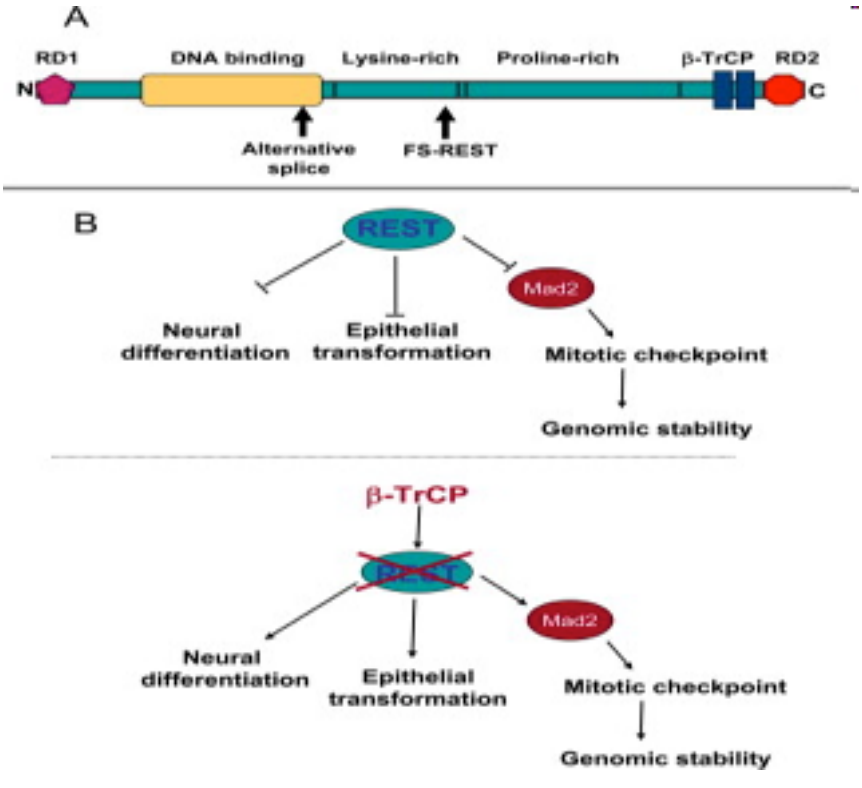

via an RNeasy column (QIAGEN) and DNase treated (DNA-free™, Ambion). First strand cDNA synthesis was performed to generate cDNA. Q-RT-PCR was performed on this cDNA using primers designed specifically to the 3' UTR of the *REST* mRNA (Refer to appendix 2). The results were standardised to Peptidylprolyl isomerase A (PPIA), also called cyclophilin A, a mRNA previously shown to be unregulated during in vitro angiogenesis. REST was regulated at the 3 and 6h timepoints when measured by Q-RT-PCR, in a pattern very similar to that seen on the array data. Its expression peaked at 3h with a 2 fold induction. The increased expression was maintained throughout the 24hrs which was in contrast to that seen with the microarray data (Figure 3.4).

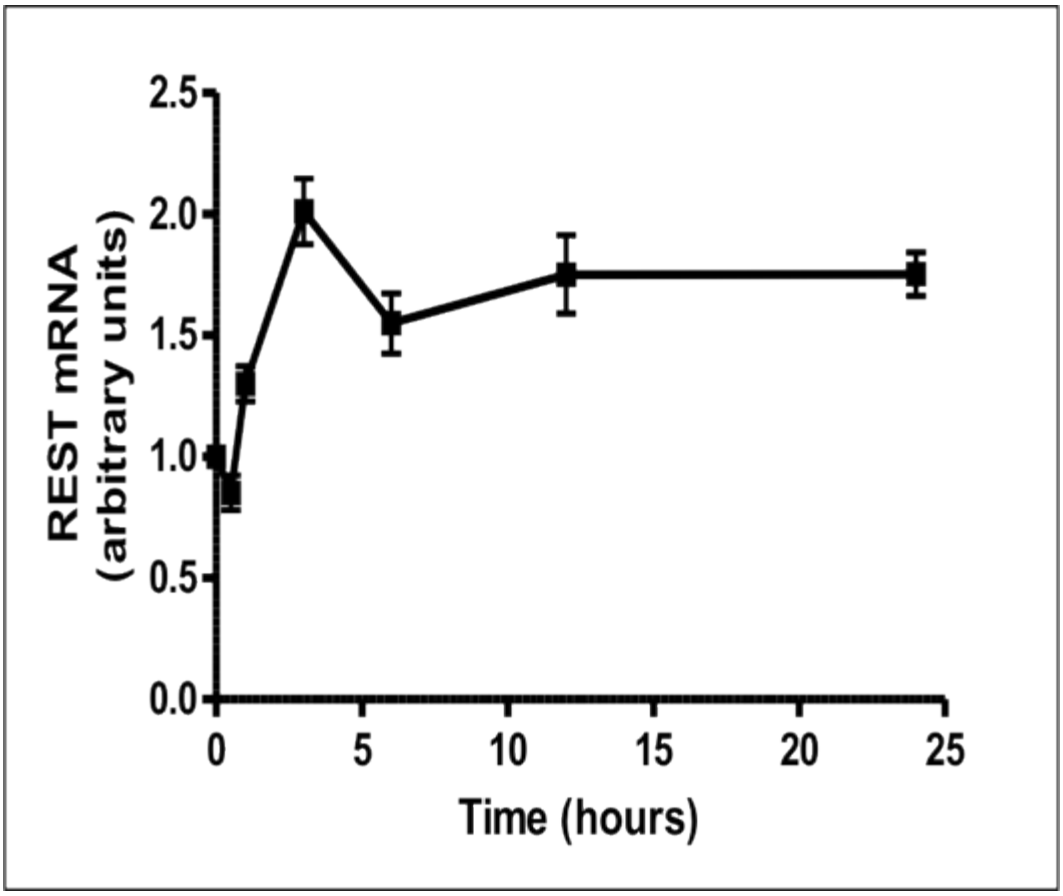

Figure 3.4. Confirmation of microarray expression profile of *REST* by Q-RT-PCR.

Expression profile of *REST* using Q-RT-PCR. The expression profile of *REST* by Q-RT-PCR confirmed the upregulation of the gene at the early timepoints, but the peak upregulation occurred at 3h. The expression stayed elevated unlike the downregulation in the microarray. Results from each timepoint were standardised to PPIA.

3.2. Regulation of REST Expression Levels

We initially investigated whether there was a link between REST regulation and proliferation.

3.2.1 Confluent versus non confluent

The levels of *REST* mRNA were investigated in response to confluency. HUVEC were plated at either 100% confluency where cells were 'contact inhibited' and therefore not proliferating or at subconfluent levels where there is little cell-cell contact and the cells are induced to undergo proliferation. *REST* mRNA expression levels were measured by Q-RT-PCR, in both confluent and non-confluent cells 3 and 24 hours after stimulation. REST was significantly more highly expressed in subconfluent proliferating cells compared to the confluent quiescent cells (Figure 3.5A). Furthermore, after 24 hours the initial subconfluent cells were starting to grow to confluence and this was associated with a decrease in the levels of *REST*.

3.2.2 Response to angiogenic stimuli

To investigate whether *REST mRNA* levels are regulated by angiogenic factors, HUVEC were treated with stimuli including Tumour Necrosis Factor α (TNFα), VEGFA , bFGF and PMA. Confluent HUVECs, (thus eliminating the proliferative element in the regulation) were exposed to factors for 3 or 24h. Q-RT-PCR was performed using *REST* specific primers and the results were standardised to PPIA. After 3h exposure to the stimuli, little regulation was seen although TNFα induced *REST* mRNA levels slightly (by 1.2 fold) and bFGF reduced *REST* expression slightly (by 0.8 fold) (Figure 3.5B). Similarly, after 24h, no response to TNFα, VEGFA occurred although PMA induction rose slightly to 1.5 fold and bFGF rose 1.2 fold (Figure 3.5C). Therefore, at least at time points 3 and 24h, *REST* mRNA is not significantly regulated by TNFα, VEGFA or bFGF, but does increase marginally in response to PMA.

The above experiment was then repeated using subconfluent HUVECs which were stimulated in the same fashion. There were no significant changes seen after 3h stimulation (Figure3.5D).The only significant change was noticed after 24hrs of stimulation with PMA. This induced a 1.3 fold increase of *REST* expression (Figure 3.5E). There was no change with 3h or 24h treatment of HUVECs with TNFα, VEGFA, bFGF. These results indicate that *REST* is downregulated by confluency but is not regulated by classic regulators of EC function

3.3 Cloning of REST cDNA

To investigate the role of *REST* in EC function we adopted the strategy to regulate the levels either by using knockdown or overexpression. However, HUVEC are notoriously difficult to transfect by physical or chemical methods. Adenoviral vectors provide the capacity to achieve high levels of gene transfer (even up to 100%) without the need for selection, as would be necessary with other viral systems such as retroviruses. To construct the adenovirus it was therefore necessary to clone the full length cDNA for *REST*.

HUVEC were harvested and total cell RNA was extracted and reverse transcribed to produce cDNA. The cDNA was then used as a template for PCR amplification of the full coding region of *REST*. To do this, REST specific primers, REST(f) and REST(r), were designed (Refer to appendix 2). The reverse (r) primer added a myc-tag onto the C-terminus of REST. Both primers introduced EcoRI sites at the extremities of the product to aid in cloning. These primers were used in combination with the high fidelity proof reading enzyme *Pfu* (Stratagene,CA) to amplify the cDNA. Confirmation of

A

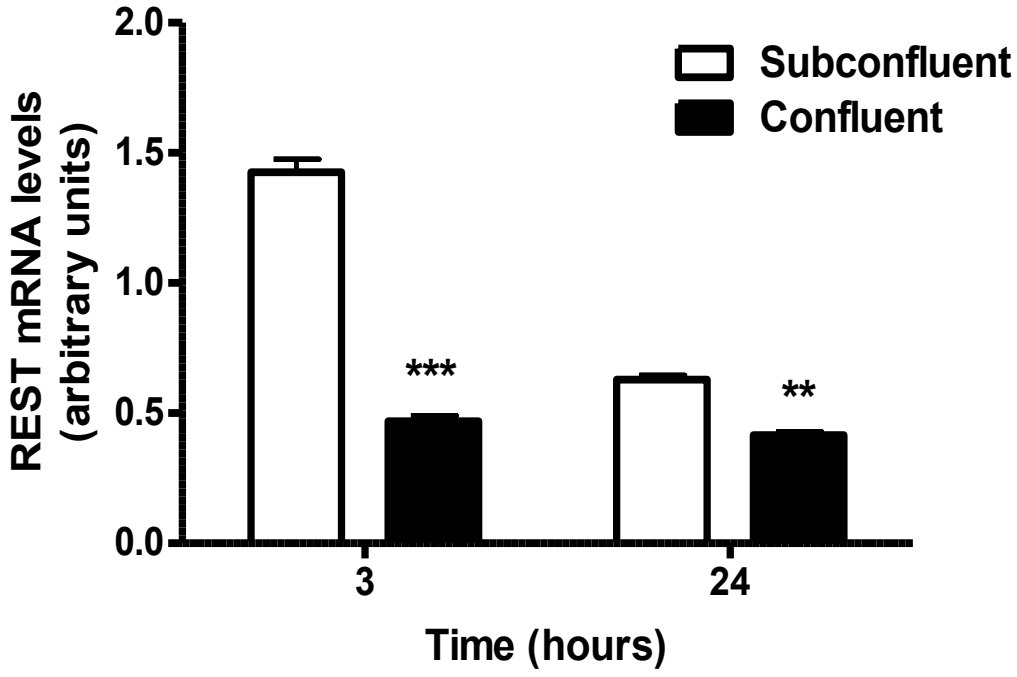
2.0
1.5
1.0
0.5
0.0
REST mRNA levels
(arbitrary units)
Subconfluent
Confluent
***
**
3
24
Time (hours)

B

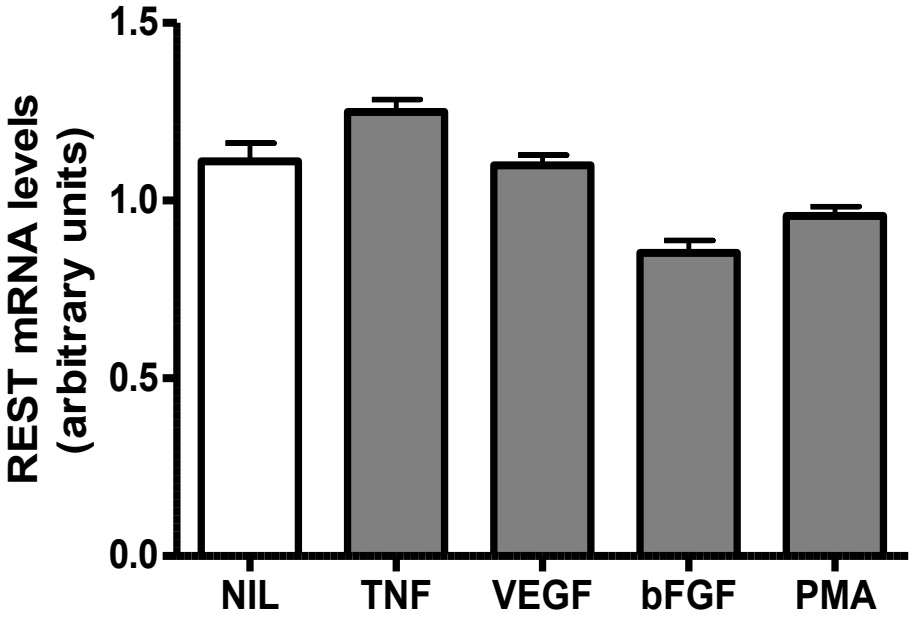
1.5
1.0
0.5
0.0
REST mRNA levels
(arbitrary units)
NIL
TNF
VEGF
bFGF
PMA

C

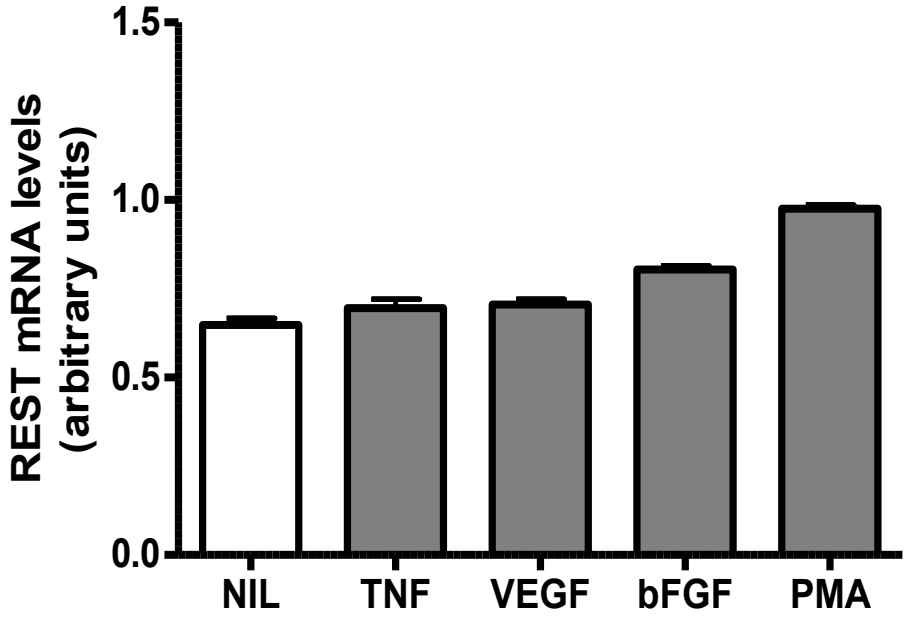
REST mRNA levels
(arbitrary units)
1.5
1.0
0.5
0.0
NIL
TNF
VEGF
bFGF
PMA

D

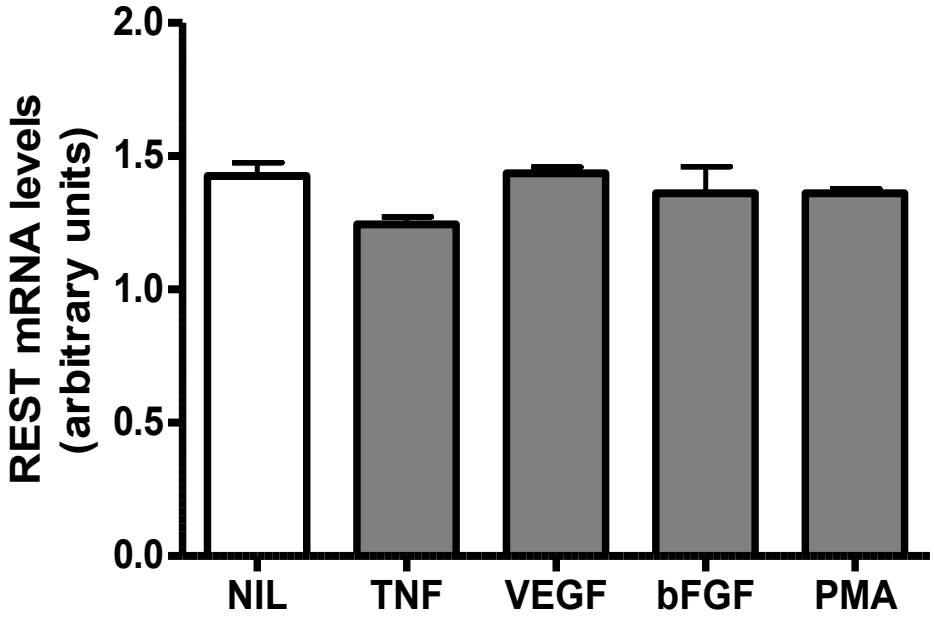
REST mRNA levels
(arbitrary units)
2.0
1.5
1.0
0.5
0.0
NIL
TNF
VEGF
bFGF
PMA

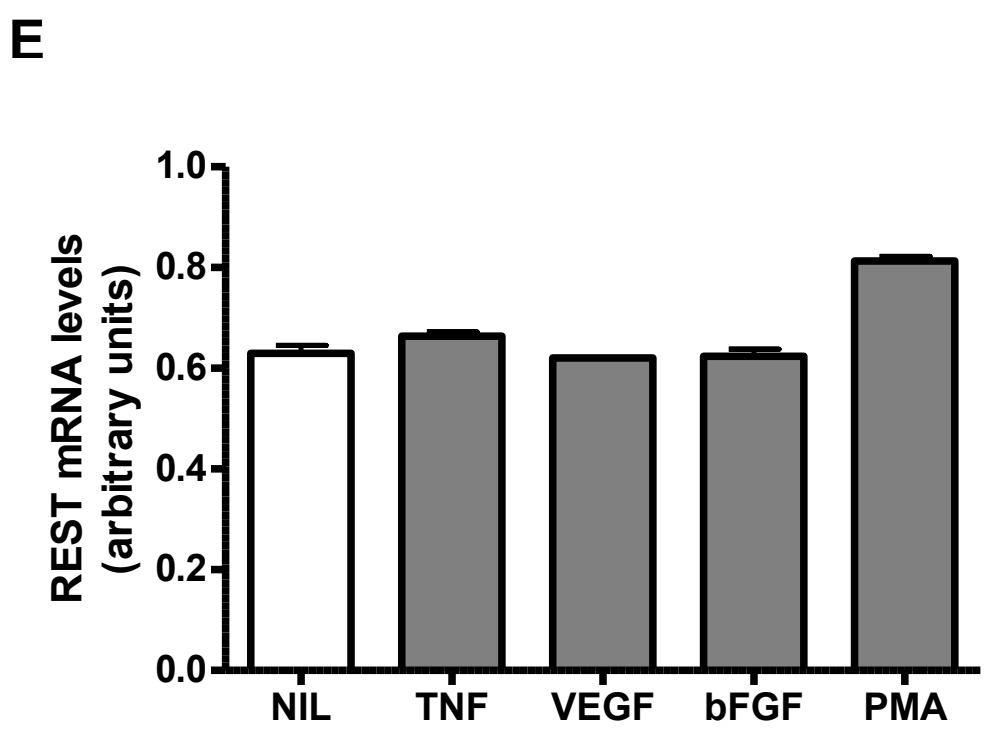

Figure 3.5. Response of *REST* expression to various stimuli. **(A).** REST regulation in a proliferating vessel versus a quiescent vessel model of tube formation. The expression level of REST was measured in a proliferating (subconfluent HUVEC) versus a quiescent (confluent HUVEC) model of tube formation via Q-RT-PCR. Each group was performed in triplicate, result shown are mean +/- SEM and are standardised to PPIA.. ** $p<0.01$ and *** $p<0.001$ compared to subconfluent **(B)**. Response of REST expression after 3h subject to various stimuli in quiescent vessel model. Confluent HUVEC were exposed to 0.5ng/ml TNFα, 20ng/ml VEGF, 5ng/ml bFGF and 20ng/ml PMA for 3h and expression levels were determined via Q-RT-PCR. Each group was performed in triplicate, results shown are mean +/- SEM and are standardised to PPIA. **(C).** Response of REST expression after 3h subject to various stimuli in quiescent vessel model. Confluent HUVEC were exposed to 0.5ng/ml TNFα, 20ng/ml VEGF, 5ng/ml bFGF and 20ng/ml PMA for 24h and expression levels were determined via Q-RT-PCR. Each group was performed in triplicate, results shown are mean +/- SEM and are standardised to PPIA.**(D).** Response of REST expression after 3h subject to various stimuli in proliferating vessel model. Subconfluent HUVEC were exposed to 0.5ng/ml TNFα, 20ng/ml VEGF, 5ng/ml bFGF and 20ng/ml PMA for 3h and expression levels were determined via Q-RT-PCR. Each group was performed in triplicate, results shown are mean +/- SEM and are standardised to PPIA. **(E).** Response of REST expression after 3h subject to various stimuli in proliferating vessel model. Subconfluent HUVEC were exposed to 0.5ng/ml TNFα, 20ng/ml VEGF, 5ng/ml bFGF and 20ng/ml PMA for 24h and expression levels were determined via Q-RT-PCR. Each group was performed in triplicate, results shown are mean +/- SEM and are standardised to PPIA.

the appropriate size product was via agarose gel electrophoresis. The PCR product was then purified via the QIAquick® PCR purification kit (QIAGEN), digested with EcoRI and cloned into the pEG shuttle vector for sequencing (Figure 3.6). The amplified cDNA sequence was confirmed and identified to be identical to the REST sequence accession, NM_005612, submitted to Genbank™.

3.4 Generation of Recombinant Adenoviral Constructs

Delivery of the gene of interest, in this case *RES*T, to cells can be achieved by adenoviral infection, which provides efficient, transient expression. For the generation of recombinant adenovirus, the GATEWAY® system (Invitrogen, VIC) of recombination was employed to enable introduction of the REST cDNA into the very large 37kb adenoviral vector. This requires use of the pEG (entry vector) and pAEATG (destination vector).

In order to generate recombinant adenoviral constructs the adenoviral entry vector pEG-REST-myc and the destination vector pAEATG were recombined via the LR Recombinase protocol (Invitrogen) (Figure 3.7). This method homogously recombines attL1 with attR1 and attL2 with attR1 and then transforms recombination products in to *E.coli* which are then selected for with Kanamycin. Since the parent entry vector is only gentamicin resistant, its ccdB 'death' gene selects against it in non-permissive DH5∝. The construction which results from this recombination, pAEATG-REST-myc, was then linearised with *Pac*I and used to transfect HEK293 cells for viral production. The pEG-REST-myc sense and antisense were recombined with pAEATG-F and pAEATG-R, respectively, to give adenoviral constructs in both orientations. In the antisense construct, the attR1 and attR2 sites are swapped.

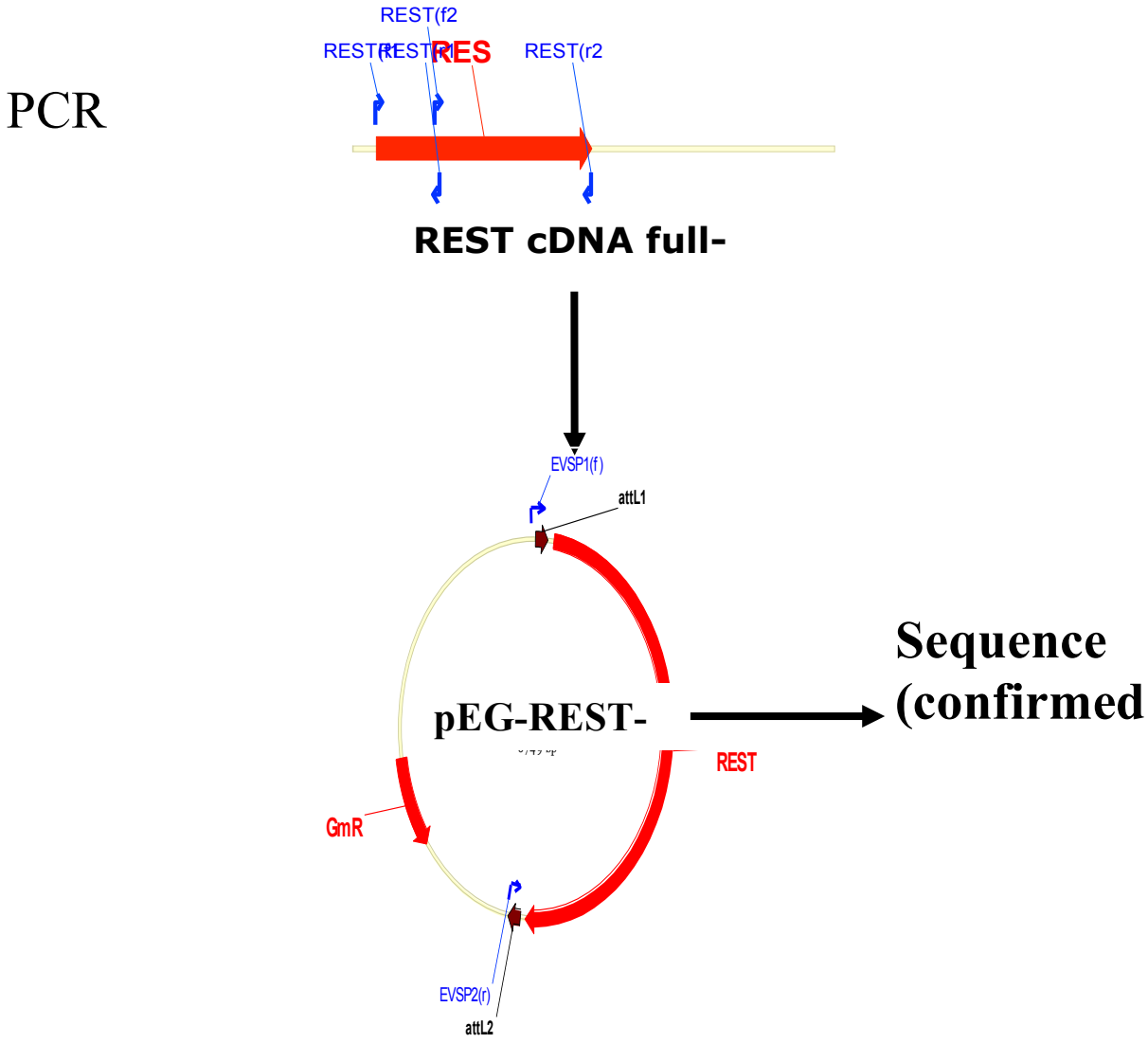

Figure 3.6 Cloning Strategy for REST cDNA into the pEG Entry Vector. The shuttle vector pEG-REST was made from the PCR amplified coding region of REST-myc. The REST PCR product and the pEG were both EcoRI digested and ligated to give pEG-REST-myc. This vector was then used for sequence confirmation of the REST insert.

Figure 3.7 Generation of Recombinant REST Adenovirus. The adenoviral entry vector pEG-REST-myc and destination vector pAEATG, were recombined in a test tube using LR clonase which recombines attL1 with attR1 and attL2 with attR2 in an orientation specific manner. The recombination products were then transformed into E.coli, and recombinants selected with Kanamycin. The parent entry vector is selected against, since it is only gentamicin resistant and the ccdB death gene selects against the parent destination vector in non-permissive DH5α cells. The resulting pAEATG-REST-myc, was then linearised with pac I and used to transfect HEK293 cells for viral production.

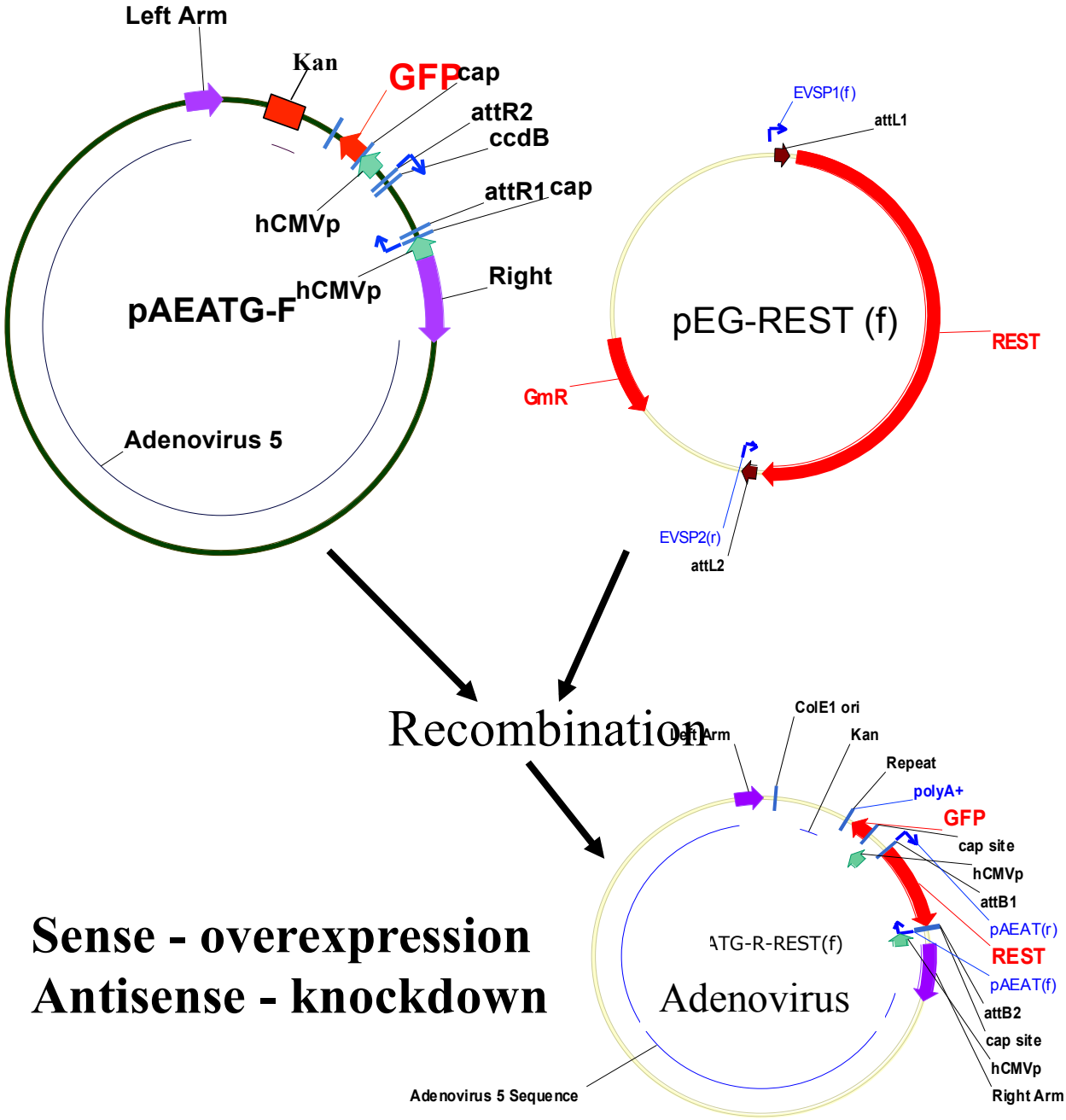

3.5 Generation of REST Adenovirus

Prior to large-scale plasmid DNA production in competent *E.coli* DH5α cells, successful recombination to generate pAEATG-REST-myc recombinants was confirmed by *Pac*I and *BstX*I restriction enzyme digestion patterns. The pAEATG empty vector (EV) was generously provided by Michelle Parsons from the Vascular Biology Laboratory. The EV can be used as a control for adenovirus infection when we knockdown or overexpress our gene of interest in this vector.

Purification of plasmid DNA was performed using the Qiafilter™ MIDIprep procedure. After purification, plasmid DNA was linearised in preparation for transfection of HEK293 cells via digestion with *Pac*I. This is required for efficient adenovirus production. Linearised pAEATG EV and REST-myc sense and antisense DNA was transfected into HEK293 cells (via the Lipofectamine™2000 procedure) to produce the initial preparation of EV, sense and antisense adenovirus.

After the initial viral particles were harvested from transfected HEK293 cells, up scaling of adenovirus required sequential adenovirus infection cycles with an increase in cell culture size as suggested in the Qbiogene Version 1.4 AdEasy™ Vector System manual. Each infection cycle (3 expansion cycles) was synchronised with subsequent cell culture growth to attain optimal virus yield in a minimum time period (approximately 3-4 days after infection where cells were starting to aggregate and detach from the flask). For the final virus growth approximately 30 T175 flasks were infected and the resultant virus collected for purification, through a three-step purification process. The first step required a discontinuous CsCl gradient aimed at removal of the majority of cellular components and defective viral particles generated in the large scale production. The second step involved the use of a continuous CsCl gradient to completely separate the defective particles from infectious viral particles and required overnight centrifugation. The final step was

dialysis to remove CsCl which is toxic to cells and may also interfere with subsequent cell infection. Large scale production and purification of the recombinant adenovirus was kindly performed by Michelle Parsons in the Vascular Biology Laboratory.

In order to confirm the authenticity, completeness and orientation of the inserted cDNA and vector components, specific restriction digestions were performed throughout the entirety of the cloning procedure. To confirm both identity and orientation of each of the final recombinant adenoviral preparations, PCR amplification with vector specific primers (pAEAT(f) and pAEAT(r)) and a gene specific primer was performed. This also enabled detection of other contaminating adenoviruses due to the possibility of airborne cross contamination from other laboratory recombinant adenoviruses. All prepared viruses were found to be correct and contamination free (data not shown).

.

3.6 Determination of Recombinant Adenoviral Titres – $TCID_{50}$

Adenovirus should be used at an infection level that gives 100% or close to 100% transfection of the cells but at a level where cytotoxicity is not encounted. Furthermore the levels of virus used for the EV and the test viruses should give similar levels of infection.

In order to obtain titres for each of the recombinant adenoviral constructs (REST sense (F), REST antisense (R) and the pAEATG empty vector control (EV)) the tissue culture infectious dose 50 ($TCID_{50}$) was determined using HEK293 cells. This assay is a ten day assay relying on the development of a cytopathic effect (CPE) in HEK293 cells and uses end-point dilutions in order to estimate the titre (http://www.qbiogene.com/products/adenovirus/adeasy/shtml). It is a very sensitive assay designed to measure down to one infectious virus particle. This is becoming the standard assay used worldwide for determining adenovirus plaque forming units (pfu). For each of the recombinant adenoviruses, the $TCID_{50}$ values were calculated according to the

equation available in the Qbiogne Version 1.4 AdEasy™ Vector System manual (website above). The $TCID_{50}$ values measured were: EV = $0.5x10^{10}$ pfu/ml, REST F = $0.8x10^{10}$ pfu/ml and REST R = $1x10^{10}$ pfu/ml.

3.7 Functional effects of REST sense and antisense constructs

3.7.1 Determination of levels of Protein

In order to ensure that overexpression and knockdown of REST F and REST R was occurring, levels of protein expression were confirmed via western blot by detection with an anti-myc antibody against the myc-tagged constructs. HUVECs were infected with EV, REST F and REST R at an MOI of 4, 0.9 and 0.8, respectively, which gave equivalent levels of GFP reporter expression. HUVECs were also infected with an adenovirus containing a control gene which is known to overexpress the gene and myc when HUVECs are infected. It was important to ensure expression and knockdown of REST protein was occurring at this level of infection for the functional assays to be relevant and determine if a change in phenotype occurred. From Figure 3.8 it is unfortunately obvious that there is no myc-tagged REST protein present in EV or REST R as would be expected, but there is also no overexpression in REST F which is what we would expect if the overexpression was working. In an attempt to obtain expression of REST, a number of changes were investigated. The dose of virus was increased, and the time between infection and harvest of the cells was varied. However no obvious overexpression of REST was measured. Therefore, our overexpression construct was not functional.

The determination of the functional effect of REST R to reduce endogenous REST levels was also a problem. Endogenous REST cannot be visualised via western blot since we did not have an antibody to REST that was able function on western blots. Therefore we could not determine

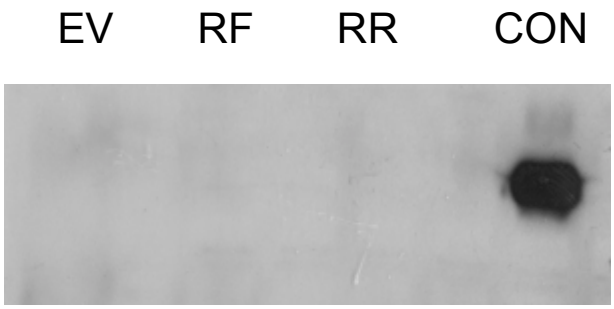

Figure 3.8 Western blot of REST-myc using an anti-myc antibody. Cell lysates at 24h of EV and RESTF-myc (RF), RESTR-myc (RR) and a control adenovirus known to overexpress myc (CON) infected HUVECs. Lysates were run on 12% SDS-PAGE gel, and a Western blot carried out using an anti-myc antibody, then detected using the Amstersham ECL kit. The protein detected was 76Kd.

whether the antisense to REST was effective. Also without a REST antibody we couldn't determine if there was knockdown of REST when the antisense adenovirus was used. There is also no change in mRNA expression when using adenovirus with the antisense construct because using the adenovirus technique prevents translation of the mRNA but does not decrease the amount of total mRNA in the cells.

3.7.2 Establishment of Viral Dose

Because of the above detection problems we became reliant on the effects of knockdown of REST in order to determine the possible functions of REST in EC. A number of functional assays were performed using HUVEC as the cell model. These assays; attachment, proliferation, migration and tube formation are hallmarks of angiogenesis. The approach is to alter the expression of REST, and then analyse the functional phenotype. In this way I should be able to determine whether REST is essential for any of the functions or whether the level of REST plays a role in these functions. Due to the problems associated with the inability to overexpress REST, the functional analysis involved in REST knockdown was only performed.

HUVEC were infected at passage 3 with adenoviral constructs containing REST antisense (R). Adenovirus constructs containing pAEATG empty vector (EV) were used as a control. In all experiments, unless stated otherwise, HUVEC were harvested 48h post infection and subsequently used for the chosen functional assay.

Initially, each adenovirus was titred further on HUVEC in order to ascertain the dose of virus which should be used to give approximately 100% infection as judged by GFP expression without compromising cell viability. In the pAEATG recombinant adenoviral vectors, two identical expression cassettes drive GFP and the gene of interest. Both contain strong CMV

promoter/enhancer elements and an efficient polyadenylation signal. Therefore, measurement of GFP enables determination of not only the efficiency of the HUVEC infection, but also of the strength of the CMV promoter in the cells and an indirect indication of the amount of inserted gene being expressed.

Previous experience has demonstrated that GFP readings between 100-200 mean fluorescence intensity, as determined by the analysis on the fluorescence activated cell sorter (FACS), results in good knockdown of expression of most proteins. From such titres of my viruses, I have used adenoviral constructs at MOI values from 2 to 4.16 for EV, and 0.125 to 0.80 for REST R, in order to obtain comparable levels of GFP and therefore comparable levels of infection.

3.7.3 Effect of REST Knockdown on Capillary Tube Formation

Matrigel® is a basement membrane matrix which provides the essential components required for tube formation to occur. This includes the provision of extracellular matrix (ECM) proteins as well as growth factors. The assay allows the formation of tubes to be visualised over a 1-2 day period. The assay is analysed microscopically at various times and cells are photographed. This assay was performed on 5 HUVEC lines and similar results were observed in all experiments. All groups received similar numbers of cells as can be seen in the photographs taken 15min after plating, at a time when the cells were just contacting the matrix (Figure 3.9A). In the first 2 experiments performed when REST R infected cells were used the tubes formed at a slower rate and the tubes were of a poorer quality, but with further experiments these results were not confirmed and it was found that there was no difference between EV and REST R in tube formation after 23hrs (Figure 3.9B). The tubes in both EV control and REST R appeared very similar, and formed in a similar time.

Overall, these tube formation assays on Matrigel® showed that in HUVEC, REST R had no effect on either the quality, number or time of tube formation. The matrigel experiments were also repeated using siRNAs targeting REST. When 70% knockdown of REST mRNA was achieved there was still no change in tube formation between REST knockdown and control siRNAs.

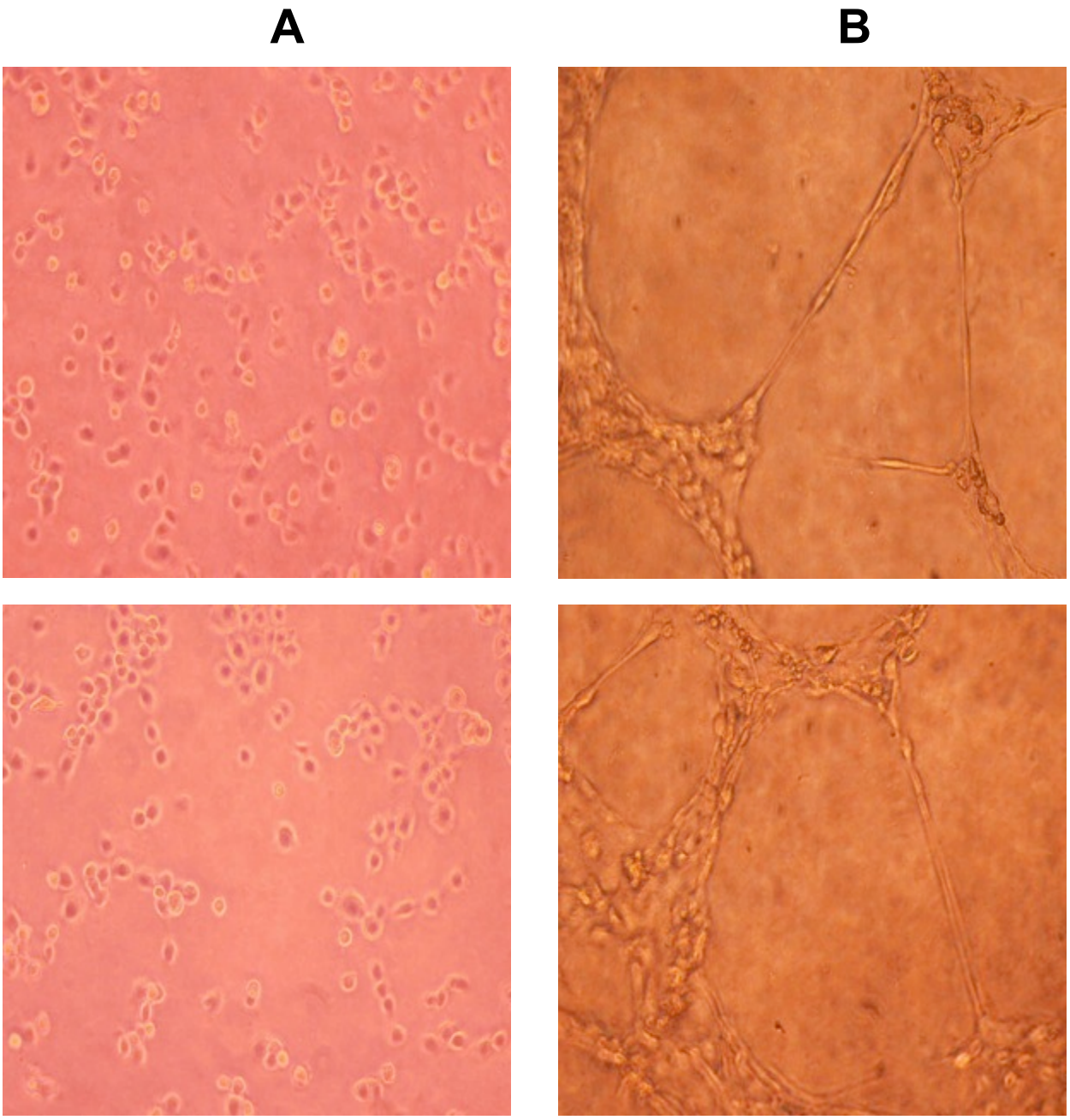

Figure 3.9. Effect of REST Regulation on the matrigel tube formation assay. HUVEC were infected with pAEATG empty vector (Top Photos) and REST antisense (Bottom Photos) 48h prior to plating on Matrigel. **(A).**. Shows EV and REST R 15min after plating. **(B)** shows EV and REST R 23h post plating. Bar=250μm

3.7.4 Effect of REST on EC Proliferation.

This assay measures the amount of cell division which occurs over a three day period. Previous work in the laboratory suggested that HUVECS double in cell number every 2-3 days. The conditions have been established so that either a decrease or increase in cell number will be measureable. The number of cells is measured by the MTS assay in which a colourless compound is converted to a coloured formazan product when cells are metabolically active. This is measured at an absorbance of 490nm, and directly correlates to the number of viable cells in culture. For the number of cells used here, the absorbance and cell number are within the linear range.

Two independent HUVEC lines were infected with EV and REST R and analysed for differences in proliferation (Figure 3.10). Both of these experiments were performed in normal medium (20% FCS plus growth factors and heparin). In no experiment was there a noticeable change in proliferation of the antisense infected cells.

3.7.5 Effect of REST on HUVEC Migration

The assay used was a very classic one to measure EC migration whereby, a wound was inflicted on the monolayer of EC and then the rate of closure of the wound was assessed. Photographs were taken over a 24h time frame to chart the progression of wound closure. The rate of wound closure is dependent on the initial size of the wound and therefore wounds of similar magnitude were compared.

The results shown in Figure 3.11 of one of the 2 HUVEC lines assayed shows that in REST R infected cells the rate of wound closure was not changed compared to EV.

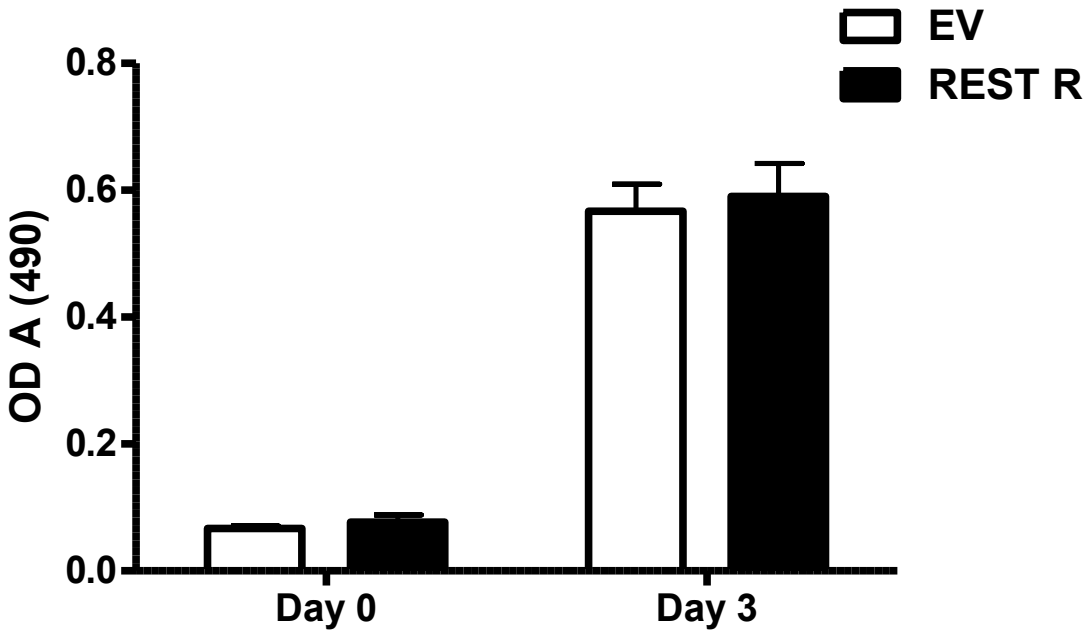

Figure 3.10. Regulation of EC proliferation by REST. HUVEC were infected with pAEATG empty vector (EV) and REST antisense (REST R) and proliferation was measured over 3 days and is given as OD (A490) +/- SEM. This is the pooled data from 2 experiments, each group was performed with 8 repeats.

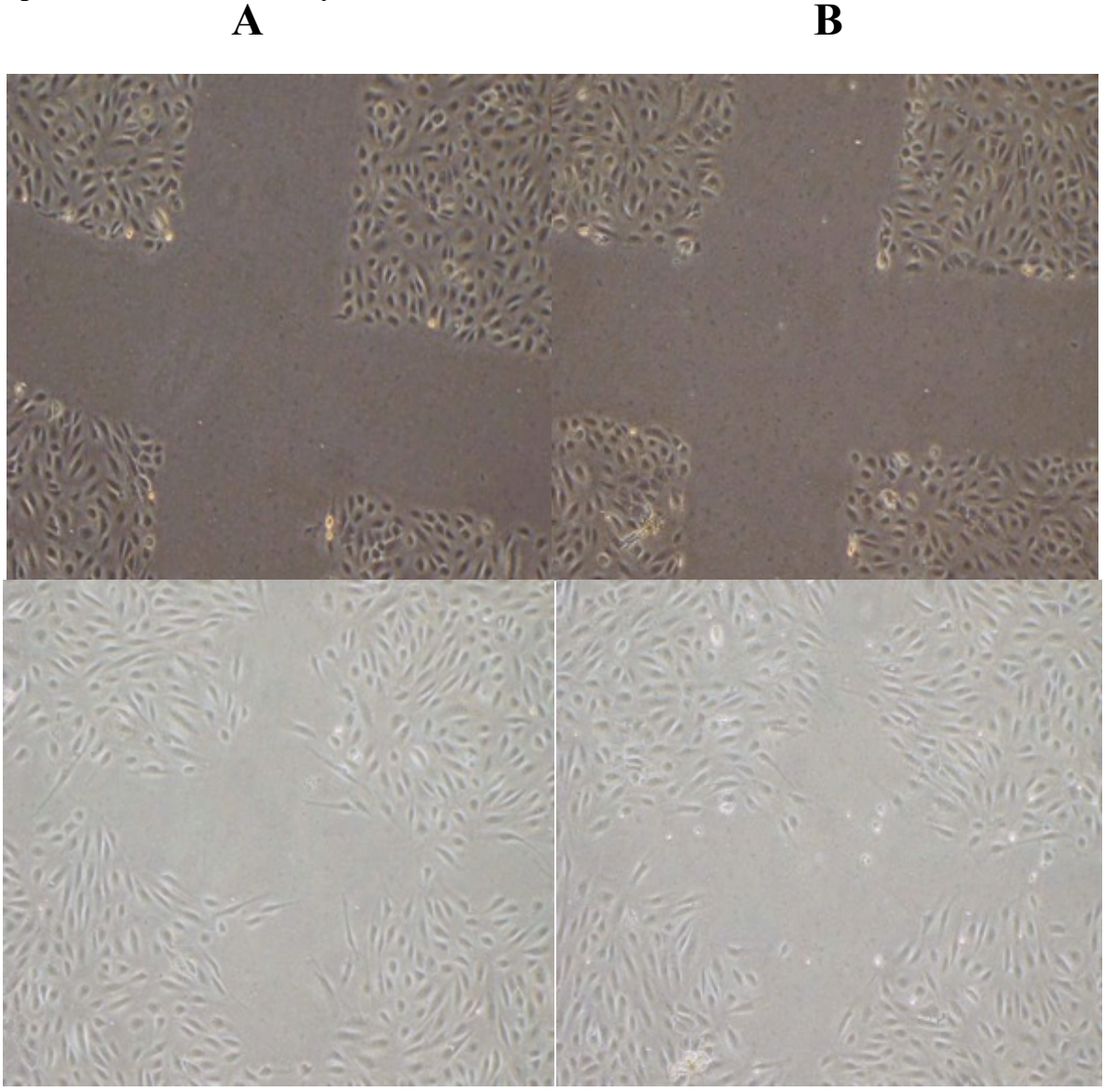

Figure 3.11. Migration Assay of HUVEC infected with REST adenovirus. The response in cell migration to pAEATG empty vector (Top Photos) and REST antisense (Bottom Photos) was tested over 24 hours in 20% FCS + growth factors. Photographs were taken at **(A).** 10 min post wounding and **(B).** 18h post wounding. This is a representative of 3 experiments.

3.7.6 Effect of REST on Attachment

The ability of HUVECS to attach to different matrices after depletion of REST was also tested. HUVEC infected with the various adenoviral constructs were plated on different matrices and the level of attachment was measured after 60min. The matrices were gelatin, collagen, fibronectin and laminin. Gelatin was chosen because it is denatured collagen, which is what the cells would experience in a wound. Laminin was chosen because it is the major component in tissues. The pooled results of 2 lines assayed are shown in Figure 3.12. There was a no significant change in attachment when compared with EV control.

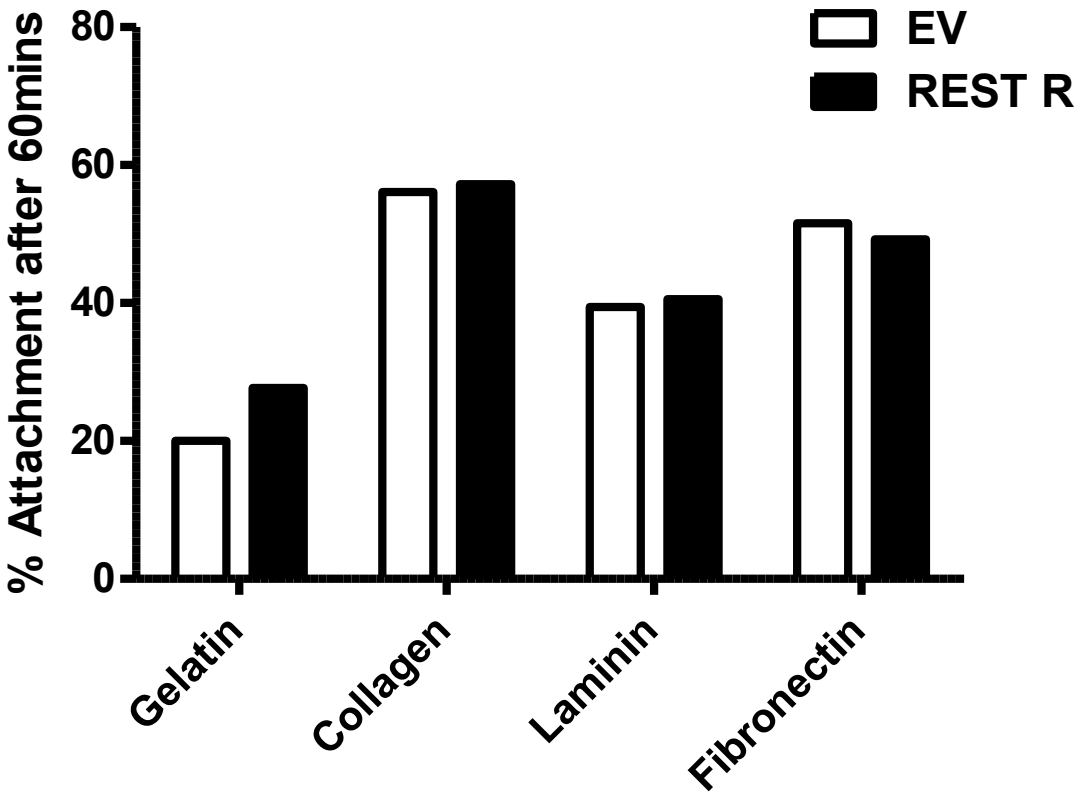

Figure 3.12. **Regulation of EC attachment by REST**. Cells were infected with pAEATG empty vector (EV) and REST antisense (REST R). Attachment to gelatin, collagen, laminin and fibronectin after 60min is given as the mean percentage of cells attached +/- SEM. This is one experiment where each group was performed in quadruplicate.

3.8 Summary

REST is upregulated between 3 and 6 hours after plating, at a time when cells are in contact but junctions are not mature and is classified as a time of sub-confluence. After 6 hours the expression of REST is decreased, at a time when the cells are starting to become confluent and the junctions are more mature. These observations were confirmed when the levels of the mRNA expression of *REST* were analysed in subconfluent and confluent cells over a 24 hour time period. The expression of *REST* was consistently and statistically downregulated in confluent cells. These results together suggested that *REST* was an important gene in angiogenesis.

Although the regulation of *REST* during capillary tube formation indicates that the gene maybe playing a role in the angiogenesis process, our results have shown that the downregulation of REST does not change capillary tube formation significantly. These results are a surprise as *REST* is significantly upregulated during capillary tube formation and it would therefore be predicted that a decrease in REST expression would have some effect on this process. Unfortunately we were unable to overexpress REST and could therefore not determine if a significant upregulation would affect angiogenesis. This was despite extensive attempts. The *REST* insert cloned into the vectors was sequenced and found to be perfectly correct. We also repeatedly confirmed that the gene was inserted into the vector in the correct orientation to achieve overexpression. We also made attempts with cloning the myc tag at both ends of the gene and found this had no effect on overexpression. For these reasons it was decided that I would stop working on REST for my PhD and move onto another gene which was also found to be regulated on the microarray. We did not attempt to transducer into other cell lines because REST was found to be involved in angiogenesis and we wanted to see the affect of overexpression and knockdown on HUVECs. We also did not use other non viral vectors because

the system we were using involved adenovirus which was the current best method for gene expression syudies in endothelial cells.

CHAPTER 4

Functional Analysis of SENEX

The gene *ARHGAP18* (also called *MacGAP*) was chosen for further study based on its regulation profile during capillary morphogenesis, high expression in endothelial cells and that it was a gene with an unknown function. It will be referred to in all subsequent chapters as *SENEX*, based on its function in EC. The name *SENEX* was chosen by my supervisors Professor Jenny Gamble and Professor Mathew Vadas. *SENEX* was the second gene which I have worked on during my PhD. The remainder of my thesis will concentrate on *SENEX.*

4.1 Isolation of ARHGAP18

One gene found to be regulated in the angiogenesis screen was *MacGAP* (RefSeq NM_33515), named since it was originally isolated from a macrophage library, had a suspected role in macrophage degranulation, and because it contained a GTPase activating protein (GAP) domain. This gene has since been assigned to the ARHGAP family of proteins, as *ARHGAP18* (Homo sapiens- a Rho GTPase activating protein 18), in accordance with the naming system for RhoGAPs but will be referred to as *SENEX* in this thesis. The microarray profile for *SENEX* during capillary tube formation showed that expression decreases through the first 6 hours and is at it's lowest during the apoptosis stage of tube formation. *SENEX* expression then increases for the remainder of the tube formation up to the 24 hour timepoint when the cell survival stage of tube formation is occurring (Figure 4.1A). This is a unique profile with only two genes from the 550 having this profile. The microarray data was confirmed by virtual northern blot and also showed a similar pattern of regulation (Figure 4.1B) and further confirmed by Q-RT-PCR (Figure 4.1C).

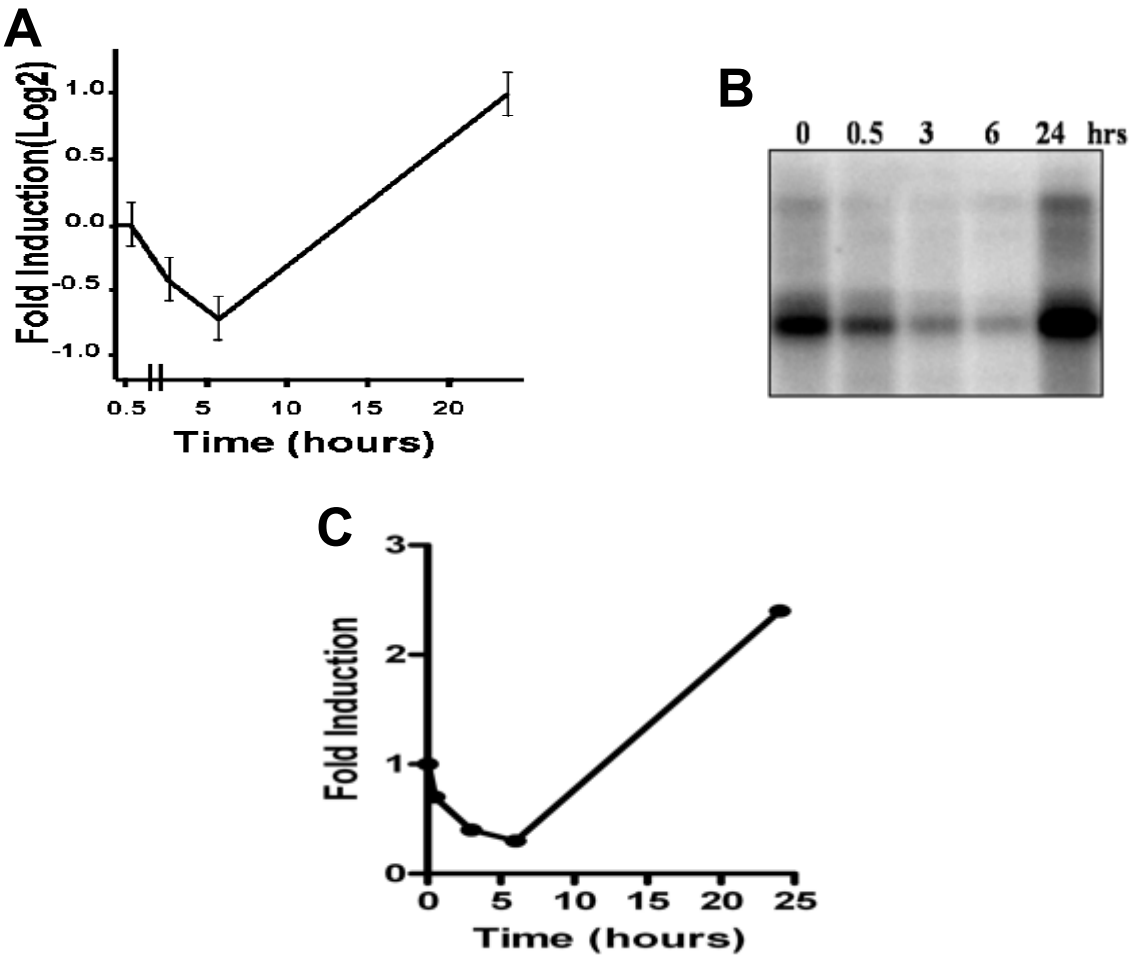

Figure 4.1. SENEX regulation during capillary tube formation. (A). A microarray profile was generated for the *SENEX* clone on the microarray slide. Plotted is the fold induction (log2) with respect to *time 0* (*y*-axis) versus time (in h; *x*-axis). **(B).** Expression profile of *SENEX* mRNA during *in vitro* capillary tube formation. Total RNA was harvested at the time points shown from cells undergoing angiogenesis in a 3D collagen assay, and virtual northern blots were probed with *SENEX* cDNA fragment. **(C).** Expression profile of *SENEX* using Q-RT-PCR. The expression profile of *SENEX* by Q-RT-PCR confirmed the upregulation of the gene at the early timepoints, but the peak upregulation occurred at 3hours. The expression stayed elevated unlike the downregulation in the microarray. Results from each timepoint were standardised to cyclophilin A.

4.1.1 Cytogenic Location

The gene is located on chromosome 6q22.33, spanning 133130 bp, from 130031370 to 129898241 on the reverse strand of chromosome 6. (GeneView, UniGene, locus link, Acembly,).

4.1.2 Expression

The *SENEX* gene is conserved in chimpanzee, dog, cow, mouse, rat, chicken, and zebrafish. Acembly and Ensembl automatic analysis were used to derive the following information about the predicted gene expression. The sequence of this gene is defined by 246 GenBank accessions from 233 cDNA clones, some from uterus (seen 22 times), lung (19), placenta (12), trachea (12), liver (11), kidney (10), leiomyosarcoma cell line (10) and 97 other tissues.

In EC, there is likely only one predominant mRNA (214 cDNA clones out of 233 cDNA clones support this mRNA species) and one protein generated of 663 aa, although post-translational processing may act on this protein. The possibility of other mRNA and their role in EC biology has not been investigated to date.

4.1.3 SENEX Protein

The protein produced by this gene, (ID = NP_277050.2) is Rho GTPase activating protein 18 and predicted to consist of 663 aa, with a molecular weight of 76.5 kDa and isoelectric point of 6.4. It belongs to the Ensembl protein family, ENSF00000002705 (AMBIGUOUS), which contains two other Ensembl gene members. One of these members (HUGO ID= C20orf95) is a putative RhoGAP domain containing protein fragment and the other (RefSeq ID= NM_030672) has no description recorded.

4.1.4 Predicted Motifs and Localisation

The most significant domain predicted to be contained within the protein is a RhoGAP domain found in 2 isoforms from this gene, (Pfam ID= PF00620, SMART ID = SM00324). In both isoforms this spans from 340 – 520 aa. There are seventy-two other genes in the (Pfam) database which also contain this RhoGAP motif, also known as the breakpoint cluster region-homology (BH) domain (Figure 4.2).

According to Psort2, the most likely localization of the protein is in the nucleus (52%) or mitochondria (30%), but possibly in the cytoplasm (8%), cytoskeleton (4%) or secreted (4%). As the protein contains no signal peptides or transmembrane domains, it is unlikely the protein is secreted or directly inserted into the membrane.

Functionally, the gene has been proposed to participate in signal transduction because of its RhoGAP domain, although this has not been formally demonstrated. Furthermore the protein is proposed to localize to the cytoplasm but, since it has a potential nuclear localization sequence it may have the possibility of shuttling between these compartments

4.1.5 Publications

Until this year there were no published data detailing a functional role for *SENEX*. Details on *SENEX* had only been published in papers screening for polymorphisms in disease. So far *SENEX* has been found to contain a polymorphisms in patients suffering from amyotrophic lateral sclerosis [151] and imaging genetics found a single nucleotide polymorphism in schizophrenia[152]. The work contained in this thesis has been recently published in Blood. Our work is the first published data detailing a functional role for *SENEX* [153].

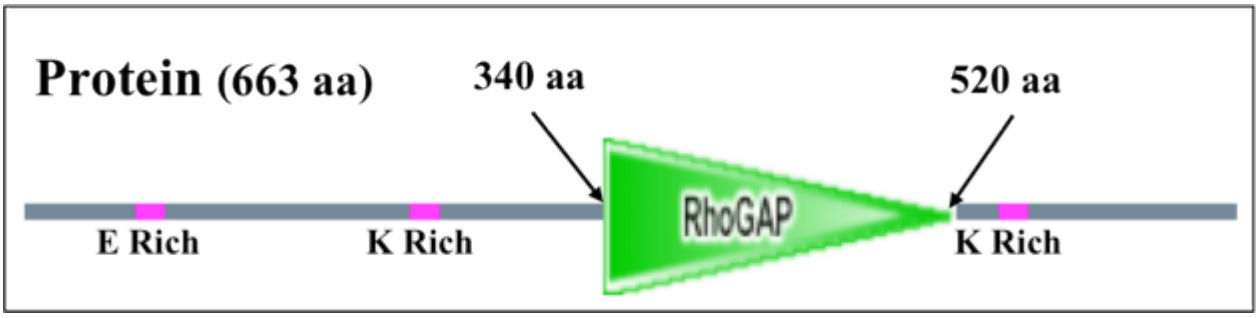

Figure 4.2 SENEX protein. The SENEX protein consists of 663 amino acids. It contains a RhoGAP domain between residues 340 and 520, two lysine-rich regions and a glutamate rich region. It contains no apparent transmembrane domain or signal peptide. The calculated molecular weight of the protein is 76.5kDa.

4.1.6 Preparation of SENEX constructs and adenovirus

SENEX constructs and adenovirus was prepared in the same manner as was described in Chapter 3 for REST and were prepared by Dr Chris Hahn. An assay to determine the tissue culture infectious dose 50 ($TCID_{50}$) was performed by titrating adenovirus in HEK293 cells. The $TCID_{50}$ values for each adenovirus, as shown in table 4.1, relate to the number of plaque forming units (viable virus particles) per ml (pfu/ml).

In addition to determination of $TCID_{50}$ assay, a titration of SENEX adenovirus in HUVECs was set up to determine infection efficiency as well as the strength of the CMV promoter by measurement of mean GFP production. This is important to determine the relative level of gene expression in infected cells so that comparisons between constructs may be made in functional assays. The level of GFP production in infected HUVECs after 48 hours was measured by flow cytometry analysis. The percentage of cells expressing GFP was determined for each construct to give an approximate level of infection of HUVECs (Figure 4.3). The adenoviral delivery system is quite efficient, and titres were determined which resulted in approximately 98-100% infection, with similar mean GFP levels. It should be noted that the mean GFP levels could be increased by increasing the MOI to a level that the adenovirus itself causes the cells to die.

Multiplicities of infection (MOI) was calculated in order to relate levels of infection of cells to the literature. MOI for each construct as shown in table 4.1, were calculated by converting pfu/ml ($TCID_{50}$ value) to pfu/cell. This was then multiplied by the 'HUVEC titre' value (µl), to give the ratio of infected cells with respect to the number of cells transfected.

However, subsequent to this we have prepared another 3 batches of virus and they all produce the same phenotype in the EC.

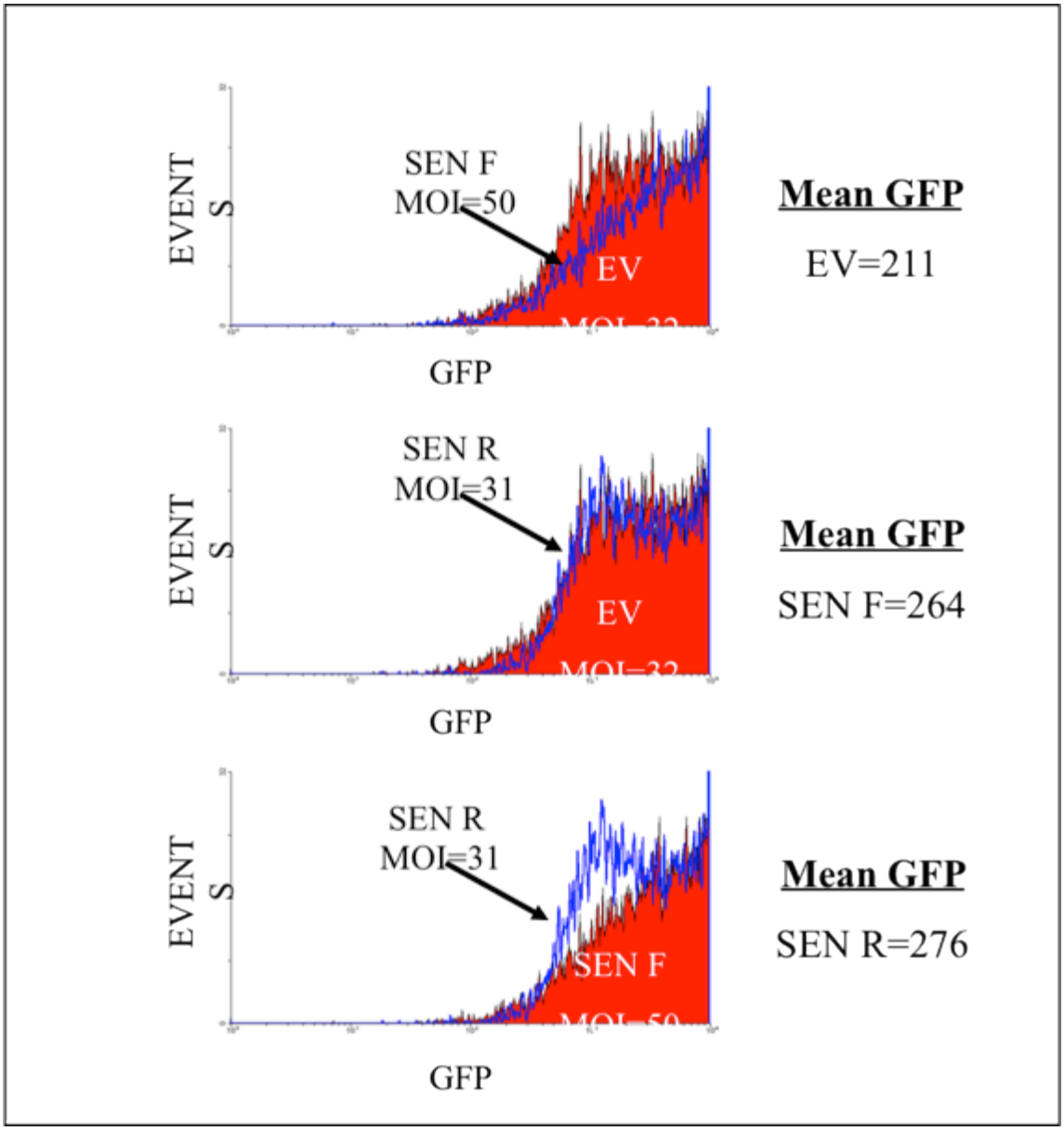

Figure 4.3. GFP expression levels of recombinant adenoviruses. The histograms show GFP expression levels, obtained by FACS analysis, of infected HUVEC. EV refers to pAEATG empty vector, SEN F to SENEX sense, and SEN R to SENEX antisense. Results show that mean GFP levels were quite comparable between the different adenoviruses.

Table 4.1 $TCID_{50}$ and MOI Values for Recombinant Adenovirus

Adenovirus	$TCID_{50}$ (pfu/ml)	MOI
SENEX F-myc	1.3×10^{10}	88
SENEX F (wild type)	1.4×10^{10}	81
SENEX R	1.58×10^{10}	47
EV (control)	3.16×10^{10}	48

Knockdown or overexpression of the gene was achieved by adenoviral infection of either antisense or sense constructs in EC, respectively. Essentially, HUVEC (passage 3 or 4) were infected with adenovirus containing the gene of interest, full length SENEX with (SENEX F-myc) and without myc tag (SENEX F-wild type) and antisense (SENEX R) orientations, as well as a control, pAEAT empty vector (EV). HUVEC were harvested 48 hours after infection. An aliquot was used for GFP measurement and the rest used for the desired assays. A description of the effects of knockdown of SENEX is given in Chapter 5.

4.2 Determination of SENEX expression.

The pAEATG-SENEXF-myc and EV adenovirus was used to determine whether overexpression of SENEX was achieved. HEK293 cells were used initially and lysates from EV (pAEATG) infected cells as a control. Lysates were run on a 12% SDS-PAGE gel and SENEXF-myc was detected with an anti-myc antibody. As seen in Figure 4.4, SENEXF-myc was highly expressed as compared to the control. It also showed a protein of approximately 76 kDa, similar to that predicted from the sequence (including myc tag). This work was completed by Milena Babic. This was repeated with HUVECs and a similar result obtained. The protein was found to be around 80kD.

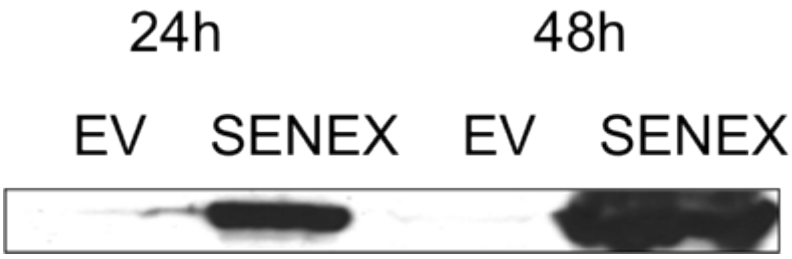

Figure 4.4. Western blot of SENEXF-myc using an anti-myc antibody. Cell lysates at 24 and 48 hours of EV and SENEXF-myc infected HEK293 cells were run on 12% SDS-PAGE gel, and a Western blot carried out using an anti-myc antibody, then detected using the Amstersham ECL kit. The protein detected was 76Kd.

4.2.1 SENEX antibody

The antibody to SENEX was raised in rabbits against the whole SENEX protein and was affinity purified. Western blots using the antibody against the purified protein and cell lysates showed that SENEX runs as an approximate 80kd protein with detection of 1 or 2 smaller proteins, which have not been identified but are presumed to be breakdown products. The increase in size of the detected protein from the predicted size of 75kD is likely a result from post translational modification. We are confident that the rabbit antibody is detecting SENEX since it detects similar sized products as that seen with the anti-myc antibody from cells infected with the SENEX-myc tagged construct

4.3 SENEX overexpression induces a unique phenotype in EC

In HUVECs using the adenovirus system for gene delivery we routinely achieved overexpression of 5-10 fold after 24hours and 15-25 fold after 48hours (Figure 4.5) compared to basal levels of SENEX. The change in protein expression was consistent over 5 HUVEC lines and when using two different batches of virus. During capillary tube formation SENEX expression increases by 2.5 fold at the 24 hour timepoint. We are therefore increasing SENEX expression by a much greater degree when adenovirus is used.

4.3.1 SENEX overexpression has no effect on capillary tube formation

To determine whether overexpression of this protein influences angiogenesis we performed the *in vitro* capillary tube formation assay on Matrigel. The cells were harvested 24 hours after infection and then plated onto Matrigel. They aligned and formed capillary tubes to the same extent as the control cells and the timing of tube formation was also not altered, (Figure 4.6), suggesting that SENEX overexpression did not alter tube formation.

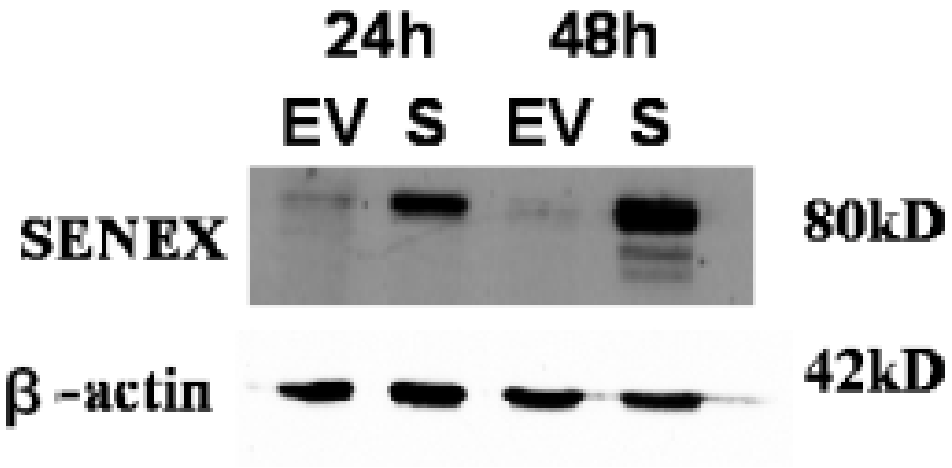

Figure 4.5. Western Blotting of SENEX overexpression using the SENEX antibody. Expression levels of SENEX protein in HUVECs at 24 and 48 h after infection with EV (EV) or *SENEX* (S) adenovirus and detected by western blot analysis using anti-SENEX antibody. Protein molecular masses (in kD) appear on the right. This is a representatative of 5 experiments

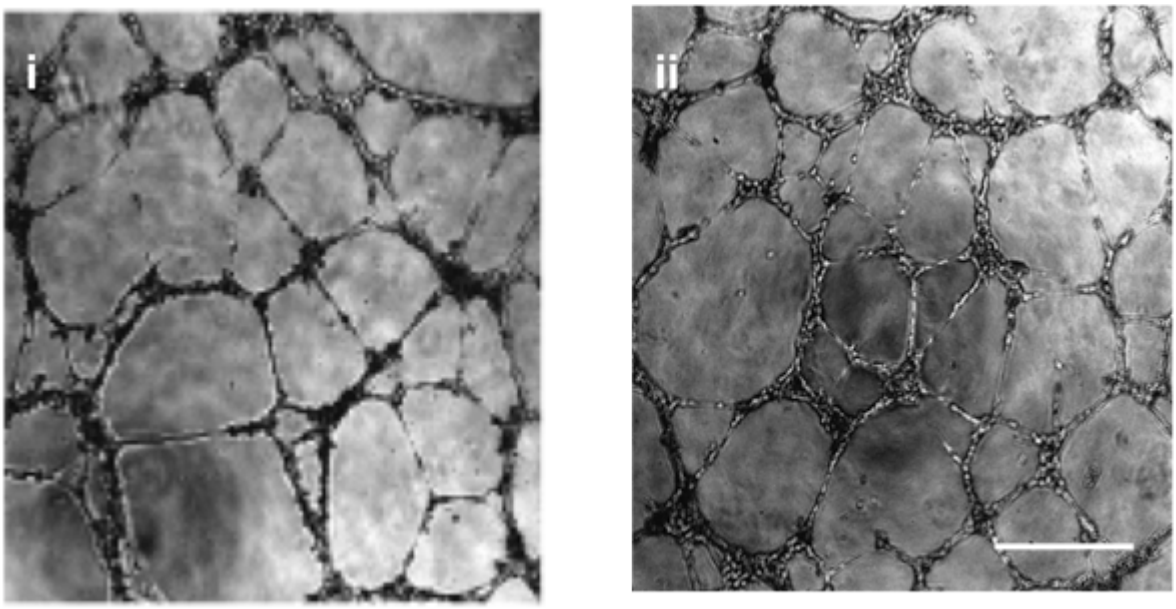

Figure 4.6. Effect of SENEX overexpression on Matrigel tube formation. HUVECs were infected with EV (i) or *SENEX* (ii) containing adenovirus. After 24 h cells were plated onto Matrigel, and capillary tube formation was observed over a 24 h time course. Photographs taken 12 h after plating are shown. This is a representative of 3 similar experiments performed. Bars =100 μm.

4.3.2 SENEX overexpression alters EC phenotype

Growth of the SENEX overexpressing cells however did result, after 2-3 days, in a substantially changed morphology of the cells. In comparison to the normal HUVECs infected with EV, the cells overexpressing SENEX became flattened and large cells were observed which contained large vacuoles and exhibited polyploidy, judged using DAPI staining of the nuclei (Figure 4.7).

4.3.3 The SENEX overexpression phenotype is not adenoviral dependent

One possibility is that the phenotype generated through the use of the adenovirus is due to the combination of the gene and the adenovirus. Therefore SENEX overexpression was also achieved through plasmid transfection. SENEX-3'myc was cloned into the mammalian expression vector, pcDNA3.

Creation of these constructs was performed as follows (refer to Figure 4.8). SENEX-3'myc was excised from pEG-SENEX-3'myc (full length, sequenced) with *EcoR* I and inserted into the unique *EcoR* I site in pcDNA3 to create pcDNA-SENEX-3'myc. *EcoR* I digestion was performed to check for the insert. An *Xho* I/ *BstE* II digest was also conducted in order to confirm orientation of the insert, and purified plasmid containing the insert in both sense and antisense orientations, as well as pcDNA3, were prepared in large scale. Plasmids were then purified using Qiagen EndoFree Plasmid MAXI kit as described in the manufacturer's manual, ensuring that all equipment, tips and tubes used were endotoxin free. Endotoxin removal is important for nucleofection into HUVEC, as they are sensitive to endotoxin (a bacterial toxin responsible for pyrogenic fever). All DNA was quantified by spectrophotometry and redigested to confirm authenticity prior to nucleofection into HUVEC. Constructs were then nucleofected into HUVEC using the Amaxa HUVEC (Vs.2) Nucleofector™ Kit.

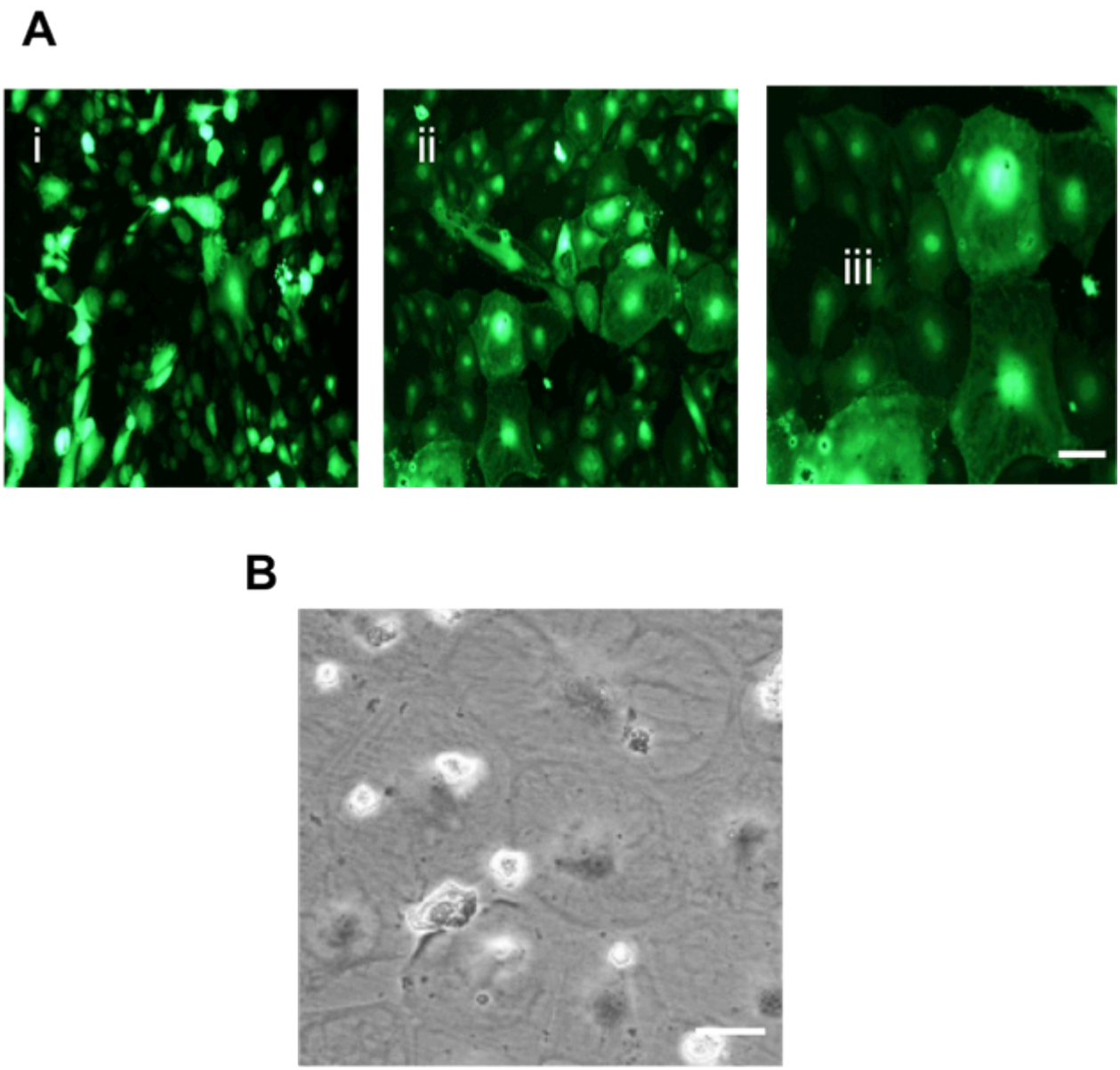

Figure 4.7. SENEX overexpressions effect on the EC phenotype. (A). HUVECs were infected with EV (i) or SENEX (ii) containing adenovirus. Infected cells are visualized with green fluorescent protein (GFP). Photographs were taken after 48 h. Bar=220 μm. (iii) Enlarged area of cells from (ii). Bar=80 μm. **(B).** Phase contrast photograph of a number of enlarged cells. Bar=80 μm

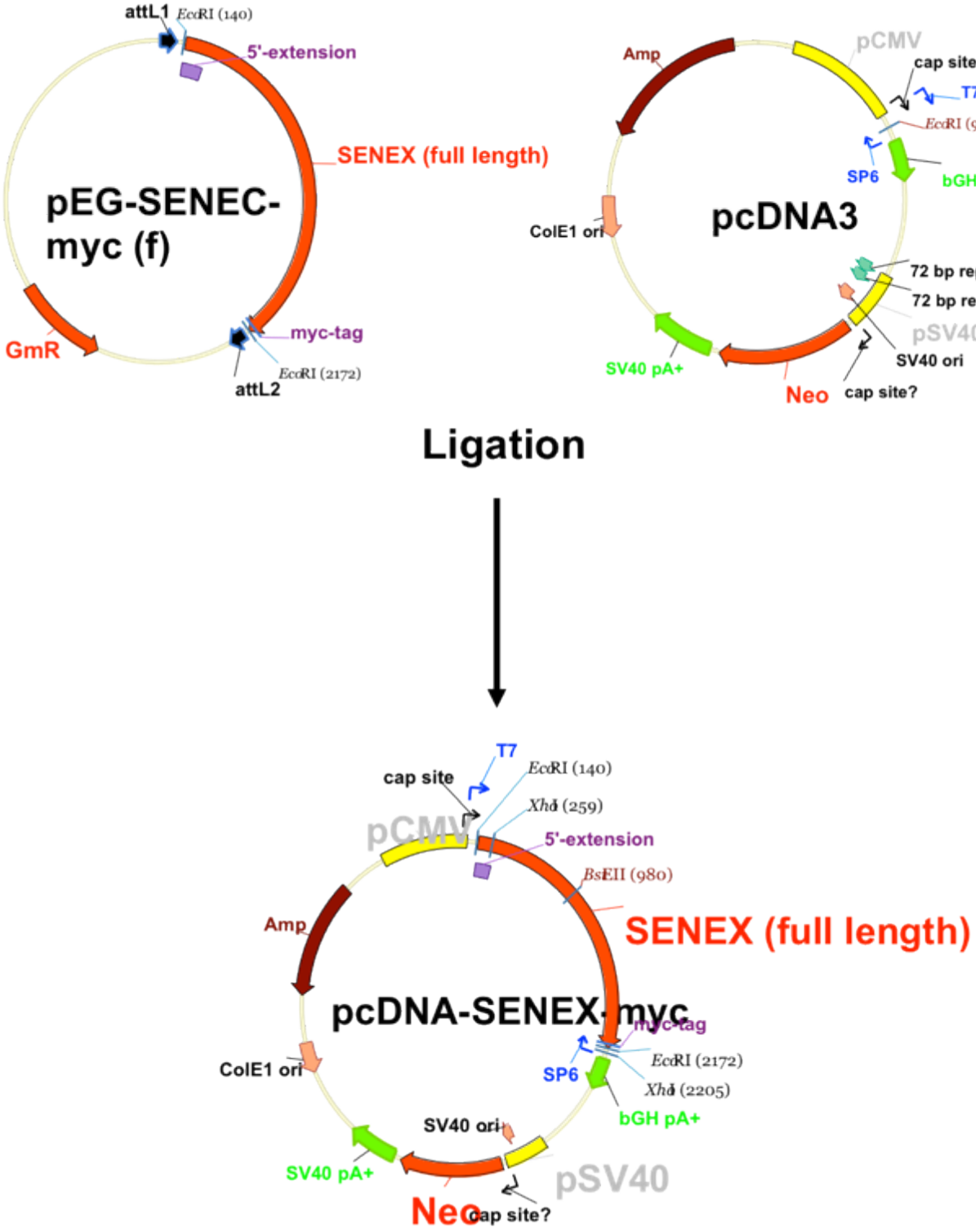

Figure 4.8. Generation of pcDNA-SENEX construct. pEG-A18-3'myc(f) and pcDNA3 were *EcoR* I digested and purified fragments were ligated together to produce pcDNA-SENEXmyc in both sense and antisense directions (only the sense orientation is depicted above). Plasmids were then amplified and purified, including endotoxin removal before being nucleofected into HUVEC.

After 24-48 hrs a large flattened morphology was seen in the cells successfully transfected with SENEX. Thus, the induction of the large flattened cells was independent of the use of adenovirus (Figure 4.9). For the remainder of the experiments adenovirus will be used because of its superior ability to infect nearly 100% of the cells compared to about 5-20% for plasmid transfections.

4.4. Confirmation that the morphological changes are a senescent cell

The change in phenotype with SENEX overexpression was reminiscent of senescent cells. The characteristics of senescent cells are a large flattened morphology, polyploidy, resistance to cell death, irreversible exit from the cell cycle. The classic marker used to identify senescent cells is β Galactosidase and is known as senescence-associated β-galactosidase activity (SA-β-gal), [2]. SA-β-gal enables the detection of increased lysosomal β-galactosidase evident in senescent cells at a pH 6.0. It is visualised by means of a cytochemical reaction which stains cells blue. Although its function is unknown, β-gal is generally accepted as a marker of senescence *in vitro* and *in vivo*.

4.4.1 Senescent-associated β-Galactosidase staining

The SA-β-gal assay was performed *in vitro* as described previously by Dimri (1996). Infection with SENEX adenovirus significantly increased the number of HUVECs with SA-β-gal activity compared with the EV (Figure 4.10A). In 4 experiments performed the numbers of SA-β-gal positive staining cells were counted and the percentage positive was calculated based on the number of total cells. In SENEX overexpressing cells the number of positive staining cells peaked at 48 hrs at approximately 12% compared to 5% in the EV (Figure 4.10B).

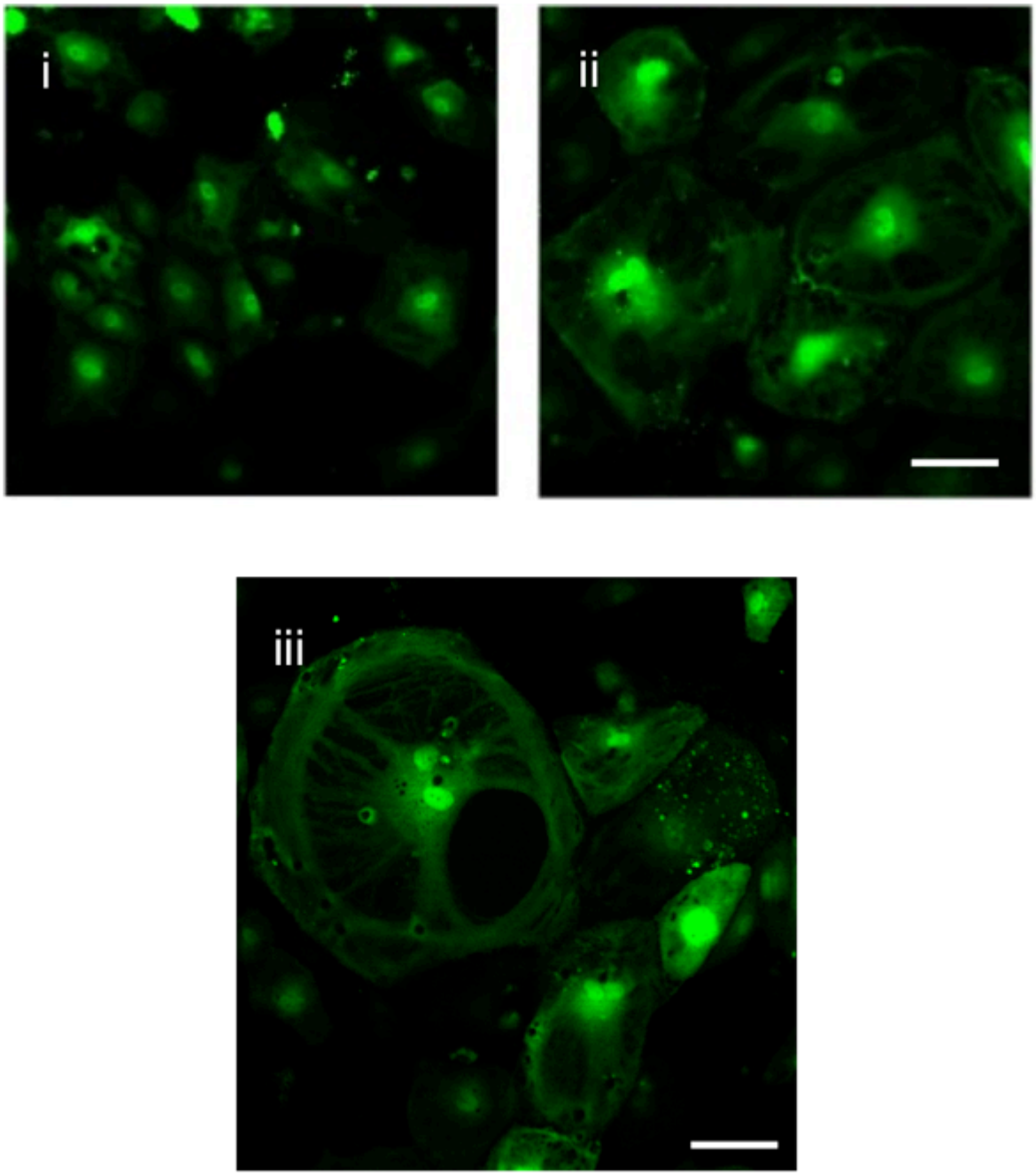

Figure 4.9. Overexpression of SENEX with plasmid transfection. HUVECs were transfected with control (i) or SENEX (ii) expressing plasmid using Amaxa nucleofector kit. Bar=100µm. (iii) Senescent cells induced by transfection of a plasmid containing *SENEX*. Bar=100µm

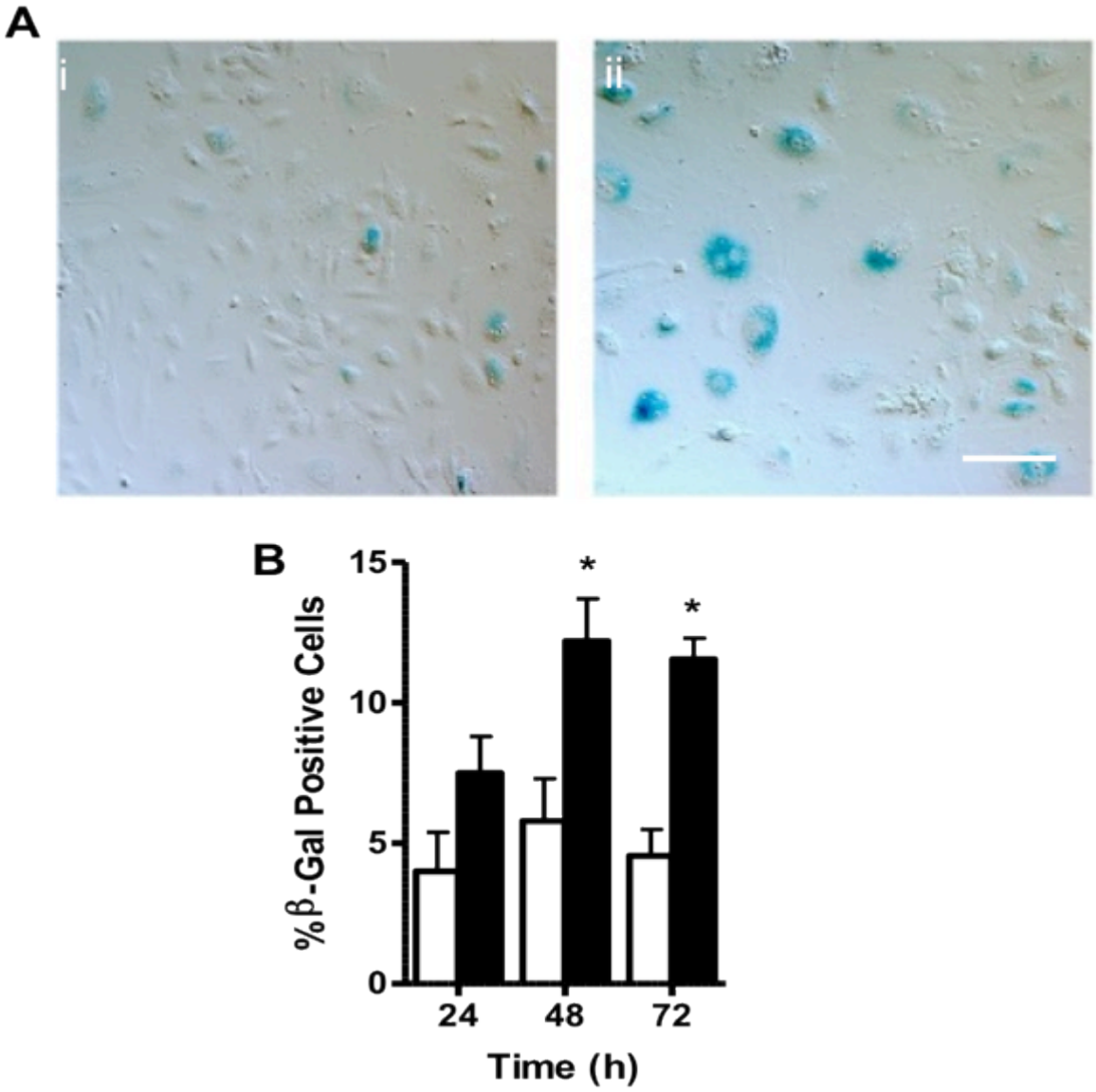

Figure 4.10. SENEX overexpressing ECs stained for the senescence marker, Senescent Associated β- galactosidase. (A). HUVECs were infected with EV (i) and SENEX (ii) adenovirus for 72hrs. The cells were then fixed and stained SA-β-Gal for 24 hrs. The blue staining represents cells positive for SA-β-Gal. Photographs were then taken at 20x magnification. The photographs are a representation of 4 separate experiments. Bars =220 μm **(B).** EV (white bars) and SENEX (black bars) overexpressing cells were harvested after 24, 48 and 72 h of culture and stained for SA-β-gal expression. At least 1000 cells on each day were counted. The percentage of cells positive for SA-β-Gal +/-SEM is given for 3 different HUVEC lines analysed. *p<0.05 compared to EV.

4.4.2 Cell Cycle arrest

Senescent cells also enter a state of permanent growth arrest and the cells are normally trapped in the G1 phase of the cell cycle [154]. ECs were infected with EV and SENEX adenovirus for 24 hours and then reseeded at the same confluence in normal growth factor and medium. Using MTS to determine the number of the ECs after 3 days we found, there was a 61 ± 4% inhibition in cell proliferation after SENEX overexpression compared to EV (Figure 4.11). We also looked at which stage of the cell cycle SENEX overexpression was able to stop EC proliferation. ECs were infected with EV and SENEX adenovirus at a very low confluence. After 24 hours when the cells are still sub confluent and proliferating they were harvested and stained with propidium iodide to detect what stage of the cell cycle the cells were in. After analysis by flow cytometry (Figure 4.12), we observed an increase of 5.8+/- 2% in cells in the G1 phase and a 3+/-1% decrease in the S and G2 phases confirming the cell cycle arrest is at the G1 phase, as would be expected. The results are not statistically significant but with only a small number of cells been senescent at this time we would only expect a small increase in the number of cells halted in the G1 stage. Further experiments are needed at later timepoints to determine if all the senescent cells are stuck in the G1 phase of the cell cycle.

4.4.3 eNOS expression

Senescent EC have been reported to show decreased expression of the endothelial specific nitric oxide synthase, eNOS [128]. SENEX induced senescent cells also showed decreased eNOS expression when measured by western blotting after 48 hours of infection (Figure 4.13).

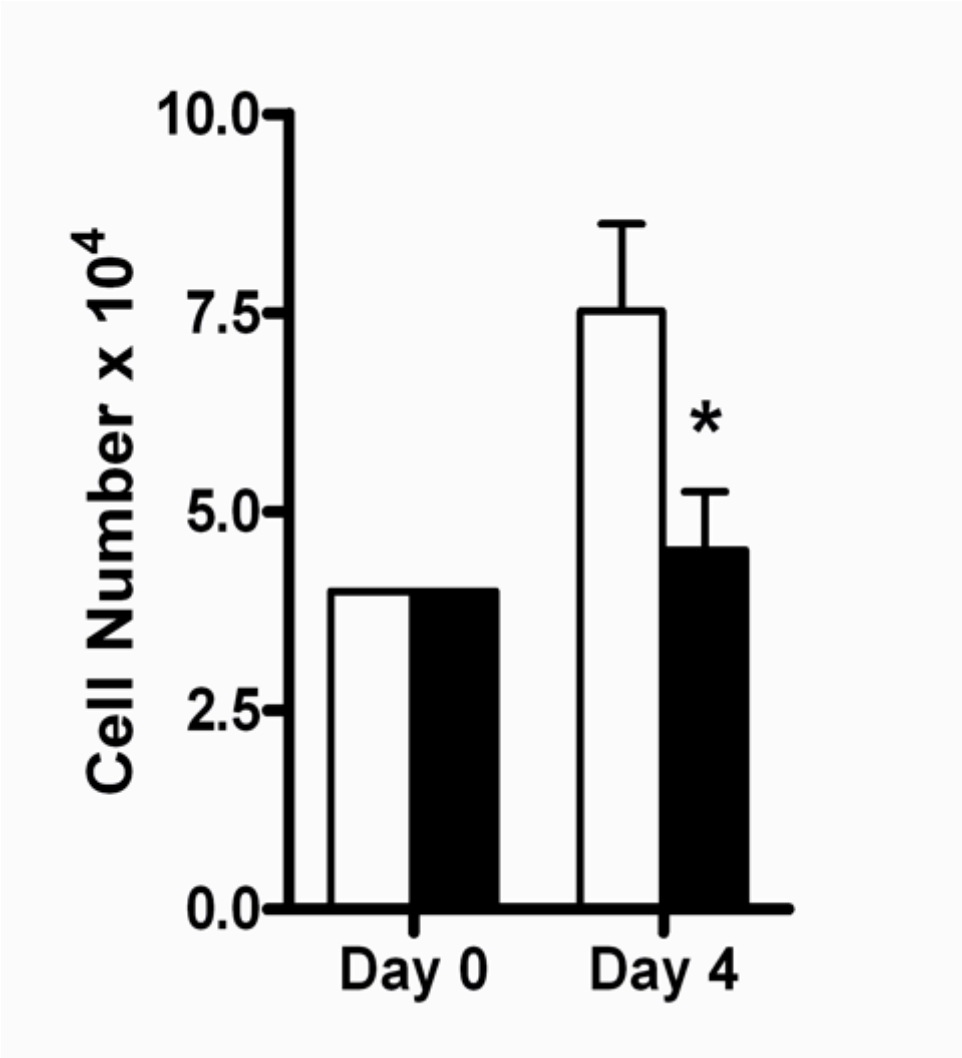

Figure 4.11. Regulation of EC proliferation by SENEX overexpression. HUVECs infected with EV (white bars) or SENEX (black bars) containing adenovirus were assessed for cell proliferation after 3 days using the MTS assay. OD490nm for cells at Day 0 and Day 3 are given. Results are the mean +/-SEM of 4 replicates of each group. This is a representative of 3 experiments, * $p<0.05$ compared to EV on Day 4.

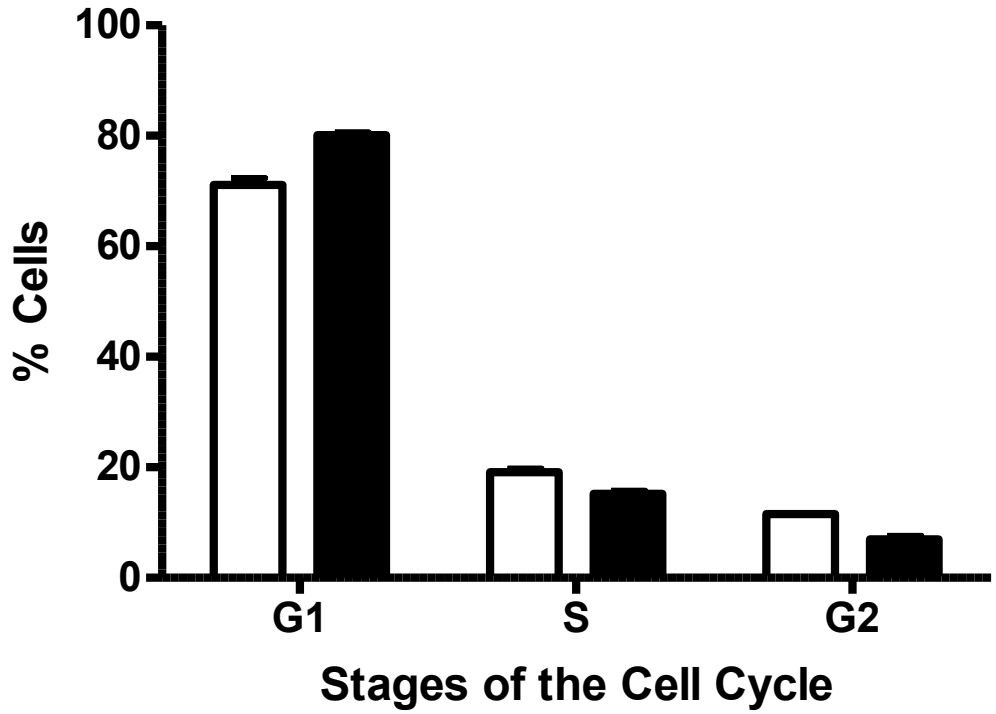

Figure 4.12. Determination of the stage in the cell cycle of ECs overexpressing SENEX. EV (white bars) and SENEX (black bars) overexpressing cells were harvested after 24h then fixed with 80% methanol and stained with propidium iodide and flow cytometry was performed to determine the cell cycle status of the cells after infection. The results are a combination of 3 individual HUVEC lines.

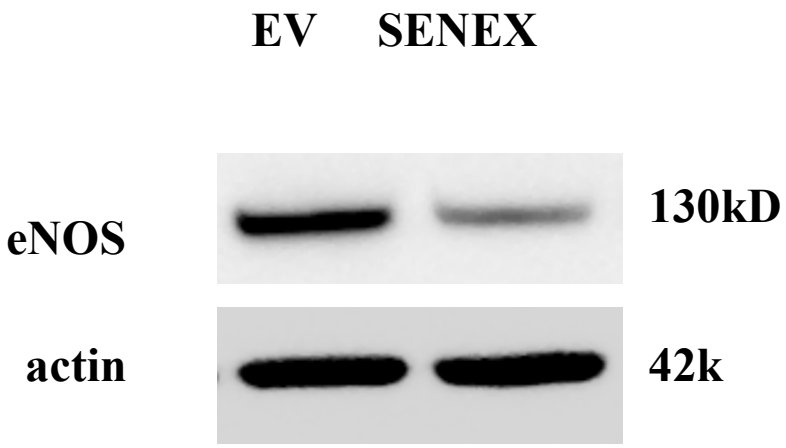

Figure 4.13. Regulation of eNOS protein expression by SENEX. HUVECs were infected with SENE*X* and EV adenovirus for 48 h. Total protein was used for western blotting with a eNOS antibody. β-actin was used as a loading control. This is a representative of 3 experiments.

4.4.4 Resistance to Apoptosis

Senescent cells have been found to be resistant to apoptotic stimuli [155]. ECs overexpressing SENEX showed increased survival under growth factor deprivation. Cells survived in the cell culture flask for over a month without any addition of new media or growth factors (Figure 4.14). This is in contrast to cells infected with EV which became apoptotic after 7 days if no new media containing growth factors was added to the cells.

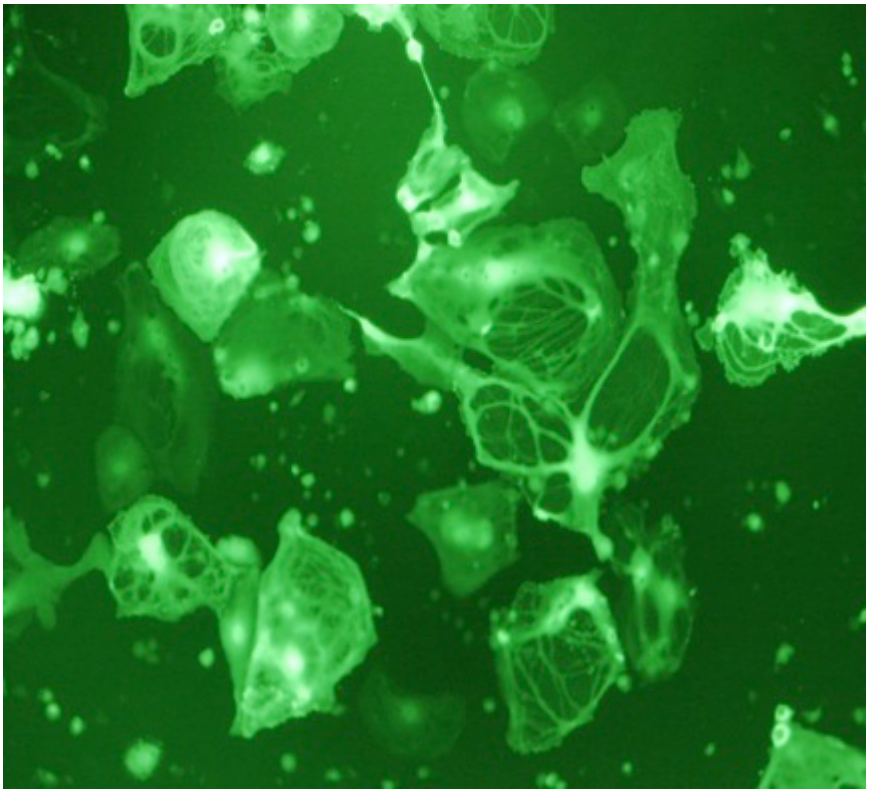

Figure 4.14. Effect of SENEX overexpression on EC apoptosis from growth factor deprivation. HUVECs were infected with SENEX and EV adenovirus. The cells were then left for 40 days without splitting or media change. The cells above are senescent cells which are overexpressing SENEX and are still alive after the 40 day period. There are no photographs of the EV overexpressing cells as these have all died.

Thus, on the basis of morphology, expression of β-gal, cell cycle arrest, longevity of maintenance in culture and eNOS downregulation, overexpression of SENEX induces senescence in EC.

4.4.5 Timecourse of morphological change

To determine a timecourse of the development of the altered morphology, HUVECs were infected with adenovirus and then photographed over 72hrs (Figure 4.15). The number of senescent cells, based on morphology and a percentage was calculated based on total cell numbers. Approximately 34% of the cells had a senescent morphology compared to 11.5% in the EV (Figure 4.16) after 72hrs. The percentage of cells that become senescent did slowly increase with further time and we found that the non senescent cells began to die after this point, especially in the EV infected cells. For this reason 72hrs was the limit for which we extended experiments when looking at the effects of SENEX overexpression. Senescent cells are known to have multi nuclei and for this reason cells overexpressing SENEX were stained with DAPI to highlight the nuclei (Figure 4.17A). We then counted the number of cells which became polyploidy and a percentage was calculated based on total cell numbers (Figure 4.17B). After 72 hours approximately 25% of the total cells were multi nucleated in the cells overexpressing SENEX compared to 12% of the total cells in the EV. The increase in SENEX overexpressing cells was not as high as when we counted based on morphology most likely because not all senescent EC exhibit polyploidy. At the time point chosen we did not observe any heterochromatin foci present in the senescent cells.

4.4.6 The senescent phenotype is not dependent on the RhoGAP domain in SENEX

SENEX is a member of the RhoGAP family of proteins. Rho GTPases are a subgroup of the family of Ras GTPases, which also includes the small G proteins Ras, Rab, Arf and Ran. GTPases act as molecular switches which cycle between an active, GTP-bound form and an inactive, GDP-bound form in response to extracellular stimuli. They mediate a number of

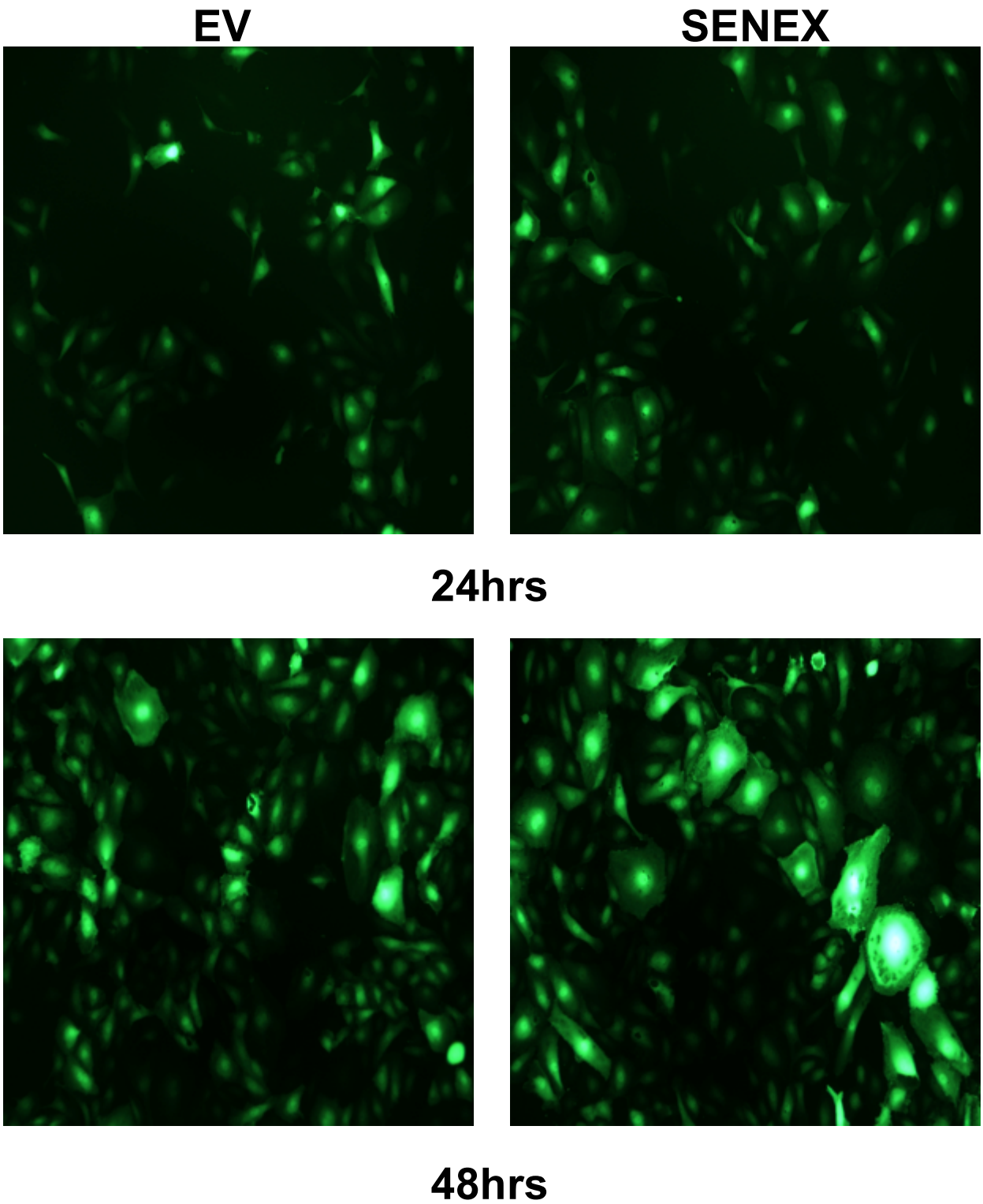
EV
SENEX
24hrs
48hrs

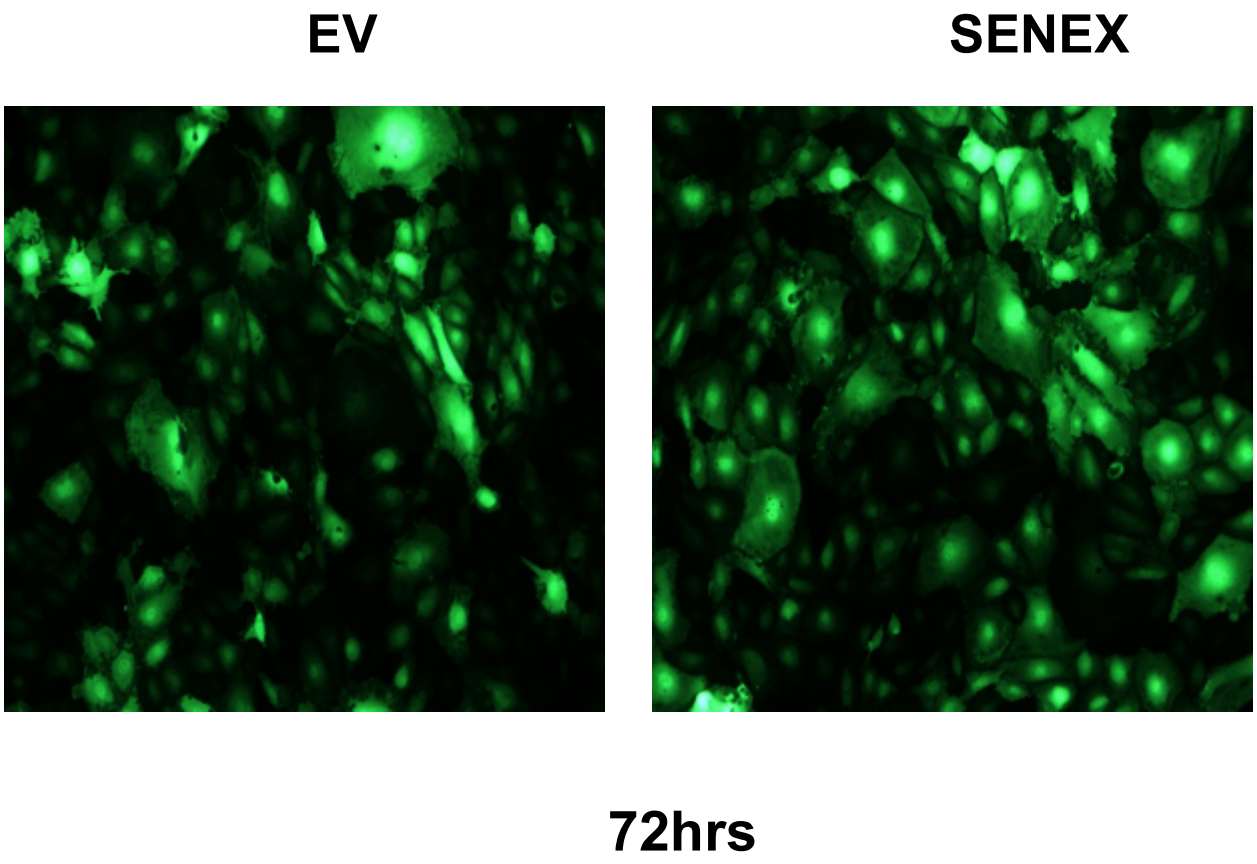

Figure 4.15. Timecourse of senescence development after SENEX overexpression. HUVECs were infected with EV and SENEX adenovirus. The cells were then visualised over a 72 hr

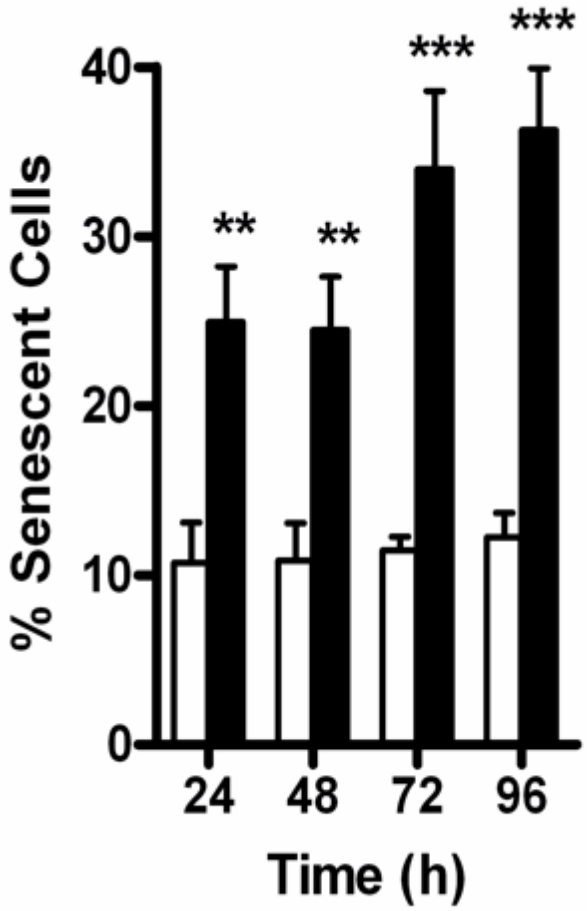

Figure 4.16. Timecourse of senescence development after SENEX overexpression quantification. HUVECs were infected with EV (white bars) or SENEX (black bars) containing adenovirus. Photographs were taken at 24 h time intervals for 4 days. The number of senescent cells, based on an enlarged morphology, were counted and presented as a percentage of total cells counted. At least 1000 cells were counted for each of the three individual HUVEC lines. The mean +/-SEM is shown. ** $p<0.01$ and *** $p<0.001$ compared to EV.

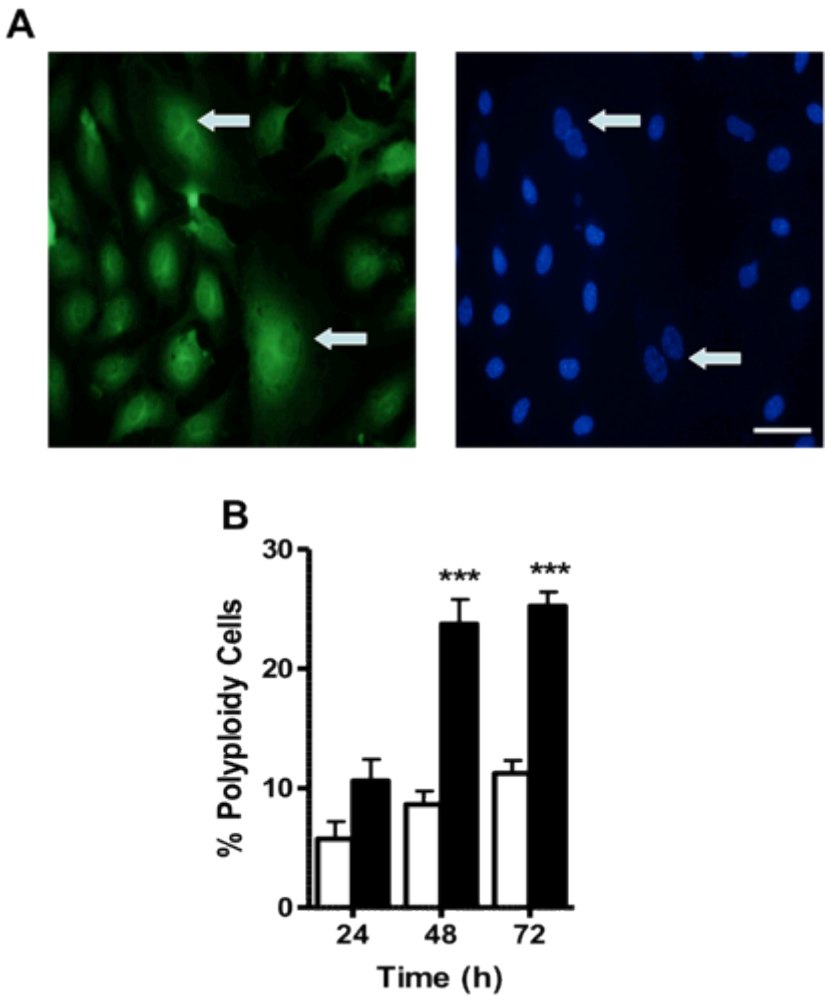

Figure 4.17. Quantification of the number of polyploidy cells after SENEX overexpression. **(A).** HUVECs were infected with SENEX containing adenovirus. The cells were stained with DAPI every 24 hrs for the next 3 days. Left photo shows the cells at 24 hrs with the GFP field with cells exhibiting polyploidy marked with an arrow. DAPI stain is shown in the right photo. Bar=100um. **(B).** SENEX overexpression induces polyploidy. HUVECs infected with EV (white bars) or SENEX (black bars) containing adenovirus and were assessed for polyploidy. At least 1000 cells were counted each day in each group for each of 3 individual cell lines and are presented as a percentage of senescent cells. The mean+/- SEM is shown. ***$p<0.001$ compared to EV.

complex signal transduction pathways in response to extracellular stimuli, including reorganisation of the actin cytoskeleton to cause changes in cell shape polarity, migration, adhesion and proliferation, membrane trafficking and vesicular transport, gene transcription, apoptosis, cell survival and enzymatic reactions including NADPH oxidase production [156, 157]. To determine whether the GAP domain is essential for SENEX induced senescence, an R365A mutant was generated. A single amino acid mutation changed an arginine to an alanine in the GAP domain. The positive charged alanine is crucial for the RhoGAP activity and by changing it to a neutral alanine the mutation eliminated the Rho activity (data not shown). However, overexpression of this mutant protein with adenovirus was still able to confer the senescence phenotype on ECs (Figure 4.18), suggesting that the GAP domain is not essential for this aspect of its function. We are currently looking at creating different mutations of SENEX in an attempt to determine the senescence induction domain of the protein.

4.5 SENEX does not induce replicative senescence

There are two broad forms of senescence, replicative and stress induced senescence. Replicative senescence (RS) is mediated through the shortening of telomeres that occurs during each cell division. This shortening eventually registers as DNA damage and triggers ATM activation and initiates a program of cell cycle arrest. Stress induced premature senescence (SIPS) is induced by oncogene activity, oxidative stress, or suboptimal culture conditions and occurs independent of a change in telomere length [158].

Overexpression of *SENEX* induced senescence within 24 hours using gene delivery through adenovirus or by transient transfection. Given the rapidity of induction of senescence with SENEX in EC, it was unlikely that it was a replicative form of senescence and this was confirmed using two criteria.

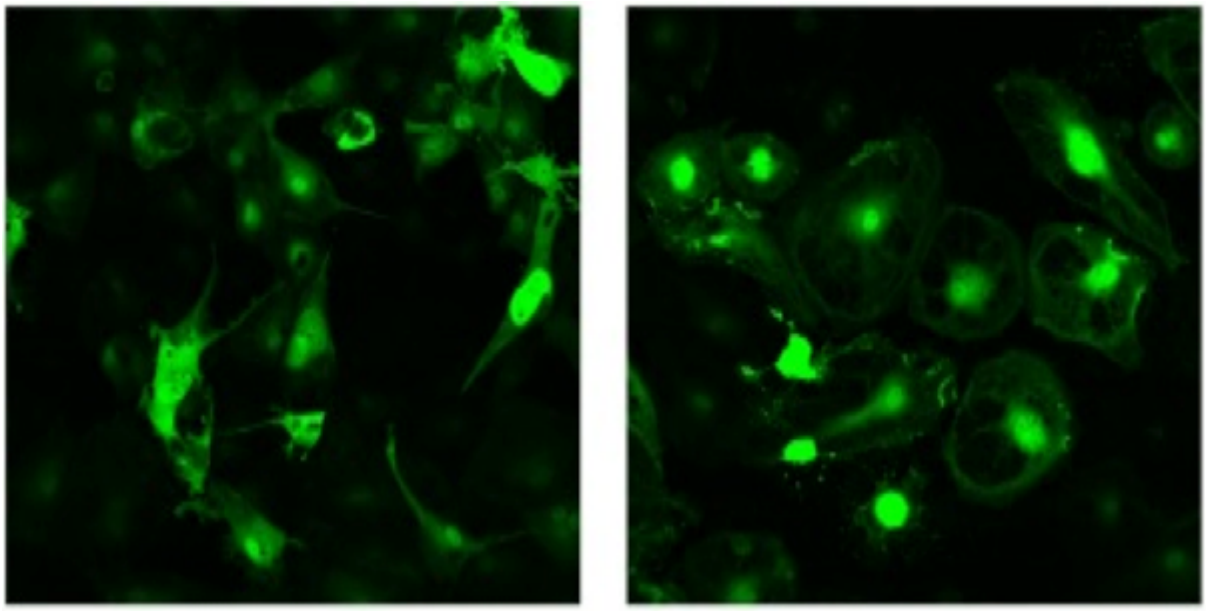

Figure 4.18. Overexpression of SENEX containing a mutation of the RhoGAP domain. HUVECs were infected with SENEX -R365A mutant construct and EV containing adenovirus. Cells were visualized 48 h after infection. Large flattened and vacuolated cells were seen in the SENEX mutant overexpressing cells (red arrows) and at a similar frequency to the wild type SENEX. Bar=220μm

4.5.1 SENEX does not alter telomere length

A shortening in telomeres after *in vitro* passaging of cell lines is the cause of replicative senescence. Telomeres are sequences - $(TTAGGG)_n$ - that cap the ends of linear chromosomes and maintain the stability of the genome by preventing DNA ends from degradation and recombination [159]. Under normal conditions, DNA base pairs are lost from the telomeric ends of each chromosome with every round of cell division. Telomeres eventually reach a critical minimum length and cell division is inhibited to prevent the chromosomes from becoming dysfunctional. A DNA damage response is initiated and cells are induced to stop dividing permanently [160]. Firstly we investigated telomere length by Southern blot analysis in SENEX induced senescent ECs. We found that even at 72 hours after infection with SENEX there was no change in telomere length compared to EV, even though at least 35% of the cells had become senescent as judged by a change in morphology (Figure 4.19).

4.5.2 SENEX overexpression does not induce a replicative senescence gene profile

We then induced replicative senescent ECs by repeatedly passaging the cells. EC were maintained under subconfluent conditions at all times and were passaged every 3–4 days. In general the cells become senescent after 15-20 passages. We used 4 different HUVEC lines. They all took on the enlarged flattened senescent morphology and were stained with SA-β-gal. There was a significant increase in senescent cells after 20 passages compared to endothelial cells passaged twice (Figure 4.20). These replicative senescent cells also displayed increased expression of 3 genes considered markers of replicative EC senescence, PAI-1[161], IL1-α[162] and cyclooxygenase-2 (COX2)[163]. However there was no concurrent increase in SENEX expression (Figure 4.21A). There was also no significant change in the expression level of these same genes in SENEX induced senescent EC (Figure 4.21B). The experiment was only performed twice so further experiments may be needed to conclusively say that SENEX does not

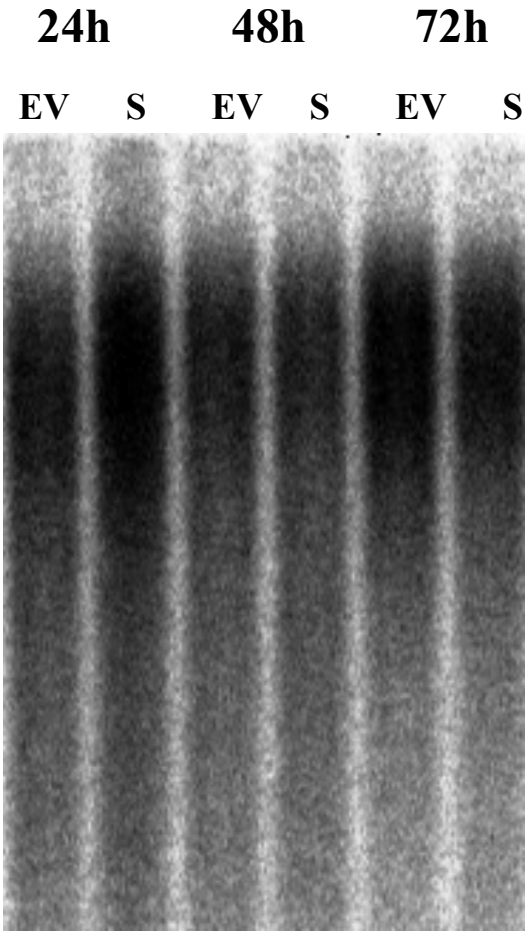

Figure 4.19. Measurement of telomere length in ECs after SENEX overexpression. HUVECs were infected with *SENEX (S)* or EV (EV) containing adenovirus. Cells were harvested after 24, 48 and 72 h of culture and telomere length was measured by southern blot analysis.

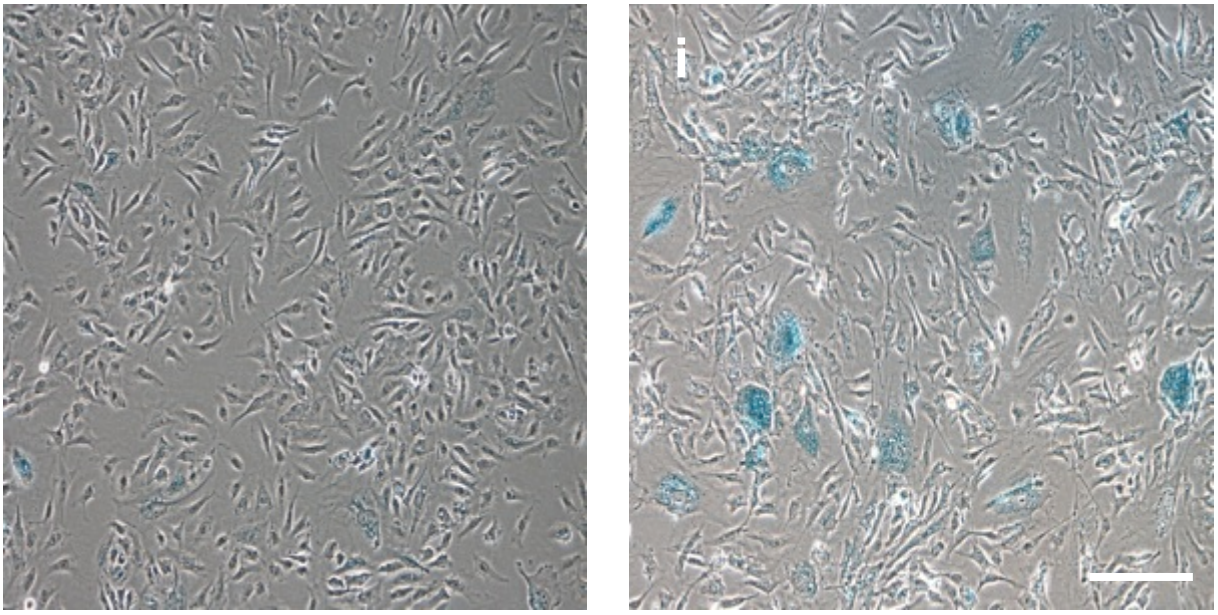

Figure 4 20. Induction of replicative senescence in ECs. Replicative senescence in HUVECs was induced through constant passaging of the cells. After 20 passages (ii) the cells stained positive for the senescent marker β-galactosidase compared to cells only passaged twice (i) which did not stain. The positive staining confirmed we had induced replicative senescence. Bar= 220 μm

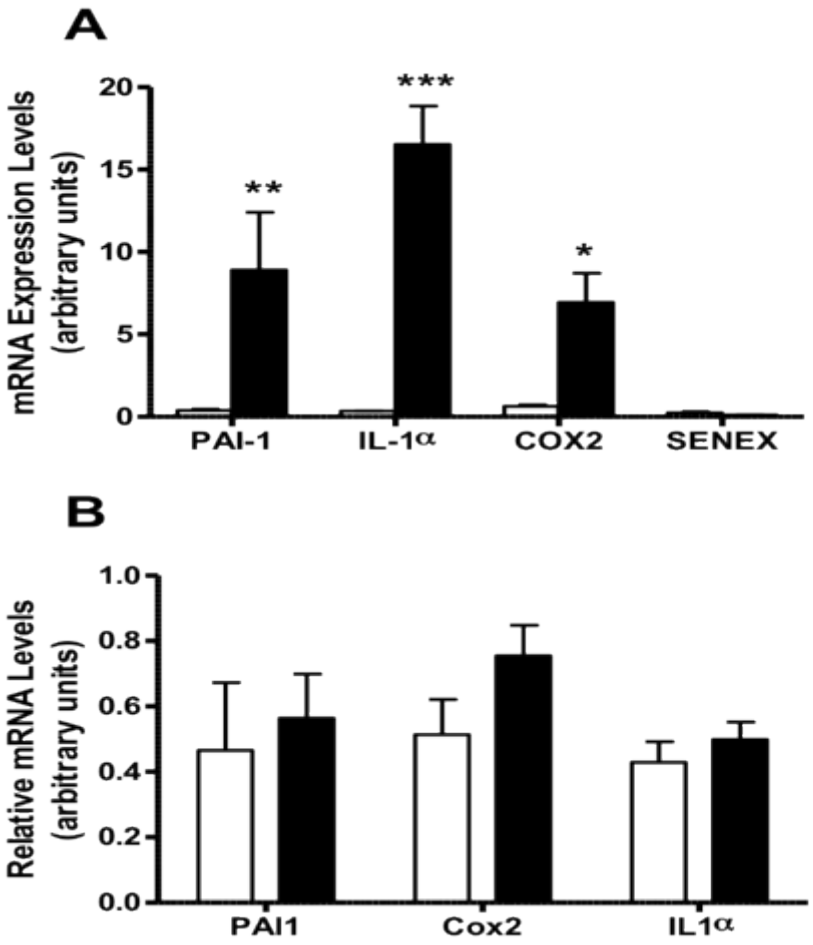

Figure 4.21. Role of SENEX in replicative senescence. (A). Replicative senescence in HUVECs was induced through constant passaging and the cells were harvested when the senescent morphology was evident in the majority of cells. mRNA expression was measured by Q-RT-PCR of COX2, IL-1α, PAI-1 and *SENEX* and standardized to cyclophilin *A*. The mean +/-SEM of 6 replicates from two lines of HUVECs is shown. Early passage cells (white bar) and late passage senescent cells (black bar). *** $p<0.001$ compared to early passage. **(B).** HUVECs were infected with *SENEX* (black bars) and EV (white bars) containing adenovirus. After 2-4 days when at least 50% senescence was seen, the cells were harvested and mRNA levels determined for PAI-1, COX-2 and IL-1α by Q-RT-PCR. There were no significant differences seen between the EV and *SENEX* groups. This is a representative of the mean +/-SEM of 2 experiments performed.

regulate these genes. Together these results suggest that SENEX overexpression is not causing replicative senescence. Given the rapidity of induction of the senescence phenotype we would suggest that this is an example of stress induced premature senescence (SIPS) and not replicative senescence.

4.6. SENEX induces Senescence through the p16 pathway

There are currently two signaling pathways known to be involved in senescence formation in either the RS or SIPS. They involve the p16/pRb pathway and the p53/p21 pathway [155].

4.6.1 SENEX regulates p16 and pRb expression

To determine the potential pathway through which SENEX induces senescence, mRNA arrays were performed on known cell cycle genes. Cells were taken at 24 and 72 hrs after infection, at a time when the morphological changes are becoming evident. Of the 96 genes analysed on the array 2 changed significantly at the 24h time point and 3 at the 72h timepoint. One gene of interest was *p16 (INK4A) CDKN2A, or p16*. This was increased in expression at the 72 hr time point when the amount of senescence is reaching its peak (Figure 4.22). The increase in expression of *p16* was confirmed using Q-RT-PCR on the same samples (Figure 4.23). *SENEX* overexpression also induced an increase in the protein levels for p16. Retinoblastoma (Rb) is a downstream target of p16 and p16 activation prevents the phosphorylation of Rb. Rb in its active hypo-phosphorylated form inhibits the expression of genes regulated by the E2F transcriptions factor halting cells in the G1 phase of the cell cycle. SENEX overexpression resulted in a decrease in the protein expression of the inactive hyper-phosphorylated form of Rb (Figure 4.24). These results indicate that SENEX overexpression is initiating the p16/pRb pathway.

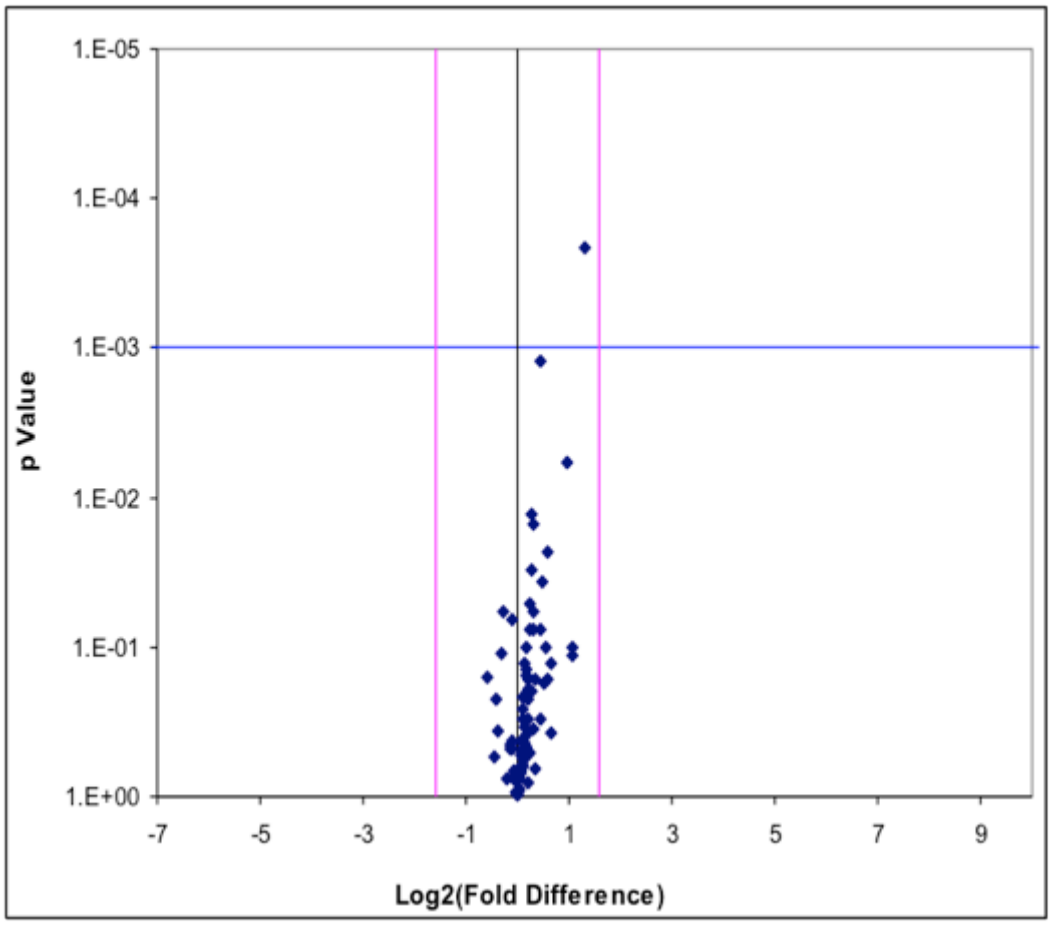

Figure 4.22. Measurement of *p16* mRNA expression after SENEX overexpression using PCR arrays. A PCR array from superarray was used to look at the mRNA changes after ECs were infected with SENEX adenovirus for 24 and 72 hrs. 3 lines of HUVECs were combined after mRNA was harvested. The results for 72 hours are shown as a volcano plot. The Y axis represent the p value for each gene measured. Any point above the blue line represent a change with a p value less than .05. The x axis represents the fold change of each gene. The pink line indicate a fold change of 2. The circled dot represent p16

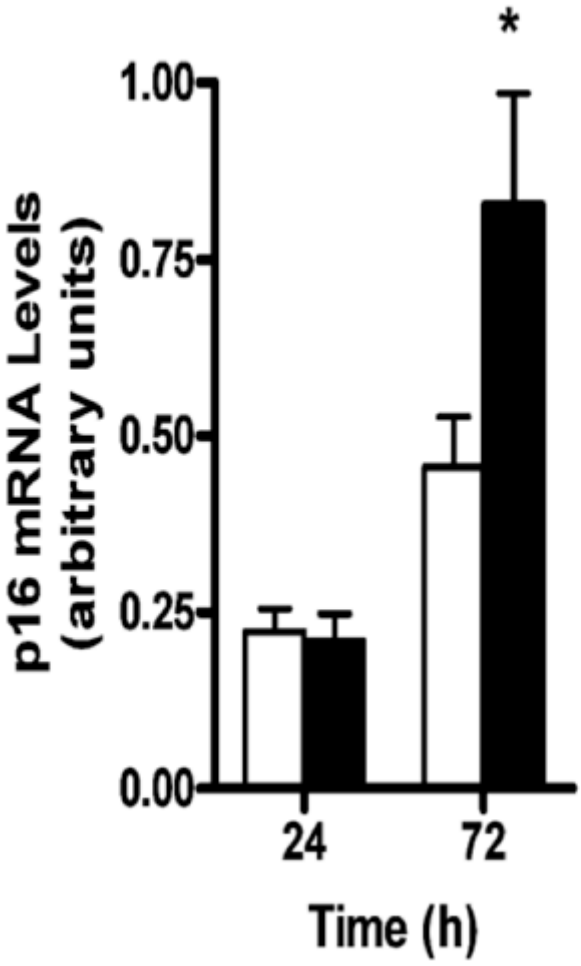

Figure 4.23. Q-RT-PCR of *p16* mRNA expression after SENEX overexpression. HUVECs were infected with *SENEX* (black bar) or EV (white bar) adenovirus for 24 and 72 h. Total RNA was extracted and Q-RT-PCR used to determine levels of p16 standardized to Cyclophilin A. This is a representative of3 experiments. Results are the mean +/-SEM of 3 replicates of each group. * $p<0.05$ compared to EV.

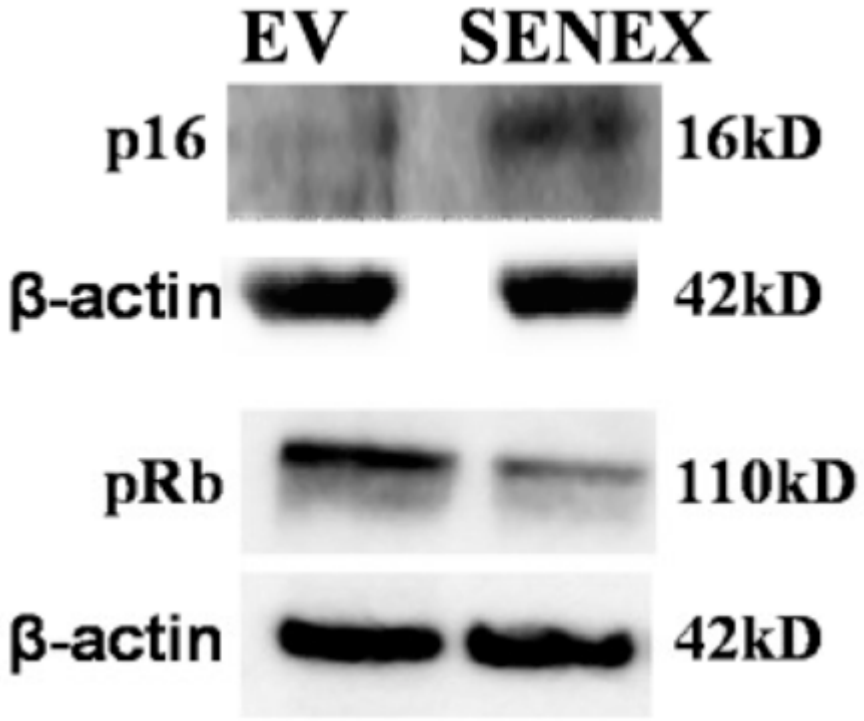

Figure 4.24. Western blot of p16 and pRb after SENEX overexpression. HUVECs were infected with SENEX and EV adenovirus for 48 h. Total protein was used for western blotting using p16 or phosphorylated Rb specific antibodies. β-actin was used as a loading control. This is a representative of 3-4 experiments performed using different EC lines.

4.6.2 SENEX expression does not change the p53 pathway.

SIPS has been reported to initiate both the p16/pRb and the p53/p21 pathways in endothelial cells [67]. Therefore the p53/p21 pathway was also investigated. Western blotting showed that there was no change in the protein expression of p53 or p21 at 48hours when 30-50% of the cells display the senescence phenotype and at the same timepoint which p16 and pRb are regulated (Figure 4.25). Thus *SENEX* activates the p16/pRb pathway but not the p53/p21 pathway in the senescence induction. To determine whether activation of p16 is essential for SENEX induced senescence we attempted to knockdown p16 using siRNA and then induce senescence using SENEX overexpression. To date this experiment has not been successful. We have been unable to determine if the p16 siRNA is actually working because the basal levels of p16 in ECs are undetectable. It is also very difficult to use two different techniques to manipulate gene expression in the primary cells. This experiment would involve transfection of the siRNAs to deplete p16 followed by an infection to overexpress SENEX. This is an important experiment but more work is needed to optimize the experiment.

4.7 Hydrogen peroxide induced EC senescence regulates SENEX expression

Hydrogen peroxide (H_2O_2), a ROS implicated in cardiovascular disease and in cancer is a known inducer of senescence when delivered in a subcytotoxic dose [27]. The senescence that results can occur through the oxidative stress pathway, without a shortening in telomere length, similar to that for SENEX. To investigate whether our SENEX overexpression is biologically relevant and not just an artifact of protein overexpression we investigated whether H_2O_2 may act to induce senescence through SENEX regulation.

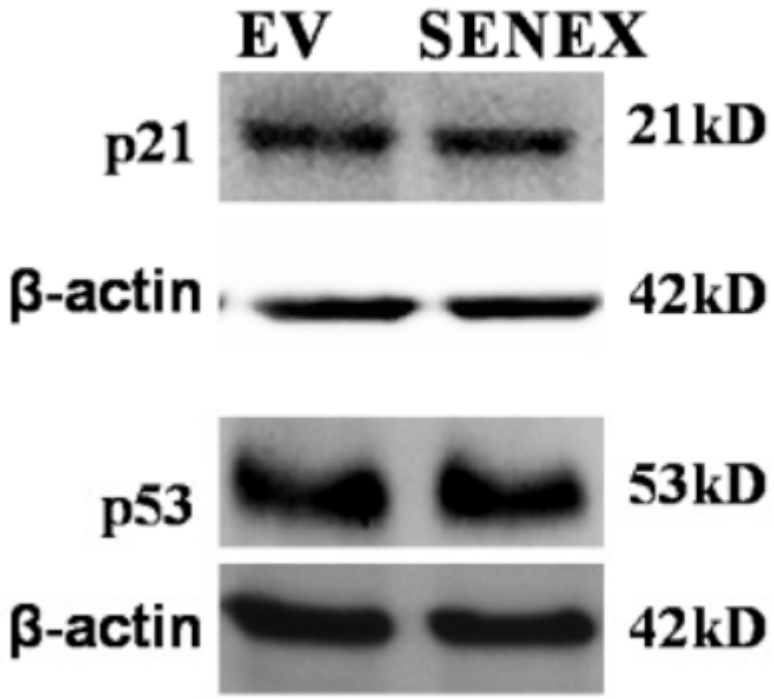

Figure 4.25. Western blot of p53 and p21 after SENEX overexpression. HUVECs were infected with SENEX and EV containing adenovirus for 48 h. Total protein was used for western blotting with p53 and p21 antibodies. β-actin was used as a loading control. Analysis of each protein was performed in 3-5 different HUVEC lines

4.7.1 H_2O_2 induced senescence increases SENEX expression

Subcytotoxic doses of hydrogen peroxide (10μM and 100μM) were administered to EC for 2 hrs and the cells were then placed in fresh normal medium for a further 24-48 hours. The H_2O_2 treatment induced senescence after 48 hours as judged by the enlarged cellular morphology and β-gal staining (Figure 4.26A). Furthermore, these cells showed an increase in SENEX protein levels in a dose dependent manner (Figure4.26B). This indicates that SENEX may be playing a role in H_2O_2 induced senescence. To confirm the role of SENEX in oxidative stress induced senescence a knockdown of SENEX with siRNA during hydrogen peroxide induced senescence would be the next experiment to attempt. But due to the apoptotic effects of SENEX knockdown which will be explained in Chapter 5 the cells are not viable after siRNA transfection. This makes it very difficult to then create senescence with H_2O_2.

At present we cannot conclusively conclude that SENEX is crucial for oxidative stress induced senescence but since low dose H_2O_2 induces senescence and upregulates SENEX the results suggest that this could be the case.

4.8 SENEX produces a senescence which is anti-inflammatory

4.8.1 SENEX induced senescence does not support neutrophil or mononuclear cell adhesion.

Published work has suggested that senescent cells are proinflammatory [93]. To determine the inflammatory phenotype of the *SENEX* induced EC, we tested their capacity to support neutrophil adhesion. HUVECs were infected with SENEX and EV adenovirus and left for 72 hours. They were then treated with TNFα (5 ng/ml) for 5 hours in order to upregulate the expression of adhesion molecules such as E-selectin which is critical for neutrophil adhesion to the EC [164, 165]. The TNFα was removed by washing. The neutrophils and mononuclear cells

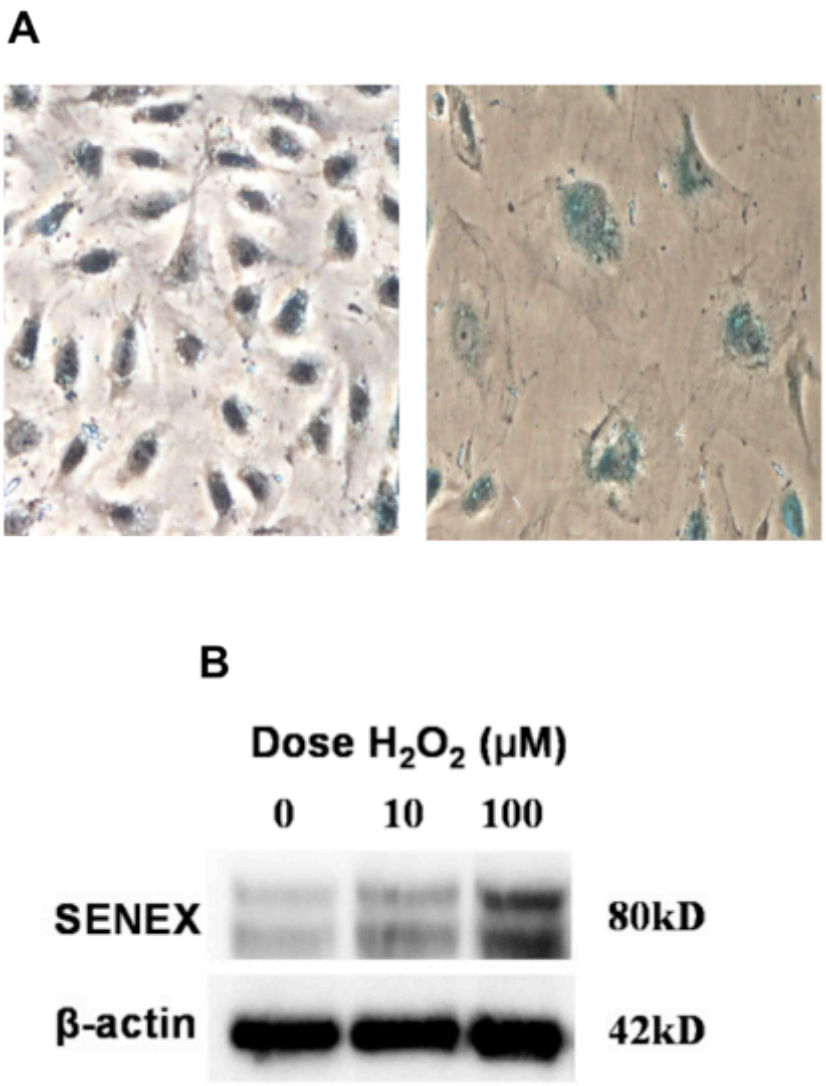

Figure 4.26. Regulation of SENEX by hydrogen peroxide induced senescence. **(A).** HUVECs were stimulated with 100 μM H_2O_2 for 2 h and then placed in normal HUVEC medium for 48 h (ii) or kept in normal HUVEC medium for 48 h (i). Cells were then stained for β-galactosidase activity. Bar= 220 μm **(B).** HUVECs were stimulated with 10 μM or 100 μM H_2O_2 for 2 h and then placed in normal HUVEC medium for 48 h. SENEX expression was measured by western blot. β-actin was used as a loading control. This is a representative of 3 experiments.

separated from blood using histopaque gradient separation, were plated onto the pretreated HUVECs and left for 2 hours. There was a striking lack of neutrophil adhesion to TNFα stimulated morphologically enlarged senescent EC (Figure 4.27). ECs which had been infected with *SENEX* but did not show the change in cell size in general displayed levels of neutrophil attachment similar to that seen with EV control cells. Quantification based on the number of neutrophils attached per large senescent cell versus non-enlarged ECs occupying the same area showed a 75% inhibition in the capacity of neutrophils to adhere to senescent ECs (Figure 4.28). There was no preferential binding of the neutrophils to the junctions of the senescent cells and we saw little or no neutrophil transmigration across the senescent EC (data not shown).

Mononuclear cell adhesion was also measured and the results were very similar to that seen for neutrophils, where there was a significant decrease in the number of mononuclear cells adhering to large senescent cells compared to the surrounding non senescent cells (Figure 4.29). There was a 74% inhibition of mononuclear cells attached to the large SENEX induced senescent cells compared to smaller infected cells (Figure 4.30).

4.8.2 SENEX induced senescence decreases adhesion molecule expression

Neutrophil attachment is mediated predominantly through the adhesion molecule E-selectin [164, 165], which is induced with 4-6 hours upon inflammatory cytokines stimulation. Therefore the levels of E-selectin were measured following stimulation for 5 hours with 5ng/ml of TNFα. Immunostaining was used to measure the amount of E-selectin on individual cells. ECs were infected with SENEX and after 48 hours the cells were harvested and plated onto labtek slides. The cells were then left for a further 24 hours before stimulated with TNFα and then fixed with 4% paraformaldehyde and stained for E-selectin. The large senescent cells induced by SENEX infection had a significant decrease in E-selectin staining on the cell surface (Figure 4.31A). This

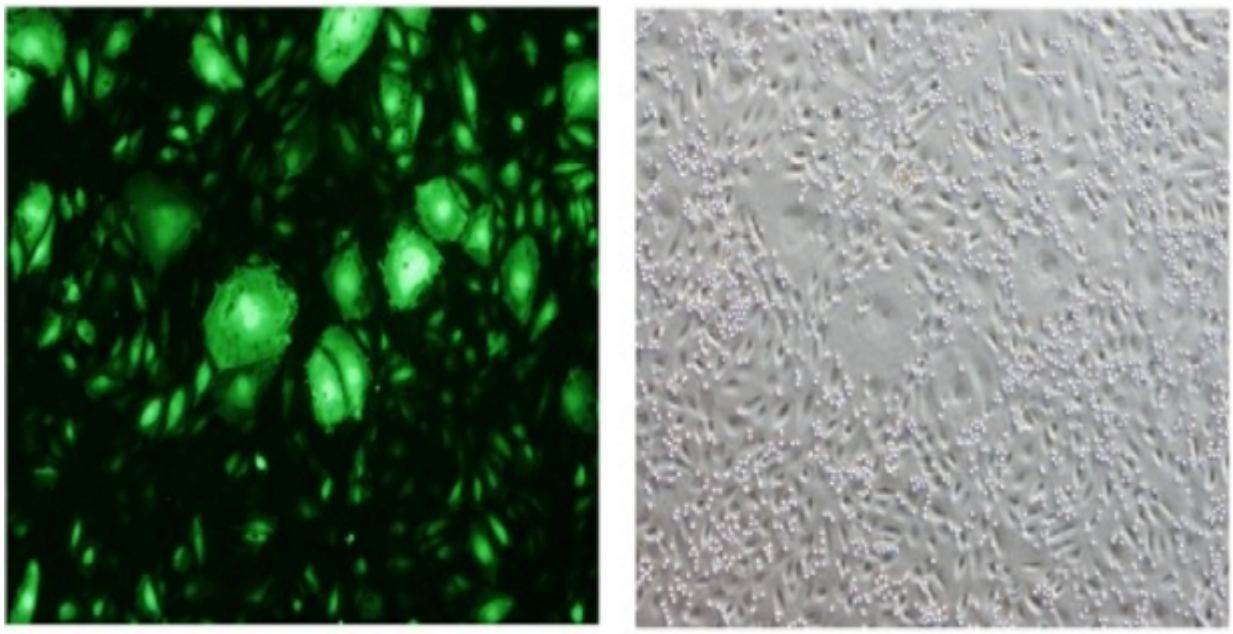

Figure 4.27. Neutrophil attachment to TNFα stimulated SENEX induced senescent ECs. HUVECs were plated on fibronectin coated labtek slides at $6x10^4$ for 24 h, then infected with *SENEX* and EV containing adenovirus and after 48 h stimulated with TNFα (5 ng/ml) for 5 h (i). Adhesion of neutrophils was then assessed (ii). This is a representative of 3 experiments. Arrows show senescent cells from the corresponding fluorescence view (i). Bar= 220 μm.

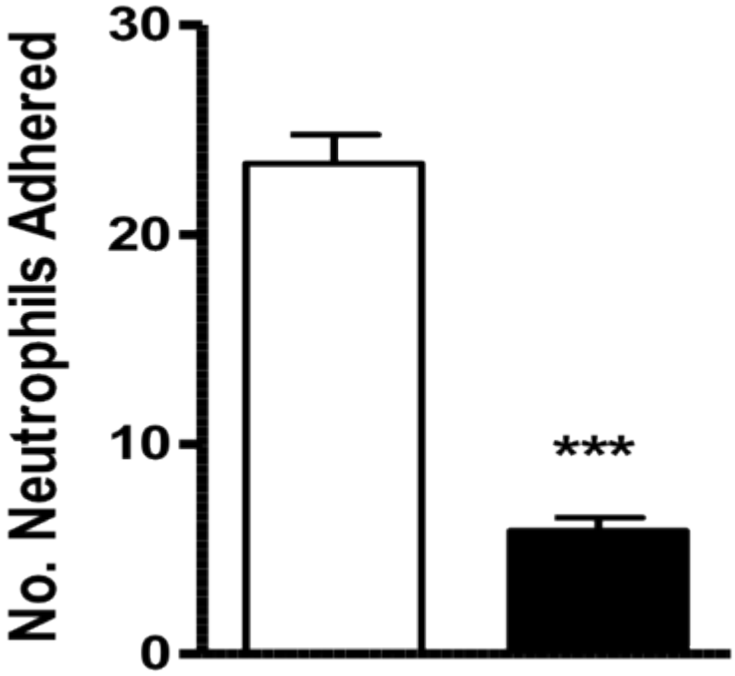

Figure 4.28. Quantification of neutrophil adhesion to SENEX induced senescent ECs. From the photographs taken in (Figure 4.27) counts were made of the number of adherent neutrophils on a senescent cell (black bar). Neutrophils were then counted in the same surface area on neighboring nonsenescent cells (white bar). This is a representative of 42 senescent cells and the corresponding area of non-senescent cells from three HUVEC lines. *** $p<0.001$ compared to non senescent cells..

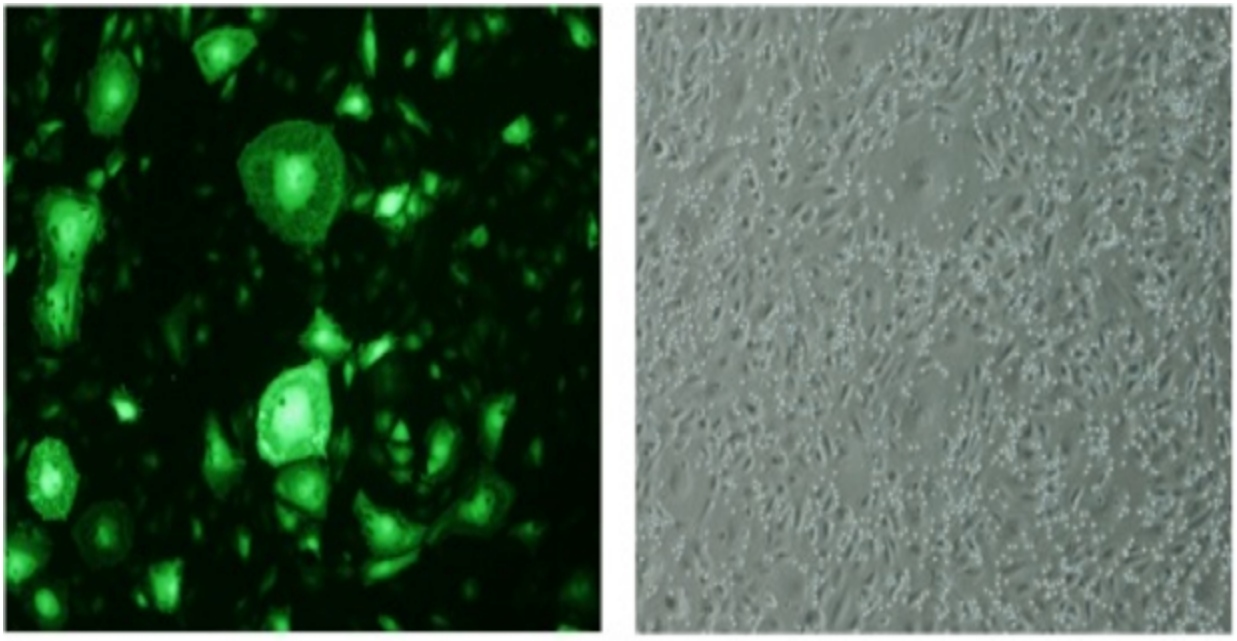

Figure 4.29. Mononuclear cell attachment to TNFα stimulated SENEX induced senescent ECs. HUVECs were plated on fibronectin coated labtek slides at $6x10^4$ for 24 h, infected with *SENEX* and EV containing adenovirus and after 48 h stimulated with TNFα (5 ng/ml) for 5 h (i). Adhesion of mononuclear cells was then assessed (ii). This is a representative of 3 experiments. Arrows show senescent cells from the corresponding fluorescence view (i). Bar= 220 μm.

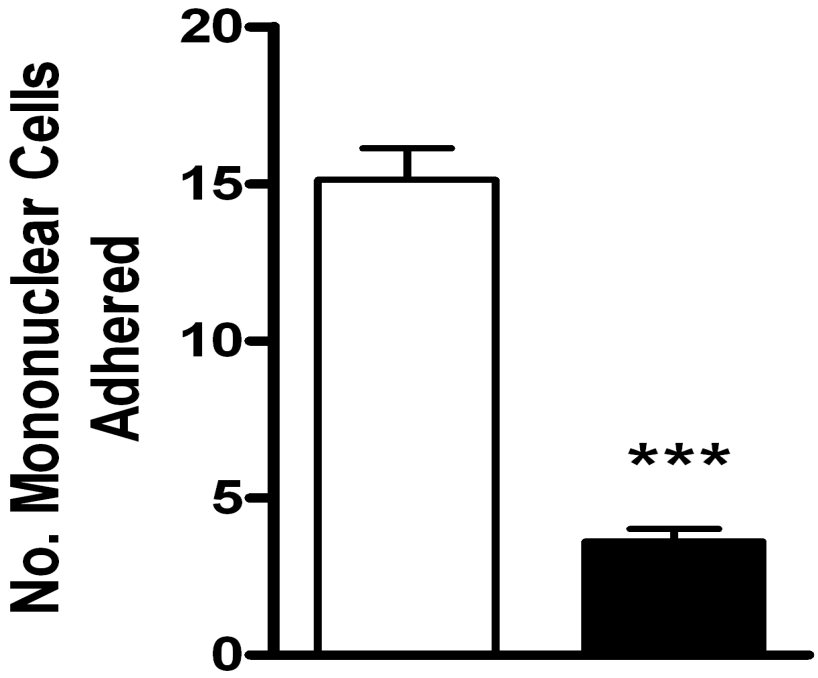

Figure 4.30. Quantification of mononuclear cell adhesion to SENEX induced senescent ECs. From the photographs taken in (Figure 4.29) counts were made of the number of adherent mononuclear cells on a senescent cell (black bar). Mononuclear cells were then counted in the same surface area on neighboring nonsenescent cells (white bar). This is a representative of 102 senescent cells and the corresponding area of non-senescent cells from three HUVEC lines. *** $p<0.001$ compared to non senescent cells.

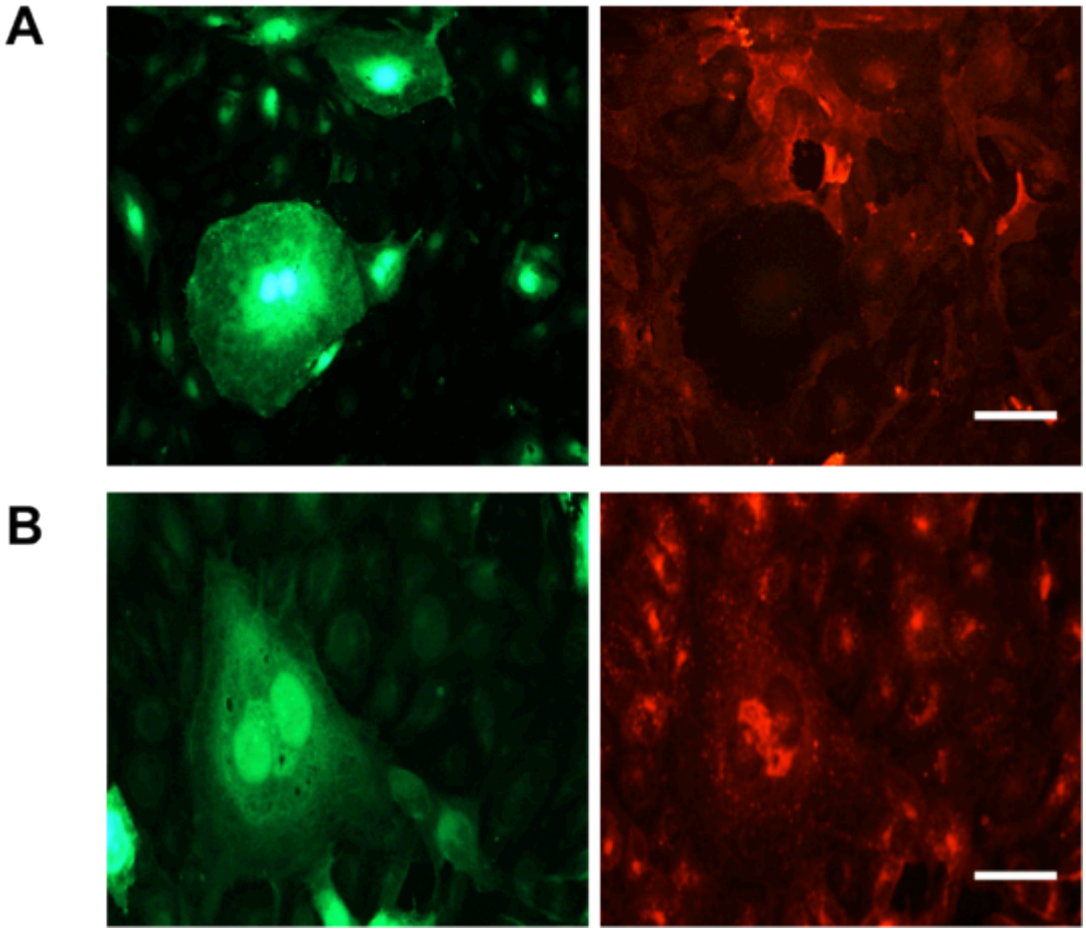

Figure 4.31. E-selectin immunostaining of SENEX induced senescent ECs. HUVECs were infected with *SENEX* adenovirus for 72 h. They were treated with 5 ng/ml of TNFα in normal HUVEC medium for 5 h and then stained for surface expression of E selectin **(A)** Bar= 220 μm. GFP photos of the area photographed for adhesion molecule expression is given in the left hand panels. In **(B)** the cells were permeabilised and then stained for intracellular E-selectin Bar= 220 μm.

decrease in expression as judged by immunostaining could be because of the size of the cell. It is possible that there is the same amount of E-selectin been expressed in the large senescent cells but it is spread over a significantly larger area. To account for this possibility the levels of E-selectin staining were measured using mean pixel intensity measurements for each individual cell. This was quantified using image J pixel intensity calculations (Figure 4.32). The results demonstrate that on a per cell basis there is a 35% decrease in the amount of E-selectin staining on the surface of large senescent cells compared to the amount on the surface of surrounding non senescent cells.

Interestingly when the cells were permeabilised to investigate the intracellular levels of E-selectin, similar levels of E-selectin were seen between senescent and non senescent cells (Figure 4.31B). This indicates that SENEX induced senescent cells are able to make E-selectin in response to TNFα stimulation but it is not translocated to the cell surface.

We next measured VCAM1 expression, a major adhesion molecule for leucocytes and which is also induced after cytokine stimulation [166]. ECs were infected with SENEX adenovirus and then treated with TNFα for 24 hours since VCAM1 requires a longer period of cytokine stimulation to induce maximum levels. The VCAM1 was then measured using immunostaining. There was a decrease in cell surface expression but no change in intracellular expression of VCAM1 (Figure 4.33). The levels of VCAM1 staining were measured using mean pixel intensity measurements for each individual cell. This was quantified using image J pixel intensity calculations (Figure 4.34). The results demonstrate that on a per cell basis there is a 50% decrease in the amount of VCAM1 staining on the surface of large senescent cells compared to the surrounding non senescent cells. In a similar fashion to E-selectin there was similar cytoplasmic staining of VCAM1 in senescent and non senescent cells.

Flow cytometry was used to confirm the immunostaining data. The ECs were treated in the same method as was used for immunostaining but instead of visualizing the cells, they were trypsinised

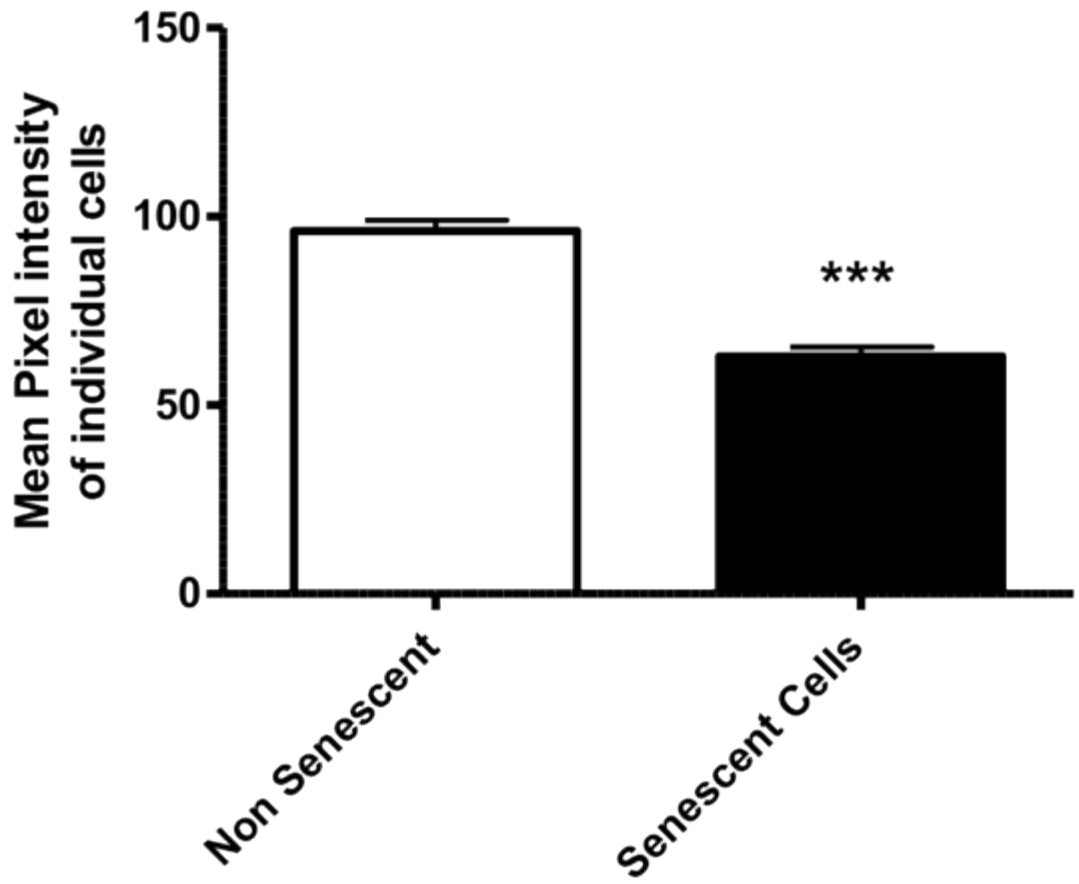

Figure 4.32. Quantification of surface expression of E-selectin staining on SENEX induced senescent ECs. Senescent and non senescent cells were analysed for cell surface expression of E-selectin. The mean pixel intensity per cell was measured using Image J for senescent cells (black bar) and for non senescent cells (white bar). The E-selectin data is a representative of the mean +/-SEM of 14 senescent cells and the corresponding area of non-senescent cells from two HUVEC lines. *** $p<0.001$ compared to non senescent cells.

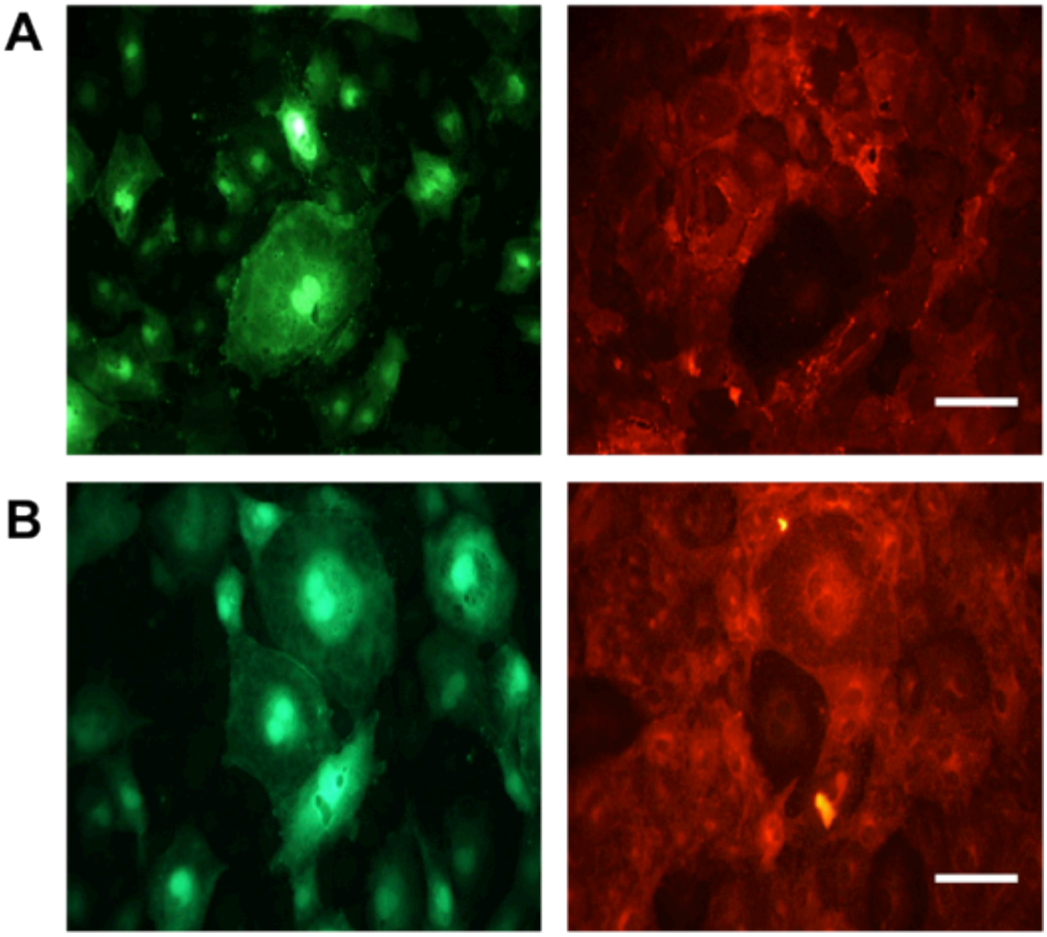

Figure 4.33. VCAM1 immunostaining of SENEX induced senescent ECs. HUVECs were infected with SENEX adenovirus for 48 h. They were treated with 5 ng/ml of TNFα in normal HUVEC medium for 24 h and then stained for surface expression of VCAM1 **(A)** Bar= 220 μm. GFP photos of the area photographed for adhesion molecule expression is given in the left hand panels. In **(B)** the cells were permeabilised and then stained for intracellular VCAM1. Bar= 220 μm.

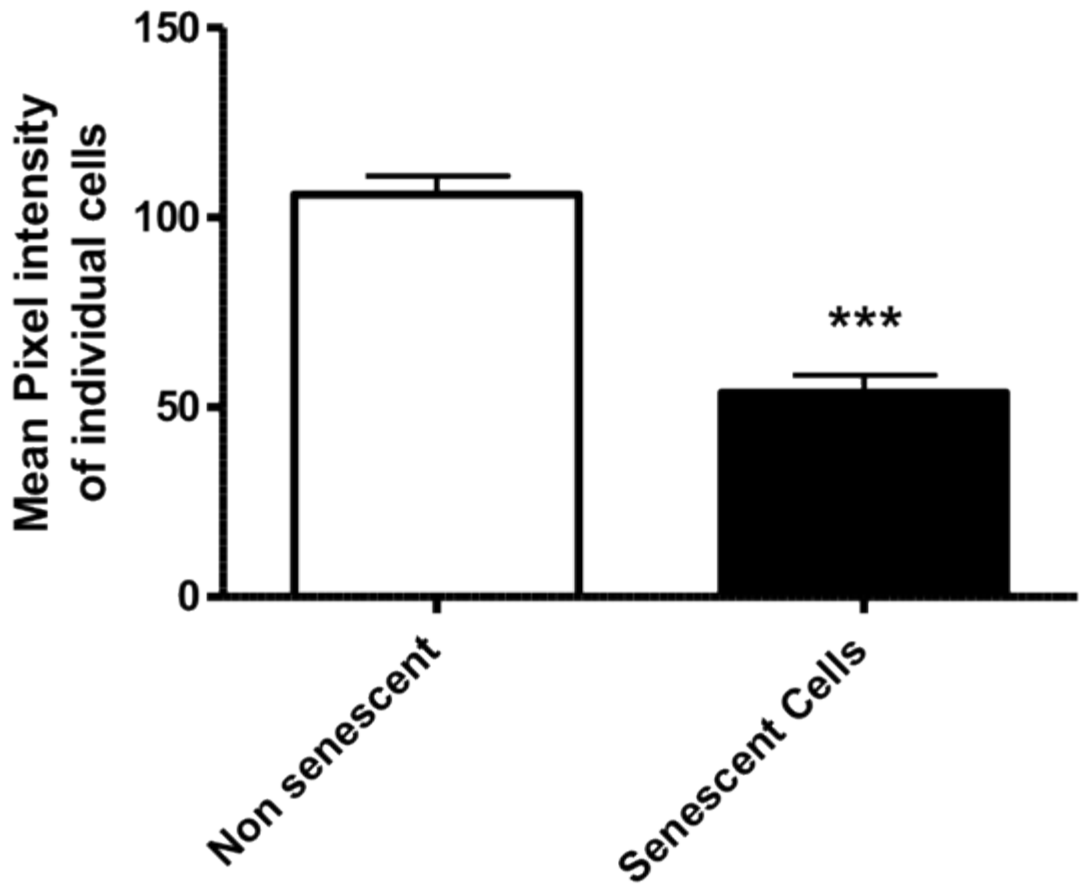

Figure 4.34. Quantification of surface expression of VCAM1 staining on SENEX induced senescent ECs. Senescent and non senescent cells were analysed for cell surface expression of VCAM1. The mean pixel intensity per cell was measured using Image J for senescent cells (black bar) and for non senescent cells (white bar). The VCAM1 data is a representative of the mean +/-SEM of 25 senescent cells and non-senescent cells from two HUVEC lines. *** $p<0.001$ compared to non senescent cells.

and fixed in FACS Fix and the surface expression of E-selectin and VCAM was measured using FACS. As with the immunostaining there was a decrease in the amount cell surface staining of E-selectin and VCAM1 in SENEX overexpressing cells compared to EV (Figure 4.35). These results together indicate that SENEX induced senescence is in fact anti-inflammatory which is the opposite that what has been found in published work on senescence to date.

4.8.3 H_2O_2 induced senescence decreases the expression of adhesion molecules

Since SENEX appears to be involved in H_2O_2 induced senescence we would predict that H_2O_2 induced senescence would show similar changes in the expression of E-selectin and VCAM1. Cells were given low dose H_2O_2 and then treated with TNFα. As with the SENEX overexpression experiments the levels of E-selectin and VCAM1 were measured using immunostaining (Figure 4.36) and the staining intensity measured using mean pixel intensity. We found with both E-selectin and VCAM1 there was a 50% decrease in the surface expression of both E-selectin and VCAM1 (Figure 4.37). Thus, both SENEX overexpression and H_2O_2 induced senescent cells demonstrate an anti-inflammatory phenotype suggesting that our overexpression studies may reflect a biologically meaningful phenotype.

4.8.4 SENEX induced senescent cells have a reduced permeability response

Inflammation is also associated with an increase in the permeability of the endothelium. Thrombin is a major inducer of EC permeability acting rapidly, within 10-30 minutes to induce the response [167]. Endothelial cells were infected with SENEX and EV and then stimulated with thrombin. The amount of EC permeability was measured by the passage of FITC-dextran across the monolayer. There was a small but not significant change in the basal permeability with SENEX overexpression. The SENEX induced senescent ECs had a significantly lower response to thrombin than did the control EV infected cells (Figure 4.38).

These results further confirm that SENEX induced senescence is resulting in an anti-inflammatory phenotype.

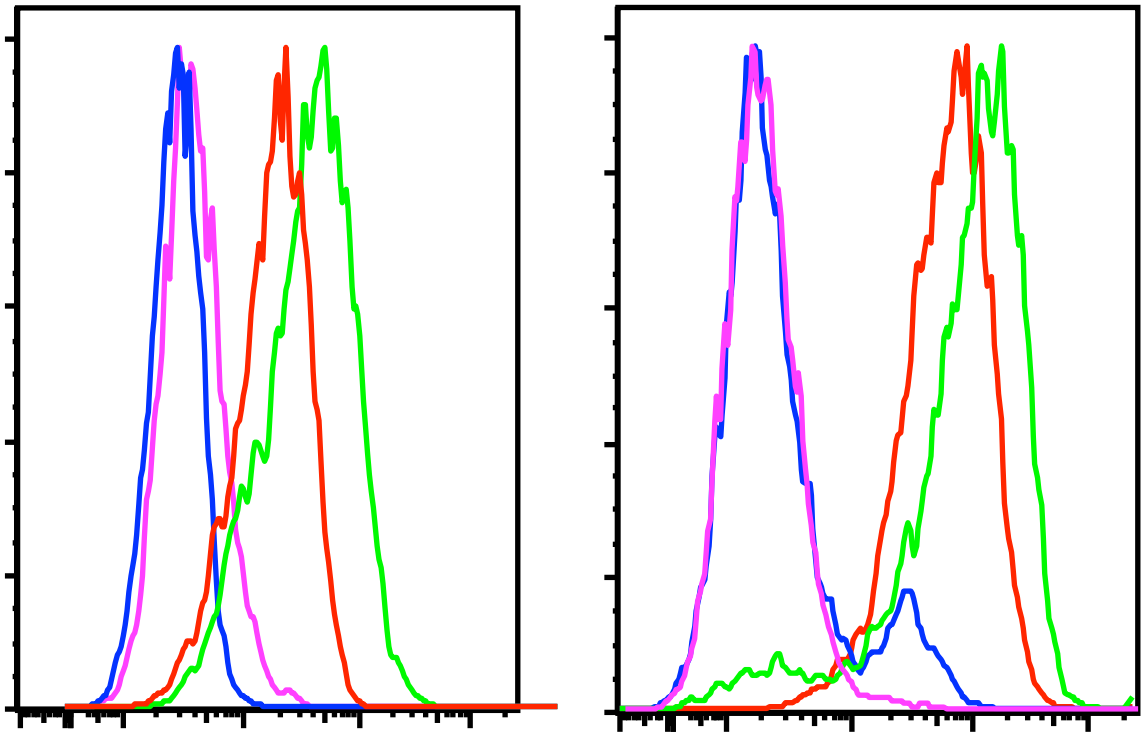

Figure 4.35. FACS analysis of E-selectin and VCAM1 surface expression after SENEX overexpression. EV and SENEX infected cells were left for 3 days and then were either stimulated or unstimulated with 5 ng/ml of TNFα for 5 h for E-selectin or 24 h for VCAM1,, then stained for E-selectin and VCAM1 expression. Cells were analysed for E-selectin and VCAM1 expression using FACS analysis. No TNFα stimulated EV = purple line, No TNFα stimulated SENEX = blue line, TNFα stimulated EV = green line, TNFα stimulated SENEX = red line. This is a representative of 3 experiments.

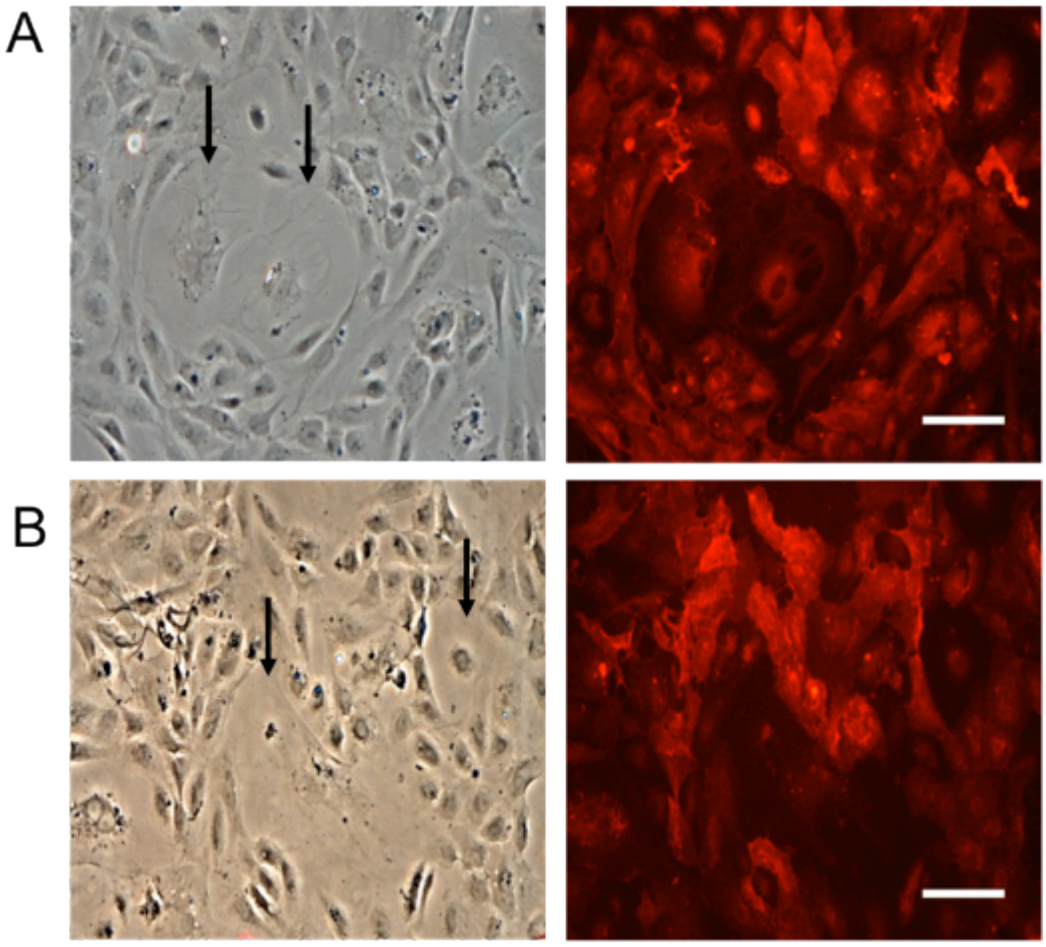
A
B

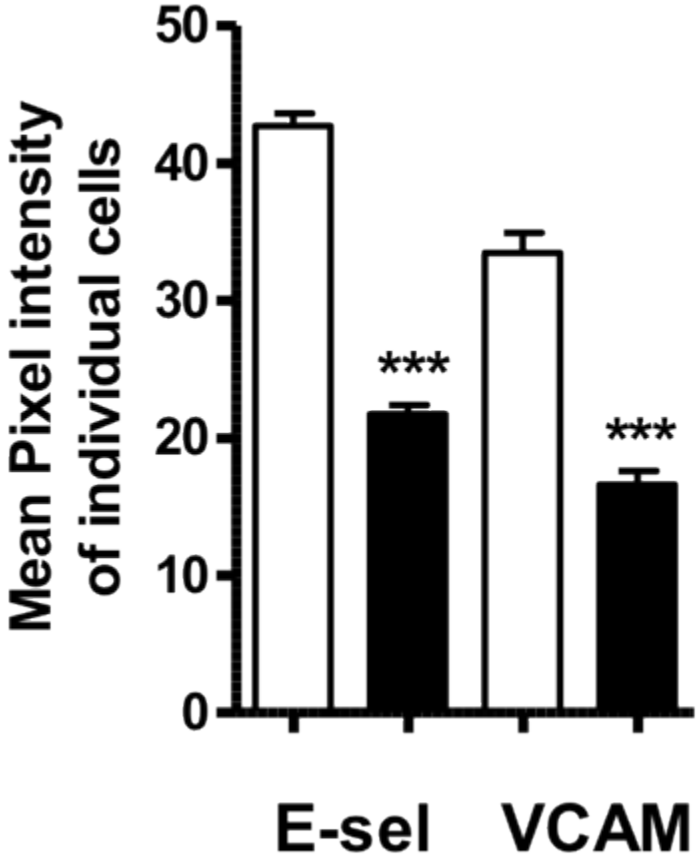
Mean Pixel intensity of individual cells
50
40
30
20
10
0
***
***
E-sel
VCAM

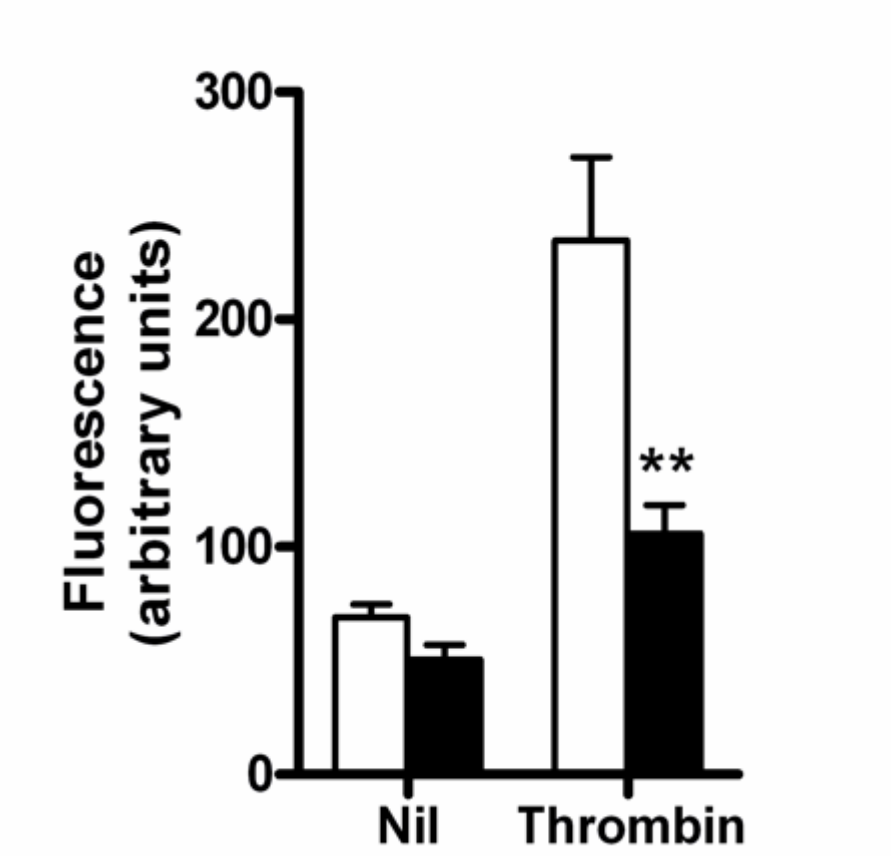

4.9 SENEX in atherosclerotic plaques

Increases in oxidative stress are associated with atherosclerosis and are postulated to lead to EC damage and aging. Furthermore, senescent ECs, as judged by β galactosidase positivity, have been detected in human atherosclerotic plaques [130] and in vascular cells in injured rabbit carotid arteries [115]. To determine whether SENEX is regulated during atherosclerosis, we

investigated the mRNA levels in the aortic region of apoE gene knockout mice fed a western diet. Sections were taken from the aorta. No atherosclerosis is seen after 1 month of Western diet. However after 5 months on the diet there is an increase in atherosclerotic plaques and at the same time there is an increase in mRNA levels of *SENEX* in relation to Pbgd and Hrpt (Figure 4.39). These results were obtained in collaboration with Roland Stockers group at the Bosch institute. The data is preliminary and has not conclusively shown that the *SENEX* overexpression is related to an increase in senescent cells at the site of the atherosclerotic plaques. We are currently using immunohistochemistry to try and show co-staining of β-galactosidase and SENEX on the surface of the plaques. These results will hopefully confirm that senescence is actually occurring as a plaques forms and the senescence that is forming requires the regulation of SENEX.

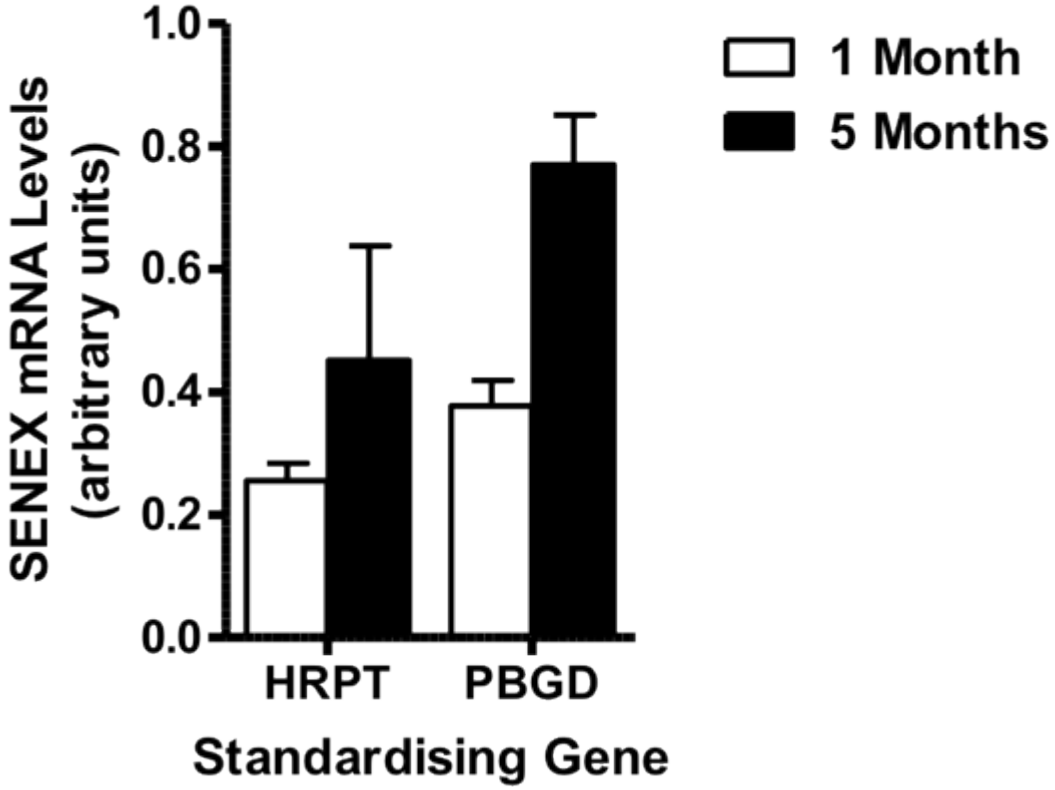

4.10 Summary

SENEX or *MacGAP* or *ARHGAP18* gene is a novel gene that to date had no biological function. The work described in this thesis, shows that SENEX, named from the Latin, *senex,* for old age or old man induces senescence in EC. Thus our work describes a new gene responsible for this major phenotypic change in cells.

The induction of senescence by SENEX in EC is a striking and robust observation, with overexpression resulting in 35 % of the ECs becoming senescent in 3 days and this proportion increases over several weeks. Furthermore, SENEX induced senescent endothelial cells exhibit the established senescence criteria of inhibited proliferation, a flattened, large vacuolated cellular morphology, polyploidy, positive staining with the senescence marker, S-A β-galactosidase and a reduction in the endothelial specific nitric oxide synthase, eNOS [132].The senescent phenotype induced by SENEX overexpression with adenovirus is reproducible with each new infection and each new batch of virus. These results indicate that SENEX can now be classified as a senescent inducing gene in EC.

The p53/p21/Rb and the p16/Rb axes are both important signaling pathways involved in the induction of senescence [158]. SENEX activates the p16/Rb pathway by increasing both p16 mRNA and protein levels together with the hypophosphorylation of the p16 downstream mediator of cell cycle arrest Rb. The reduced phosphorylation of Rb leads to its activation and causes the cell cycle arrest. In contrast, SENEX overexpression did not alter the expression of either p53 or p21 at the protein level. We also show that SENEX induced senescence is the result of stress and does not cause replicative senescence since it fails to affect telomere length [42], induces senescence within a few days and does not induce the usual RS gene profile in EC. Consistent with this, *SENEX* is not induced upon RS formation in our EC. Currently p16 and Rb are the only proteins known to be involved in SENEX induced senescence. Further work is being performed to identify both upstream and downstream molecules which may contribute to the SENEX -induced senescence in EC.

SENEX not only is capable of inducing senescence when overexpressed, it also is likely to be involved in low dose H_2O_2 induced senescence. H_2O_2 induces an oxidative stress form of

senescence which also can occur without any change in telomere length [27, 168]. SENEX protein expression increases in a dose dependent manner after H_2O_2 is added and is at its highest expression with a dose that also causes senescence. These results would indicate that SENEX is playing a role in H_2O_2 induced senescence. We have currently not been able to conclusively demonstrate that SENEX is essential for H_2O_2 induced senescence. To demonstrate that SENEX is crucial during H_2O_2 induced senescence we are currently attempting the knockdown of SENEX with siRNAs and then the induction of senescence with H_2O_2. We would predict that there will be a significant decrease in the level of senescence formation when SENEX expression is reduced in the ECs. This would indicate that the H_2O_2 induced senescence requires that SENEX is expressed and would demonstrate that SENEX is essential in this process.

The most notable feature of *SENEX* induced senescent cells and contrary to SIPS induced in other cell types,[8] is their anti-inflammatory nature. SENEX- induced senescent EC are not activated by TNFα to support neutrophil or mononuclear cell adhesion. The lack of immune adhesion seems to be the result of a decrease in cell surface expression of TNFα induced E-selectin and VCAM1, although there is some induction of these proteins in the cytoplasm of the cells. These results would suggest that the signaling pathway is partially intact but there is a block in the translocation of these proteins to the cell surface. Furthermore the SENEX induced senescent cells also exhibit reduced permeability in response to thrombin, again confirming their anti-inflammatory phenotype.

Since H_2O_2 induced senescent EC display a similar phenotype the results suggests that our results have biological meaning and also suggest that SIPS in EC displays an anti-inflammatory nature in contrast to SIPS induced in all other cell types investigated by others where they display a pro-inflammatory state [169].

The results obtained for SENEX overexpressing have so far produced very exciting results. The members of the Vascular Biology Laboratory are currently trying to expand on these areas to solidify a place for SENEX in the senescence field.

CHAPTER 5

The role of SENEX knockdown in Endothelial Cell Apoptosis

5.1 SENEX and Endothelial Cell Survival

Although SENEX overexpression induced senescence as demonstrated in Chapter 4, the question remained as to whether the basal levels of SENEX expression have a specific function in the cells. As was shown in the previous chapter, SENEX expression during tube formation increases after the 6 hour timepoint and is increased compared to the 0 timepoint at 24 hours. For this reason we would expect that a certain level of SENEX needs to remain for angiogenesis to occur. To address this question we chose to knockdown the basal levels of SENEX with either adenovirus containing the antisense version of SENEX or siRNA techniques against *SENEX* and determine the phenotype of the cells and how knockdown of SENEX effects tube formation.

5.1.1 SENEX knockdown prevents capillary tube formation

To determine whether SENEX basal expression is important in EC function, HUVECs were infected with adenovirus containing constructs of SENEX in the antisense orientation or empty vector (EV) as control. At the time of the experiments we were unable to determine if the expression of SENEX was actually decreased as there is no change in mRNA expression when using adenovirus with the antisense construct because using the adenovirus technique prevents translation of the mRNA but does not decrease the amount of total mRNA in the cells and the antibody specifically detecting SENEX was not yet available. Therefore functional analysis was conducted on the assumption that we had achieved knockdown. Capillary tube formation on Matrigel was used to determine if SENEX expression is important for EC function. The EV control cells formed tubes normally. In contrast, cells infected with antisense containing adenovirus failed to form capillary tubes with changes evident as early as 3 hrs after plating.

Although they initially aligned, the antisense infected cells failed to join and were unable to form tubes and the cells appeared to undergo apoptosis (Figure 5.1).

5.2 SENEX knockdown results in cell death.

Initially the knockdown of SENEX was performed with adenovirus. As an alternate approach knockdown was also achieved using siRNA. A set of Invitrogen validated stealth siRNAs were trialed in the HUVECs. With the purchase of a Stealth Select RNAi™ siRNA Set, Invitrogen guarantees the results that at least 2 out of the 3 sequences will result in at least 70% transcript knockdown, given that the transfection efficiency in your experiment is at least 80%. Following Invitrogens instructions we initially tested the set of 3 siRNAs at concentrations of 15nM and 25nM. With these concentrations we were unable to achieve a knockdown greater than 50% (Figure 5.2). We did not believe that this was a high enough knockdown so the amount of siRNA was increased to 50nM and we found that 80% knockdown was achieved in two of the three siRNAs (Figure 5.3). During the capillary tube formation array we found that SENEX expression was decreased by 50% at the 6 hour timepoint. We are therefore knocking down a greater percentage using siRNA. From these results one siRNA from the set was chosen and for the experiments in this chapter this siRNA was used at 50nM for all knockdown experiments. We then repeated the capillary tube formation assay using the siRNAs. HUVECS were transfected with either the siRNA to *SENEX* or a control siRNA and then 24 hours later plated onto Matrigel. After a further 12 hours photos were taken (Figure 5.4). In a similar manner to when we infected the cells with SENEX antisense containing adenovirus, we found that the tubes started to form as would be expected but cells would begin to die which would lead to the disintegration of the tubes.

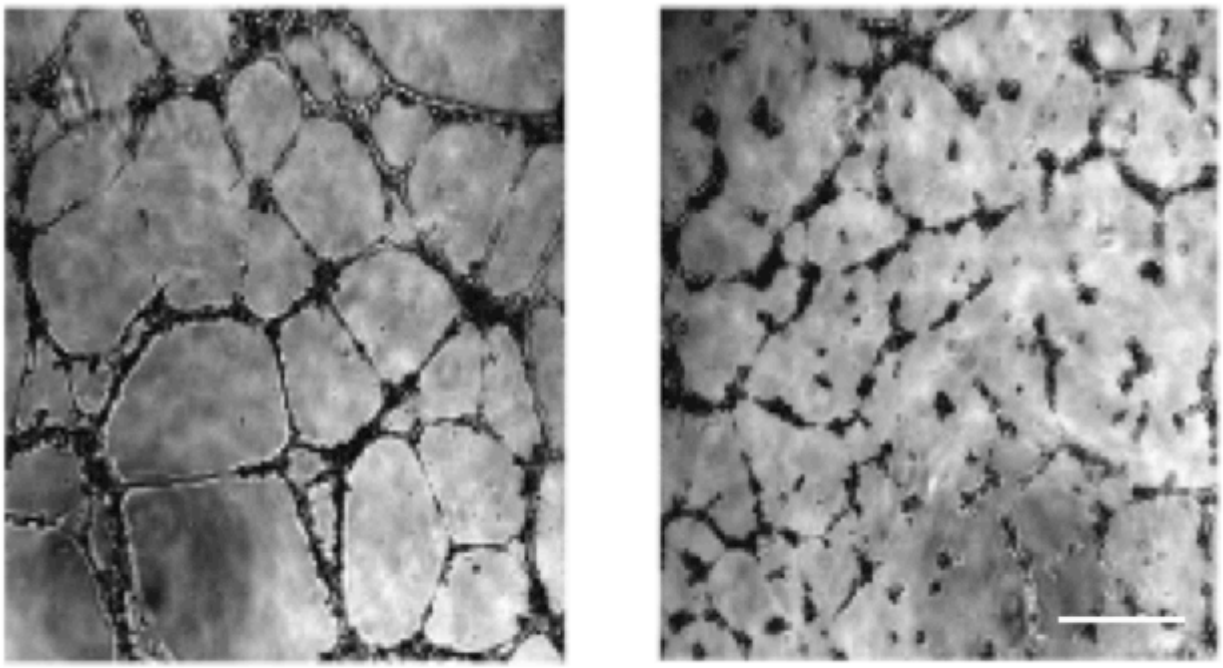
EV
SENEX(R)

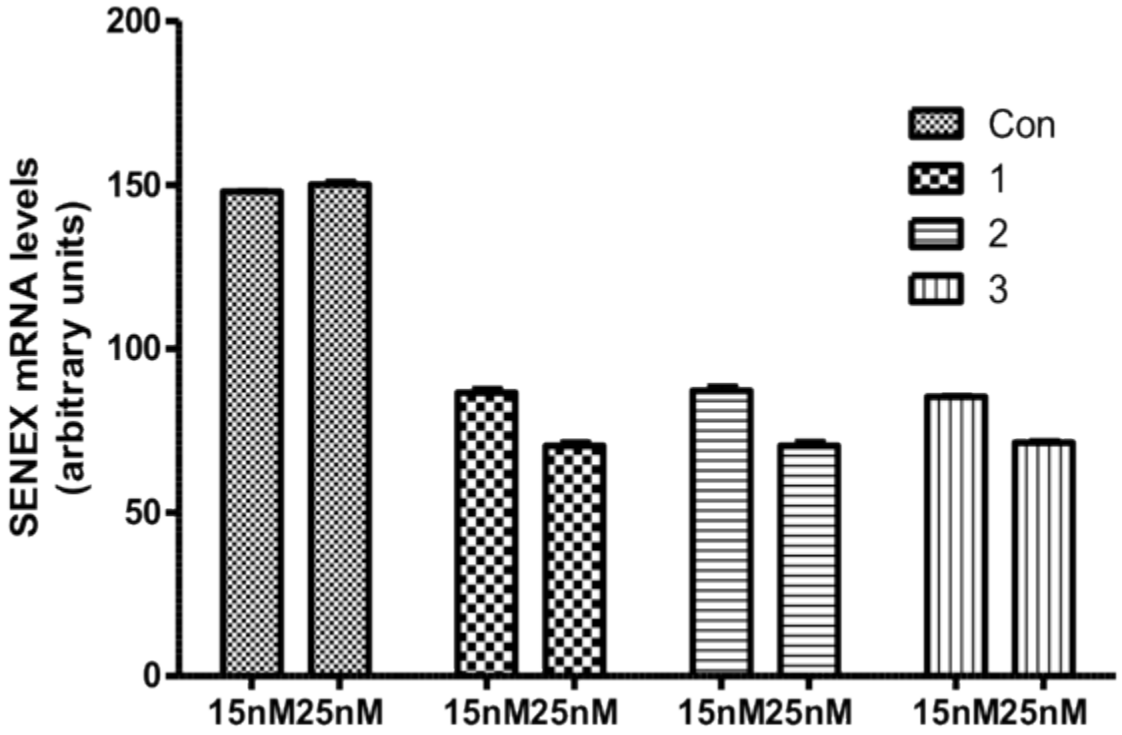
SENEX mRNA levels
(arbitrary units)
200
150
100
50
0
Con
1
2
3
15nM25nM
15nM25nM
15nM25nM
15nM25nM

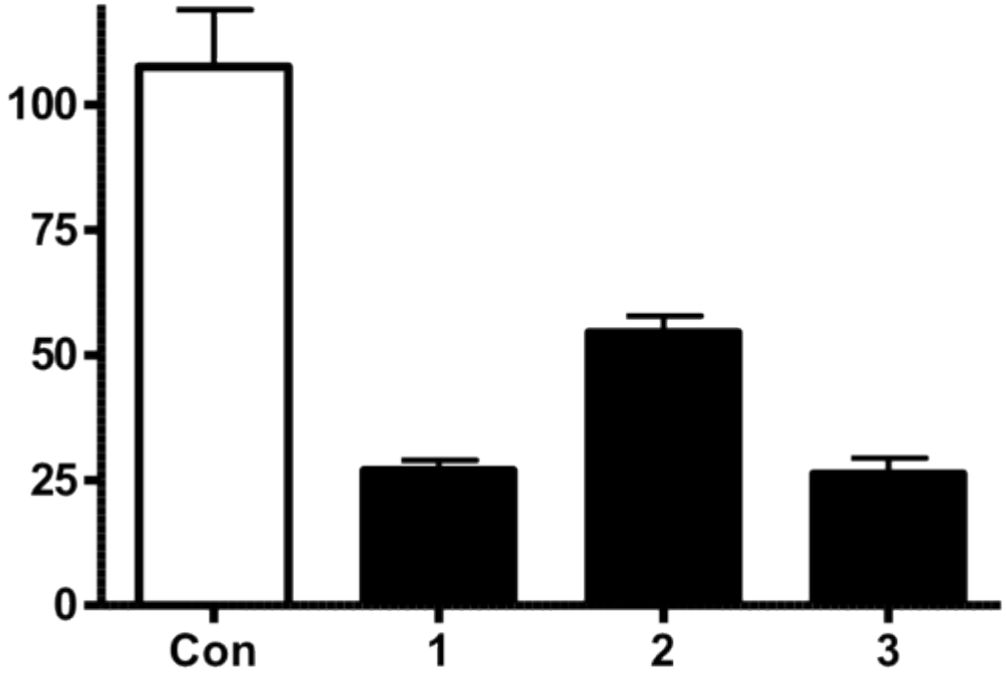
100
75
50
25
0
Con
1
2
3

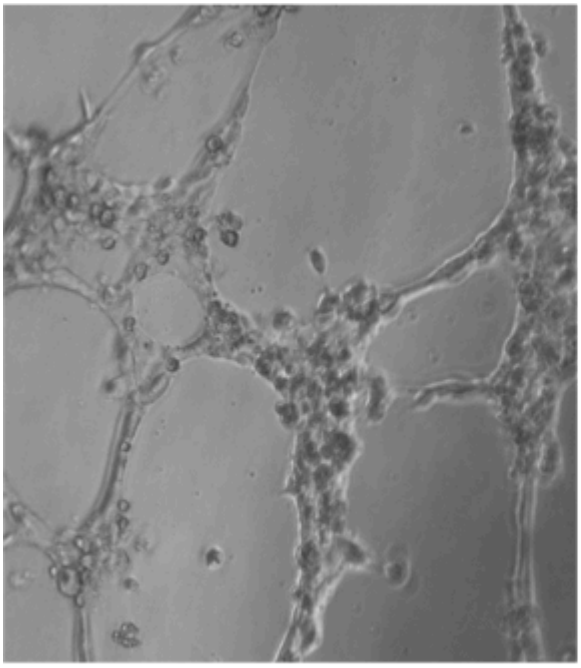

EV

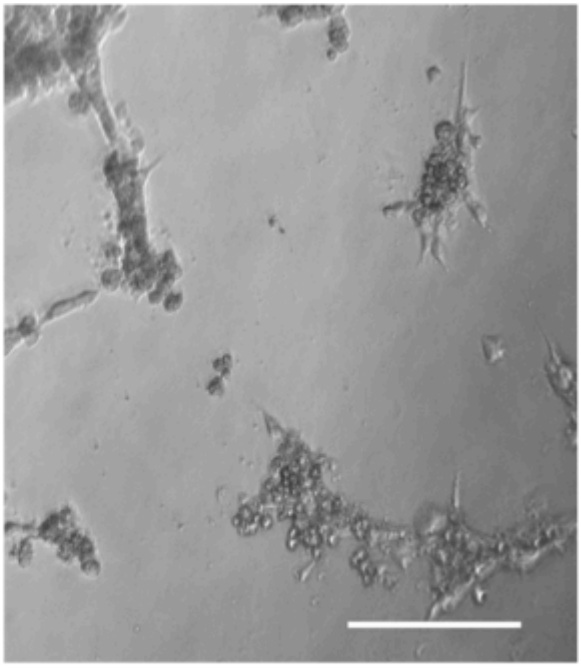

SENEX

5.2.1 Confirmation that SENEX knockdown causes apoptosis

siRNA treatment achieved a depletion of *SENEX* mRNA expression by 70% and at the protein level by 75% (Figure 5.5) and after siRNA treatment cell death was observed. To determine whether this cell death was apoptotic in nature, caspase 3 levels were measured. There are two types of apoptotic caspases: initiator (apical) caspases and effector (executioner) caspases. Initiator caspases (e.g., caspase-2, -8, -9 and-10) cleave inactive pro-forms of effector caspases, thereby activating them. Effector caspases (e.g., caspase-3, -6, -7) in turn cleave other protein substrates within the cell resulting in the apoptotic process. At least fourteen caspases have so far been implicated in human apoptotic pathway cascade. Among these, caspase-3 is considered to be a major executioner protease in apoptosis [170]. Detection of active caspase-3 in cells and tissues is an important method for assessing apoptosis induced by a wide variety of apoptotic signals. Knockdown of *SENEX* caused a >2 fold increase in apoptosis as measured by caspase 3 expression (Figure 5.6). Apoptosis was further confirmed by DAPI staining. DAPI is a DNA-specific dye that displays a blue fluorescence. This dye can pass through intact, living cell membranes, but apoptosis increases cell membrane permeability and uptake of DAPI, leaving a stronger stain. In addition, the nuclear morphology of normal cells is round, clear-edged, uniformly stained. Apoptotic cells show irregular edges around the nucleus, chromosome concentration in the nucleus, heavier coloring, and, with nuclear pyknosis, an increased number of nuclear body fragments. For these reasons, the intensity of the fluorescence can help researchers identify apoptotic samples [171]. Staining for DAPI showed an increase in apoptosis after SENEX knockdown (Figure 5.7).

Together, these results indicate that SENEX expression is essential for EC survival because without a normal basal level of SENEX the ECs will die.

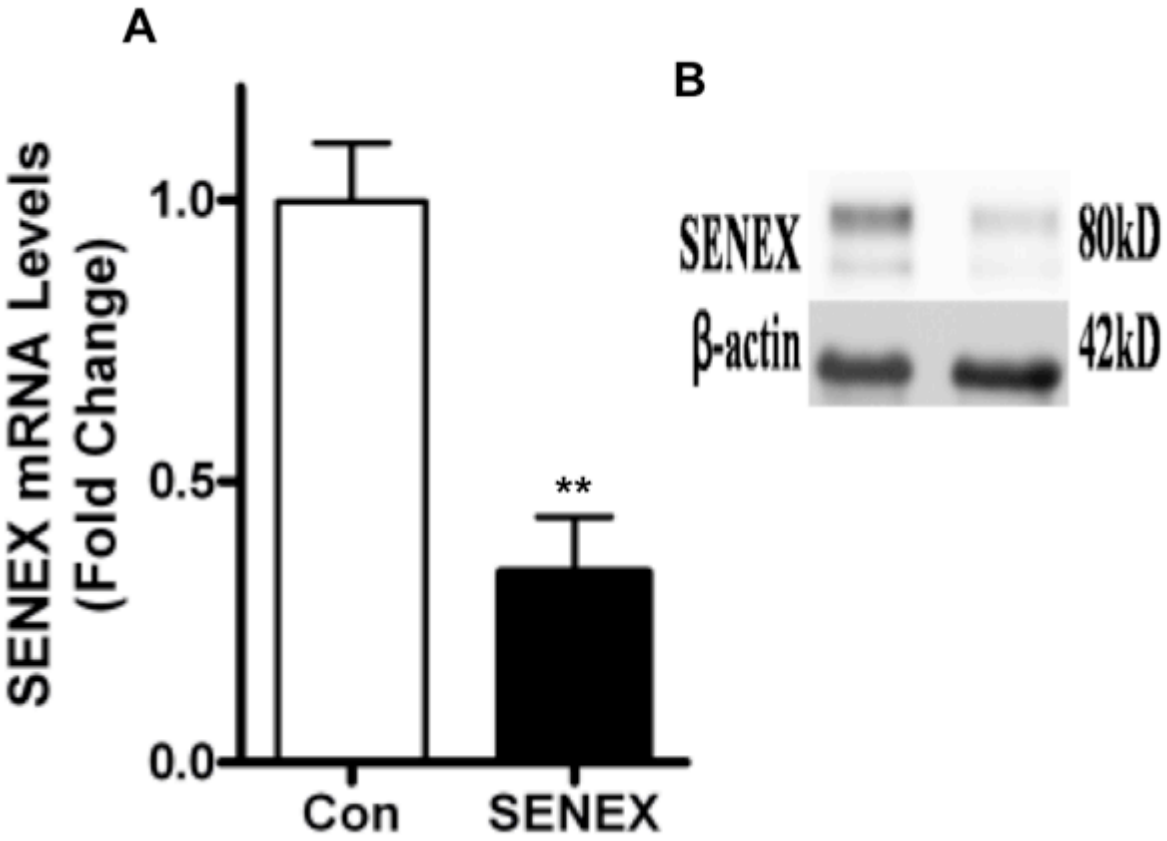
A
SENEX mRNA Levels
(Fold Change)
1.0
0.5
0.0
**
Con
SENEX
B
SENEX
80kD
β-actin
42kD

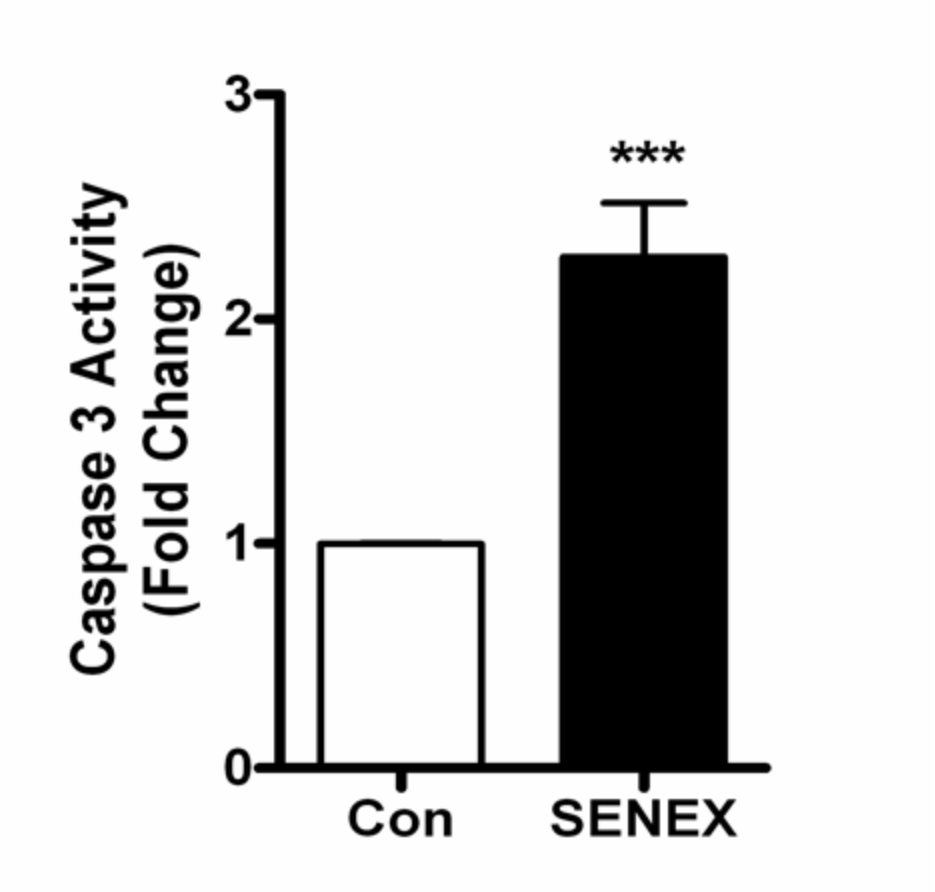
Caspase 3 Activity
(Fold Change)
3
2
1
0
***
Con
SENEX

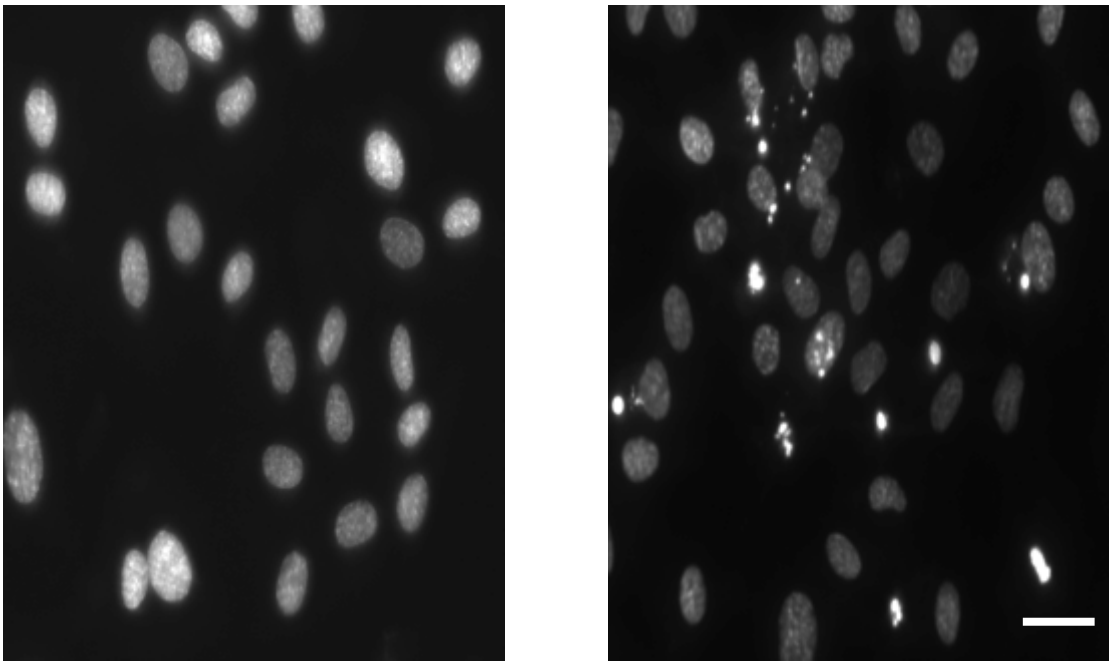

5.2.2 SENEX knockdown does not act through the intrinsic pathway

There are currently two well known pathways controlling the initiation of apoptosis. The death receptor or extrinsic pathway mediated by the activation of death receptors, and the BCL2 regulated mitochondrial or intrinsic pathway, which is mediated by noxious stimuli that ultimately leads to mitochondrial injury. In the intrinsic pathway, BCL-2 or BCL-XL inhibit the action of BAX and BAK to prevent mitochondrial leak. Activation of the pro-apoptotic BH3 proteins by the apoptotic stimuli, for example, in a serum free environment inhibits the action of BCL-2 and allows Bax and Bak to induce mitochondrial permeabilisation and the release of cytochrome c. This ultimately activates the caspase pathway and leads to apoptosis [172]. We initially looked at the levels of a range of proteins in the intrinsic pathway. They included the BH3 proteins Bid and Bax, and the antiapoptotic proteins BCL2 and MCL1. Cells were harvested for protein 48 hours after siRNA transfection as this is a time when the cells are starting to show signs of apoptosis. There was no change in the amount of Bid, Bax, MCL1 or BCL2 protein levels as measured by western blotting (Figure 5.8). Cells were also taken at 24 hours after siRNA transfection in case the signals for apoptosis were time dependent. However no changes in any of these proteins were seen (data not shown). These results suggest that the apoptosis induced by downregulation of *SENEX* is not occurring through the intrinsic apoptosis pathway. To help confirm no involvement of the intrinsic pathway a larger panel of proteins should be included. We further analysed SENEX involvement in the intrinsic pathway by using low serum containing media to induce apoptosis and there was no change in the levels of *SENEX* mRNA expression (Figure 5.9). Indicating that the mRNA levels of *SENEX* do not need to be regulated for the intrinsic pathway of apoptosis to occur. To confirm no involvement of the intrinsic pathway in SENEX knockdown further experiments are needed.

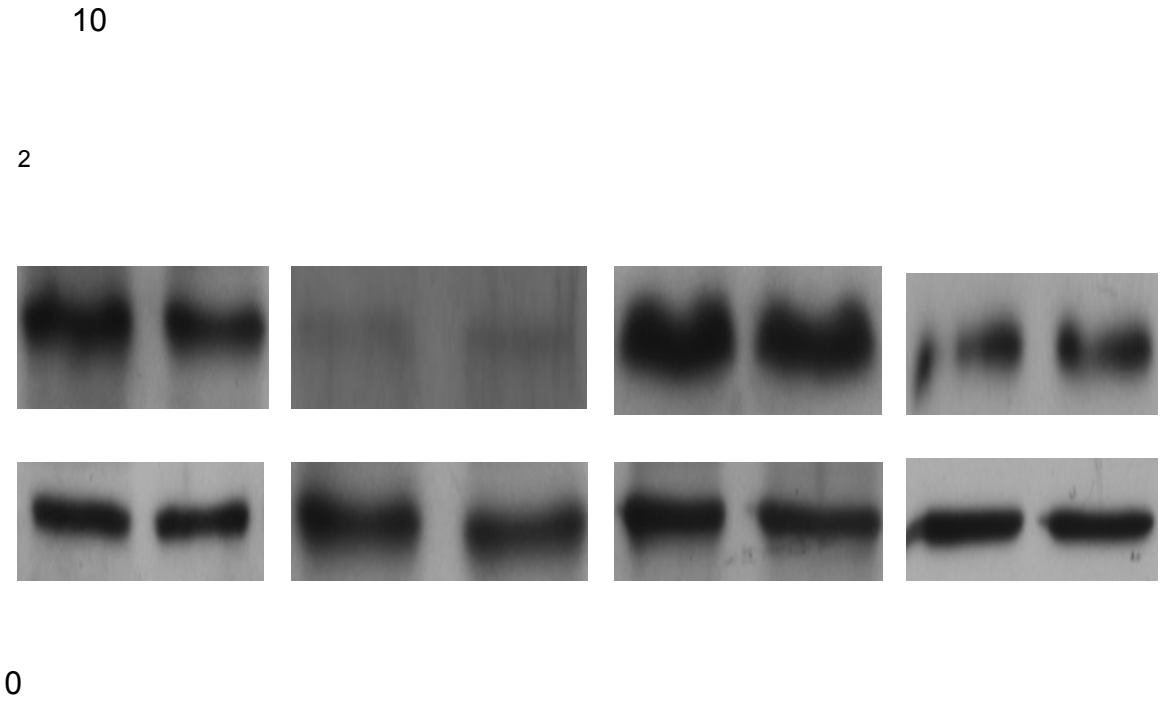
10
2
0

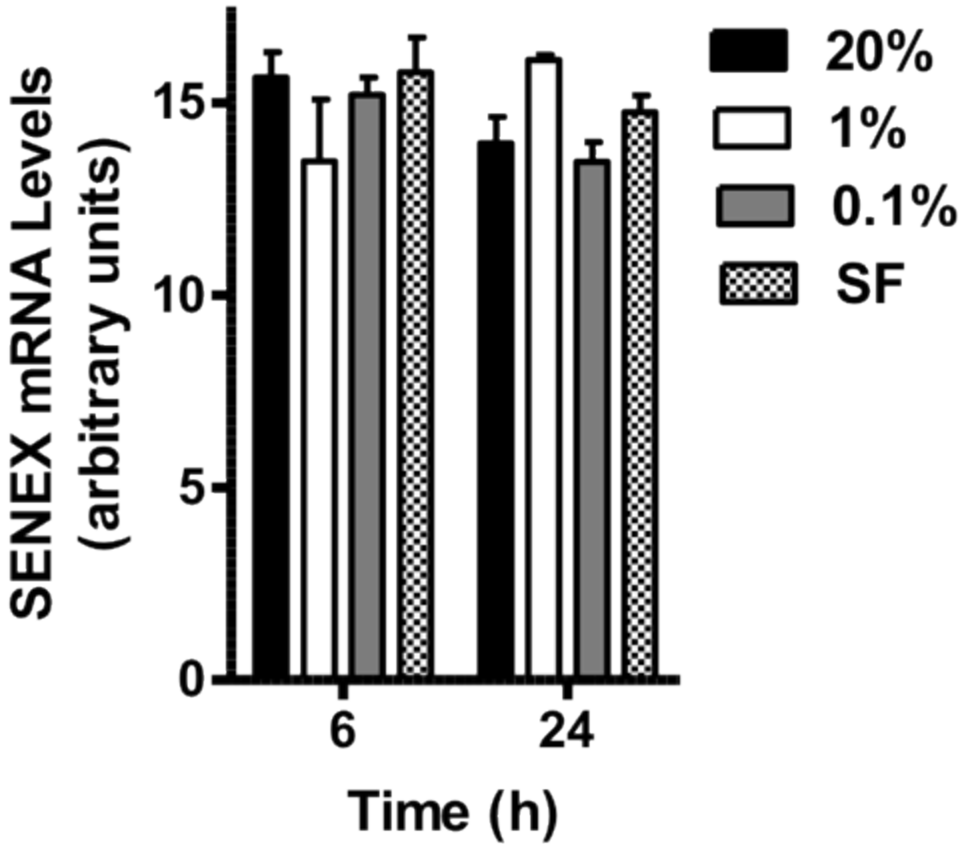

10

5.2.3 SENEX knockdown occurs during TNFα induced apoptosis

TNFα initiates apoptosis through an alternative mechanism than the intrinsic pathway, which is known as the extrinsic pathway [173]. ECs were treated with high dose TNFα and apoptosis was measured using the caspase 3 assay. At the same doses of TNFα which caused apoptosis the

mRNA levels of *SENEX* were down regulated (Figure 5.10A). At the same time periods the protein expression of SENEX was also downregulated (Figure 5.10B). This indicates that SENEX may play a role in TNFα induced apoptosis which acts through the extrinsic apoptosis pathway, but has no role in serum deprivation induced apoptosis which is induced through the intrinsic pathway.

5.2.4 SENEX overexpression protects against TNFα induced apoptosis

Since TNFα induces apoptosis and SENEX downregulation, the question was raised as to whether SENEX is directly involved in the TNFα induced apoptosis pathway. Therefore, EC were infected with SENEX containing adenovirus to induce SENEX overexpression for 24hrs and then treated with high dose TNFα or serum free HUVEC media. The amount of apoptosis induced by the conditions was then measured using the caspase 3 assay. High dose TNFα induced apoptosis (Figure 5.11, middle columns) and overexpression of SENEX protected against this TNFα induced apoptosis. Interestingly, SENEX overexpression did not protect against serum deprivation (Figure 5.11 last columns). These results further confirmed the involvement of SENEX in the induction of the extrinsic apoptosis pathway and no involvement in the intrinsic apoptosis pathway.

As was shown earlier in Chapter 4 SENEX is regulated by low dose H_2O_2 when senescence is formed. It is also known that a high dose of H_2O_2 will cause apoptosis in endothelial cells and for

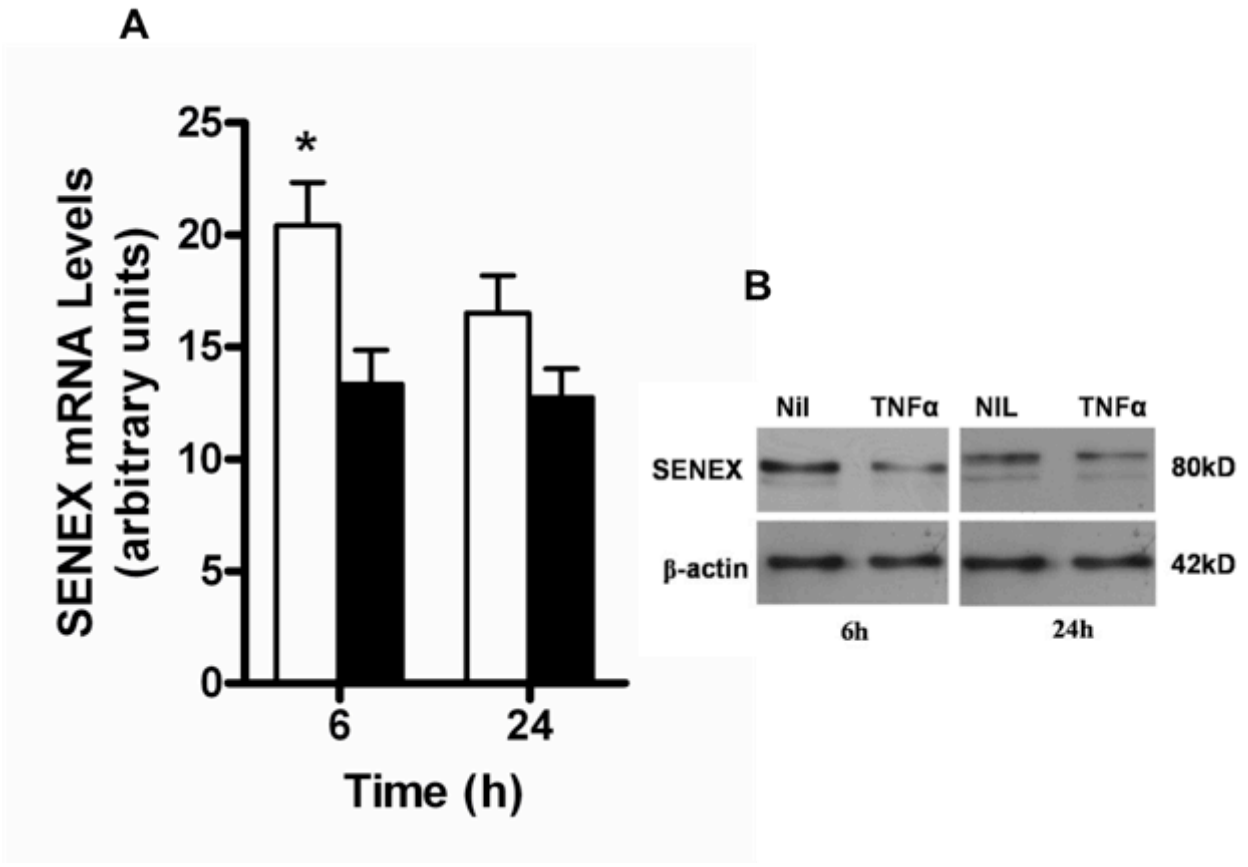
A
SENEX mRNA Levels (arbitrary units)
25
20
15
10
5
0
*
6
24
Time (h)
B
Nil
TNFα
NIL
TNFα
SENEX
80kD
β-actin
42kD
6h
24h

3

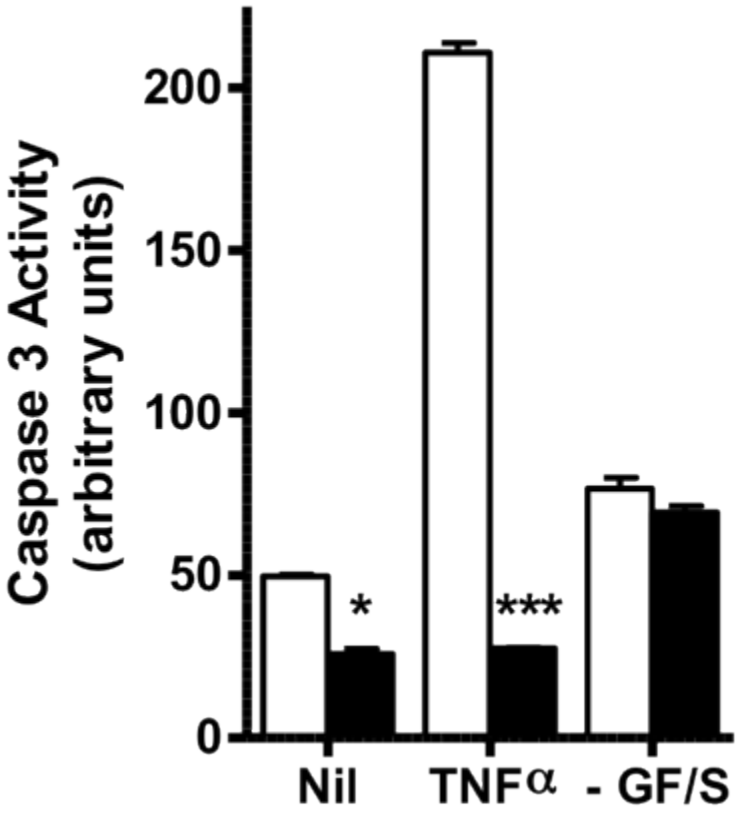
Caspase 3 Activity
(arbitrary units)
200
150
100
50
0
*
***
Nil
TNFα
- GF/S

10

this reason we also investigated whether SENEX was regulated during H_2O_2 induced apoptosis.

5.2.5 SENEX is regulated during hydrogen peroxide induced apoptosis.

HUVECs were treated with 500 μM of H_2O_2 for 6 hours and then the protein was harvested from attached and detached cells. The amount of apoptosis induced by high dose H_2O_2 was then measured using a caspase 3 assay. We found a 3 fold increase in the amount of apoptosis after treatment (Figure5.12A). SENEX protein levels were also decreased in cells treated with the same high dose H_2O_2 for the same period (Figure 5.12B). These results demonstrate that SENEX is not only regulated during H_2O_2 induced senescence but also during H_2O_2 induced apoptosis. Initial results indicate that SENEX expression needs to be downregulated for apoptosis to occur when it is caused by H_2O_2.

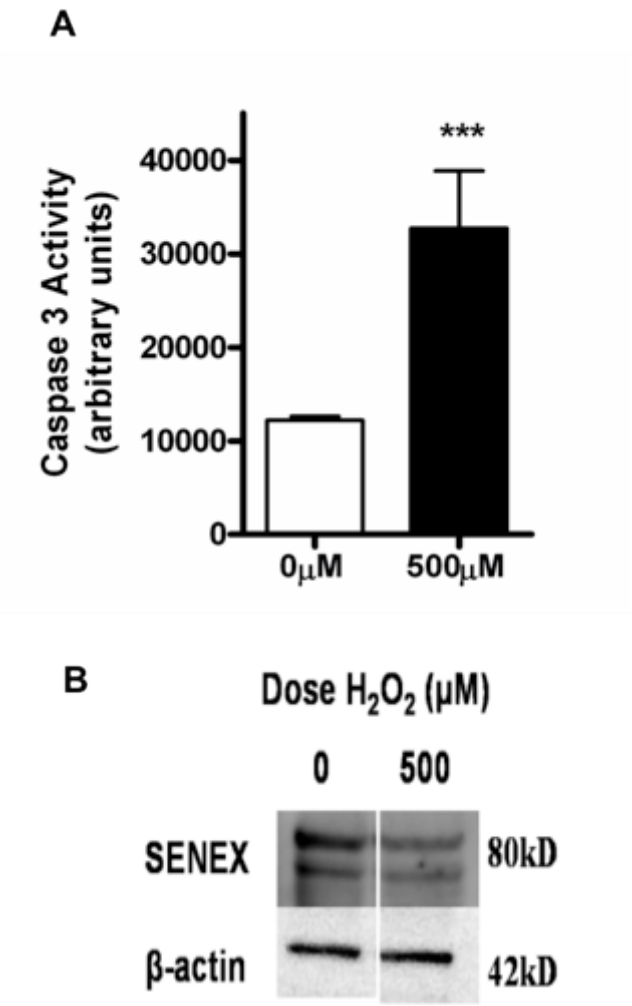
A
Caspase 3 Activity (arbitrary units)
40000
30000
20000
10000
0
***
0μM
500μM
B
Dose H_2O_2 (μM)
0
500
SENEX
80kD
β-actin
42kD

4

5.3 Summary

The work in this chapter demonstrates that SENEX is essential for endothelial cell survival. Loss of expression, as can be induced by siRNA or by high dose H_2O_2 or high dose TNFα results in the induction of apoptosis. The apoptosis which results from the knockdown of SENEX makes tube formation impossible and therefore has a serious effect on angiogenesis. Thus the maintenance of a basal level of SENEX not only is vital for EC survival but also for angiogenesis. This theory is further confirmed by the fact that all knockdown experiments were performed on subconfluent. Indicating the importance of SENEX expression during a time when the cells are active and dividing in a similar fashion during angiogenesis.

Our results indicate that SENEX is not involved in regulation of the intrinsic apoptosis signaling pathway and the overexpression of SENEX also does not protect against apoptosis initiated by this pathway. There is also no regulation of the BH3 proteins or BCL family which are all essential for the intrinsic pathway to cause apoptosis. High dose TNFα results in apoptosis which is mediated through the extrinsic pathway of apoptosis and here SENEX expression was downregulated. Also when we overexpressed SENEX to prevent its downregulation we found that the ECs were protected from TNFα induced apoptosis. These results indicate that the knockdown of SENEX is essential for apoptosis to occur and that this is through the extrinsic pathway. This area of research involving SENEX is still on going and more work is needed to determine how SENEX maybe involved in the extrinsic apoptosis pathway.

Chapter 6

Conclusion and future directions

The aim of my project was to identify novel genes which have integral functions during the angiogenesis process. From an angiogenesis array to identify genes regulated during capillary tube formation, a short list of interesting genes was made. The criteria for selection was a) high level of expression in EC, b) previous information about the gene, c) a pattern of regulation which was appropriate for the information about the gene, d) the uniqueness of the gene for angiogenesis. The first gene chosen for my studies was *REST*. *REST* has been implicated in neuronal development [145]. Since previous work has shown a link between the neuronal and vascular systems[150], *REST* appeared a potentially interesting possibility. I determined that the expression of the gene is regulated by the confluence level of endothelial cells, but there were no significant differences in any of the functional processes upon downregulation of REST expression levels. Furthermore, there were problems in overexpressing REST which limited analysis. Therefore, after 12 months of work to clone, sequence and manipulate the levels of expression of REST, it was decided to switch focus to another novel gene found on the angiogenesis array.

SENEX was the gene chosen for further work since some interesting results were being generated by other members of the laboratory. *SENEX* had been cloned and produced in the adenovirus system in both the forward and reverse orientations, using techniques analogous to those which I had used for REST. *SENEX* was a novel gene which although had been submitted to the data base as MacGAP, was without a described function. The dramatic alteration in phenotype of the

EC upon overexpression of SENEX formed the basis for the new project, to determine the phenotype induced and the consequences to EC function.

My investigations showed that the large flattened highly vacuolated, polyploidy cells were in fact senescent EC. The cells which resulted from overexpressing SENEX had all the features of a senescent EC. They had the morphological features of senescence, they stained positive for the published marker of senescence SA β-galactosidase, they had withdrawn from the cell cycle at the G1 stage and could no longer proliferate when stimulated with growth factors. The senescent cells were also resistant to the apoptotic stimuli and had a decreased expression of eNOS, which is a published marker of senescent endothelial cells [132]. These results together confirmed that by overexpressing SENEX we were inducing the EC to become senescent.

There are two well described signaling pathways which lead to the development of senescence. They are the p53/p21 pathway and the p16/Rb pathway [155]. SENEX was able to increase the expression of p16 which resulted in hypophosphorylated Rb but did not alter the p53/p21 pathway. These results further confirmed that SENEX was able to initiate senescence through a known signaling pathway. To determine the importance of the p16/Rb pathway in SENEX induced senescence it would be interesting in the future to use siRNA to knockdown the expression of p16 and determine if SENEX is still capable of inducing senescence. This experiment would also confirm the importance of p16 in SENEX induced senescence.

There are two known forms of senescence, replicative senescence which results from the shortening of telomeres during repeated replication and stress induced premature senescence which results from different stimuli, causes a rapid development of senescence and does not involve telomere shortening [174]. We found that SENEX does not alter telomere length and

causes a rapid induction of the senescent phenotype. These results point to the involvement of SENEX in SIPS and not RS development.

Oxidative stress is able to induce senescence either by causing DNA damage [69], but can also induce senescence through the p38 pathway[68]. Oxidative stress is an inducer of senescence in EC and is also involved in cardiovascular disease[130]. For these reasons we chose to determine if SENEX is involved in oxidative stress induced senescence. Low dose H_2O_2 induces an increase in the protein levels of SENEX and also induces senescence. The upregulation of SENEX after hydrogen peroxide treatment points to the involvement of SENEX during senescence formation after oxidative stress. Furthermore it suggests that the phenotype seen after SENEX overexpression is not purely a result of excess protein expression but rather has a biological foundation. We are currently performing the experiments to determine if SENEX is essential for oxidative stress induced senescence in endothelial cells. To do this we will knockdown the expression of SENEX with siRNA and then attempt to induce senescence with H_2O_2. The aim would be to knockdown expression at a reduced level from which causes apoptosis, but prevents the upregulation indiced by hydrogen peroxide. If there is a reduction in the amount of senescence this will establish that SENEX has an integral role in oxidative stress induced senescence.

Our results have shown that SENEX is a novel gene that is able to induce a new and important physiological change to EC which is senescence. We currently have shown a role for SENEX in oxidative stress but there are also many other published inducers of stress induced senescence. These include a range of oncogenes and chemotherapeutic agents [175]. We are currently inducing senescence in the EC with different oncogenes and agents and looking for regulation of SENEX. If SENEX is shown to be regulated during other forms of stressed induced senescence

in EC, then SENEX may be used in the future as a marker of SIPS in EC. Since there are limited markers for senescence, especially a marker of SIPs the possibility of SENEX being such a marker is very exciting.

The most surprising result from investigations into the effects of SENEX overexpression however was the functional consequence on ECs. These senescent cells were powerfully anti-inflammatory since they failed to support neutrophil and lymphocyte adhesion after TNFα activation, they failed to show surface expression of appropriate adhesion molecules E-selectin and VCAM1 and the permeability response to thrombin was impaired. This phenotype of SIPS induced EC is in contrast to SIPS induced in other cell types where a strongly pro-inflammatory phenotype has been reported [24]. Indeed senescence is associated with the secretion of multiple factors (hence the name, senescence-associated secretory phenotype)[103] which are strongly pro-inflammatory. These include increased levels of IL-8, IL-6, MCP-1 and shed proteins such as uPAR, VCAM1and ICAM1/[83, 176]

Thus, we have postulated that this SIPS phenotype in EC may serve a protective role in the vasculature at sites of chronic inflammation. In support of this it was shown that SENEX, at least at the mRNA level is increased in atherosclerotic plaques in ApoE knockout mice fed a western diet. Further work now is focusing on confirming that SENEX is expressed on the EC in such lesions. Thus, the phenotype of SENEX induced senescence maybe beneficial and protective to decrease inflammation at known senescent sites such as in atherosclerotic plaques, and thus may serve as a mechanism to limit the progression of plaque formation. The work published to date in the atherosclerotic plaque area has concentrated on late chronic lesions. It may be possible that the induction of senescence in early lesions by SENEX would provide a way to prevent the

progression of atherosclerosis. The decrease in eNOS observed in our SENEX induced senescent cells would appear contradictory. However, since it is the "available' NO derived from eNOS rather than eNOS expression per se which is critical, further work is required to delineate the role of NO in our observed phenotype.

The phenotype of senescent cells maybe cell type and inducer specific. In non vascular cells the pro-inflammatory phenotype seen in senescent cells may have specific disease related consequences. For example, senescence in tumours may not only inhibit tumour growth but may also recruit in immune cells. The stimulation of immune cells, particularly the innate immune system contributes to tumour clearance [83]. Induction of senescence in hepatic stellate cells prevents the progression of liver fibrosis by inhibiting the proliferation of these activated cells. The senescent stellate cells upregulate a pattern of gene expression associated with enhanced immune surveillance and indeed these senescent cells are sensitive to NK mediated killing as a mechanism for their removal from the fibrotic lesion.[8] Thus although senescence was originally considered to be a mechanism, together with apoptosis, for controlling cell proliferation and malignant transformation, the data would suggest that senescence plays a broader role in disease progression or resolution.

In contrast to what we have shown here, replicative senescent EC, as induced by Akt,[63] Rac1,[177] Duffy Antigen/Receptor for Chemokines (DARC) [177] and the metabolite homocysteine [119] result in an endothelium that is pro- inflammatory as judged by increased monocyte adhesion with upregulation of adhesion molecule expression [119, 177] and upregulation of IL-8.[96] Interestingly, IL-8 is not only a cytokine responsible for neutrophil transendothelial cell migration [178] but is also a downstream effector of C reactive protein, an activator of EC and involved in promoting the inflammatory response during atherogenesis [179]. Thus, my work together with previous publications would suggest that the mechanism and

signaling pathway (RS versus SIPS) activated to achieve senescence in EC clearly impacts on the consequence to cellular function (inflammatory versus anti-inflammatory, respectively).

SENEX is of further interest since its expression is essential for EC survival. Knockdown of SENEX in EC results in apoptosis. In addition, SENEX overexpression inhibits TNFα induced EC apoptosis. These studies were performed at times where there is a significant level of senescent cells and could be merely explained by the previously documented, anti-apoptotic phenotype of senescent cells.[16] However, the failure of SENEX to protect against growth factor and serum deprivation suggests that the protection seen in TNFα treated cells is through SENEX effects on specific signaling pathways, not a general effect of the senescence. The most likely apoptotic pathway activated by depletion of SENEX is the extrinsic pathway. SENEX does not protect against serum starvation induced apoptosis and the knockdown of SENEX does not regulate any of the BH3 proteins or the BCL family, proteins known to be important in the induction of intrinsic apoptosis. .Further work on delineating these signaling pathways is currently being done.

The fact that overexpression of SENEX induces senescence whereas depletion induces apoptosis highlights the fact that the SENEX dosage (or a more complicated change in its subcellular distribution) governs a balance between these two vital cellular mechanisms. The changes induced by oxidative stress in the form of H_2O_2 support this notion. Low doses of H_2O_2 induce *SENEX* and senescence, whereas higher doses inhibit SENEX expression and induce apoptosis. H_2O_2 has been implicated in senescence induction in other cell types. Although in primary fibroblasts H_2O_2 targets TGFβ and caveolin-1 to induce the senescence phenotype,[180] these downstream targets are not involved in apoptosis signaling. Thus, the characterization of *SENEX*

shows novel features of being highly expressed in EC but that further changes regulate a senescence/apoptosis arm.

The structure function analysis of SENEX is still to be elucidated. SENEX is a member of the RhoGAP family of proteins. However, mutation of one of the essential amino acids in the RhoGAP domain that eliminates the Rho activity, does not affect the senescence inducing capacity of the protein. Thus, it is likely that SENEX can exert multiple functions. In this regard, it is interesting to note that *SENEX* is predicted to interact with the RNA binding protein m phase phosphoprotein 6 (MPP6) (www.thebiogrid.org/SearchResults/summary/119675) and MPP6 interacts with the RNA polymerase II (POL II) binding protein, Che-1. Che-1 is a protein involved in the control of cell proliferation through interactions with Rb and regulation of the transcription of E2F target genes. More recently Che-1 has been shown to regulate DNA damage and cell-cycle checkpoint control [181]. Further investigations are underway to determine whether such potential interactions are involved in the senescence inducing ability of *SENEX*. In addition, we are performing yeast 2 hybrid screens in order to identify any interacting proteins which may function to regulate SENEX levels or function.

The *SENEX* gene is located on chromosome 6q22.33.and recently this locus has been identified as a novel susceptibility locus for breast cancer [182]. This is also another area which we may be looking at in the future.

In summary, we have described the gene *SENEX* as a major fulcrum for the fine tuning of function in EC, regulating senescence and apoptosis. The identification of *SENEX* as a senescence-inducing gene, specifically through the SIPS pathway, allows us to probe the consequences of this on cellular function and its role in disease. Our results indicate that SIPS not only limits excessive proliferation but also activates an anti-inflammatory profile in EC. Thus

while *SENEX* mediated senescence is likely to be beneficial in limiting vascular disease, we would predict that excessive and prolonged accumulation of these cells in the vasculature may ultimately result in chronic vascular dysfunction.

REFERENCES

[1] Hayflick L, Moorhead PS. The serial cultivation of human diploid cell strains. Exp Cell Res. 1961 Dec;25:585-621.
[2] Dimri GP, Lee X, Basile G, Acosta M, Scott G, Roskelley C, et al. A biomarker that identifies senescent human cells in culture and in aging skin in vivo. Proc Natl Acad Sci U S A. 1995 Sep 26;92(20):9363-7.
[3] Braig M, Lee S, Loddenkemper C, Rudolph C, Peters AH, Schlegelberger B, et al. Oncogene-induced senescence as an initial barrier in lymphoma development. Nature. 2005 Aug 4;436(7051):660-5.
[4] Chen Z, Trotman LC, Shaffer D, Lin HK, Dotan ZA, Niki M, et al. Crucial role of p53-dependent cellular senescence in suppression of Pten-deficient tumorigenesis. Nature. 2005 Aug 4;436(7051):725-30.
[5] Collado M, Gil J, Efeyan A, Guerra C, Schuhmacher AJ, Barradas M, et al. Tumour biology: senescence in premalignant tumours. Nature. 2005 Aug 4;436(7051):642.
[6] Michaloglou C, Vredeveld LC, Soengas MS, Denoyelle C, Kuilman T, van der Horst CM, et al. BRAFE600-associated senescence-like cell cycle arrest of human naevi. Nature. 2005 Aug 4;436(7051):720-4.
[7] Lowe SW, Cepero E, Evan G. Intrinsic tumour suppression. Nature. 2004 Nov 18;432(7015):307-15.
[8] Krizhanovsky V, Yon M, Dickins RA, Hearn S, Simon J, Miething C, et al. Senescence of activated stellate cells limits liver fibrosis. Cell. 2008 Aug 22;134(4):657-67.
[9] Ben-Porath I, Weinberg RA. When cells get stressed: an integrative view of cellular senescence. The Journal of clinical investigation. 2004 Jan;113(1):8-13.
[10] Campisi J, d'Adda di Fagagna F. Cellular senescence: when bad things happen to good cells. Nat Rev Mol Cell Biol. 2007 Sep;8(9):729-40.
[11] Kurz DJ, Decary S, Hong Y, Erusalimsky JD. Senescence-associated (beta)-galactosidase reflects an increase in lysosomal mass during replicative ageing of human endothelial cells. J Cell Sci. 2000 Oct;113 (Pt 20):3613-22.
[12] Severino J, Allen RG, Balin S, Balin A, Cristofalo VJ. Is beta-galactosidase staining a marker of senescence in vitro and in vivo? Exp Cell Res. 2000 May 25;257(1):162-71.
[13] Cotter MA, Florell SR, Leachman SA, Grossman D. Absence of senescence-associated beta-galactosidase activity in human melanocytic nevi in vivo. The Journal of investigative dermatology. 2007 Oct;127(10):2469-71.
[14] Narita M, Nunez S, Heard E, Narita M, Lin AW, Hearn SA, et al. Rb-mediated heterochromatin formation and silencing of E2F target genes during cellular senescence. Cell. 2003 Jun 13;113(6):703-16.
[15] Rodier F, Campisi J. Four faces of cellular senescence. The Journal of cell biology. Feb 21;192(4):547-56.
[16] Wang E. Senescent human fibroblasts resist programmed cell death, and failure to suppress bcl2 is involved. Cancer Res. 1995 Jun 1;55(11):2284-92.
[17] Hampel B, Malisan F, Niederegger H, Testi R, Jansen-Durr P. Differential regulation of apoptotic cell death in senescent human cells. Exp Gerontol. 2004 Nov-Dec;39(11-12):1713-21.
[18] Ohshima S. Apoptosis in stress-induced and spontaneously senescent human fibroblasts. Biochem Biophys Res Commun. 2004 Nov 5;324(1):241-6.
[19] Unterluggauer H, Hampel B, Zwerschke W, Jansen-Durr P. Senescence-associated cell death of human endothelial cells: the role of oxidative stress. Exp Gerontol. 2003 Oct;38(10):1149-60.

[20] Chan SW, Chang J, Prescott J, Blackburn EH. Altering telomere structure allows telomerase to act in yeast lacking ATM kinases. Curr Biol. 2001 Aug 21;11(16):1240-50.
[21] Smogorzewska A, de Lange T. Regulation of telomerase by telomeric proteins. Annual review of biochemistry. 2004;73:177-208.
[22] Harley CB, Futcher AB, Greider CW. Telomeres shorten during ageing of human fibroblasts. Nature. 1990 May 31;345(6274):458-60.
[23] de Lange T, Shiue L, Myers RM, Cox DR, Naylor SL, Killery AM, et al. Structure and variability of human chromosome ends. Molecular and cellular biology. 1990 Feb;10(2):518-27.
[24] Campisi J. Senescent cells, tumor suppression, and organismal aging: good citizens, bad neighbors. Cell. 2005 Feb 25;120(4):513-22.
[25] Toussaint O, Medrano EE, von Zglinicki T. Cellular and molecular mechanisms of stress-induced premature senescence (SIPS) of human diploid fibroblasts and melanocytes. Exp Gerontol. 2000 Oct;35(8):927-45.
[26] Bartkova J, Rezaei N, Liontos M, Karakaidos P, Kletsas D, Issaeva N, et al. Oncogene-induced senescence is part of the tumorigenesis barrier imposed by DNA damage checkpoints. Nature. 2006 Nov 30;444(7119):633-7.
[27] Chen QM, Bartholomew JC, Campisi J, Acosta M, Reagan JD, Ames BN. Molecular analysis of H2O2-induced senescent-like growth arrest in normal human fibroblasts: p53 and Rb control G1 arrest but not cell replication. The Biochemical journal. 1998 May 15;332 (Pt 1):43-50.
[28] Lee AC, Fenster BE, Ito H, Takeda K, Bae NS, Hirai T, et al. Ras proteins induce senescence by altering the intracellular levels of reactive oxygen species. J Biol Chem. 1999 Mar 19;274(12):7936-40.
[29] Serrano M, Lin AW, McCurrach ME, Beach D, Lowe SW. Oncogenic ras provokes premature cell senescence associated with accumulation of p53 and p16INK4a. Cell. 1997 Mar 7;88(5):593-602.
[30] Courtois-Cox S, Genther Williams SM, Reczek EE, Johnson BW, McGillicuddy LT, Johannessen CM, et al. A negative feedback signaling network underlies oncogene-induced senescence. Cancer cell. 2006 Dec;10(6):459-72.
[31] Serrano M, Blasco MA. Putting the stress on senescence. Current opinion in cell biology. 2001 Dec;13(6):748-53.
[32] Haber DA. Splicing into senescence: the curious case of p16 and p19ARF. Cell. 1997 Nov 28;91(5):555-8.
[33] Pavletich NP. Mechanisms of cyclin-dependent kinase regulation: structures of Cdks, their cyclin activators, and Cip and INK4 inhibitors. Journal of molecular biology. 1999 Apr 16;287(5):821-8.
[34] Harbour JW, Dean DC. Corepressors and retinoblastoma protein function. Current topics in microbiology and immunology. 2001;254:137-44.
[35] Artandi SE, Attardi LD. Pathways connecting telomeres and p53 in senescence, apoptosis, and cancer. Biochem Biophys Res Commun. 2005 Jun 10;331(3):881-90.
[36] Prieur A, Peeper DS. Cellular senescence in vivo: a barrier to tumorigenesis. Curr Opin Cell Biol. 2008 Apr;20(2):150-5.
[37] Kastan MB, Bartek J. Cell-cycle checkpoints and cancer. Nature. 2004 Nov 18;432(7015):316-23.
[38] von Zglinicki T. Oxidative stress shortens telomeres. Trends Biochem Sci. 2002 Jul;27(7):339-44.
[39] Mah LJ, El-Osta A, Karagiannis TC. gammaH2AX: a sensitive molecular marker of DNA damage and repair. Leukemia. Apr;24(4):679-86.

[40] Appella E, Anderson CW. Post-translational modifications and activation of p53 by genotoxic stresses. Eur J Biochem. 2001 May;268(10):2764-72.
[41] Lambert PF, Kashanchi F, Radonovich MF, Shiekhattar R, Brady JN. Phosphorylation of p53 serine 15 increases interaction with CBP. J Biol Chem. 1998 Dec 4;273(49):33048-53.
[42] Herbig U, Jobling WA, Chen BP, Chen DJ, Sedivy JM. Telomere shortening triggers senescence of human cells through a pathway involving ATM, p53, and p21(CIP1), but not p16(INK4a). Mol Cell. 2004 May 21;14(4):501-13.
[43] Freiberg RA, Hammond EM, Dorie MJ, Welford SM, Giaccia AJ. DNA damage during reoxygenation elicits a Chk2-dependent checkpoint response. Mol Cell Biol. 2006 Mar;26(5):1598-609.
[44] Prives C. Signaling to p53: breaking the MDM2-p53 circuit. Cell. 1998 Oct 2;95(1):5-8.
[45] Levine AJ. p53, the cellular gatekeeper for growth and division. Cell. 1997 Feb 7;88(3):323-31.
[46] Bringold F, Serrano M. Tumor suppressors and oncogenes in cellular senescence. Exp Gerontol. 2000 May;35(3):317-29.
[47] Sherr CJ, McCormick F. The RB and p53 pathways in cancer. Cancer Cell. 2002 Aug;2(2):103-12.
[48] Giaccia AJ, Kastan MB. The complexity of p53 modulation: emerging patterns from divergent signals. Genes Dev. 1998 Oct 1;12(19):2973-83.
[49] Jacobs JJ, de Lange T. Significant role for p16INK4a in p53-independent telomere-directed senescence. Curr Biol. 2004 Dec 29;14(24):2302-8.
[50] Stein GH, Drullinger LF, Soulard A, Dulic V. Differential roles for cyclin-dependent kinase inhibitors p21 and p16 in the mechanisms of senescence and differentiation in human fibroblasts. Mol Cell Biol. 1999 Mar;19(3):2109-17.
[51] Campisi J. Cellular senescence as a tumor-suppressor mechanism. Trends Cell Biol. 2001 Nov;11(11):S27-31.
[52] Wajapeyee N, Serra RW, Zhu X, Mahalingam M, Green MR. Oncogenic BRAF induces senescence and apoptosis through pathways mediated by the secreted protein IGFBP7. Cell. 2008 Feb 8;132(3):363-74.
[53] Davies H, Bignell GR, Cox C, Stephens P, Edkins S, Clegg S, et al. Mutations of the BRAF gene in human cancer. Nature. 2002 Jun 27;417(6892):949-54.
[54] Wang W, Chen JX, Liao R, Deng Q, Zhou JJ, Huang S, et al. Sequential activation of the MEK-extracellular signal-regulated kinase and MKK3/6-p38 mitogen-activated protein kinase pathways mediates oncogenic ras-induced premature senescence. Molecular and cellular biology. 2002 May;22(10):3389-403.
[55] Sun P, Yoshizuka N, New L, Moser BA, Li Y, Liao R, et al. PRAK is essential for ras-induced senescence and tumor suppression. Cell. 2007 Jan 26;128(2):295-308.
[56] Bihani T, Chicas A, Lo CP, Lin AW. Dissecting the senescence-like program in tumor cells activated by Ras signaling. J Biol Chem. 2007 Jan 26;282(4):2666-75.
[57] Huot TJ, Rowe J, Harland M, Drayton S, Brookes S, Gooptu C, et al. Biallelic mutations in p16(INK4a) confer resistance to Ras- and Ets-induced senescence in human diploid fibroblasts. Molecular and cellular biology. 2002 Dec;22(23):8135-43.
[58] Brookes S, Rowe J, Ruas M, Llanos S, Clark PA, Lomax M, et al. INK4a-deficient human diploid fibroblasts are resistant to RAS-induced senescence. Embo J. 2002 Jun 17;21(12):2936-45.
[59] Sewing A, Wiseman B, Lloyd AC, Land H. High-intensity Raf signal causes cell cycle arrest mediated by p21Cip1. Molecular and cellular biology. 1997 Sep;17(9):5588-97.

[60] Sarkisian CJ, Keister BA, Stairs DB, Boxer RB, Moody SE, Chodosh LA. Dose-dependent oncogene-induced senescence in vivo and its evasion during mammary tumorigenesis. Nature cell biology. 2007 May;9(5):493-505.
[61] Drayton S, Rowe J, Jones R, Vatcheva R, Cuthbert-Heavens D, Marshall J, et al. Tumor suppressor p16INK4a determines sensitivity of human cells to transformation by cooperating cellular oncogenes. Cancer cell. 2003 Oct;4(4):301-10.
[62] Guney I, Wu S, Sedivy JM. Reduced c-Myc signaling triggers telomere-independent senescence by regulating Bmi-1 and p16(INK4a). Proc Natl Acad Sci U S A. 2006 Mar 7;103(10):3645-50.
[63] Miyauchi H, Minamino T, Tateno K, Kunieda T, Toko H, Komuro I. Akt negatively regulates the in vitro lifespan of human endothelial cells via a p53/p21-dependent pathway. Embo J. 2004 Jan 14;23(1):212-20.
[64] Graeber TG, Peterson JF, Tsai M, Monica K, Fornace AJ, Jr., Giaccia AJ. Hypoxia induces accumulation of p53 protein, but activation of a G1-phase checkpoint by low-oxygen conditions is independent of p53 status. Mol Cell Biol. 1994 Sep;14(9):6264-77.
[65] Finkel T. Oxygen radicals and signaling. Curr Opin Cell Biol. 1998 Apr;10(2):248-53.
[66] Chen Q, Ames BN. Senescence-like growth arrest induced by hydrogen peroxide in human diploid fibroblast F65 cells. Proc Natl Acad Sci U S A. 1994 May 10;91(10):4130-4.
[67] Chen J, Goligorsky MS. Premature senescence of endothelial cells: Methusaleh's dilemma. American journal of physiology. 2006 May;290(5):H1729-39.
[68] Iwasa H, Han J, Ishikawa F. Mitogen-activated protein kinase p38 defines the common senescence-signalling pathway. Genes Cells. 2003 Feb;8(2):131-44.
[69] Zhan H, Suzuki T, Aizawa K, Miyagawa K, Nagai R. Ataxia telangiectasia mutated (ATM)-mediated DNA damage response in oxidative stress-induced vascular endothelial cell senescence. J Biol Chem. Jul 16.
[70] Macip S, Igarashi M, Berggren P, Yu J, Lee SW, Aaronson SA. Influence of induced reactive oxygen species in p53-mediated cell fate decisions. Molecular and cellular biology. 2003 Dec;23(23):8576-85.
[71] Kurz DJ, Decary S, Hong Y, Trivier E, Akhmedov A, Erusalimsky JD. Chronic oxidative stress compromises telomere integrity and accelerates the onset of senescence in human endothelial cells. J Cell Sci. 2004 May 1;117(Pt 11):2417-26.
[72] Petersen S, Saretzki G, von Zglinicki T. Preferential accumulation of single-stranded regions in telomeres of human fibroblasts. Exp Cell Res. 1998 Feb 25;239(1):152-60.
[73] Schmitt CA. Senescence, apoptosis and therapy--cutting the lifelines of cancer. Nat Rev Cancer. 2003 Apr;3(4):286-95.
[74] Gray-Schopfer VC, Cheong SC, Chong H, Chow J, Moss T, Abdel-Malek ZA, et al. Cellular senescence in naevi and immortalisation in melanoma: a role for p16? British journal of cancer. 2006 Aug 21;95(4):496-505.
[75] Adams PD. Healing and hurting: molecular mechanisms, functions, and pathologies of cellular senescence. Mol Cell. 2009 Oct 9;36(1):2-14.
[76] Ha L, Ichikawa T, Anver M, Dickins R, Lowe S, Sharpless NE, et al. ARF functions as a melanoma tumor suppressor by inducing p53-independent senescence. Proc Natl Acad Sci U S A. 2007 Jun 26;104(26):10968-73.
[77] Di Cristofano A, Pandolfi PP. The multiple roles of PTEN in tumor suppression. Cell. 2000 Feb 18;100(4):387-90.
[78] Vogelstein B, Lane D, Levine AJ. Surfing the p53 network. Nature. 2000 Nov 16;408(6810):307-10.
[79] Feldser DM, Greider CW. Short telomeres limit tumor progression in vivo by inducing senescence. Cancer cell. 2007 May;11(5):461-9.

[80] Cosme-Blanco W, Shen MF, Lazar AJ, Pathak S, Lozano G, Multani AS, et al. Telomere dysfunction suppresses spontaneous tumorigenesis in vivo by initiating p53-dependent cellular senescence. EMBO reports. 2007 May;8(5):497-503.
[81] Harris SL, Levine AJ. The p53 pathway: positive and negative feedback loops. Oncogene. 2005 Apr 18;24(17):2899-908.
[82] Sherr CJ. Principles of tumor suppression. Cell. 2004 Jan 23;116(2):235-46.
[83] Xue W, Zender L, Miething C, Dickins RA, Hernando E, Krizhanovsky V, et al. Senescence and tumour clearance is triggered by p53 restoration in murine liver carcinomas. Nature. 2007 Feb 8;445(7128):656-60.
[84] Ventura A, Kirsch DG, McLaughlin ME, Tuveson DA, Grimm J, Lintault L, et al. Restoration of p53 function leads to tumour regression in vivo. Nature. 2007 Feb 8;445(7128):661-5.
[85] Emadi A, Jones RJ, Brodsky RA. Cyclophosphamide and cancer: golden anniversary. Nat Rev Clin Oncol. 2009 Nov;6(11):638-47.
[86] Schmitt CA, Fridman JS, Yang M, Lee S, Baranov E, Hoffman RM, et al. A senescence program controlled by p53 and p16INK4a contributes to the outcome of cancer therapy. Cell. 2002 May 3;109(3):335-46.
[87] Pommier Y, Leteurtre F, Fesen MR, Fujimori A, Bertrand R, Solary E, et al. Cellular determinants of sensitivity and resistance to DNA topoisomerase inhibitors. Cancer investigation. 1994;12(5):530-42.
[88] te Poele RH, Okorokov AL, Jardine L, Cummings J, Joel SP. DNA damage is able to induce senescence in tumor cells in vitro and in vivo. Cancer Res. 2002 Mar 15;62(6):1876-83.
[89] Coppe JP, Patil CK, Rodier F, Sun Y, Munoz DP, Goldstein J, et al. Senescence-Associated Secretory Phenotypes Reveal Cell-Nonautonomous Functions of Oncogenic RAS and the p53 Tumor Suppressor. PLoS biology. 2008 Dec 2;6(12):e301.
[90] Chen J, Brodsky SV, Goligorsky DM, Hampel DJ, Li H, Gross SS, et al. Glycated collagen I induces premature senescence-like phenotypic changes in endothelial cells. Circulation research. 2002 Jun 28;90(12):1290-8.
[91] Kamino H, Hiratsuka M, Toda T, Nishigaki R, Osaki M, Ito H, et al. Searching for genes involved in arteriosclerosis: proteomic analysis of cultured human umbilical vein endothelial cells undergoing replicative senescence. Cell structure and function. 2003 Dec;28(6):495-503.
[92] Shelton DN, Chang E, Whittier PS, Choi D, Funk WD. Microarray analysis of replicative senescence. Curr Biol. 1999 Sep 9;9(17):939-45.
[93] Coppe JP, Desprez PY, Krtolica A, Campisi J. The senescence-associated secretory phenotype: the dark side of tumor suppression. Annual review of pathology.5:99-118.
[94] Davalos AR, Coppe JP, Campisi J, Desprez PY. Senescent cells as a source of inflammatory factors for tumor progression. Cancer Metastasis Rev. Jun;29(2):273-83.
[95] Kuilman T, Michaloglou C, Vredeveld LC, Douma S, van Doorn R, Desmet CJ, et al. Oncogene-induced senescence relayed by an interleukin-dependent inflammatory network. Cell. 2008 Jun 13;133(6):1019-31.
[96] Acosta JC, O'Loghlen A, Banito A, Guijarro MV, Augert A, Raguz S, et al. Chemokine signaling via the CXCR2 receptor reinforces senescence. Cell. 2008 Jun 13;133(6):1006-18.
[97] Sparmann A, Bar-Sagi D. Ras-induced interleukin-8 expression plays a critical role in tumor growth and angiogenesis. Cancer cell. 2004 Nov;6(5):447-58.
[98] Bordoni R, Fine R, Murray D, Richmond A. Characterization of the role of melanoma growth stimulatory activity (MGSA) in the growth of normal melanocytes, nevocytes, and malignant melanocytes. Journal of cellular biochemistry. 1990 Dec;44(4):207-19.
[99] Liu D, Hornsby PJ. Senescent human fibroblasts increase the early growth of xenograft tumors via matrix metalloproteinase secretion. Cancer Res. 2007 Apr 1;67(7):3117-26.

[100] Krtolica A, Parrinello S, Lockett S, Desprez PY, Campisi J. Senescent fibroblasts promote epithelial cell growth and tumorigenesis: a link between cancer and aging. Proc Natl Acad Sci U S A. 2001 Oct 9;98(21):12072-7.
[101] Bavik C, Coleman I, Dean JP, Knudsen B, Plymate S, Nelson PS. The gene expression program of prostate fibroblast senescence modulates neoplastic epithelial cell proliferation through paracrine mechanisms. Cancer Res. 2006 Jan 15;66(2):794-802.
[102] Coppe JP, Patil CK, Rodier F, Sun Y, Munoz DP, Goldstein J, et al. Senescence-associated secretory phenotypes reveal cell-nonautonomous functions of oncogenic RAS and the p53 tumor suppressor. PLoS biology. 2008 Dec 2;6(12):2853-68.
[103] Coppe JP, Kauser K, Campisi J, Beausejour CM. Secretion of vascular endothelial growth factor by primary human fibroblasts at senescence. J Biol Chem. 2006 Oct 6;281(40):29568-74.
[104] Yoon IK, Kim HK, Kim YK, Song IH, Kim W, Kim S, et al. Exploration of replicative senescence-associated genes in human dermal fibroblasts by cDNA microarray technology. Exp Gerontol. 2004 Sep;39(9):1369-78.
[105] Schnabl B, Purbeck CA, Choi YH, Hagedorn CH, Brenner D. Replicative senescence of activated human hepatic stellate cells is accompanied by a pronounced inflammatory but less fibrogenic phenotype. Hepatology (Baltimore, Md. 2003 Mar;37(3):653-64.
[106] Mason DX, Jackson TJ, Lin AW. Molecular signature of oncogenic ras-induced senescence. Oncogene. 2004 Dec 9;23(57):9238-46.
[107] Hong DS, Angelo LS, Kurzrock R. Interleukin-6 and its receptor in cancer: implications for Translational Therapeutics. Cancer. 2007 Nov 1;110(9):1911-28.
[108] Rodier F, Coppe JP, Patil CK, Hoeijmakers WA, Munoz DP, Raza SR, et al. Persistent DNA damage signalling triggers senescence-associated inflammatory cytokine secretion. Nature cell biology. 2009 Aug;11(8):973-9.
[109] Freund A, Patil CK, Campisi J. p38MAPK is a novel DNA damage response-independent regulator of the senescence-associated secretory phenotype. The EMBO journal. 2011 Apr 20;30(8):1536-48.
[110] Collado M, Blasco MA, Serrano M. Cellular senescence in cancer and aging. Cell. 2007 Jul 27;130(2):223-33.
[111] Krtolica A, Campisi J. Cancer and aging: a model for the cancer promoting effects of the aging stroma. The international journal of biochemistry & cell biology. 2002 Nov;34(11):1401-14.
[112] Ogami M, Ikura Y, Ohsawa M, Matsuo T, Kayo S, Yoshimi N, et al. Telomere shortening in human coronary artery diseases. Arteriosclerosis, thrombosis, and vascular biology. 2004 Mar;24(3):546-50.
[113] Valdes AM, Andrew T, Gardner JP, Kimura M, Oelsner E, Cherkas LF, et al. Obesity, cigarette smoking, and telomere length in women. Lancet. 2005 Aug 20-26;366(9486):662-4.
[114] Erusalimsky JD, Kurz DJ. Cellular senescence in vivo: its relevance in ageing and cardiovascular disease. Exp Gerontol. 2005 Aug-Sep;40(8-9):634-42.
[115] Fenton M, Barker S, Kurz DJ, Erusalimsky JD. Cellular senescence after single and repeated balloon catheter denudations of rabbit carotid arteries. Arteriosclerosis, thrombosis, and vascular biology. 2001 Feb;21(2):220-6.
[116] Minamino T, Komuro I. Role of telomeres in vascular senescence. Front Biosci. 2008;13:2971-9.
[117] Balcer-Kubiczek EK, Yin J, Lin K, Harrison GH, Abraham JM, Meltzer SJ. p53 mutational status and survival of human breast cancer MCF-7 cell variants after exposure to X rays or fission neutrons. Radiation research. 1995 Jun;142(3):256-62.
[118] Scalera F, Borlak J, Beckmann B, Martens-Lobenhoffer J, Thum T, Tager M, et al. Endogenous nitric oxide synthesis inhibitor asymmetric dimethyl L-arginine accelerates

endothelial cell senescence. Arteriosclerosis, thrombosis, and vascular biology. 2004 Oct;24(10):1816-22.
[119] Xu D, Neville R, Finkel T. Homocysteine accelerates endothelial cell senescence. FEBS Lett. 2000 Mar 17;470(1):20-4.
[120] Voghel G, Thorin-Trescases N, Farhat N, Nguyen A, Villeneuve L, Mamarbachi AM, et al. Cellular senescence in endothelial cells from atherosclerotic patients is accelerated by oxidative stress associated with cardiovascular risk factors. Mechanisms of ageing and development. 2007 Nov-Dec;128(11-12):662-71.
[121] Najjar SS, Scuteri A, Lakatta EG. Arterial aging: is it an immutable cardiovascular risk factor? Hypertension. 2005 Sep;46(3):454-62.
[122] Kunieda T, Minamino T, Nishi J, Tateno K, Oyama T, Katsuno T, et al. Angiotensin II induces premature senescence of vascular smooth muscle cells and accelerates the development of atherosclerosis via a p21-dependent pathway. Circulation. 2006 Aug 29;114(9):953-60.
[123] Minamino T, Yoshida T, Tateno K, Miyauchi H, Zou Y, Toko H, et al. Ras induces vascular smooth muscle cell senescence and inflammation in human atherosclerosis. Circulation. 2003 Nov 4;108(18):2264-9.
[124] Schleicher M, Shepherd BR, Suarez Y, Fernandez-Hernando C, Yu J, Pan Y, et al. Prohibitin-1 maintains the angiogenic capacity of endothelial cells by regulating mitochondrial function and senescence. The Journal of cell biology. 2008 Jan 14;180(1):101-12.
[125] Ballinger SW, Patterson C, Knight-Lozano CA, Burow DL, Conklin CA, Hu Z, et al. Mitochondrial integrity and function in atherogenesis. Circulation. 2002 Jul 30;106(5):544-9.
[126] Comi P, Chiaramonte R, Maier JA. Senescence-dependent regulation of type 1 plasminogen activator inhibitor in human vascular endothelial cells. Exp Cell Res. 1995 Jul;219(1):304-8.
[127] Celermajer DS, Sorensen KE, Spiegelhalter DJ, Georgakopoulos D, Robinson J, Deanfield JE. Aging is associated with endothelial dysfunction in healthy men years before the age-related decline in women. Journal of the American College of Cardiology. 1994 Aug;24(2):471-6.
[128] Matsushita H, Chang E, Glassford AJ, Cooke JP, Chiu CP, Tsao PS. eNOS activity is reduced in senescent human endothelial cells: Preservation by hTERT immortalization. Circulation research. 2001 Oct 26;89(9):793-8.
[129] van der Loo B, Labugger R, Skepper JN, Bachschmid M, Kilo J, Powell JM, et al. Enhanced peroxynitrite formation is associated with vascular aging. The Journal of experimental medicine. 2000 Dec 18;192(12):1731-44.
[130] Minamino T, Miyauchi H, Yoshida T, Ishida Y, Yoshida H, Komuro I. Endothelial cell senescence in human atherosclerosis: role of telomere in endothelial dysfunction. Circulation. 2002 Apr 2;105(13):1541-4.
[131] Maier JA, Statuto M, Ragnotti G. Senescence stimulates U937-endothelial cell interactions. Exp Cell Res. 1993 Sep;208(1):270-4.
[132] Minamino T, Komuro I. Vascular cell senescence: contribution to atherosclerosis. Circulation research. 2007 Jan 5;100(1):15-26.
[133] Brodsky SV, Gealekman O, Chen J, Zhang F, Togashi N, Crabtree M, et al. Prevention and reversal of premature endothelial cell senescence and vasculopathy in obesity-induced diabetes by ebselen. Circulation research. 2004 Feb 20;94(3):377-84.
[134] Hayashi T, Iguchi A. Possibility of the regression of atherosclerosis through the prevention of endothelial senescence by the regulation of nitric oxide and free radical scavengers. Geriatrics & gerontology international. Apr;10(2):115-30.

[135] Patschan S, Chen J, Polotskaia A, Mendelev N, Cheng J, Patschan D, et al. Lipid mediators of autophagy in stress-induced premature senescence of endothelial cells. American journal of physiology. 2008 Mar;294(3):H1119-29.
[136] Wu DY, Ugozzoli L, Pal BK, Qian J, Wallace RB. The effect of temperature and oligonucleotide primer length on the specificity and efficiency of amplification by the polymerase chain reaction. DNA Cell Biol. 1991;10(3):233-8.
[137] Ehrt S, Schnappinger D. Isolation of plasmids from E. coli by alkaline lysis. Methods Mol Biol. 2003;235:75-8.
[138] Gamble J, Meyer G, Noack L, Furze J, Matthias L, Kovach N, et al. B1 integrin activation inhibits in vitro tube formation: effects on cell migration, vacuole coalescence and lumen formation. Endothelium. 1999;7(1):23-34.
[139] Madhusudan S, Harris AL. Drug inhibition of angiogenesis. Current opinion in pharmacology. 2002 Aug;2(4):403-14.
[140] Bergers G, Hanahan D. Modes of resistance to anti-angiogenic therapy. Nat Rev Cancer. 2008 Aug;8(8):592-603.
[141] Nussenbaum F, Herman IM. Tumor angiogenesis: insights and innovations. Journal of oncology.2010:132641.
[142] Gamble JR, Matthias LJ, Meyer G, Kaur P, Russ G, Faull R, et al. Regulation of in vitro capillary tube formation by anti-integrin antibodies. The Journal of cell biology. 1993 May;121(4):931-43.
[143] Meyer GT, Matthias LJ, Noack L, Vadas MA, Gamble JR. Lumen formation during angiogenesis in vitro involves phagocytic activity, formation and secretion of vacuoles, cell death, and capillary tube remodelling by different populations of endothelial cells. The Anatomical record. 1997 Nov;249(3):327-40.
[144] Hahn CN, Su ZJ, Drogemuller CJ, Tsykin A, Waterman SR, Brautigan PJ, et al. Expression profiling reveals functionally important genes and coordinately regulated signaling pathway genes during in vitro angiogenesis. Physiological genomics. 2005 Jun 16;22(1):57-69.
[145] Westbrook TF, Martin ES, Schlabach MR, Leng Y, Liang AC, Feng B, et al. A genetic screen for candidate tumor suppressors identifies REST. Cell. 2005 Jun 17;121(6):837-48.
[146] Coulson JM, Edgson JL, Woll PJ, Quinn JP. A splice variant of the neuron-restrictive silencer factor repressor is expressed in small cell lung cancer: a potential role in derepression of neuroendocrine genes and a useful clinical marker. Cancer Res. 2000 Apr 1;60(7):1840-4.
[147] Palm K, Metsis M, Timmusk T. Neuron-specific splicing of zinc finger transcription factor REST/NRSF/XBR is frequent in neuroblastomas and conserved in human, mouse and rat. Brain Res Mol Brain Res. 1999 Sep 8;72(1):30-9.
[148] Coulson JM. Transcriptional regulation: cancer, neurons and the REST. Curr Biol. 2005 Sep 6;15(17):R665-8.
[149] Majumder S. REST in good times and bad: roles in tumor suppressor and oncogenic activities. Cell Cycle. 2006 Sep;5(17):1929-35.
[150] Branco-Price C, Johnson RS. Tumor vessels are Eph-ing complicated. Cancer cell. Jun 15;17(6):533-4.
[151] Cronin S, Tomik B, Bradley DG, Slowik A, Hardiman O. Screening for replication of genome-wide SNP associations in sporadic ALS. Eur J Hum Genet. 2009 Feb;17(2):213-8.
[152] Potkin SG, Turner JA, Fallon JA, Lakatos A, Keator DB, Guffanti G, et al. Gene discovery through imaging genetics: identification of two novel genes associated with schizophrenia. Molecular psychiatry. 2009 Apr;14(4):416-28.
[153] Coleman PR, Hahn CN, Grimshaw M, Lu Y, Li X, Brautigan PJ, et al. Stress-induced premature senescence mediated by a novel gene, SENEX, results in an anti-inflammatory phenotype in endothelial cells. Blood. Jul 27.

[154] Afshari CA, Vojta PJ, Annab LA, Futreal PA, Willard TB, Barrett JC. Investigation of the role of G1/S cell cycle mediators in cellular senescence. Exp Cell Res. 1993 Dec;209(2):231-7.
[155] Muller M. Cellular senescence: molecular mechanisms, in vivo significance, and redox considerations. Antioxidants & redox signaling. 2009 Jan;11(1):59-98.
[156] Etienne-Manneville S, Hall A. 02.
[157] Van Aelst L, D'Souza-Schorey C. Rho GTPases and signaling networks. Genes Dev. 1997 Sep 15;11(18):2295-322.
[158] Ben-Porath I, Weinberg RA. The signals and pathways activating cellular senescence. The international journal of biochemistry & cell biology. 2005 May;37(5):961-76.
[159] McElligott R, Wellinger RJ. The terminal DNA structure of mammalian chromosomes. Embo J. 1997 Jun 16;16(12):3705-14.
[160] d'Adda di Fagagna F, Reaper PM, Clay-Farrace L, Fiegler H, Carr P, Von Zglinicki T, et al. A DNA damage checkpoint response in telomere-initiated senescence. Nature. 2003 Nov 13;426(6963):194-8.
[161] Kortlever RM, Higgins PJ, Bernards R. Plasminogen activator inhibitor-1 is a critical downstream target of p53 in the induction of replicative senescence. Nature cell biology. 2006 Aug;8(8):877-84.
[162] Garfinkel S, Brown S, Wessendorf JH, Maciag T. Post-transcriptional regulation of interleukin 1 alpha in various strains of young and senescent human umbilical vein endothelial cells. Proc Natl Acad Sci U S A. 1994 Feb 15;91(4):1559-63.
[163] Ota H, Akishita M, Eto M, Iijima K, Kaneki M, Ouchi Y. Sirt1 modulates premature senescence-like phenotype in human endothelial cells. Journal of molecular and cellular cardiology. 2007 Nov;43(5):571-9.
[164] Gamble JR, Harlan JM, Klebanoff SJ, Vadas MA. Stimulation of the adherence of neutrophils to umbilical vein endothelium by human recombinant tumor necrosis factor. Proc Natl Acad Sci U S A. 1985 Dec;82(24):8667-71.
[165] Ley K. Integration of inflammatory signals by rolling neutrophils. Immunological reviews. 2002 Aug;186:8-18.
[166] Ley K, Laudanna C, Cybulsky MI, Nourshargh S. Getting to the site of inflammation: the leukocyte adhesion cascade updated. Nat Rev Immunol. 2007 Sep;7(9):678-89.
[167] Mehta D, Malik AB. Signaling mechanisms regulating endothelial permeability. Physiological reviews. 2006 Jan;86(1):279-367.
[168] Finkel T, Holbrook NJ. Oxidants, oxidative stress and the biology of ageing. Nature. 2000 Nov 9;408(6809):239-47.
[169] Tsirpanlis G. Cellular senescence and inflammation: a noteworthy link. Blood purification. 2009;28(1):12-4.
[170] Slee EA, Adrain C, Martin SJ. Executioner caspase-3, -6, and -7 perform distinct, non-redundant roles during the demolition phase of apoptosis. J Biol Chem. 2001 Mar 9;276(10):7320-6.
[171] Kapuscinski J. DAPI: a DNA-specific fluorescent probe. Biotech Histochem. 1995 Sep;70(5):220-33.
[172] Cory S, Adams JM. The Bcl2 family: regulators of the cellular life-or-death switch. Nat Rev Cancer. 2002 Sep;2(9):647-56.
[173] Locksley RM, Killeen N, Lenardo MJ. The TNF and TNF receptor superfamilies: integrating mammalian biology. Cell. 2001 Feb 23;104(4):487-501.
[174] Passos JF, Simillion C, Hallinan J, Wipat A, von Zglinicki T. Cellular senescence: unravelling complexity. Age (Dordrecht, Netherlands). 2009 Jul 18.
[175] FK MCD, Turner SD. Jailbreak: Oncogene-induced senescence and its evasion. Cellular signalling. Jul 13.

[176] Borrello MG, Alberti L, Fischer A, Degl'innocenti D, Ferrario C, Gariboldi M, et al. Induction of a proinflammatory program in normal human thyrocytes by the RET/PTC1 oncogene. Proc Natl Acad Sci U S A. 2005 Oct 11;102(41):14825-30.
[177] Deshpande SS, Qi B, Park YC, Irani K. Constitutive activation of rac1 results in mitochondrial oxidative stress and induces premature endothelial cell senescence. Arteriosclerosis, thrombosis, and vascular biology. 2003 Jan 1;23(1):e1-6.
[178] Smith WB, Gamble JR, Clark-Lewis I, Vadas MA. Chemotactic desensitization of neutrophils demonstrates interleukin-8 (IL-8)-dependent and IL-8-independent mechanisms of transmigration through cytokine-activated endothelium. Immunology. 1993 Mar;78(3):491-7.
[179] Kibayashi E, Urakaze M, Kobashi C, Kishida M, Takata M, Sato A, et al. Inhibitory effect of pitavastatin (NK-104) on the C-reactive-protein-induced interleukin-8 production in human aortic endothelial cells. Clin Sci (Lond). 2005 Jun;108(6):515-21.
[180] Volonte D, Zhang K, Lisanti MP, Galbiati F. Expression of caveolin-1 induces premature cellular senescence in primary cultures of murine fibroblasts. Molecular biology of the cell. 2002 Jul;13(7):2502-17.
[181] Bruno T, De Nicola F, Iezzi S, Lecis D, D'Angelo C, Di Padova M, et al. Che-1 phosphorylation by ATM/ATR and Chk2 kinases activates p53 transcription and the G2/M checkpoint. Cancer cell. 2006 Dec;10(6):473-86.
[182] Kirchhoff T, Chen ZQ, Gold B, Pal P, Gaudet MM, Kosarin K, et al. The 6q22.33 locus and breast cancer susceptibility. Cancer Epidemiol Biomarkers Prev. 2009 Sep;18(9):2468-75.

Appendices

Appendix 1. Buffers

FACs analysis

FACS wash 0.02% sodium azide (Chem-Supply, SA, Australia), 5% FCS, in PBS

FACS fix 2% glucose (Chem-Supply), 0.02% sodium azide, 2.5% formaldehyde (Chem-Supply), in PB

Whole cell protein fractionation

Lysis solution Lysis buffer (100 mM Tris/HCl, 1% NP40, 150 mM NaCl, 1 mM EDTA, 100 μM NaF (Chem-Supply), 100 μM Sodium pyrophosphate) 1x Protease inhibitor (Sigma-Aldrich)

Western blotting

20X MOPS buffer 50 mM MOPS, 50 mM Tris Base, 0.1% SDS, 1 mM EDTA (pH 7.7)

20X MES buffer 50 mM MES, 50 mM Tris base, 0.1% SDS, 1 mM EDTA (pH 7.3)

20X transfer buffer 25 mM Bicine, 25mM Bis Tris, 1mM EDTA (pH 7.2)

Appendix 2. PCR Primers

REST – Cloning Primers
Forward – CGGAATTCACAGTTATGGCCACCCAGGTAATG
Reverse – CGGAATTCATGGCTTCTCACCTGAATGAGTACG

REST-Q-RT-PCR Primers
Forward – CTGTTTTGCGTATGAGTGCTGAT
Reverse – GGTATTCCTTCCATTGTCAACATTC

REST – Myc Primer
Reverse
CGGAATTCACAGGTCCTCCTCGCTGATCAGCTTCTGCTCCTCCTGCCCTTGAGCTGCTTC

Cyclophilin A
Forward – GGCAAATGCTGGACCCAACACAAA
Reverse – CTAGGCATGGGAGGGAACAAGGAA

SENEX
Forward – TTGCTCTGTTTTCCAGATTGGA
Reverse – GCCCCAGTGCTTGAGGCT

PAI1
Forward – GGTAGGGCACAAAGATGGATGA
Reverse – CCCAGGCTGGTCTTGAACTC

IL-1α
Forward – TTACCTGGGCATTCTTGTTTCA
Reverse – CAGTGGTCTCATGGTTGTCAAAGT

Cox2
Forward – TGTTATTAACATTGATCTGCTGACAAAA
Reverse – ACACATTTGTCTGAGGCACTGAA

p16
Forward – TGCCTTTTCACTGTGTTGGAGTT
Reverse – GCAAGAAATGCCCACATGAAT

Appendix 3. Antibodies

ANTIBODY	CLONALITY	SOURCE	DILUTION	MANUFACTURER
Anti-SENEX	Polyclonal	Rabbit	1/500	Vascular Biology Lab
Anti-p16	Polyclonal	Rabbit	1/200	Santa Cruz
Anti-p53	Monoclonal	Mouse	1/1000	Invitrogen
Anti-p21	Monoclonal	Mouse	1/1000	Zymed Laboratories
Anti-phosph Rb (Ser807/811)	Polyclonal	Rabbit	1/200	Cell Signalling Technologies
Anti-actin	Monoclonal	Mouse	1/1000	Sigma Aldrich
Anti-myc	Polyclonal	Rabbit	1/1000	BD Biosciences
Anti-Bid	Monoclonal	Mouse	1/1000	BD Biosciences
Anti-BCL2	Polyclonal	Rabbit	1/1000	BD Biosciences
Anti-MCL	Polyclonal	Rabbit	1/1000	BD Biosciences
Anti-Bax	Polyclonal	Rabbit	1/1000	BD Biosciences
Anti-E-selectin	Polyclonal	Rabbit	20µg/ml	Vascular Biology Lab
Anti-VCAM1	Polyclonal	Rabbit	20µg/ml	Vascular Biology Lab

ANTIBODY	CONJUGATE	HOST	MANUFACTURER
Anti-rabbit IgG	Alexa Fluor® 594	Goat	Invitrogen
Anti-mouse IgG	Alexa Fluor® 594	Goat	Invitrogen
Anti-mouse IgG	HRP	Goat	Cayman Chemical
Anti-rabbit IgG	HRP	Goat	Cayman Chemical